New Polygeneration Processes for Power Generation and Liquid Fuel Production with Zero CO_2 Emissions

New Polygeneration Processes for Power Generation and Liquid Fuel Production with Zero CO_2 Emissions

By
Yaser Khojasteh-Salkuyeh, B.Eng., M.A.Sc

A Thesis

Submitted to the School of Graduate Studies

in Partial Fulfillment of the Requirements

for the Degree

Doctor of Philosophy

McMaster University

Ph.D. Candidate (2015) McMaster University

Chemical Engineering Hamilton, Ontario

TITLE: **New Polygeneration Processes for Power Generation and Liquid Fuel Production with Zero CO_2 Emissions**

AUTHOR: Yaser Khojasteh-Salkuyeh

B.Eng. (Tehran University)

M.A.Sc (Sharif University of Technology)

SUPERVISOR: Professor Thomas A. Adams II

NUMBER OF PAGES: xii, 179

Abstract

The price and accessibility of fossil fuels, especially crude oil, are subject to considerable fluctuations due to growing demand on energy, limited resources, and energy security concerns. In addition, climate change caused by burning of fossil fuels is a challenge that energy sector is currently facing. These challenges incentivize development of alternative processes with no greenhouse gas emissions that can meet transportation fuels, chemical liquids, and electricity demands. Coal-based processes are of particular interest because coal price is both low and stable. However, these processes have a large environmental impact and are also less economically attractive than natural gas based plants due to the recent significant drop in natural gas price. However, even for natural gas plants, attempts to reduce CO_2 emissions by using traditional CO_2 capture and sequestration technologies not only decrease the thermal efficiency and profitability of the plant significantly but still release some CO_2 to the atmosphere.

The aim of this thesis is to develop, simulate and optimize an integrated polygeneration plant that uses multiple feedstocks and produces multiple products with low to zero CO_2 emissions. Several process alternatives are investigated in this work to show the effect of each feedstock and product on the performance of the proposed plant. A comprehensive study is performed in each section, including process simulation in Aspen Plus software, development of custom models required for some units, as well as cost analysis by using Aspen Icarus software and empirical cost estimations from literature.

Moreover, derivative free optimization techniques such as particle swarm optimization (PSO), genetic algorithm (GA) and simulated annealing (SA) are implemented to drive the design to economically optimum conditions as a function of the market price and carbon taxes. The final model will also introduce emerging technologies that can achieve higher efficiency and lower CO_2 emissions compared to commercial systems, such as chemical looping gasification, chemical looping combustion, nuclear heat reforming, etc. By integrating multiple feedstocks and processes, the model can exploit certain synergies which are unavailable to traditional plants, resulting in significant efficiency improvements. In addition to power and liquid fuels, this polygeneration process offers benefits for petrochemical plants. Despite limited worldwide crude oil reserves, the demand for petrochemical products is still growing fast and it is highly important for petrochemical industry to find new resources as feedstock and diversify their supply chain network. By integration of the polygeneration plant in the same facility with novel processes that produce olefins (petrochemical feedstock) not from oil, but from syngas, it is possible to supply the required feed at lower cost than commercial steam cracking plants.

Research Contributions

- Development and techno-economic analysis of the first integrated system which converts coal-natural gas-nuclear heat to transportation fuels are investigated.

- Carbon efficiency up to 72% can be achieved which is around 40% higher than the carbon efficiency of typical coal-to-liquid plants.

- Economic analysis results showed that the minimum CO_2 emission tax to incentivize using the CCS and nuclear heat enabled scenarios is around \$25/tonne CO_2

- By incorporation of the chemical looping system, a new zero-carbon emission system can be achieved that its efficiency is up to 6 percentage points greater than the efficiency of traditional coal-based systems.

- Production of olefins from shale gas and also petroleum coke waste product has been investigated in this work. The techno-economic performances of two new olefin production technologies are studied for a variety of process configurations and market fluctuations. Optimization results showed that it is more economical to convert the feedstock to methanol and then produce olefins from methanol using MTO process. However, the direct conversion option (OCM based system) is also profitable, especially by coproduction of electricity as an optional byproduct. Noting that 100% carbon capture system is considered for both options.

- Using the proposed model, up to 74% of the input can be petcoke while still having a profitable plant.

- The required hydrogen of the FT transportation liquid production process is supplied by using the chemical looping gasification system to reduce the hydrogen production energy demand.

Acknowledgements

Firstly, I would like to express my gratitude to my Ph.D. supervisor, Prof. Thomas A. Adams II for his continued support and mentorship throughout my research work. I am grateful for his support, constant encouragement, positive attitude and invaluable guidance while providing me with a remarkable freedom to research and explore new ideas in my own way.

I would also like to thank Prof. Vladimir Mhalec, Prof. Christopher Swartz and Prof. Jim Cotton from the Mechanical Engineering Department for their valuable suggestions and advice.

Special thanks are also to the McMaster Advanced Control Consortium and the Department of Chemical Engineering at McMaster University for their financial support.

I also would also like to thank Jaffer Ghouse, Jake Nease, Vida Meidanshahi, Chinedu Okoli, Yanan Cao, Nor Farida Harun, Kyle Lefebvre, Kushlani Wijesekera, Yasser Ghobara and other MACC members for their support and help during this project.

Last but not least, I would like to thank my family and express my love and gratitude to my wife Dr. Sana Jahanshahi Anbuhi, my parents Mrs. Bemani Asgharian Salkuyeh and Mr. Yaghub Khojasteh Salkuyeh for their endless love and for supporting me spiritually throughout my life. Finally, thanks to God for giving me the opportunity and the ability to proceed with my doctoral research work.

Table of Contents

List of Acronyms

ANN	Artificial Neural Network
Ar	Argon
ASU	Air Separation Unit
CCS	Carbon Capture and Sequestration
CEPCI	Chemical Engineering Plant Cost Index
CGNTL	Coal-And-Gas-And-Nuclear-To-Liquids
CGTL	Coal-And-Gas-To-Liquid
CLC	Chemical Looping Combustion
COS	Carbonyl Sulfate
CTL	Coal-To-Liquid
DGA	Diglycolamine
DME	Dimethyl Ether
EOR	Enhanced Oil Recovery
FT	Fischer-Tropsch
GA	Genetic Algorithm
GCR	Gas Cooled Reactor
GCT	Gas Combustion Turbine
GE	General Electric
GEE	General Electric Energy
GT	Gas Turbine
GTL	Gas-To-Liquid
HHV	Higher Heating Value
HP	High Pressure
HRSG	Heat Recovery Steam Generation

HTL	Heat-To-Liquid
IGCC	Integrated Gasification Combined Cycle
IP	Intermediate Pressure
IRR	Internal Rate of Return
LHV	Lower Heating Value
LPS	Low Pressure Steam
MDEA	Methyl-Diethanol Amine
MHR	Modular Helium Reactor
MINLP	Mixed Integer Nonlinear Programming
MIP	Mixed Integer Programming
MPS	Medium Pressure Steam
MTO	Methanol to Olefins
NBS/NRC	National Bureau of Standards/National Research Council
NETL	National Energy Technology Laboratory
NFE	Number of Function Evaluations
NGCC	Natural Gas Combined Cycle
NPV	Net Present Value
NRTL	Nonrandom-Two-Liquid
OCM	Oxidative Coupling Of Methane
PR-BM	Peng Robinson with Boston-Matthias
PSO	Particle Swarm Optimization
R-50	Methane Refrigerant
R-1150	Ethylene Refrigerant
R-1270	Propylene Refrigerant
SA	Simulated Annealing

SG	Shale Gas
TIT	Turbine Inlet Temperature
VBA	Visual Basic For Applications
WGS	Water Gas Shift

Chapter 1 Introduction

According to the United Nations report, the world's population is projected to grow more than 33% by 2050, compared to 2013 [1]. Population growth along with considerable increase in global Gross Domestic Product (GDP) poses a significant challenge to the world energy consumption. Thus, it is not surprising that the global energy consumption is anticipated to grow at 1.4% per year [2]. As another example, global demand for ethylene, as the main feedstock of petrochemical industry, is forecast to raise at 4% per year [3].

Although crude oil is still one of the main energy sources that both industry and transportation sectors significantly rely on, its market fluctuations, supply security concerns and also greenhouse gas emissions have provided great long term incentives for researchers to study alternative processes. Therefore, diversification of supply chain networks by introducing new processes that are capable of using carbon-based and noncarbon-based feedstocks such as coal, biomass, natural gas, nuclear heat and also renewable energy is the main interest of recent research. For example, gasification of coal and converting the produced synthesis gas to transportation fuels (gasoline and diesel) via Fischer-Tropsch process is an alternative to the conventional oil refineries. The water gas shift (WGS) section, which is used to increase the H_2/CO ratio of syngas, causes a significant efficiency loss in the coal-to-liquid (CTL) process though.

Incorporation of natural gas is an alternative approach that can be coupled with coal or biomass gasification train to improve the performance of the plant [4]. Natural gas is a fossil fuel that can produce synthesis gas with higher H_2/CO ratio compared to the syngas produced by coal gasifier [5]. Due to rapid growth of shale gas resources, natural gas market price has started to decline since 2009, which makes natural gas a more attractive resource for hybrid systems. However, there have been no prior works considering different varieties of shale gas for a large scale polygeneration process (to the best of our knowledge).

By blending the syngas produced by shale gas reformer with the one produced by coal gasifier, the H_2/CO ratio can be adjusted to the optimum value required by downstream units. The

blended syngas can be used as the feedstock of a polygeneration system to generate multiple products: electricity, chemicals such as ethanol, methanol and dimethyl ether (DME), gasoline, diesel and kerosene. Thus, the integrated system can use the benefits of each feedstock and product, which can be more efficient than standalone strategies. For example, Baliban et al. [6-9] focused on development and optimization of a hybrid system that uses coal, biomass and natural gas to coproduce FT liquids, electricity and olefins. Various configurations were tested in their works, showing that there are some process flow sheets that can be competitive with the conventional petrochemical based processes while having 50% reduction on CO_2 emissions compared to refineries. However, further reduction of CO_2 emissions can still be achieved by incorporation of novel technologies, which will be presented in this thesis.

It should be also noted that due to the emergence of new energy resources, development of novel hybrid systems is still an active area of research. For instance, petroleum coke (or petcoke), which is the byproduct of heavy oil refineries or oil sands upgraders, can be considered as an alternative to coal. The global production rate of petcoke is projected to grow 4% per year [10]. As a result, finding an economic strategy with minimal environmental impacts that is capable of converting petcoke to valuable products is the new challenge of most oil refineries. Economical utilization of petcoke can reduce the refining waste and CO_2 emissions, while potentially improves the profitability of plant.

Incorporation of advanced nuclear power plants to supply the process energy demand is the other possibility that can reduce the fossil fuel depletion rate. For example, a modular helium reactor (MHR) can be integrated into the hydrogen production unit to produce high purity hydrogen from this non-carbon resource [11]. In the novel system proposed in this thesis, a modular helium reactor (MHR) is coupled with the polygeneration process to provide the heat required in the plant without any additional CO_2 emissions. Reduction of fossil fuel consumption, as well as greenhouse gas emissions, can yield a considerable improvement on the efficiency of polygeneration process.

As mentioned before, despite several studies on the improvement of the performance of polygeneration systems, the efficiency and financial loss caused by CO_2 removal and

sequestration steps is still a major concern [12, 13]. Among the several technologies that have been proposed for CO_2 capture currently under development, the chemical looping combustion system has been identified as one of the most promising technologies with significant reduction in CO_2 removal cost [14]. In this option, the main combustion reaction is divided into two sub-reactions. A solid oxygen carrier, such as iron-oxide (Fe_2O_3) or nickel-oxide (NiO), is used to combust the feedstock in the first reactor. The reduced metal is then regenerated with air in the combustion reactor and recycled back to the first reactor. In addition, chemical looping gasification is the other option that can attain high purity hydrogen by regenerating the oxygen carrier with steam, instead of air [15]. Introduction of these technologies to polygeneration systems can improve both the profitability and CO_2 capture performance of plant, which hasn't been studied before and is a subject of further research.

1.1 Research outline

The main objective of this project is to develop and optimize a polygeneration plant that produces chemicals, fuels, olefins and electricity by using a hybrid system with minimum to zero CO_2 emissions at maximum thermal efficiency and profitability. A simplified schematic of this system is shown in Figure 1. Therefore, in this thesis, incorporation of new feedstocks and novel technologies are studied to develop a polygeneration process which offers an innovative alternative to traditional processes. The use of shale gas, nuclear energy and petroleum coke are considered as the main alternative feedstocks. In addition, several design configurations are investigated including chemical looping systems, oxy-fuel combustion, OCM reaction, CO_2 hydration, etc.

Chapter 2. The first achievement of this project deals with the development of an integrated coal, natural gas and nuclear heat to coproduce transportation fuels (gasoline and diesel via Fischer-Tropsch process) and electricity with zero CO_2 emissions with remarkably high carbon efficiency (70%). In terms of energy resources, it is tried to incorporate the modular helium reactor (MHR), as the 4^{th} generation of nuclear power plants, with the natural gas reformer and take the advantage (price, CO_2 emission rate, availability, etc.) of each feedstock. Details of this system are described in chapter 2. This work has led to 2 publications in *Computer Aided*

Chemical Engineering [16] and *Energy Conversion and Management* [17] journals.

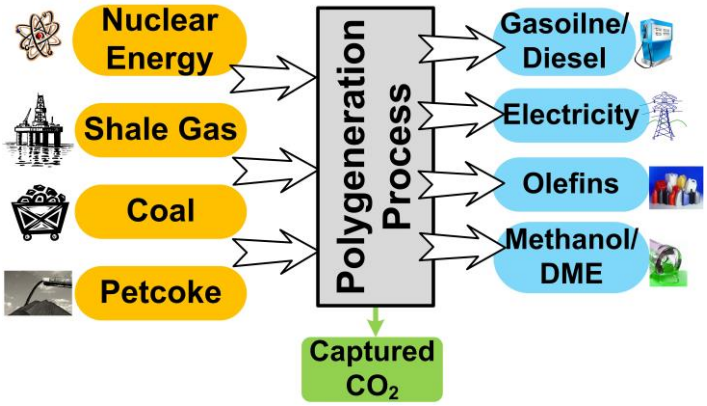

Figure 1. Schematic of the proposed polygeneration process.

Chapter 3. The second contribution deals with the improvement of the efficiency of plant by using new emerging CO_2 removal techniques, as described in chapter 3. Chemical looping, as one of the promising approaches that can be used for a diverse range of fuel and power production processes, is applied to the coal-natural gas-nuclear energy polygeneration system. Multiple gasification options, and integrated methanol/DME and power generation are the key promising features of this model. This process has higher thermal efficiency than previous works with essentially zero carbon emissions. In addition, the liquefaction and pumping of CO_2 product to the supercritical pressure can be replaced with a new concept based on gas hydrate formation, to decrease the energy consumption. This work has led to a publication in *Energy Conversion and Management* [18].

Chapter 4. The next achievement of this work is the introduction of a shale gas-to-olefin system based on oxidative coupling of methane (OCM) process. As described in chapter 4, different optimization techniques are also developed and linked to the simulation model to determine the optimum conditions as a function of market prices. In addition, a custom model is developed to simulate the actual behaviour of the electricity generation system. Unlike the simple models built in traditional simulation software, the cooling system that is an important part of gas turbines is modeled. This model can also be used for the simulation and optimization of the traditional natural gas combined cycle (NGCC) plants. Therefore, by using this model, less expensive electricity for both traditional power plants and also new zero-emission large scale

polygeneration units is achievable. This work has led to a publication in *Energy Conversion and Management* [19].

Chapter 5. In addition to OCM system, production of olefins based on indirect conversion of shale gas to olefins, using the methanol-to-olefins (MTO) option is investigated in chapter 5. Various zero-emission power generation strategies are investigated and the techno-economic optimization is performed to determine the optimum conditions for different scenarios. The results presented in this chapter is published in *Computer Aided Chemical Engineering* [20]. The text and materials provided in this chapter are submitted to the Energies journal for peer review [21].

Chapter 6. The final accomplishment introduces petcoke to the polygeneration process (chapter 6). Petcoke can be used instead of coal or mixed with coal and fed to the petcoke gasifier. Conversion of stockpiled petcokes to marketable products with zero CO_2 emissions has the capability of raising the profitability of heavy crude oil refineries and tar san upgraders with substantial environmental benefits. The text and materials provided in this chapter are submitted to the *Fuel Processing Technology* journal for peer review.

Chapter 7. Finally, the main conclusions of this work and future research suggestions are described in chapter 7.

1.2 References

[1] World population projected to reach 9.6 billion by 2050 – United Nations report. 2013.
[2] BP Energy Outlook 2035. BP plc, London, United Kingdom. (February 2015).
[3] Ethylene, Information Handling Services (IHS) Report. (October 2014).
[4] H. Li, H. Hong, H. Jin, R. Cai. Analysis of a feasible polygeneration system for power and methanol production taking natural gas and biomass as materials. Applied Energy. 87 (2010) 2846-53.
[5] T.A. Adams II, P.I. Barton. Combining coal gasification and natural gas reforming for efficient polygeneration. Fuel Processing Technology. 92 (2011) 639-55.
[6] R.C. Baliban, J.A. Elia, C.A. Floudas. Optimization framework for the simultaneous process synthesis, heat and power integration of a thermochemical hybrid biomass, coal, and natural gas facility. Computers & Chemical Engineering. 35 (2011) 1647-90.
[7] R.C. Baliban, J.A. Elia, C.A. Floudas. Simultaneous process synthesis, heat, power, and water integration of thermochemical hybrid biomass, coal, and natural gas facilities.

Computers & Chemical Engineering. 37 (2012) 297-327.
[8] R.C. Baliban, J.A. Elia, V. Weekman, C.A. Floudas. Process synthesis of hybrid coal, biomass, and natural gas to liquids via Fischer–Tropsch synthesis, ZSM-5 catalytic conversion, methanol synthesis, methanol-to-gasoline, and methanol-to-olefins/distillate technologies. Computers & Chemical Engineering. 47 (2012) 29-56.
[9] R.C. Baliban, J.A. Elia, C.A. Floudas. Toward Novel Hybrid Biomass, Coal, and Natural Gas Processes for Satisfying Current Transportation Fuel Demands, 1: Process Alternatives, Gasification Modeling, Process Simulation, and Economic Analysis. Industrial & Engineering Chemistry Research. 49 (2010) 7343-70.
[10] L. Stockman. Petroleum Coke: the coal hiding in the tar sands. Oil Chance International, Washington DC, USA. (2013).
[11] M. Richards, A. Shenoy. H_2-MHR Pre-Conceptual Design Summary for Hydrogen Production. Nuclear Engineering and Technology. 39 (2007) 1-8.
[12] M. Bracht, P.T. Alderliesten, R. Kloster, R. Pruschek, G. Haupt, E. Xue, et al. Water gas shift membrane reactor for CO_2 control in IGCC systems: techno-economic feasibility study. Energy Conversion and Management. 38, Supplement (1997) S159-S64.
[13] B.S. Hoffmann, A. Szklo. Integrated gasification combined cycle and carbon capture: A risky option to mitigate CO_2 emissions of coal-fired power plants. Applied Energy. 88 (2011) 3917-29.
[14] J. Adanez, A. Abad, F. Garcia-Labiano, P. Gayan, L.F. de Diego. Progress in Chemical-Looping Combustion and Reforming technologies. Progress in Energy and Combustion Science. 38 (2012) 215-82.
[15] L.S. Fan. Chemical Looping Systems For Fossil Energy Conversions. John Wiley & Sons, Inc., , Hoboken, NJ, USA, 2010.
[16] Y. Khojasteh Salkuyeh, T.A. Adams II. Combining coal, natural gas, and nuclear heat for liquid fuels production with reduced CO_2 emissions. in: B. Ian David Lockhart, F. Michael, (Eds.), Computer Aided Chemical Engineering. Elsevier2012. pp. 247-51.
[17] Y. Khojasteh Salkuyeh, T.A. Adams II. Combining coal gasification, natural gas reforming, and external carbonless heat for efficient production of gasoline and diesel with CO_2 capture and sequestration. Energy Conversion and Management. 74 (2013) 492-504.
[18] Y. Khojasteh Salkuyeh, T.A. Adams II. A new power, methanol, and DME polygeneration process using integrated chemical looping systems. Energy Conversion and Management. 88 (2014) 411-25.
[19] Y. Khojasteh Salkuyeh, T.A. Adams II. A novel polygeneration process to co-produce ethylene and electricity from shale gas with zero CO_2 emissions via methane oxidative coupling. Energy Conversion and Management. 92 (2015) 406-20.
[20] Y. Khojasteh Salkuyeh, T.A. Adams II. Shale gas for the petrochemical industry: Incorporation of novel technologies. in: J.D.S. Mario R. Eden, P.T. Gavin, (Eds.), Computer Aided Chemical Engineering. Elsevier2014. pp. 603-8.
[21] Y. Khojasteh Salkuyeh, T.A. Adams II. Co-Production of Olefins, Fuels, and Electricity from Conventional Pipeline Gas and Shale Gas with Near-Zero CO_2 Emissions, (Under Final Review). Energies. 18 (2015).

Chapter 2

Combining Coal Gasification, Natural Gas Reforming, and External Carbonless Heat for Efficient Production of Gasoline and Diesel with CO_2 Capture and Sequestration

Energy Conversion and Management 74 (2013) 492–504

Contents lists available at ScienceDirect

Energy Conversion and Management

journal homepage: www.elsevier.com/locate/enconman

Combining coal gasification, natural gas reforming, and external carbonless heat for efficient production of gasoline and diesel with CO_2 capture and sequestration

Yaser Khojasteh Salkuyeh, Thomas A. Adams II *

Department of Chemical Engineering, McMaster University, 1280 Main Street West, Hamilton, Ontario L8S 4L7, Canada

ARTICLE INFO

Article history:
Received 12 June 2013
Accepted 11 July 2013
Available online 9 August 2013

Keywords:
Coal gasification
Natural gas reforming
Fischer–Tropsch
Helium-heated steam reformer
CO_2 capture

ABSTRACT

In this paper, several novel polygeneration systems are presented which convert natural gas, coal, and a carbonless heat source such as high-temperature helium to gasoline and diesel. The carbonless heat source drives a natural gas reforming reaction to produce hydrogen rich syngas, which is mixed with coal-derived syngas to produce a syngas blend ideal for the Fischer–Tropsch reaction. Simulations and techno-economic analyses performed for 16 different process configurations under a variety of market conditions indicate significant economic and environmental benefits. Using a combination of coal, gas, and carbonless heat, it is possible to reduce CO_2 emissions (both direct and indirect) by 79% compared to a traditional coal-to-liquids process, and even achieve nearly zero CO_2 emissions when carbon capture and sequestration technology is employed. Using a carbonless heat source, the direct fossil fuel consumption can be reduced up to 22% and achieve a carbon efficiency up to 72%. Market considerations for this analysis include prices of coal, gas, high-temperature helium, gasoline, and CO_2 emission tax rates. The results indicate that coal-only systems are never the most economical choice, unless natural gas is more than 5 $/MMBtu.

1. Introduction

1.1. Background

The rising price of crude oil, energy security concerns, and greenhouse gas emission challenges are motivating new efforts to find alternative processes for the production of transportation fuels with improved energy and environmental efficiencies. Coal-based processes are of particular interest because coal prices are both low and stable (lower cost per usable energy compared to crude oil [1]), coal is plentiful, and coal is ubiquitous [1,2] (approximately 50% of the power in the United States and 40% of all power world-wide is coal-derived [1,3]). The coal-to-liquids (CTL) process can be used to produce diesel and gasoline from coal rather than crude oil. In a traditional CTL process, coal is gasified to produce synthesis gas (or "syngas", consisting mainly of CO and H_2 [4]) and subsequently convert the syngas to liquid fuels such as diesel and gasoline by using the well-known Fischer–Tropsch (FT) process [5]. However, although coal is a cheap energy resource, it has a large environmental impact because of the high rate of air pollution. For example, carbon dioxide, which is produced in both the gasifier and the FT reactor, is exhausted to atmosphere at a rate of around 15–20 kg per gallon of liquid fuel produced [6]. In addition, attempts to reduce CO_2 emissions by using solvent-based CO_2 capture and sequestration technologies (CCS) decrease the thermal efficiency of the plant and yet still release some CO_2 to the atmosphere [7–9]. Furthermore, CO_2 capture and sequestration is very expensive, thus incentivizing the use of other techniques [10].

To improve the thermodynamic efficiency and flexibility of coal-based processes, polygeneration systems [11] have been introduced. Polygeneration couples power generation with the production of liquid fuels like gasoline, diesel [12], alcohols [13] and dimethyl ether (DME) [14]. Often, coal gasification is used to generate synthesis gas which is utilized for liquid fuel production. By taking advantage of certain synergies, the thermal efficiency of coal-based polygeneration plants is generally higher than stand-alone power or liquid fuels plants of the same size [9]. This helps

Abbreviations: ASU, air separation unit; CCS, carbon capture and sequestration; CTL, coal-to-liquids; CGTL, coal-and-gas-to-liquids; CGNTL, coal-and-gas-and-nuclear-to-liquids; DME, dimethyl ether; FT, Fischer–Tropsch; GCR, gas cooled reactor; GT, gas turbine; GTL, gas-to-liquid; IGCC, integrated gasification combined cycle; HHV, higher heating value; HTL, heat-to-liquid; HRSG, heat recovery steam generation; IRR, internal rate of return; MHR, modular helium reactor; MINLP, mixed integer nonlinear programming; MIP, mixed integer programming; NPV, net present value.

* Corresponding author. Tel.: +1 (905) 525 9140x24782.
E-mail address: tadams@mcmaster.ca (T.A. Adams II).

0196-8904/$ - see front matter © 2013 Elsevier Ltd. All rights reserved.
http://dx.doi.org/10.1016/j.enconman.2013.07.023

to make coal-based processes economically competitive compared to crude oil refineries [15].

The improvement of polygeneration systems is an area of active research. A techno-economic evaluation of a coal-based polygeneration system with carbon capture was performed by Hu et al. [16] for different configurations. They found that system efficiencies varied from 42–70% (LHV) without CO_2 capture and 30–48% with CO_2 Capture. The lowest carbon emission achieved (with CCS) was 16 kg per GJ of products. Yu et al. [17] investigated the process of converting coal to liquid fuels and electricity with carbon capture for four different design configurations in which FT tail gases are combusted in a gas turbine and concluded that maximizing the fuel production (as a percentage of the total product portfolio) also maximizes the thermal efficiency (48.3% (LHV) for 100% of syngas converted to the FT liquids, compared to 34.6% for 100% of syngas used for power generation). This is because the thermal efficiency of a gas-turbine combined cycle is approximately 60% of the thermal efficiency of a Fischer–Tropsch synthesis plant. Later studies by Adams and Barton [18,19] reached a similar conclusion. Liu et al. used mixed-integer nonlinear methods to optimize a polygeneration plant producing methanol and electricity from coal and obtained around $128 per tonne coal as the maximum annual profit of polygeneration system [20]. He et al. [21] analyzed a similar process using improved catalysts which helped improve the thermal efficiency. However, for all of these processes, carbon emissions remain relatively high at around 20% of the inlet carbon [22] (even with CCS) mainly due to tail gas emissions from the liquid fuel production section.

Instead of using coal as the only fuel, it can be advantageous to use combinations of feedstocks (such as coal and biomass [23,24], coal and natural gas [18,19,25,26], coal and coke-oven gas [27], and biomass and natural gas [28]) in order to take advantage of certain synergies between the two fuels. For example, Yi et al. [27] developed and optimized a polygeneration plant using coal and clean coke-oven gas (mainly H_2 and CO) to make dimethyl ether (DME) and methanol. They achieved a total plant thermal efficiency 62.8% (HHV) by using an optimal ratio of 0.56 for the rate of coke-oven gas to coal gasified gas. They also proposed a novel dual feed system (coal–coke oven gas) with CO_2 recycle to the gasifier to increase the carbon conversion and decrease CO_2 emissions [29]. Li et al. [28] examined a similar system using a combined biomass-natural gas feedstock to get 9% fuel input saving compared with individual systems which use either biomass or natural gas as resource for methanol/power production. Gangadharan et al. [30] compared two different DME/power polygeneration systems, using coal and natural gas in a variety of configurations. It was found that natural gas as co-feed to coal can improve both the thermal efficiency and the CO_2 emissions rate. Adams and Barton examined other combinations of coal and natural gas and reached similar conclusions [18]. However, carbon emissions are still present from syngas or tail gas combustion (around 25 kg per GJ output [18]).

Another novel approach is to incorporate carbonless energy sources such as nuclear energy since nuclear-based electricity can be produced with essentially zero CO_2 emissions, thus providing a source of energy largely free of direct greenhouse gas emissions. While commonly used for electricity production, there has been recent interest in using nuclear energy for the production of fuels such as hydrogen gas and gasoline. For example, heat produced by nuclear energy can be integrated with a coal-to-liquids plant to supply some of the heat or steam generation needs of that plant. This helps to reduce CO_2 emissions to the atmosphere since less coal must be burned for heat, meaning that a greater percentage of the coal ends up as gasoline or diesel fuel. Thus, fossil fuels can be used more efficiently while reducing CO_2 emissions. Therefore, in this paper, several novel potential polygeneration processes are introduced using this approach in which coal, natural gas, and nuclear energy are converted into diesel and gasoline. These are evaluated and compared with several coal-only and coal-and-natural gas polygeneration processes.

1.2. CGTL and CGNTL process descriptions

Most coal-and-gas-to-liquids (CGTL) processes follow the same general process strategy (as shown in Fig. 1a). Coal is gasified to produce syngas with a low H_2 concentration (having a H_2/CO mole ratio of less than 1) which is then cleaned by removing H_2S with a solvent-based process. The H_2S collected is then converted to elemental sulfur compounds in the Claus process for sale. In parallel, natural gas is reformed into syngas with a high H_2 content (H_2/CO mole ratio greater than 3). This is then blended with the cleaned coal syngas such that the H_2/CO ratio is approximately 2, the ratio needed for FT synthesis. CO_2 is then removed from the blended gas with a solvent-based process, and optionally compressed and sent to a sequestration site. The remaining syngas is then used as feed to the FT synthesis reactor to produce a mixture of hydrocarbons ranging from light to heavy. The liquid hydrocarbons are then separated, purified, and blended into diesel and gasoline mixtures via distillation and other processes. The lightest hydrocarbons and waste syngas is collected as a vapor and used for some other purpose as described below.

In the present study, several new process design strategies are explored using coal, natural gas, and optionally nuclear energy and evaluate each for its potential to improve the profitability, carbon efficiency, thermal efficiency, and atmospheric emissions. The processes under consideration fall into two categories, described below.

CGTL: Unreacted FT waste gases (light hydrocarbons) are recycled to the process at various places upstream, rather than combusting for electricity as was the case in prior studies [18,19,31]. This also helps to decrease the rate of natural gas burning in the primary natural gas reformer. Four different process design configurations are considered by using the FT waste gases in different ways, as summarized in Fig. 1a:

- Case 1 – The light gas wastes which must be purged from the FT synthesis section are mixed with the main natural gas feed to replace some of the natural gas. The remaining waste gases are burned in the natural gas reformer to provide the necessary heat, eliminating the need to use fresh natural gas for that purpose there as well.
- Case 2 – Like case 1, 20% of the FT light gas wastes are used to replace natural gas burned in the natural gas reformer, and the remaining 80% are reformed in their own gas reformer and recycled directly to the FT process.
- Case 3 – Unlike cases 1 and 2, the main natural gas reformer continues to use some of the natural gas as the main heat source. A portion (80%) of the FT light gas wastes is sent to a separate reformer and recycled directly to the FT reactor, and the balance (20%) is mixed with the main natural gas feed.
- Case 4 – Like case 3, natural gas is used as a heat source in the main natural gas reformer, except that main natural gas feed is mixed with 100% of the FT light gas wastes beforehand.

CGNTL: Carbonless heat is delivered to the process from some external source. This heat is then used to displace fossil-based heating (such as the burning of natural gas used for natural gas reforming) by indirect contact in a heat exchanger which can reach above 900 °C. The high-temperature heat carrier can be chosen from several options, including helium gas, heavy metals, and

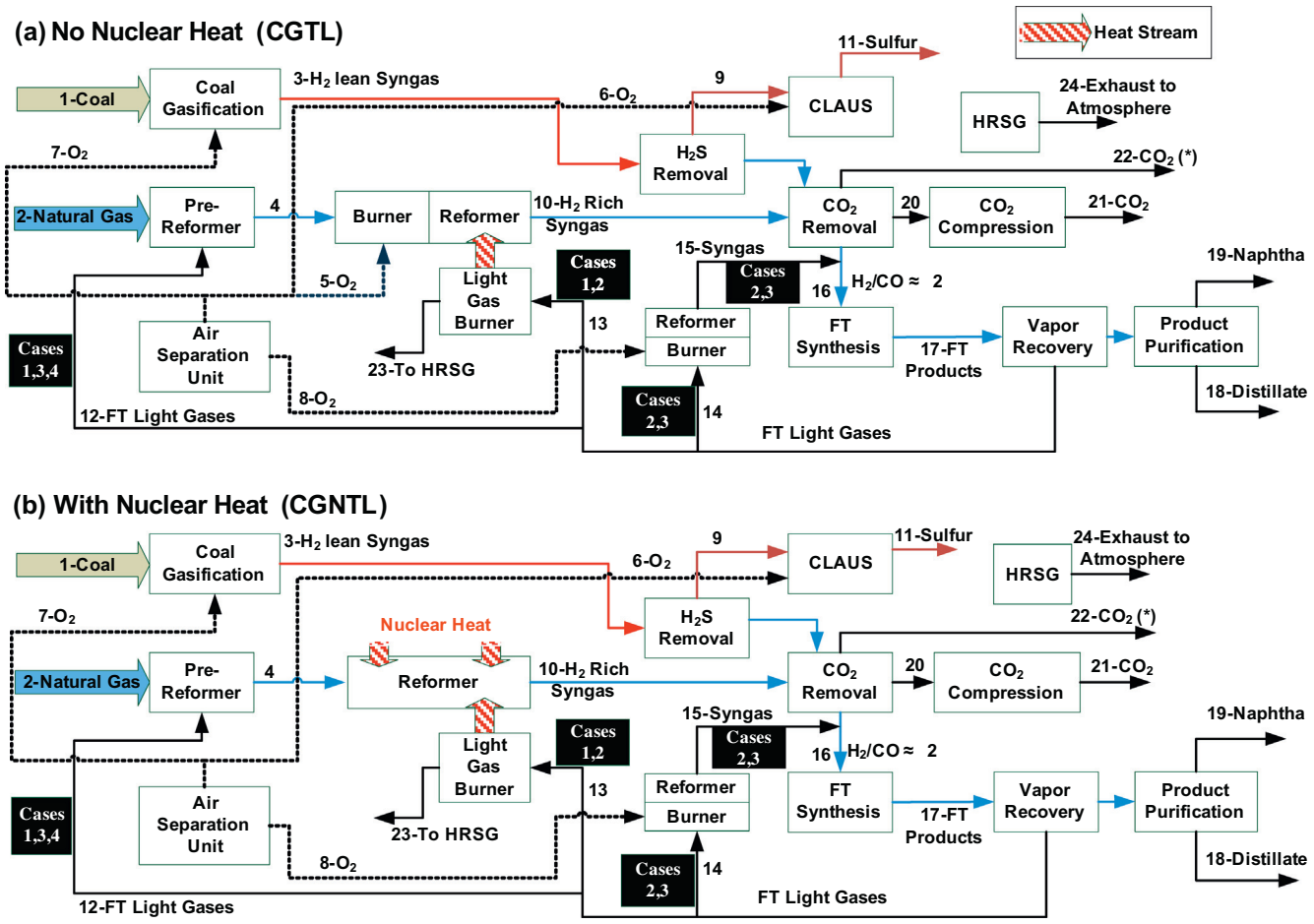

Fig. 1. Superstructures for all design options considered in the paper, divided into processes which do not use nuclear heat (a) and processes which do use nuclear heat (b). Heat integration is not shown for simplicity. *For "No CCS" cases the CO_2 stream (22) is directly sent to the atmosphere.

molten salts [32]. These are currently used as reactor coolants capable of achieving the required high temperatures [33]. For example, helium is used as the coolant for a modular helium reactor (MHR), a type of nuclear reactor in which the high-temperature helium coolant spins a turbine to produce electricity [34–40]. The use of these coolants as a heat temperature heat source has been studied in other applications, such as generating H_2 fuels via the sulfur-iodide cycle [41], and it has been shown that such plants can be safe [42]. The same principles can be applied to natural gas reforming with very few changes to the fundamental design [41]. In this study, we use high-temperature helium produced in an MHR as the high-temperature heat source delivered to the natural gas former. This results in the coal-gas-and-nuclear-to-liquids (CGNTL) process shown in Fig. 1b. Note that the same four design configurations described for CGTL (cases 1–4) are also considered for CGNTL.

In this study, the CGTL and CGNTL cases considered are further subdivided depending on whether or not carbon capture and sequestration (CCS) is employed, resulting in a total of 16 novel process configurations previously unexplored in the open literature, to the best of our knowledge. Each case is simulated in a chemical process flowsheet simulator to compute the steady-state mass and energy balances, stream conditions, efficiencies, and atmospheric emissions for each. The results are used to inform a profitability analysis under uncertain market conditions to determine the conditions in which one design configuration is more profitable than the rest.

2. Methodology

The simulation of each case was carried out using Aspen Plus 2006.5 to compute the mass and energy balances for each of the 16 process configurations. Steady-state flowsheet simulation models were developed based on previously published models of coal-and-natural-gas-to-liquids-and-electricity processes by Adams and Barton [18,19,43,44] and details of the model components used are described in those works. The properties of the coal (Illinois #6) and natural gas used are shown in Table 1 and were selected to be consistent with our prior work as well as commonly cited baseline studies [10]. Most equation of state calculations use the Peng–Robison with Boston–Mathias model, except for water-only streams in which NBS/NRC steam tables were used.

A GE-type entrained-flow gasifier is used to generate syngas at high temperature and pressure by employing a pulverized coal slurry as feed and almost pure oxygen from an air separation unit (ASU) for partial oxidization. The gasification step is modeled with the Gibbs Reactor block in Aspen Plus (which assumes chemical and phase equilibrium) with certain design parameters selected such that the output matches that of an existing GE gasifier. The hot syngas produced in the gasifier is cooled with a radiant syngas cooler followed by a quench cooler. After cooling, the coal-derived synthesis gas is cleaned of HCl and NH_3 in a scrubber, producing H_2-lean syngas (stream 3 in Fig. 1). Details of the models for the gasifier, ASU, and scrubber portions (which constitute the Coal Gasification box in Fig. 1) are described in [43].

Table 1
Properties of Illinois Bituminous coal and natural gas used in this study [10].

Coal: proximate analysis (weight%)					
Moisture	Ash	Volatile matter	Fixed carbon	HHV, Btu/lb	
11.12	9.7	34.99	44.19	13,126	
Coal: ultimate analysis (dry, weight%)					
Carbon	Hydrogen	Nitrogen	Chlorine	Sulfur	Oxygen
71.72	5.06	1.41	0.33	2.82	7.75
Natural gas composition (% molar)					
Methane	Ethane	Propane	n-Butane	CO_2	N_2
93.9	3.2	0.7	0.4	1	0.8

Then, sulfur is removed from the coal-derived syngas by first hydrolyzing the COS contained in the syngas into H_2S using a COS hydrolysis reactor. The H_2S is then removed using the solvent Selexol in an absorption-based process. Models for these steps (which constitute the H_2S Removal box in Fig. 1) are described in [18].

Natural gas is converted to H_2-rich syngas (H_2/CO ratio above 3) by reacting with steam in two stages: a pre-reformer, in which ethane, butane, and propane are reformed into H_2 and CO, and the main reformer, in which the bulk of the methane is converted to H_2 and CO. Depending on the configuration used in this project, natural gas or other hydrocarbon fuels may be burned in a furnace which encompasses the reforming chamber and provides the heat required for the endothermic reforming reaction. Alternatively, a high-purity oxygen feed from the ASU may be used to oxidize the natural gas inside of the natural gas reforming chamber as opposed to or in addition to the furnace. The purpose of this is to keep any CO_2 generated from natural gas oxidation in the syngas stream so that it can be readily captured downstream. The reformed natural gas is cooled and any remaining water is condensed out. Together, these steps constitute the Pre-reformer, Reformer, and associated Burner blocks in Fig. 1. The reformers are modeled using equilibrium models considering reactions with various hydrocarbons and the water–gas-shift reaction, with modeling details described in [44].

For the CGNTL processes, heat delivery from the helium is modeled by introducing a heat stream into the natural gas reformer of the appropriate magnitude and ensuring that temperature crossover does not occur. It is assumed that the helium stream from the MHR reactor is delivered to the reformer at 1200 °C and exits the reactor at 950 °C, which is high enough for use in a Brayton cycle [45]. It is also assumed that 2.9% of the heat delivered to the reformer is lost to the environment, which is an appropriate estimate based onto other high temperature heat transfer unit operations [46]. In the economic analysis, this high-temperature helium stream is treated as a utility with cost estimates described in Section 2.1.

The H_2-lean coal-derived syngas (after sulfur removal) and the H_2-rich natural-gas-derived syngas are mixed to create a syngas mixture with a H_2/CO molar ratio of about 2, which is ideal for downstream FT synthesis. To achieve this, the flow rate of natural gas and coal are adjusted for each case such that the correct ratio is achieved. Then, the absorption-based Selexol process is used to remove CO_2 from the blended syngas stream, leaving essentially only H_2 and CO remaining in the syngas. The captured CO_2 is optionally compressed and sent to off-site sequestration. These steps constitute the CO_2 removal and CO_2 compression blocks in Fig. 1. Details of the models for the Selexol section and the CO_2 compression section can be found in [18] and [43] respectively.

The blended synthesis gas then enters the FT reactor and passes through the cobalt catalyst solid particles and FT liquid products. The hydrogenation reaction of CO into paraffinic hydrocarbons with various carbon numbers (1–60) is [47]:

$$n(2H_2 + CO) \rightarrow -(CH_2)_n- + nH_2O$$

The FT product mixture is sent to a flash drum in order to recover unreacted syngas and light hydrocarbons as vapors (the Vapor Recovery box in Fig. 1). The vapor product is then recycled to various places in the process depending on which design option is being considered. The liquid product is then sent to the separation column for product upgrading to get liquid hydrocarbon blends which constitute the primary diesel (or rather its precursor called "distillate") and gasoline (or rather, "naphtha") products. The ratio of gasoline to diesel produced is determined by the specific hydrocarbon blend produced by the FT reaction and subsequent separation. This results in a fixed ratio of about 1:3 (gasoline:diesel) by volume. The FT synthesis reaction is modeled using Anderson-Schulz-Flory hydrocarbon distribution theory and the product separation and most of the auxiliary separations are modeled using either PetroFrac or RadFrac models within Aspen Plus. Details of these models can be found in [18].

The Heat Recovery and Steam Generation (HRSG) section is designed to contribute to the heat and steam requirements of all remaining sections of the process using the waste heat available in the plant. The rate and quality of each type of steam is selected appropriately to cover all of the heat sinks in the process and produce electricity via steam turbines using any surplus waste heat. This was modeled in Aspen Plus using the available heat exchanger, pump, and compressor models. The operating conditions of each section are based on optimized values calculated by Adams and Barton [18] and selected design parameters are summarized in Table 2. Each of the design cases considered is scaled to produce 3300 barrels per day of gasoline equivalent.

2.1. Cost estimation for high temperature helium utility

An integrated gas turbine modular helium reactor (GT-MHR) process uses a MHR with helium as the coolant and Brayton cycle fluid, as shown in Fig. 2. In this example, high pressure helium at 7.07 MPa and 750 °C enters the MHR and is heated to 1200 °C [48]. The hot helium then powers a gas turbine to produce electric-

Table 2
Main design parameters.

Unit	Parameters
ASU	Oxygen purity (molar): 99.5% Delivery condition: T = 32 °C, P = 10 bar
Gasifier	P = 55 bar, T = 1370 °C Oxygen/coal ratio (kg/kg): 0.787
Scrubber	Delivery condition: T = 203 °C
Auto-thermal reforming section	Outlet H_2/CO ratio >3 Coal COS hydrolysis: adiabatic reaction; catalyst bed with 98% conversion $COS + H_2O \rightarrow H_2S + CO_2$ Pre-reformer and reformer: adiabatic, equilibrium reactions; T = 480 °C (pre-reformer) and 980 °C (reformer)
Acid Gas Removal (AGR)	Coal COS hydrolysis: adiabatic reaction; catalyst bed with 98% conversion $COS + H_2O \rightarrow H_2S + CO_2$ Selexol H_2S/CO_2 removal
Claus process	Three-stage oxygen blown reactors; Tail gas to acid gas recovery unit
CO_2 compression	LP/HP compression stages, delivery conditions: T = 44 °C, P = 153 bar Triethyleneglycol used for water removal
FT section	Products ASTM specification (95% vol.): gasoline = 170 °C, diesel = 340 °C

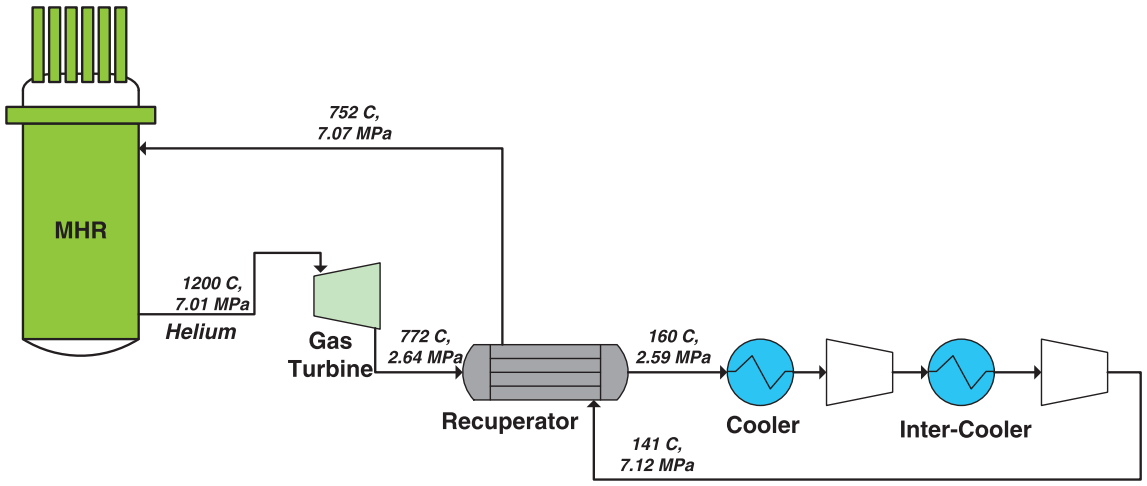

Fig. 2. Process flow diagram of a GT-MHR process.

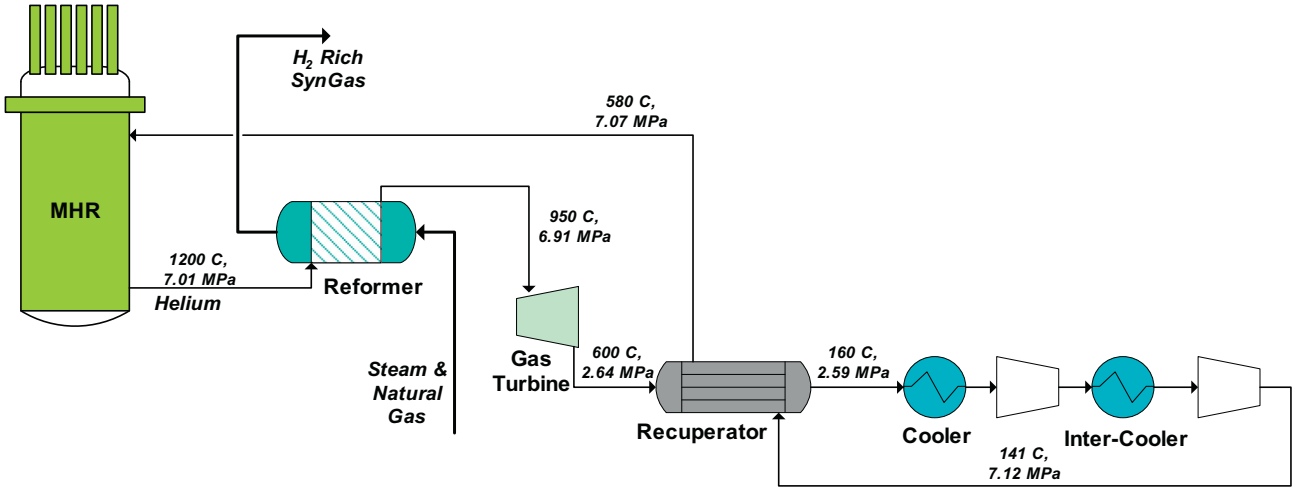

Fig. 3. Process flow diagram of a GT-MHR process combined with natural gas reformer.

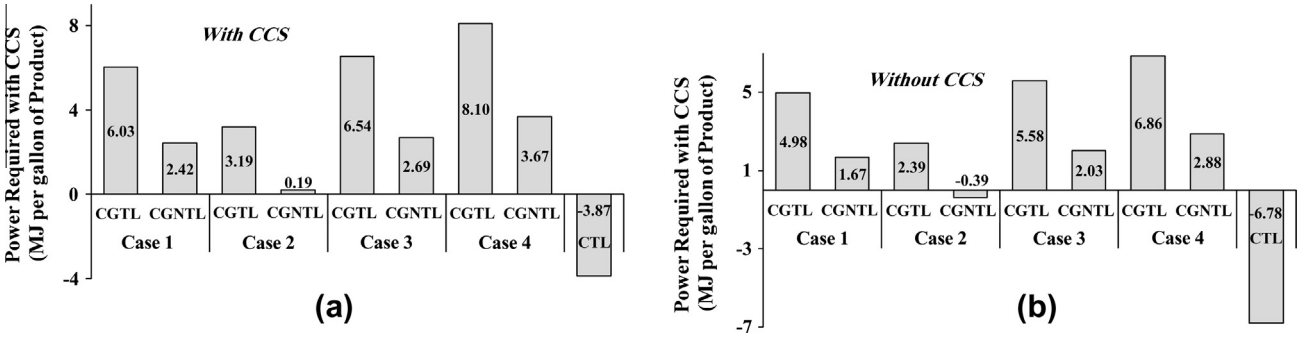

Fig. 4. Net power required for different cases – (a) with CCS; and (b) without CCS.

ity, exiting at a lower pressure and temperature (about 2.6 MPa and about 770 °C). The spent helium is then cooled, recompressed, and preheated before returning to the MHR and completing the cycle.

For our analysis, we propose an altering of the GT-MHR process as shown in Fig. 3, in which the high temperature helium leaving the MHR is used to power the natural gas reformer through direct heat exchange. For example, the natural gas and steam to be reformed could be inside of the tubes of the reformer, and the helium could enter the shell side, countercurrent to the natural gas flow direction. The helium would then exit the reformer at 950 °C and then continue into the gas turbine as in the original GT-MHR process. This would result in lower electricity production since some of the energy in the helium has been transferred to the natural gas to make hydrogen. For this analysis, we chose a helium exit temperature of 950 °C because it is low enough to keep the

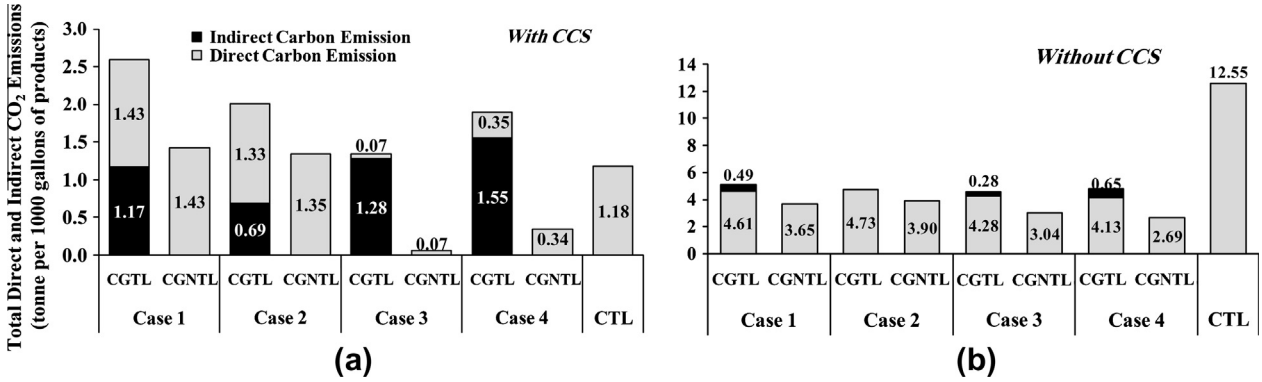

Fig. 5. CO_2 emissions (direct and indirect) for different cases for (a) CCS-enabled; and (b) CCS-disabled scenarios.

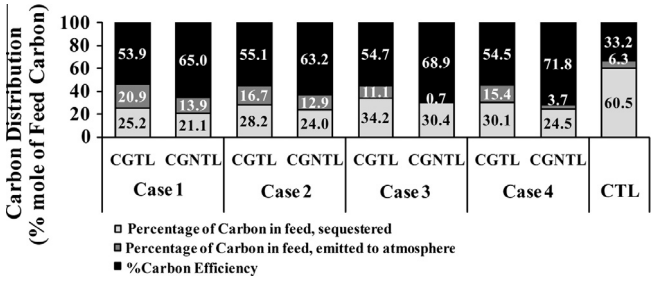

Fig. 6. How carbon in the feedstock is distributed among the products for various design options. All options use CCS where possible. Non-CCS cases have very similar carbon efficiencies and thus are not shown.

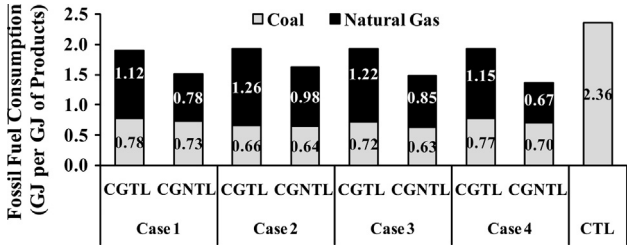

Fig. 7. Direct fossil fuel consumption for different cases with CCS. Non-CCS cases have very similar values and thus are not shown.

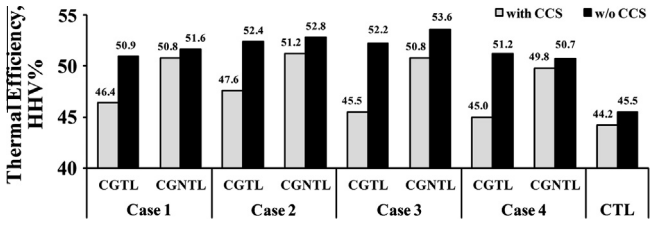

Fig. 8. Thermal efficiency of all cases.

required helium flow rate low but high enough to still produce a sufficient amount of power in the gas turbine. The determination of the optimal temperature and other GT-MHR design parameters is a subject of future work.

In order to estimate the utility price of high temperature helium used in this techno-economic analysis, the GT-MHR (Fig. 2) and modified GT-MHR (Fig. 3) processes were modeled in Aspen Plus 2006.5. The reformer, recuperator, and coolers are modeled as heat exchangers. The MHR is not modeled; by assuming the GT-MHR process has a thermal efficiency of 48%, a typical value for GT-MHR [45,49], the total nuclear energy requirement per megawatt of power produced can be computed. Then, by comparing the results of the GT-MHR and modified GT-MHR simulations, the amount of power that is lost by adding the reformer step can be determined. For an electricity price of 9.7 ¢/kW h (see Section 3.4), this results in a reduction in revenue for the owners of the GT-MHR facility due to reduced power production of 2.79 ¢ per kW h of high-temperature heat actually delivered to the reformer. Then, a 5% premium markup is assumed, giving the final estimate of the price of high-temperature helium utility of 2.93 ¢ per kW h of high-temperature heat actually delivered to the reformer.

3. Results and discussion

A summary of the detailed results of the Aspen Plus simulation is given in the Supplementary Material available on the journal's website. These include detailed process flowsheets, tables of stream conditions, and other pertinent data used for this analysis.

3.1. Required power

Using the simulation results, the external power requirement has been computed for each case. The power requirement is the total parasitic load of all pumps and compressors in the plant minus the supplementary power produced in the HRSG. As shown in Fig. 4a, case 2 has the lowest required power when CCS is enabled. This is because much of the FT off-gas is combusted to provide heat for reforming reactions, which also increases the amount of waste-heat available in the plant for power production in the HRSG. If this off-gas is instead reformed to generate syngas and displace natural gas (cases 3 and 4) the required power will be increased since less waste-heat is produced. However, when nuclear heat is used, the

Table 3
Base-case market prices for electricity, fuels and products.

Electricity	9.70[a]	¢/kW h [51]
Sulfur	$100	per tonne [18]
Water	$0.27	per million L [18]
Process steam (60.3 bar)	$19	per tonne [55,56]
Coal	$49.70	per ton [52]
Natural gas	$4.00	per MMBTU [53]
Gasoline	$3.40	per gallon [54]
Naphtha (gasoline precursor)	$3.06	per gallon [18,54]
Diesel	$3.84	per gallon [54]
Distillate (diesel precursor)	$3.45	per gallon [18,54]
High-temperature helium	2.93	¢/kW h (see Section 2.1)
Carbon emissions tax	$0	per tonne CO_2

[a] Same price for CGTL and CGNTL.

external power requirement drops dramatically (for example, from 3.19 MJ per gallon of gasoline equivalent produced to 0.19 MJ/gallon for case 2). This is because the use of nuclear heat reduces the amount of natural gas that needs to be burned (see Section 3.3), and thus reduces the parasitic load associated with natural gas compression, air compression, or O_2 production/compression needed for burning.

The power requirement for non-CCS designs is shown in Fig. 4b. For each case, the total external power load is roughly 18% lower than the comparable case with CCS enabled since compression costs for CO_2 are avoided (the captured CO_2 is simply vented to the atmosphere instead). If nuclear heat is used, then power consumption drops as it did in the with-CCS case. Note that in case 2 the effect is enough to actually result in a negative power consumption, meaning that there is sufficient waste heat in the process to generate enough electricity in the HRSG to meet all of the parasitic load requirements in the plant with some leftover for sale to the grid. In general, for all cases considered, using nuclear heat reduces the external power requirement anywhere from 55% to 116%.

For comparison, a traditional CTL process is also shown in Fig. 4. CTL produces a considerable amount of extra power because a considerable amount of waste heat is produced. For this study, the goal is to maximize liquid fuel production and thus although this extra electricity can be sold for revenue, it is not as desirable in this case since we would rather have more liquid fuels produced instead. The details of the CTL process are presented in [18]. It should be noted that some minor deviations from the original CTL process have been made for comparison purposes; specifically, methanol was produced in parallel to FT liquids in [18] but only FT liquids

Table 4
Cost analysis of each case.

Design type	CTL	CTL	CGTL Case-1	CGNTL Case-1	CGTL Case-1	CGNTL Case-1	CGTL Case-2	CGNTL Case-2	CGTL Case-2	CGNTL Case-2
Nuclear Heat Used?	No	No	No	Yes	No	Yes	No	Yes	No	Yes
CCS Enabled?	Yes	No	Yes	Yes	No	No	Yes	Yes	No	No
Capital costs by section ($1000s)										
Solids handling	161,150	161,150	68,337	75,058	68,337	75,058	63,623	68,516	63,640	68,516
Water systems	59,748	59,748	74,427	74,689	73,897	74,319	86,137	85,559	82,139	83,939
Gasifier section	286,721	286,721	121,588	133,545	121,588	133,545	113,200	121,906	113,230	121,906
Air separation unit	234,884	234,884	150,901	94,232	85,222	94,232	165,768	119,646	110,546	119,646
Gas cleaning (incud. Selexol)	163,594	163,594	73,801	73,138	73,801	73,138	69,616	68,355	69,635	68,355
CO_2 compression	28,497	0	9,746	6,911	0	0	10,326	8,081	0	0
Natural gas reforming	0	0	11,817	9,412	11,817	9,412	12,714	10,776	12,718	10,776
COS removal	13,933	13,933	5913	6451	5913	6451	12,255	13,125	12,258	13,125
Power generation	117,778	117,778	38,167	41,524	41,258	44,829	53,319	55,546	55,801	58,320
Fischer–Tropsch synthesis	277,073	277,073	284,979	284,373	284,979	284,373	295,139	295,692	295,221	295,692
Plant accessories	83,568	89,727	80,868	67,126	71,957	65,050	76,219	62,240	66,270	63,922
Solvents & catalysts	2231	2230	399	399	399	399	87	77	87	77
Cost breakdown at 85% capacity ($1000s)										
Total capital cost	1,415,245	1,392,904	915,032	860,405	833,256	854,354	946,148	896,396	869,287	891,149
Total operating cost (per yr)	70,239	46,830	32,520	66,726	25,897	62,306	33,593	62,518	26,515	57,205
Helium utility cost (per yr)	0	0	0	39,492	0	39,492	0	33,326	0	33,326
Total fuel costs (per yr)	89,233	89,233	114,786	91,230	114,786	91,230	122,368	103,110	122,414	103,110
Gasoline sales (per yr)	135,047	135,047	135,036	135,051	135,036	135,051	135,054	135,107	135,105	135,107
Diesel sales (per yr)	348,688	348,688	352,839	352,736	352,839	352,736	350,779	352,022	350,911	352,022
Gross earnings (per yr)	318,266	357,809	274,876	285,494	303,770	294,041	279,952	289,272	313,592	306,006
Net present value	610,531	785,278	667,266	736,230	827,140	774,983	674,640	735,930	851,632	807,897

Design type	CGTL Case-3	CGNTL Case-3	CGTL Case-3	CGNTL Case-3	CGTL Case-4	CGNTL Case-4	CGTL Case-4	CGNTL Case-4
Nuclear Heat Used?	No	Yes	No	Yes	No	Yes	No	Yes
CCS Enabled?	Yes	Yes	No	No	Yes	Yes	No	No
Capital costs by section ($1000s)								
Solids handling	64,795	69,910	64,795	69,910	64,828	73,185	64,828	73,185
Water systems	81,752	79,060	76,121	76,913	69,158	67,250	64,346	66,734
Gasifier section	115,284	124,386	115,284	124,386	115,344	130,213	115,344	130,213
Air separation unit	190,574	129,402	119,285	129,402	169,384	91,717	80,543	91,717
Gas cleaning (incud. Selexol)	75,249	72,202	75,249	72,202	74,676	72,630	74,676	72,630
CO_2 compression	12,622	9,293	0	0	11,039	7,292	0	0
Natural gas reforming	12,769	10,023	12,769	10,023	11,931	8,551	11,931	8,551
COS removal	5,628	6,039	5,628	6,039	5,631	6,302	5,631	6,302
Power generation	45,793	47,778	48,165	50,582	31,682	34,489	34,126	37,660
Fischer–Tropsch synthesis	363,433	350,683	363,433	350,683	294,014	291,562	294,014	291,562
Plant accessories	84,599	68,844	70,492	61,120	94,032	84,657	83,524	82,783
Solvents & catalysts	106	92	105	91	319	221	319	221
Cost breakdown at 85% capacity ($1000s)								
Total capital cost	1,046,976	961,675	945,698	945,314	936,406	861,767	823,650	855,257
Total operating cost (per yr)	35,853	74,259	26,876	67,996	39,672	99,375	32,004	94,667
Helium utility cost (per yr)	0	45,248	0	45,248	0	62,296	0	62,296
Total fuel costs (per yr)	123,610	95,303	123,610	95,303	114,167	80,349	114,167	80,349
Gasoline sales (per yr)	135,069	135,032	135,069	135,032	135,059	135,061	135,059	135,061
Diesel sales (per yr)	376,817	372,385	376,817	372,385	357,373	356,131	357,373	356,131
Gross earnings (per yr)	280,853	290,592	324,050	310,881	260,013	259,783	297,247	268,870
Net present value	627,649	707,659	856,786	800,583	594,147	626,520	803,639	667,754

are produced in the present study, and some syngas was used for combustion in [18] whereas all syngas is used for FT liquid production in the present study.

3.2. CO_2 emissions

The CO_2 emissions for the with-CCS and without-CCS cases are shown in Fig. 5a and b respectively. The reported CO_2 emissions include both the direct CO_2 emissions from the process as well as the indirect CO_2 emissions resulting from the production of external electricity which has to be purchased (see Section 3.1). For the CGNTL scenarios, it is assumed that the external power demand is supplied by nuclear power generation since there is already a nuclear facility available, and thus has no CO_2 emissions associated with power generation. For the CGTL scenarios, it is assumed that power is purchased from the grid which is mostly derived from fossil fuels and thus has an average CO_2 emissions of 1.341 lb CO_2 per kW h (609 g per kW h) [50]. From Fig. 5, can be seen that total CO_2 emissions for case 3 is the lowest, since the waste FT light-gases are no longer burned, and thus most (98–99%) of the CO_2 directly generated by the process can be captured and sequestered. Thus, when CCS is used, all of the CO_2 emissions are a result

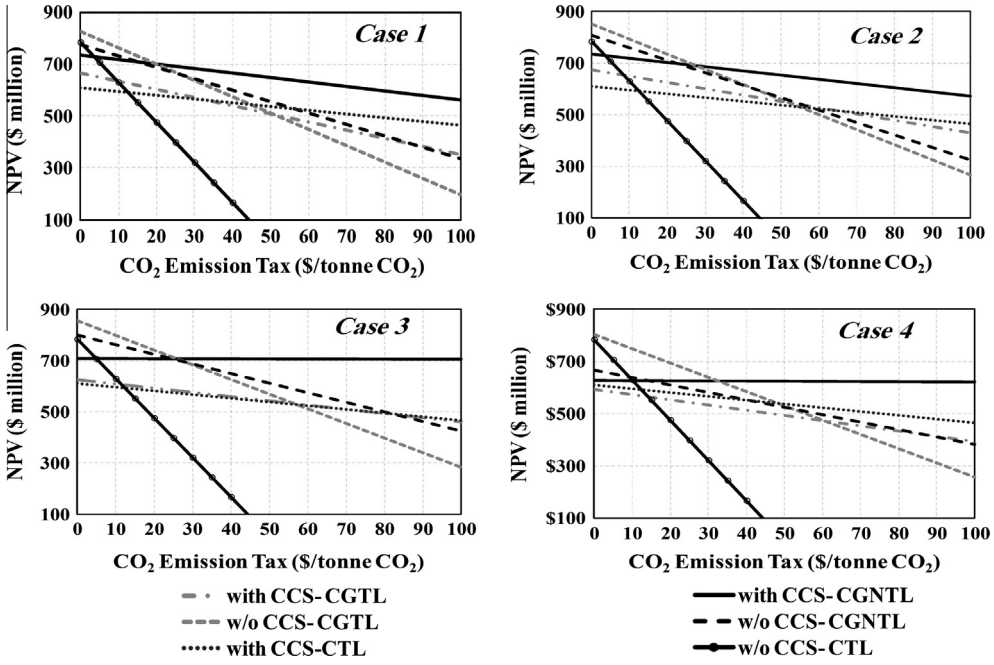

Fig. 9. Effect of CO_2 emission tax on NPV for all cases.

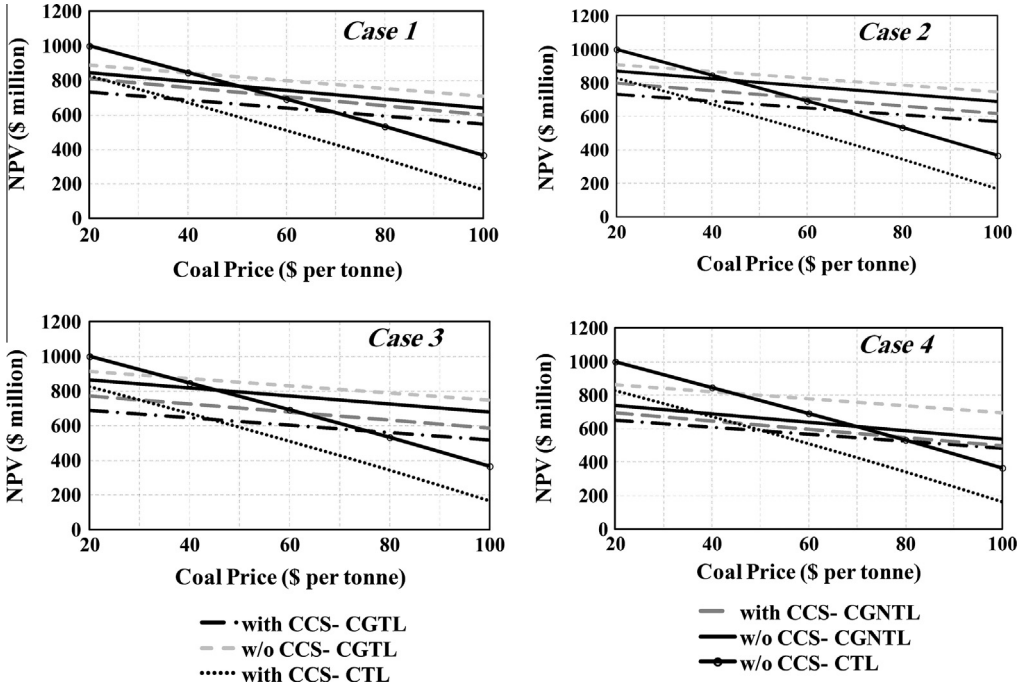

Fig. 10. Effect of coal price on NPV for all cases.

of indirect emissions arising from externally purchased power. Thus, for the CGNTL with-CCS case 3, the total direct and indirect CO_2 emissions for the process is nearly zero (about a 99.5% reduction compared to CTL). The small amount of emissions for case 3 that does exist results from minor releases in the relatively small FT purge stream. Overall, using nuclear heat reduces CO_2 emissions by about 64% on average for with-CCS cases and by about 31% for without-CCS cases. As shown in Fig. 5, the CO_2 emissions of CTL is comparable with other scenarios when CCS is used. However, without CCS a traditional CTL process has at least 2.52 times greater CO_2 emissions than the CGTL and CGNTL processes studied in this work. In fact, the CGNTL case 4 design produces 79% less CO_2 emissions per gallon of gasoline produced than CTL even when CCS techniques are not used.

3.3. Carbon and thermal efficiency

The carbon efficiency is the percentage of carbon atoms in the feed (including the fossil fuels used to produce external power) which end up in the liquid products as opposed to CO_2 wastes or other greenhouse gases. This is another important parameter which represents the amount of CO_2 generated per gallon of desired products. As can be seen in Fig. 6, the case with the highest carbon efficiency is CGNTL case 4 (having 71.8% carbon efficiency), meaning that this strategy generates the least amount of CO_2 for every gallon of gasoline produced. In other words, this option will have the lowest CO_2 emissions when CCS is not used, and requires relatively few resources to sequester CO_2 if CCS is used. For comparison, traditional CTL has a low carbon efficiency of around 33%. This is because of the CO_2 emissions generated from burning coal for heat or producing H_2 for syngas upgrading using the water–gas-shift reaction. Overall, the use of nuclear heat increases the carbon efficiency by 8–17 percentage points compared to non-nuclear CGTL options and up to 39 percentage points compared to CTL.

The relative direct fossil fuel consumption (which does not include any fossil fuels consumed for external power generation) is shown in Fig. 7. CGNTL case 4 has the lowest rates of fossil fuel consumption, with about 1.37 GJ of fossil fuels consumed for each GJ of gasoline and diesel produced. In case 4, the majority of the waste FT light gases are recycled for synthesis gas generation, thus reducing the natural gas requirement and lowering the total fossil fuel consumption. Overall, the use of nuclear heat helps reduce direct fossil fuel consumption by 15–29%, or an average of 22% for the four cases since it displaces natural gas combustion. In fact, nuclear heat is a significant contributor to the process; for CGNTL case 4 with CCS, it can be said that 20% of the energy in the gasoline originated from the nuclear source. Compared to CTL, an 18% to 42% reduction in fossil fuel consumption can be achieved by using CGTL or CGNTL.

In addition, the plant thermal efficiency of each case, shown in Fig. 8 is defined as follows:

$$\eta_{therm} = \frac{\text{HHV of fuels produced} + \text{surplus electricity produced}}{\text{HHV of fuel consumed} + \text{nuclear energy consumed} + \text{HHV of fuel consumed for input power}}$$

It can be seen that the maximum efficiency is around 53.6% which is for CGNTL case 3-without CCS. This case has higher efficiencies due to better use of waste gases. The addition of nuclear heat generally increases the efficiency 0.5–5 percentage points (except for case 4-without CCS), and the addition of CCS decreases the efficiency by 1–7 percentage points. In general, compared to CTL, the CGTL or CGNTL cases have higher thermal efficiencies by 2–7 percentage points for cases with CCS and 5–8 percentage points for cases without CCS.

3.4. Cost analysis

An economic analysis was performed for each of the 16 design cases using the simulation results in order determine the profitability of each process. Capital costs were estimated using either published costs from other works or using Aspen Icarus 2006.5 where data were available. This cost data and other economic parameters are consistent with our prior work and details can be found in [18,51–56], except that costs have been updated to May 2011 US dollars by scaling with the Chemical Engineering Plant Cost Index [55]. The plant boundaries (and therefore the scope of the capital cost considerations) includes all process units shown in Fig. 1. Water, steam, electricity and high-temperature helium are treated as utilities: therefore the capital costs of producing these utilities are not within the scope of the profitability study. Note that external steam is only purchased in the CTL case because

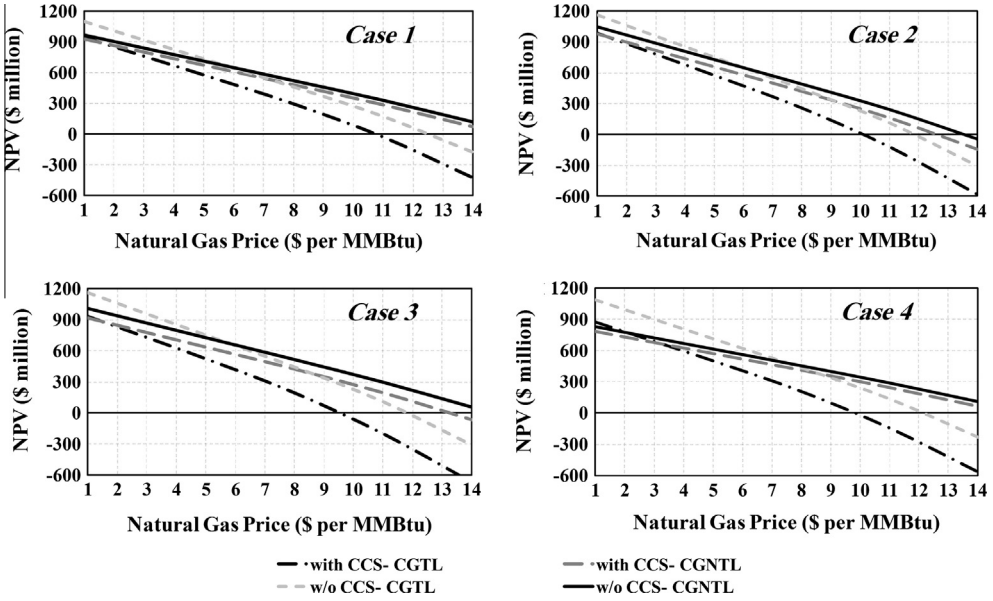

Fig. 11. Effect of Natural gas price on NPV (a) Case 1; (b) Case 2; (c) Case 3; and (d) Case 4.

the steam production in the HRSG from waste heat is insufficient for the CTL plant needs.

Key market parameters in this study, such as the product sale prices and purchase price of electricity are presented in Table 3. Other key financial parameters such as the debt-to-equity ratio, loan interest rates, and inflation rates can be found in the Supplementary Material on the journal's website, along with a detailed year-by-year breakdown of the cash-flow analysis which is used to determine the net present value (NPV) of each of the 16 designs.

A summary of the profitability analysis for each of the 16 cases using the base-case market prices is shown in Table 4, as well as a coal-to-liquids plant [18] for comparison. All design cases have been scaled to produce 3300 barrels/day of gasoline equivalent. Compared to CGTL, CGNTL has lower total capital cost by around 5–8% for with-CCS cases but higher capital costs by 0–4% for without-CCS cases. In addition, CGNTL has higher operating costs than CGTL by 85–195% for with-CCS cases; however, for the base case market prices, the net present value (NPV) of CGNTL is higher by around 5–13% for with-CCS cases but lower by 5–17% for without-CCS. To summarize, for all CCS enabled cases, using nuclear heat increases the NPV of plant for these base-case market conditions (Table 3). In addition, all 8 of the proposed CGTL and CGNTL processes with CCS had a higher NPV than the CTL cases. However, the values of the base-case market conditions can

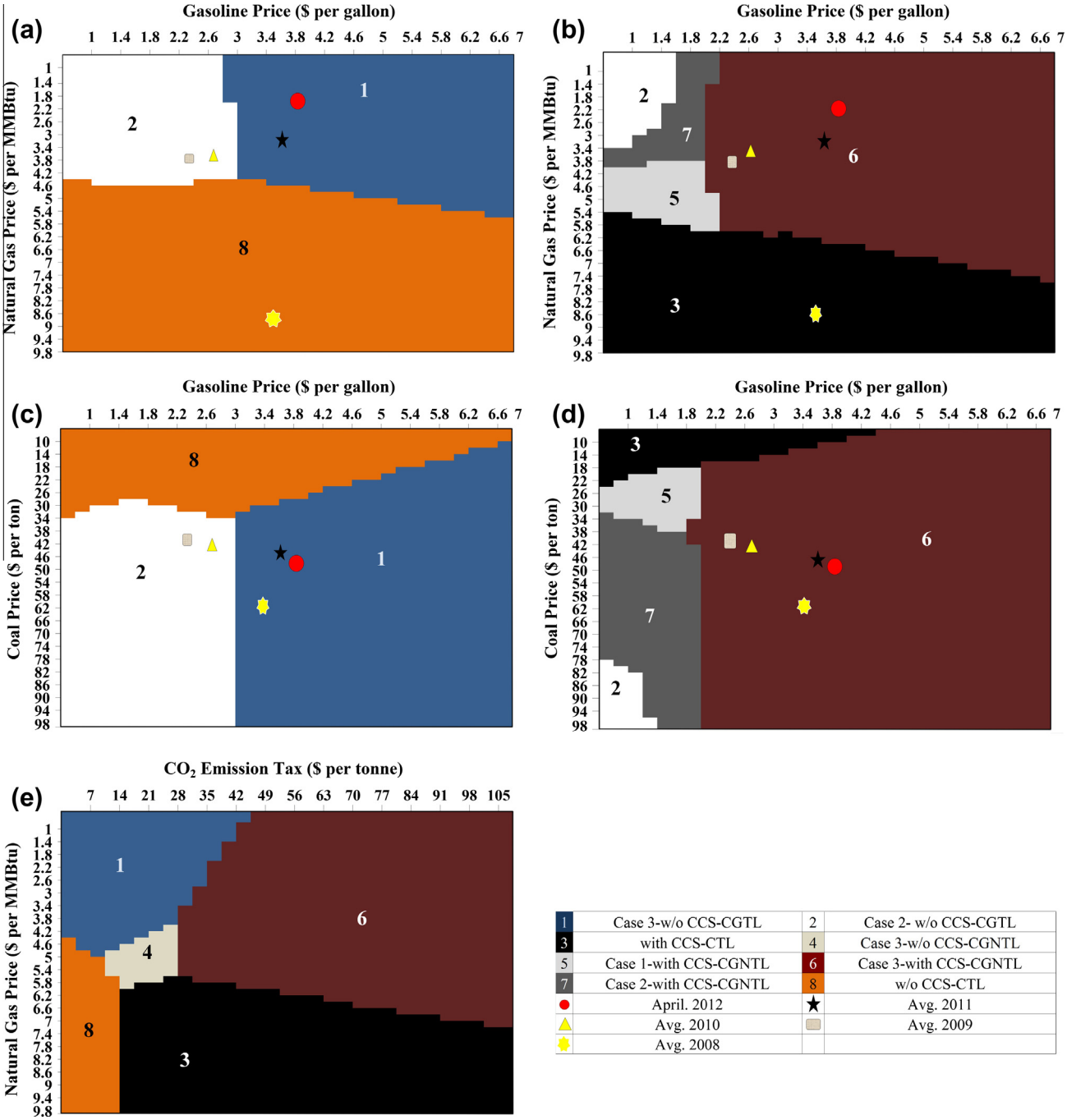

Fig. 12. The most profitable design, considering deviations of prices from the base case for: (a) Natural gas/Gasoline prices-zero CO_2 tax; (b) Natural gas/Gasoline prices-$50 CO_2 tax; (c) Coal/Gasoline prices-zero CO_2 tax; (d) Coal/Gasoline prices-$50 CO_2 tax; (e) Natural gas price/CO_2 tax.

significantly affect the profitability, and is discussed in the next section.

3.5. Sensitivity analysis

Profitability is significantly influenced by market prices, which can fluctuate widely. Therefore, a sensitivity analysis was carried out to determine how the net present value deviates from the base-case results when market conditions change. For example, the effects of imposing a CO_2 emissions tax on the NPV for the 16 cases are shown in Fig. 9, as well as the base-case CTL plant (with and without CCS) for comparison. Note that for the results of Fig. 9, all of the economic parameters are at their base case values (Table 3) except for the CO_2 tax, which is varied. It can be seen that for CO_2 taxes higher than \$20–30 per tonne of CO_2 emitted, the most profitable design for each of the four cases uses nuclear heat with CCS. Below that range, it is generally more profitable to use a design without CCS. In addition, case 3 has the highest NPV for all tax values for any variant (with or without nuclear heat, with or without CCS). Furthermore, the coal only design (CTL) is generally among the least profitable, with NPV as much as \$100–200 million lower than the most profitable option for each design case at any tax rate.

A similar sensitivity analysis is repeated for variations in the coal (Fig. 10) and natural gas (Fig. 11) prices, where all other prices are kepts at their base case values (Table 3). As shown in Fig. 10, increases in the coal price have approximately the same relative impact for all 16 design cases since they all use coal in approximately the same proportions, and so changes in the coal price do not change which plant design is the most profitable. However, the profitability of CTL drops considerably faster as coal prices rise since the process uses much more coal per gallon of product.

Changes to the price of natural gas (Fig. 11) have different effects on the different processes because they use different amounts of natural gas per gallon of product. In particular, for natural gas prices higher than \$4–7 per MMBtu the cases which use nuclear heat are the most profitable since the natural gas requirement is lowest in those cases.

A third sensitivity analysis considers the impact of changes to multiple economic parameters such as coal and natural gas prices, CO_2 tax, and the price of gasoline. The results for four sets of parameters are shown in Fig. 12, which are presented as a "map" of the best of the 17 design options (the 16 novel options plus CTL) for each combination of parameters. For example, Fig. 12a shows the map for changes in the natural gas price and the sale price of gasoline, with all other economic parameters set at their base case values (Table 3)—note also that it is assumed that the price of diesel also changes with the price of gasoline such that the gasoline price is always 13% higher than the diesel price. From Fig. 12a it can be seen that, for example, CGTL case 2 without CCS is the most profitable for low gasoline (roughly below \$3/gallon) and natural gas (roughly below \$4/MMBtu), while CTL is the most profitable only for very high natural gas prices (roughly above \$5/MMBtu). However, three design configurations (CTL, CGTL Case 2, and CGTL Case 3, all without CCS) are the most profitable at some point in the price range considered, and all of them occur at prices ranges which are quite feasible for the future considering price histories.

However, once a \$50/tonne CO_2 tax is applied (Fig. 12b), the map becomes very different. For gasoline price above \$1.8 per gallon and for natural gas prices below about \$5.8/MMBtu, the optimal design will incorporate both nuclear heat and CCS. Two design cases can be the most profitable, but CGNTL case 3 with CCS tends to dominate. This is also true as the CO_2 tax is varied (Fig. 12e), in which this configuration is the often most profitable for CO_2 taxes above \$25/tonne. In addition, Fig. 12c shows that CGTL cases 2 and 3 without CCS are the most profitable for no CO_2 tax and natural gas price at its base case. But increasing the CO_2 tax to \$50/tonne (Fig. 12d) changes the best choice to CGNTL with CCS for most points.

4. Conclusion

In this paper, simulations were performed on rigorous models of 16 different potential chemical plants which convert coal, natural gas, and possibly nuclear energy into diesel and gasoline. The use of carbon capture and sequestration technology was considered as an additional option. Taken together, the results illustrate the uncertainty in choosing the optimum process design. For example, the prices used in this analysis are effectively lifetime average prices, which cannot be predicted exactly over the lifetime of the plant (three decades). Thus, there is a large uncertainty in how economical any given plant will be once it is built due to unexpected fluctuations in price. Therefore, the consideration of the optimal design under uncertainty is a subject of future work, in which future prices are described by probability distribution functions, and the optimum decision is that which is most likely to yield the most profit. In addition, the ability to operate the plant flexibly is another topic of future work, in which the amount of coal, natural gas, or even nuclear heat may be increased or decreased during normal operation to respond to changes in market prices. For example, if the natural gas becomes seasonally high, perhaps the plant operating state could switch such that more coal could be used instead.

The primary conclusions are summarized as follows:

- The use of nuclear heat via high-temperature heat transfer can significantly decrease the amount of power which must be supplied to the process from an external source, and in some cases, actually result in a surplus of power generated from waste heat.
- Compared to a traditional coal-to-liquids plant, the total direct and indirect CO_2 emissions per gallon of gasoline or diesel produced can be reduced by up to 79% when natural gas and nuclear heat are integrated into the system using the case 4 design strategy, even when CCS technology is not used. This is a very effective way of significantly reducing CO_2 emissions without requiring CCS infrastructure.
- When CCS technology is added, it is possible to achieve nearly 100% CO_2 capture and nearly zero CO_2 emissions for some of the proposed configurations, with nuclear heat. The use of nuclear heat in these cases helps reduce the amount of CO_2 that must be sequestered by about 30% on average since less natural gas is consumed in those cases.
- Using nuclear heat can reduce the direct fossil fuel consumption by up to 22%. Furthermore, fossil fuel is used more efficiently, with an additional 8–17% of the carbon in the fuel recovered as useful gasoline or diesel products, instead of CO_2 wastes. With nuclear heat, a carbon efficiency of up to 72% is possible.
- The CGNTL design variant in which FT-off gases were partially recycled to the FT synthesis reactor and partially recycled upstream to the main natural gas reformer (case 3) with nuclear heat used to displace natural gas combustion in the reformer tended to be the most profitable design strategy in most cases for CO_2 tax above \$25/tonne CO_2. Generally, this is because it is better to convert the light purge gas to fuel than to burn it for heat and electricity.
- The use of CCS depended on the carbon tax: taxes of above about \$20–30/tonne were usually sufficient to incentivize carbon capture.

- CTL is only the most economical when the price of natural gas is more than \$5/MMBtu (the price in June 2012 is around \$2.5/MMBtu), indicating that a process using natural gas has significant advantages in the current era of low natural gas prices. Alternatively, at today's market prices, CTL is only the most economical when the coal price drops to about \$30/tonne. Otherwise, coal-and-gas solutions are preferred.
- Despite the uncertainties of cost, the results show that processes which use nuclear heat are generally more profitable than CTL or CGTL for moderate natural gas prices, and especially when carbon taxes are imposed.
- Although diesel and gasoline were the products of interest for this study, the CGTL and CGNTL concepts can be similarly applied to other types of products such as methanol and dimethyl ether by following an analogous process scheme.

Acknowledgement

We thank Dr. Harold Rosen for helpful discussions and support on this project.

Appendix A. Supplementary material

Supplementary data associated with this article can be found, in the online version, at http://dx.doi.org/10.1016/j.enconman.2013.07.023.

References

[1] Ansolabehere S, Beer J, Deutch J, Ellerman AD, Friedmann SJ, Herzog H, et al. The future of coal-options for a carbon-constrained world. Interdisciplinary MIT Study 2007.
[2] Semeniuk I. Cheap coal threat to global climate. New Scientist 2007;193:14.
[3] Fan L, Li F, Ramkumar S. Utilization of chemical looping strategy in coal gasification processes. Particuology 2008;6:131–42.
[4] Kunze C, Spliethoff H. Modelling, comparison and operation experiences of entrained flow gasifier. Energy Convers Manage 2011;52:2135–41.
[5] Liu G, Yan B, Chen G. Technical review on jet fuel production. Renew Sustain Energy Rev 2013;25:59–70.
[6] Mantripragada HC, Rubin ES. CO_2 reduction potential of coal-to-liquids (CTL) process: effect of gasification technology. Energy Procedia 2011;4:2700–7.
[7] Falcke TJ, Hoadley AFA, Brennan DJ, Sinclair SE. The sustainability of clean coal technology: IGCC with/without CCS. Process Saf Environ Prot 2011;89:41–52.
[8] Kaldis SP, Skodras G, Sakellaropoulos GP. Energy and capital cost analysis of CO_2 capture in coal IGCC processes via gas separation membranes. Fuel Process Technol 2004;85:337–46.
[9] Li LGS, Zhang X, Lin H, Jin H. Evaluation of cost reduction potential for a coal based polygeneration system with CO_2 capture. Energy 2012:1–6.
[10] Black J. Cost and performance baseline for fossil energy plants, bituminous coal and natural gas to electricity, vol. 1, DOE, National Energy Technology Laboratory (NETL), 2010.
[11] Serra LM, Lozano M-A, Ramos J, Ensinas AV, Nebra SA. Polygeneration and efficient use of natural resources. Energy 2009;34:575–86.
[12] Knoope MMJ, Meerman JC, Ramírez A, Faaij APC. Future technological and economic performance of IGCC and FT production facilities with and without CO_2 capture: combining component based learning curve and bottom-up analysis. Int J Greenhouse Gas Control 2013;16:287–310.
[13] Reyes Valle C, Villanueva Perales AL, Vidal-Barrero F, Gómez-Barea A. Techno-economic assessment of biomass-to-ethanol by indirect fluidized bed gasification: impact of reforming technologies and comparison with entrained flow gasification. Appl Energy 2013;109:254–66.
[14] Normann F, Thunman H, Johnsson F. Process analysis of an oxygen lean oxy-fuel power plant with co-production of synthesis gas. Energy Convers Manage 2009;50:279–86.
[15] Longwell JP, Rubin ES, Wilson J. Coal: energy for the future. Prog Energy Combust Sci 1995;21:269–360.
[16] Hu L, Hongguang J, Lin G, Wei H. Techno-economic evaluation of coal-based polygeneration systems of synthetic fuel and power with CO_2 recovery. Energy Convers Manage 2011;52:274–83.
[17] Yu GW, Xu YY, Hao X, Li YW, Liu GQ. Process analysis for polygeneration of Fischer–Tropsch liquids and power with CO_2 capture based on coal gasification. Fuel 2010;89:1070–6.
[18] Adams II TA, Barton PI. Combining coal gasification and natural gas reforming for efficient polygeneration. Fuel Process Technol 2011;92:639–55.
[19] Adams II TA, Barton PI. Combining coal gasification, natural gas reforming, and solid oxide fuel cells for efficient polygeneration with CO_2 capture and sequestration. Fuel Process Technol 2011;92:2105–15.
[20] Liu P, Pistikopoulosa EN, Li Z. A mixed-integer optimization approach for polygeneration energy systems design. Comput Chem Eng 2009;33:759–68.
[21] He F, Liu P, Li Z, Ni W. Integrating low steam demand CO shift process to coal based polygeneration energy systems: process design and analysis. Energy 2012:1–7.
[22] Zhang X, Gundersen T, Roussanaly S, Brunsvold AL, Zhang S. Carbon chain analysis on a coal IGCC — CCS system with flexible multi-products. Fuel Process Technol 2012.
[23] Liu G, Larson ED, Williams RH, Kreutz TG, Guo X. Making Fischer–Tropsch fuels and electricity from coal and biomass: performance and cost analysis. Energy Fuels 2011;25:415–37.
[24] Meerman JC, Knoope MMJ, Ramírez A, Turkenburg WC, Faaij APC. Technical and economic prospects of coal- and biomass-fired integrated gasification facilities equipped with CCS over time. Int J Greenhouse Gas Control 2013;16:311–23.
[25] Floudas CA, Elia JA, Baliban RC. Hybrid and single feedstock energy processes for liquid transportation fuels: a critical review. Comput Chem Eng 2012;41:24–51.
[26] Liszka M, Ziebik A. Economic optimization of the combined cycle integrated with multi-product gasification system. Energy Convers Manage 2009;50:309–18.
[27] Yi Q, Feng J, Li WY. Optimization and efficiency analysis of polygeneration system with coke-oven gas and coal gasified gas by Aspen Plus. Fuel 2012;96:131–40.
[28] Li H, Hong H, Jin H, Cai R. Analysis of a feasible polygeneration system for power and methanol production taking natural gas and biomass as materials. Appl Energy 2010;87:2846–53.
[29] Yi Q, Lu B, Feng J, Wu Y, Li W. Evaluation of newly designed polygeneration system with CO_2 recycle. Energy Fuels 2012;26:1459–69.
[30] Gangadharan P, Zanwar A, Zheng K, Gossage J, Lou HH. Sustainability assessment of polygeneration processes based on syngas derived from coal and natural gas. Comput Chem Eng 2012;39:105–17.
[31] Lin H, Jin H, Gao L, Han W. Economic analysis of coal-based polygeneration system for methanol and power production. Energy 2010;35:858–63.
[32] Marques JG. Evolution of nuclear fission reactors: third generation and beyond. Energy Convers Manage 2010;51:1774–80.
[33] Brown LC, Besenbruch GE, Schultz KR, Showalter SK, Marshall AC, Pickard PS, Funk JF. High efficiency generation of hydrogen fuels using thermochemical cycles and nuclear power, AIChE Spring Meeting, New Orleans, 2002.
[34] Yin H, Jiang S, Zhang Y, Ju H. Modeling of the helium-heated steam reformer for HTR-10. J Nucl Sci Technol 2007;44:977–84.
[35] Kugeler K, Kugeler M, Niessen HF, Hammelmann KH. Steam reformers heated by helium from high temperature reactors. Nucl Eng Des 1975;34:129–45.
[36] Yari M, Mahmoudi SMS. Utilization of waste heat from GT-MHR for power generation in organic Rankine cycles. Appl Therm Eng 2010;30:366–75.
[37] Zare V, Yari M, Mahmoudi SMS. Proposal and analysis of a new combined cogeneration system based on the GT-MHR cycle. Desalination 2012;286:417–28.
[38] Şahin HM, Erol Ö, Acır A. Utilization of thorium in a Gas Turbine-Modular Helium Reactor. Energy Convers Manage 2012;63:25–30.
[39] Şahin HM, Erol Ö. Utilization of thorium in a Gas Turbine-Modular Helium Reactor with alternative fuels. Energy Convers Manage 2012;53:224–9.
[40] Chaubey R, Sahu S, James OO, Maity S. A review on development of industrial processes and emerging techniques for production of hydrogen from renewable and sustainable sources. Renew Sustain Energy Rev 2013;23:443–62.
[41] Rosen MA. Advances in hydrogen production by thermochemical water decomposition: a review. Energy 2010;35:1068–76.
[42] Muñoz PSR. Dynamic simulation of nuclear hydrogen production systems, PhD Thesis, Massachusetts Institute of Technology, 2011.
[43] Adams II TA, Barton PI. High-efficiency power production from coal with carbon capture. AIChE J 2010;56:3120–36.
[44] Adams II TA, Barton PI. High-efficiency power production from natural gas with carbon capture. J Power Sources 2010;195:1971–83.
[45] Baldwin D, Campbell M, Ellis C, Richards M, Shenoy A. MHR design, technology and applications. Energy Convers Manage 2008;49:1898–901.
[46] Watkinson AP, Lucas JP, Lim CJ. A prediction of performance of commercial coal gasifiers. Fuel 1991;70:519–27.
[47] Meyers RA. Handbook of Petroleum Refining Processes. 3rd ed. New York: McGraw-Hill Handbooks; 2003.
[48] Şahin HM, Akbayir Ö. Alternative operating conditions for the Modular Helium Reactor. Energy Convers Manage 2012;63:31–7.
[49] LaBar MP, Shenoy AS, Simon WA, Campbell EM. Status of GT-MHR for Electricity Production, World Nuclear Association meeting, London, UK, 3–5 September, 2003.
[50] Carbon Dioxide Emissions from the Generation of Electric Power in the United States, Department of Energy and the U.S. Environmental Protection Agency, DOE, July, 2000.
[51] US Energy Information Administration, Electric Power Monthly Update, Average Retail Price of Electricity to Ultimate for All Sectors, <http://www.eia.gov/electricity/monthly/>, Average 2011.

[52] US Energy Information Administration. Coal News and Markets Report: average week coal commodity spot prices, <http://www.eia.gov/coal/news_markets/>, September 2011.
[53] US Energy Information Administration. Natural Gas Weekly Update, Henry Hub spot price, <http://www.eia.gov/naturalgas/weekly/>, September 2011.
[54] US Energy Information Administration. Gasoline and Diesel Fuel Update, <http://www.eia.gov/petroleum/gasdiesel/>, September 2011.
[55] Chemical Engineering Plant Cost Index. Chemical Engineering, 118 (2011) 10.
[56] Peters MS, Timmerhaus KD. Plant design and economics for chemical engineers, 4th ed., 1991.

Chapter 2

Supplementary Material for "Combining coal gasification, natural gas reforming, and external carbonless heat for efficient production of gasoline and diesel with CO_2 capture and sequestration"

by: Yaser Khojasteh Salkuyeh, Thomas A. Adams II

Case 1 **Without Nuclear Heat**

Stream No.	1	2	3	4	5	6	7	8	9	10	11	12	13	14	15	16	17	18	19	20*	21*	22‡	23	24
Temperature (°C)	60.0	30.0	204.8	679.4	32.0	32.0	82.0	-	46.0	80.0	188.9	15.0	15.0	-	-	34.5	240.0	229.3	108.0	-7.0	70.9	-7.0	662.2	150.0
Pressure (bar)	72.4	30.0	55.0	29.5	10.0	10.0	67.6	-	2.1	54.3	1.8	32.0	32.0	-	-	51.5	35.0	2.3	2.8	1.0	153.0	1.0	2.2	1.5
Total Flow (kg/hr)	66499	56862	171018	273187	61107	879	52623	-	5954	20670	1666	111863	27966	-	-	284426	284426	42192	15867	87129	86977	87129	222335	222335
Vapor Fraction	0.00	1.00	1.00	1.00	1.00	1.00	1.00	-	0.99	1.00	0.00	1.00	1.00	-	-	1.00	0.99	0.00	0.00	1.00	0.00	1.00	1.00	1.00
Mole Percent																								
Coal	100.00%	0.00%	0.00%	0.00%	0.00%	0.00%	0.00%	-	0.00%	0.00%	0.00%	0.00%	0.00%	-	-	0.00%	0.00%	0.00%	0.00%	0.00%	0.00%	0.00%	0.00%	0.00%
CO	0.00%	0.00%	31.40%	4.57%	0.00%	0.00%	0.00%	-	0.00%	23.41%	0.00%	27.57%	27.57%	-	-	31.09%	18.06%	0.00%	0.05%	2.52%	2.53%	2.52%	0.02%	0.02%
CO_2	0.00%	0.38%	8.42%	10.24%	0.00%	0.00%	0.00%	-	56.12%	9.18%	0.00%	7.72%	7.72%	-	-	2.87%	5.10%	0.00%	0.51%	95.79%	96.19%	95.79%	11.42%	11.42%
H_2	0.00%	0.00%	23.75%	24.49%	0.00%	0.00%	0.00%	-	0.00%	64.93%	0.00%	55.51%	55.51%	-	-	63.99%	36.36%	0.00%	0.04%	0.92%	0.93%	0.92%	0.01%	0.01%
H_2O	0.00%	0.00%	35.32%	31.14%	0.00%	0.00%	0.00%	-	5.19%	0.25%	4.97%	0.06%	0.06%	-	-	0.01%	32.89%	1.73%	1.00%	0.42%	0.00%	0.42%	18.32%	18.32%
N_2	0.00%	0.47%	0.38%	1.37%	0.19%	0.19%	0.19%	-	4.81%	1.09%	0.00%	2.70%	2.70%	-	-	1.06%	1.77%	0.00%	0.00%	0.04%	0.04%	0.04%	66.30%	66.30%
AR	0.00%	0.00%	0.06%	0.27%	0.32%	0.32%	0.32%	-	0.00%	0.24%	0.00%	0.57%	0.57%	-	-	0.23%	0.38%	0.00%	0.00%	0.02%	0.02%	0.02%	0.94%	0.94%
NH_3	0.00%	0.00%	0.00%	0.00%	0.00%	0.00%	0.00%	-	0.00%	0.00%	0.00%	0.00%	0.00%	-	-	0.00%	0.00%	0.00%	0.00%	0.00%	0.00%	0.00%	0.00%	0.00%
H_2S	0.00%	0.00%	0.57%	0.00%	0.00%	0.00%	0.00%	-	33.88%	0.00%	0.00%	0.00%	0.00%	-	-	0.00%	0.00%	0.00%	0.00%	0.00%	0.00%	0.00%	0.00%	0.00%
O_2	0.00%	0.00%	0.00%	0.00%	0.00%	0.00%	0.00%	-	0.00%	0.00%	0.00%	0.00%	0.00%	-	-	0.00%	0.00%	0.00%	0.00%	0.00%	0.00%	0.00%	2.99%	2.99%
SO_2	0.00%	0.00%	0.00%	0.00%	99.49%	99.49%	99.49%	-	0.00%	0.00%	0.00%	0.00%	0.00%	-	-	0.00%	0.00%	0.00%	0.00%	0.00%	0.00%	0.00%	0.00%	0.00%
COS	0.00%	0.00%	0.03%	0.00%	0.00%	0.00%	0.00%	-	0.00%	0.00%	0.00%	0.00%	0.00%	-	-	0.00%	0.00%	0.00%	0.00%	0.00%	0.00%	0.00%	0.00%	0.00%
Cl_2	0.00%	0.00%	0.00%	0.00%	0.00%	0.00%	0.00%	-	0.00%	0.00%	0.00%	0.00%	0.00%	-	-	0.00%	0.00%	0.00%	0.00%	0.00%	0.00%	0.00%	0.00%	0.00%
HCl	0.00%	0.00%	0.06%	0.01%	0.00%	0.00%	0.00%	-	0.00%	0.01%	0.00%	0.03%	0.03%	-	-	0.01%	0.02%	0.00%	0.00%	0.00%	0.00%	0.00%	0.01%	0.01%
Sulfur	0.00%	0.00%	0.00%	0.00%	0.00%	0.00%	0.00%	-	0.00%	0.00%	95.02%	0.00%	0.00%	-	-	0.00%	0.00%	0.00%	0.00%	0.00%	0.00%	0.00%	0.00%	0.00%
CH_4	0.00%	97.01%	0.01%	27.91%	0.00%	0.00%	0.00%	-	0.00%	0.88%	0.00%	4.42%	4.42%	-	-	0.74%	2.90%	0.00%	0.04%	0.29%	0.29%	0.29%	0.00%	0.00%
C_2H_4	0.00%	0.00%	0.00%	0.00%	0.00%	0.00%	0.00%	-	0.00%	0.00%	0.00%	0.01%	0.01%	-	-	0.00%	0.01%	0.00%	0.00%	0.00%	0.00%	0.00%	0.00%	0.00%
C_2H_6	0.00%	1.76%	0.00%	0.00%	0.00%	0.00%	0.00%	-	0.00%	0.00%	0.00%	0.25%	0.25%	-	-	0.00%	0.17%	0.00%	0.04%	0.00%	0.00%	0.00%	0.00%	0.00%
C_3H_6	0.00%	0.00%	0.00%	0.00%	0.00%	0.00%	0.00%	-	0.00%	0.00%	0.00%	0.33%	0.33%	-	-	0.00%	0.22%	0.00%	0.28%	0.00%	0.00%	0.00%	0.00%	0.00%
C_3H_8	0.00%	0.26%	0.00%	0.00%	0.00%	0.00%	0.00%	-	0.00%	0.00%	0.00%	0.16%	0.16%	-	-	0.00%	0.11%	0.00%	0.18%	0.00%	0.00%	0.00%	0.00%	0.00%
C_4H_8	0.00%	0.00%	0.00%	0.00%	0.00%	0.00%	0.00%	-	0.00%	0.00%	0.00%	0.23%	0.23%	-	-	0.00%	0.17%	0.00%	1.03%	0.00%	0.00%	0.00%	0.00%	0.00%
C_4H_{10}	0.00%	0.11%	0.00%	0.00%	0.00%	0.00%	0.00%	-	0.00%	0.00%	0.00%	0.12%	0.12%	-	-	0.00%	0.08%	0.00%	0.61%	0.00%	0.00%	0.00%	0.00%	0.00%
C_5H_{12}	0.00%	0.00%	0.00%	0.00%	0.00%	0.00%	0.00%	-	0.00%	0.00%	0.00%	0.16%	0.16%	-	-	0.00%	0.14%	0.00%	3.43%	0.00%	0.00%	0.00%	0.00%	0.00%
C_6H_{14}	0.00%	0.00%	0.00%	0.00%	0.00%	0.00%	0.00%	-	0.00%	0.00%	0.00%	0.09%	0.09%	-	-	0.00%	0.13%	0.00%	7.12%	0.00%	0.00%	0.00%	0.00%	0.00%
C_7H_{16}	0.00%	0.00%	0.00%	0.00%	0.00%	0.00%	0.00%	-	0.00%	0.00%	0.00%	0.04%	0.04%	-	-	0.00%	0.12%	0.03%	9.90%	0.00%	0.00%	0.00%	0.00%	0.00%
C_8H_{18}	0.00%	0.00%	0.00%	0.00%	0.00%	0.00%	0.00%	-	0.00%	0.00%	0.00%	0.01%	0.01%	-	-	0.00%	0.11%	0.11%	25.24%	0.00%	0.00%	0.00%	0.00%	0.00%
C_9H_{20}	0.00%	0.00%	0.00%	0.00%	0.00%	0.00%	0.00%	-	0.00%	0.00%	0.00%	0.00%	0.00%	-	-	0.00%	0.10%	0.47%	30.63%	0.00%	0.00%	0.00%	0.00%	0.00%
$C_{10}H_{22}$	0.00%	0.00%	0.00%	0.00%	0.00%	0.00%	0.00%	-	0.00%	0.00%	0.00%	0.00%	0.00%	-	-	0.00%	0.09%	3.28%	19.52%	0.00%	0.00%	0.00%	0.00%	0.00%
$C_{11}H_{24}$	0.00%	0.00%	0.00%	0.00%	0.00%	0.00%	0.00%	-	0.00%	0.00%	0.00%	0.00%	0.00%	-	-	0.00%	0.09%	5.46%	0.37%	0.00%	0.00%	0.00%	0.00%	0.00%
$C_{12}H_{26}$	0.00%	0.00%	0.00%	0.00%	0.00%	0.00%	0.00%	-	0.00%	0.00%	0.00%	0.00%	0.00%	-	-	0.00%	0.08%	33.13%	0.01%	0.00%	0.00%	0.00%	0.00%	0.00%
$C_{13}H_{28}$	0.00%	0.00%	0.00%	0.00%	0.00%	0.00%	0.00%	-	0.00%	0.00%	0.00%	0.00%	0.00%	-	-	0.00%	0.07%	4.82%	0.00%	0.00%	0.00%	0.00%	0.00%	0.00%
$C_{14}H_{30}$	0.00%	0.00%	0.00%	0.00%	0.00%	0.00%	0.00%	-	0.00%	0.00%	0.00%	0.00%	0.00%	-	-	0.00%	0.07%	22.85%	0.00%	0.00%	0.00%	0.00%	0.00%	0.00%
$C_{15}H_{32}$	0.00%	0.00%	0.00%	0.00%	0.00%	0.00%	0.00%	-	0.00%	0.00%	0.00%	0.00%	0.00%	-	-	0.00%	0.06%	4.08%	0.00%	0.00%	0.00%	0.00%	0.00%	0.00%
$C_{16}H_{34}$	0.00%	0.00%	0.00%	0.00%	0.00%	0.00%	0.00%	-	0.00%	0.00%	0.00%	0.00%	0.00%	-	-	0.00%	0.06%	11.26%	0.00%	0.00%	0.00%	0.00%	0.00%	0.00%
$C_{17}H_{36}$	0.00%	0.00%	0.00%	0.00%	0.00%	0.00%	0.00%	-	0.00%	0.00%	0.00%	0.00%	0.00%	-	-	0.00%	0.05%	3.46%	0.00%	0.00%	0.00%	0.00%	0.00%	0.00%
$C_{18}H_{38}$	0.00%	0.00%	0.00%	0.00%	0.00%	0.00%	0.00%	-	0.00%	0.00%	0.00%	0.00%	0.00%	-	-	0.00%	0.05%	3.18%	0.00%	0.00%	0.00%	0.00%	0.00%	0.00%
$C_{19}H_{40}$	0.00%	0.00%	0.00%	0.00%	0.00%	0.00%	0.00%	-	0.00%	0.00%	0.00%	0.00%	0.00%	-	-	0.00%	0.04%	2.93%	0.00%	0.00%	0.00%	0.00%	0.00%	0.00%
$C_{20}H_{42}$	0.00%	0.00%	0.00%	0.00%	0.00%	0.00%	0.00%	-	0.00%	0.00%	0.00%	0.00%	0.00%	-	-	0.00%	0.04%	2.69%	0.00%	0.00%	0.00%	0.00%	0.00%	0.00%
$C_{24}H_{50}$	0.00%	0.00%	0.00%	0.00%	0.00%	0.00%	0.00%	-	0.00%	0.00%	0.00%	0.00%	0.00%	-	-	0.00%	0.13%	0.52%	0.00%	0.00%	0.00%	0.00%	0.00%	0.00%
C_{28}+	0.00%	0.00%	0.00%	0.00%	0.00%	0.00%	0.00%	-	0.00%	0.00%	0.00%	0.00%	0.00%	-	-	0.00%	0.32%	0.00%	0.00%	0.00%	0.00%	0.00%	0.00%	0.00%
Total	100.00%	100.00%	100.00%	100.00%	100.00%	100.00%	100.00%	0.00%	100.00%	100.00%	100.00%	100.00%	100.00%	0.00%	0.00%	100.00%	100.00%	100.00%	100.00%	100.00%	100.00%	100.00%	100.00%	100.00%

Notes:

* For CCS Enabled Cases Only

‡ For CCS Disabled Cases Only

Chapter 2

Supplementary Material for "Combining coal gasification, natural gas reforming, and external carbonless heat for efficient production of gasoline and diesel with CO_2 capture and sequestration"

by: Yaser Khojasteh Salkuyeh, Thomas A. Adams II

Case 1 **With Nuclear Heat**

Stream No.	1	2	3	4	5	6	7	8	9	10	11	12	13	14	15	16	17	18	19	20*	21*	22‡	23	24
Temperature (°C)	60.0	30.0	204.8	697.2	-	32.0	82.0	-	46.0	80.0	189.8	15.0	15.0	-	-	34.7	240.0	229.3	109.7	-7.0	73.3	-7.0	682.5	150.0
Pressure (bar)	72.4	30.0	55.0	29.5	-	10.0	67.6	-	2.1	54.3	1.8	32.0	32.0	-	-	51.5	35.0	2.3	2.8	1.0	153.0	1.0	2.2	1.5
Total Flow (kg/hr)	76034	39330	195541	239365	-	1003	60169	-	5018	208633	1907	106088	26522	-	-	277100	277100	42181	15871	61094	60947	61094	235121	235121
Vapor Fraction	0.00	1.00	1.00	1.00	-	1.00	1.00	-	0.99	1.00	0.00	1.00	1.00	-	-	1.00	0.99	0.00	0.00	1.00	0.00	1.00	1.00	1.00
Mole Percent																								
Coal	100.00%	0.00%	0.00%	0.00%	-	0.00%	0.00%	-	0.00%	0.00%	0.00%	0.00%	0.00%	-	-	0.00%	0.00%	0.00%	0.00%	0.00%	0.00%	0.00%	0.00%	0.00%
CO	0.00%	0.00%	31.40%	5.29%	-	0.00%	0.00%	-	0.00%	23.15%	2.90E-13	27.76%	27.76%	-	-	31.17%	18.15%	2.12E-10	0.05%	3.55%	3.57%	3.55%	0.03%	0.03%
CO_2	0.00%	0.38%	8.42%	10.00%	-	0.00%	0.00%	-	44.71%	5.14%	2.22E-05	5.55%	5.55%	-	-	2.00%	3.66%	5.77E-09	0.38%	93.58%	94.11%	93.58%	10.59%	10.59%
H_2	0.00%	0.00%	23.75%	26.81%	-	0.00%	0.00%	-	0.00%	68.10%	3.94E-11	55.47%	55.47%	-	-	64.00%	36.25%	2.84E-10	0.05%	1.30%	1.30%	1.30%	0.01%	0.01%
H_2O	0.00%	0.00%	35.32%	31.18%	-	0.00%	0.00%	-	5.75%	0.25%	6.26%	0.06%	0.06%	-	-	9.38E-05	33.04%	1.73%	1.00%	0.57%	2.84E-06	0.57%	18.32%	18.32%
N_2	0.00%	0.47%	0.38%	1.39%	-	0.19%	0.19%	-	5.11%	1.05%	5.20E-08	2.52%	2.52%	-	-	0.99%	1.64%	1.63E-11	4.47E-05	0.05%	0.05%	0.05%	66.95%	66.95%
AR	0.00%	0.00%	0.06%	0.16%	-	0.32%	0.32%	-	0.00%	0.12%	6.54E-09	0.31%	0.31%	-	-	0.12%	0.20%	7.22E-12	1.21E-05	0.01%	0.01%	0.01%	1.12%	1.12%
NH_3	0.00%	0.00%	0.00%	0.00%	-	0.00%	0.00%	-	0.00%	0.00%	2.50E-13	0.00%	0.00%	-	-	0.00%	0.00%	0.00%	0.00%	0.00%	0.00%	0.00%	0.00%	0.00%
H_2S	0.00%	0.00%	0.57%	0.00%	-	0.00%	0.00%	-	44.43%	0.00%	1.65E-05	0.00%	0.00%	-	-	0.00%	0.00%	0.00%	0.00%	0.00%	0.00%	0.00%	0.00%	0.00%
O_2	0.00%	0.00%	0.00%	0.00%	-	0.00%	0.00%	-	0.00%	0.00%	0.00%	1.26E-12	1.26E-12	-	-	4.94E-13	8.22E-13	2.78E-21	4.96E-15	0.00%	0.00%	0.00%	2.98%	2.98%
SO_2	0.00%	0.00%	0.00%	0.00%	-	99.49%	99.49%	-	0.00%	0.00%	0.00%	0.00%	0.00%	-	-	0.00%	0.00%	0.00%	0.00%	0.00%	0.00%	0.00%	0.00%	0.00%
COS	0.00%	0.00%	0.03%	0.00%	-	0.00%	0.00%	-	0.00%	0.00%	0.00%	0.00%	0.00%	-	-	0.00%	0.00%	0.00%	0.00%	0.00%	0.00%	0.00%	0.00%	0.00%
Cl_2	0.00%	0.00%	0.00%	0.00%	-	0.00%	0.00%	-	0.00%	0.00%	0.00%	1.57E-12	1.57E-12	-	-	6.46E-13	1.07E-12	1.77E-17	1.82E-12	0.00%	0.00%	0.00%	0.00%	0.00%
HCl	0.00%	0.00%	0.06%	0.02%	-	0.00%	0.00%	-	0.00%	0.01%	0.00%	0.03%	0.03%	-	-	0.01%	0.02%	9.53E-11	4.60E-05	0.00%	0.00%	0.00%	0.01%	0.01%
Sulfur	0.00%	0.00%	0.00%	0.00%	-	0.00%	0.00%	-	0.00%	0.00%	93.74%	0.00%	0.00%	-	-	0.00%	0.00%	0.00%	0.00%	0.00%	0.00%	0.00%	0.00%	0.00%
CH_4	0.00%	97.01%	0.01%	25.15%	-	0.00%	0.00%	-	0.00%	2.18%	0.00%	6.88%	6.88%	-	-	1.70%	4.50%	5.88E-10	0.06%	0.95%	0.95%	0.95%	0.00%	0.00%
C_2H_4	0.00%	0.00%	0.00%	0.00%	-	0.00%	0.00%	-	0.00%	5.03E-08	0.00%	0.01%	0.01%	-	-	4.01E-08	8.43E-05	2.21E-11	1.11E-05	0.00%	0.00%	0.00%	0.00%	0.00%
C_2H_6	0.00%	1.76%	0.00%	0.00%	-	0.00%	0.00%	-	0.00%	3.18E-06	0.00%	0.26%	0.26%	-	-	2.54E-06	0.17%	1.13E-09	0.04%	0.00%	0.00%	0.00%	0.00%	0.00%
C_3H_6	0.00%	0.00%	0.00%	0.00%	-	0.00%	0.00%	-	0.00%	1.31E-06	0.00%	0.33%	0.33%	-	-	1.05E-06	0.22%	1.99E-08	0.29%	0.00%	0.00%	0.00%	0.00%	0.00%
C_3H_8	0.00%	0.26%	0.00%	0.00%	-	0.00%	0.00%	-	0.00%	9.78E-07	0.00%	0.17%	0.17%	-	-	7.79E-07	0.11%	1.44E-08	0.18%	0.00%	0.00%	0.00%	0.00%	0.00%
C_4H_8	0.00%	0.00%	0.00%	0.00%	-	0.00%	0.00%	-	0.00%	9.25E-07	0.00%	0.24%	0.24%	-	-	7.38E-07	0.17%	2.58E-07	1.05%	0.00%	0.00%	0.00%	0.00%	0.00%
C_4H_{10}	0.00%	0.11%	0.00%	0.00%	-	0.00%	0.00%	-	0.00%	5.98E-07	0.00%	0.12%	0.12%	-	-	4.77E-07	0.08%	1.89E-07	0.62%	0.00%	0.00%	0.00%	0.00%	0.00%
C_5H_{12}	0.00%	0.00%	0.00%	0.00%	-	0.00%	0.00%	-	0.00%	6.33E-07	0.00%	0.16%	0.16%	-	-	5.05E-07	0.14%	4.66E-06	3.45%	0.00%	0.00%	0.00%	0.00%	0.00%
C_6H_{14}	0.00%	0.00%	0.00%	0.00%	-	0.00%	0.00%	-	0.00%	3.64E-07	0.00%	0.09%	0.09%	-	-	2.91E-07	0.13%	4.34E-05	7.15%	0.00%	0.00%	0.00%	0.00%	0.00%
C_7H_{16}	0.00%	0.00%	0.00%	0.00%	-	0.00%	0.00%	-	0.00%	1.52E-07	0.00%	0.04%	0.04%	-	-	1.21E-07	0.12%	0.03%	9.91%	0.00%	0.00%	0.00%	0.00%	0.00%
C_8H_{18}	0.00%	0.00%	0.00%	0.00%	-	0.00%	0.00%	-	0.00%	4.49E-08	0.00%	0.01%	0.01%	-	-	3.58E-08	0.11%	0.10%	25.24%	0.00%	0.00%	0.00%	0.00%	0.00%
C_9H_{20}	0.00%	0.00%	0.00%	0.00%	-	0.00%	0.00%	-	0.00%	1.11E-08	0.00%	2.82E-05	2.82E-05	-	-	8.83E-09	0.10%	0.47%	30.62%	0.00%	0.00%	0.00%	0.00%	0.00%
$C_{10}H_{22}$	0.00%	0.00%	0.00%	0.00%	-	0.00%	0.00%	-	0.00%	2.34E-09	0.00%	5.95E-06	5.95E-06	-	-	1.87E-09	0.09%	3.28%	19.52%	0.00%	0.00%	0.00%	0.00%	0.00%
$C_{11}H_{24}$	0.00%	0.00%	0.00%	0.00%	-	0.00%	0.00%	-	0.00%	4.81E-10	0.00%	1.22E-06	1.22E-06	-	-	3.83E-10	0.09%	5.46%	0.37%	0.00%	0.00%	0.00%	0.00%	0.00%
$C_{12}H_{26}$	0.00%	0.00%	0.00%	0.00%	-	0.00%	0.00%	-	0.00%	8.90E-11	0.00%	2.26E-07	2.26E-07	-	-	7.10E-11	0.08%	33.13%	0.01%	0.00%	0.00%	0.00%	0.00%	0.00%
$C_{13}H_{28}$	0.00%	0.00%	0.00%	0.00%	-	0.00%	0.00%	-	0.00%	1.70E-08	0.00%	4.33E-08	4.33E-08	-	-	1.36E-08	0.07%	4.82%	3.76E-06	0.00%	0.00%	0.00%	0.00%	0.00%
$C_{14}H_{30}$	0.00%	0.00%	0.00%	0.00%	-	0.00%	0.00%	-	0.00%	3.53E-09	0.00%	8.97E-09	8.97E-09	-	-	2.81E-09	0.07%	22.85%	1.49E-07	0.00%	0.00%	0.00%	0.00%	0.00%
$C_{15}H_{32}$	0.00%	0.00%	0.00%	0.00%	-	0.00%	0.00%	-	0.00%	6.45E-10	0.00%	1.64E-09	1.64E-09	-	-	6.49E-13	0.06%	4.08%	6.29E-09	0.00%	0.00%	0.00%	0.00%	0.00%
$C_{16}H_{34}$	0.00%	0.00%	0.00%	0.00%	-	0.00%	0.00%	-	0.00%	1.33E-10	0.00%	3.39E-10	3.39E-10	-	-	1.06E-10	0.06%	11.26%	2.96E-10	0.00%	0.00%	0.00%	0.00%	0.00%
$C_{17}H_{36}$	0.00%	0.00%	0.00%	0.00%	-	0.00%	0.00%	-	0.00%	2.13E-11	0.00%	5.42E-11	5.42E-11	-	-	2.82E-15	0.05%	3.46%	1.19E-11	0.00%	0.00%	0.00%	0.00%	0.00%
$C_{18}H_{38}$	0.00%	0.00%	0.00%	0.00%	-	0.00%	0.00%	-	0.00%	4.43E-12	0.00%	1.13E-11	1.13E-11	-	-	2.31E-16	0.05%	3.18%	6.71E-13	0.00%	0.00%	0.00%	0.00%	0.00%
$C_{19}H_{40}$	0.00%	0.00%	0.00%	0.00%	-	0.00%	0.00%	-	0.00%	8.96E-13	0.00%	2.28E-12	2.28E-12	-	-	1.55E-17	0.04%	2.93%	3.57E-14	0.00%	0.00%	0.00%	0.00%	0.00%
$C_{20}H_{42}$	0.00%	0.00%	0.00%	0.00%	-	0.00%	0.00%	-	0.00%	1.47E-13	0.00%	3.74E-13	3.74E-13	-	-	0.00%	0.04%	2.69%	1.54E-15	0.00%	0.00%	0.00%	0.00%	0.00%
$C_{24}H_{50}$	0.00%	0.00%	0.00%	0.00%	-	0.00%	0.00%	-	0.00%	0.00%	0.00%	0.00%	0.00%	-	-	0.00%	0.13%	0.52%	7.34E-21	0.00%	0.00%	0.00%	0.00%	0.00%
C_{28}+	0.00%	0.00%	0.00%	0.00%	-	0.00%	0.00%	-	0.00%	0.00%	0.00%	0.00%	0.00%	-	-	0.00%	0.32%	0.00%	0.00%	0.00%	0.00%	0.00%	0.00%	0.00%
Total	100.00%	100.00%	100.00%	100.00%	0.00%	100.00%	100.00%	0.00%	100.00%	100.00%	100.00%	100.00%	100.00%	0.00%	0.00%	100.00%	100.00%	100.00%	100.00%	100.00%	100.00%	100.00%	100.00%	100.00%

Notes:

* For CCS Enabled Cases Only

‡ For CCS Disabled Cases Only

Chapter 2

Supplementary Material for "Combining coal gasification, natural gas reforming, and external carbonless heat for efficient production of gasoline and diesel with CO_2 capture and sequestration"

by: Yaser Khojasteh Salkuyeh, Thomas A. Adams II

Case 2 **Without Nuclear Heat**

Stream No.	1	2	3	4	5	6	7	8	9	10	11	12	13	14	15	16	17	18	19	20*	21*	22‡	23	24
Temperature (°C)	60.0	30.0	204.8	480.8	32.0	32.0	82.0	32.0	46.0	80.0	188.9	-	15.0	15.0	950.0	47.5	240.0	229.3	109.5	-7.0	70.9	-7.0	999.2	150.0
Pressure (bar)	72.4	30.0	55.0	29.5	10.0	10.0	67.6	10.0	2.1	54.3	1.8	-	32.0	32.0	39.0	35.9	35.0	2.3	2.8	1.0	153.0	1.0	2.2	1.5
Total Flow (kg/hr)	60043	63361	154417	99524	53589	790	47515	28008	4189	143457	1505	-	26263	102485	166061	272160	272160	41953	15853	93865	93777	93865	213924	213924
Vapor Fraction	0.00	1.00	1.00	1.00	1.00	1.00	1.00	1.00	0.99	1.00	0.00	-	1.00	1.00	1.00	1.00	0.99	0.00	0.00	1.00	0.00	1.00	1.00	1.00
Mole Percent																								
Coal	100.00%	0.00%	0.00%	0.00%	0.00%	0.00%	0.00%	0.00%	0.00%	0.00%	0.00%	-	0.00%	0.00%	0.00%	0.00%	0.00%	0.00%	0.00%	0.00%	0.00%	0.00%	0.00%	0.00%
CO	0.00%	0.00%	31.40%	0.13%	0.00%	0.00%	0.00%	0.00%	0.00%	21.51%	0.00%	-	28.46%	28.55%	21.61%	31.50%	18.46%	0.00%	0.06%	2.71%	1.63%	2.71%	0.00%	0.00%
CO_2	0.00%	0.38%	8.42%	2.62%	0.00%	0.00%	0.00%	0.00%	50.71%	7.94%	0.00%	-	5.59%	5.43%	8.22%	1.91%	3.54%	0.00%	0.38%	95.52%	97.57%	95.52%	10.79%	10.79%
H_2	0.00%	0.00%	23.75%	8.29%	0.00%	0.00%	0.00%	0.00%	0.00%	69.12%	0.00%	-	56.68%	56.99%	43.49%	64.64%	36.83%	0.00%	0.05%	1.00%	0.60%	1.00%	0.00%	0.00%
H_2O	0.00%	0.00%	35.32%	27.80%	0.00%	0.00%	0.00%	0.00%	4.97%	0.25%	5.99%	-	0.08%	0.06%	24.20%	0.07%	33.72%	1.73%	1.00%	0.57%	0.00%	0.57%	18.51%	18.51%
N_2	0.00%	0.47%	0.38%	0.29%	0.19%	0.19%	0.19%	0.19%	1.34%	0.17%	0.00%	-	2.83%	2.84%	1.98%	1.10%	1.84%	0.00%	0.01%	0.01%	0.01%	0.01%	66.68%	66.68%
AR	0.00%	0.00%	0.06%	0.00%	0.32%	0.32%	0.32%	0.32%	0.00%	0.04%	0.00%	-	0.67%	0.67%	0.48%	0.26%	0.43%	0.00%	0.00%	0.00%	0.00%	0.00%	0.97%	0.97%
NH_3	0.00%	0.00%	0.00%	0.00%	0.00%	0.00%	0.00%	0.00%	0.00%	0.00%	0.00%	-	0.00%	0.00%	0.00%	0.00%	0.00%	0.00%	0.00%	0.00%	0.00%	0.00%	0.00%	0.00%
H_2S	0.00%	0.00%	0.57%	0.00%	0.00%	0.00%	0.00%	0.00%	42.98%	0.00%	0.00%	-	0.00%	0.00%	0.00%	0.00%	0.00%	0.00%	0.00%	0.00%	0.00%	0.00%	0.00%	0.00%
O_2	0.00%	0.00%	0.00%	0.00%	0.00%	0.00%	0.00%	0.00%	0.00%	0.00%	0.00%	-	0.00%	0.00%	0.00%	0.00%	0.00%	0.00%	0.00%	0.00%	0.00%	0.00%	3.04%	3.04%
SO_2	0.00%	0.00%	0.00%	0.00%	99.49%	99.49%	99.49%	99.49%	0.00%	0.00%	0.00%	-	0.00%	0.00%	0.00%	0.00%	0.00%	0.00%	0.00%	0.00%	0.00%	0.00%	0.00%	0.00%
COS	0.00%	0.00%	0.03%	0.00%	0.00%	0.00%	0.00%	0.00%	0.00%	0.00%	0.00%	-	0.00%	0.00%	0.00%	0.00%	0.00%	0.00%	0.00%	0.00%	0.00%	0.00%	0.00%	0.00%
Cl_2	0.00%	0.00%	0.00%	0.00%	0.00%	0.00%	0.00%	0.00%	0.00%	0.00%	0.00%	-	0.00%	0.00%	0.00%	0.00%	0.00%	0.00%	0.00%	0.00%	0.00%	0.00%	0.00%	0.00%
HCl	0.00%	0.00%	0.06%	0.00%	0.00%	0.00%	0.00%	0.00%	0.00%	0.00%	0.00%	-	0.03%	0.03%	0.02%	0.01%	0.02%	0.00%	0.00%	0.00%	0.00%	0.00%	0.01%	0.01%
Sulfur	0.00%	0.00%	0.00%	0.00%	0.00%	0.00%	0.00%	0.00%	0.00%	0.00%	94.01%	-	0.00%	0.00%	0.00%	0.00%	0.00%	0.00%	0.00%	0.00%	0.00%	0.00%	0.00%	0.00%
CH_4	0.00%	97.01%	0.01%	60.86%	0.00%	0.00%	0.00%	0.00%	0.00%	0.98%	0.00%	-	4.01%	3.99%	0.00%	0.52%	2.58%	0.00%	0.04%	0.19%	0.19%	0.19%	0.00%	0.00%
C_2H_4	0.00%	0.00%	0.00%	0.00%	0.00%	0.00%	0.00%	0.00%	0.00%	0.00%	0.00%	-	0.01%	0.01%	0.00%	0.00%	0.01%	0.00%	0.00%	0.00%	0.00%	0.00%	0.00%	0.00%
C_2H_6	0.00%	1.76%	0.00%	0.00%	0.00%	0.00%	0.00%	0.00%	0.00%	0.00%	0.00%	-	0.27%	0.26%	0.00%	0.00%	0.17%	0.00%	0.04%	0.00%	0.00%	0.00%	0.00%	0.00%
C_3H_6	0.00%	0.00%	0.00%	0.00%	0.00%	0.00%	0.00%	0.00%	0.00%	0.00%	0.00%	-	0.37%	0.34%	0.00%	0.00%	0.23%	0.00%	0.31%	0.00%	0.00%	0.00%	0.00%	0.00%
C_3H_8	0.00%	0.26%	0.00%	0.00%	0.00%	0.00%	0.00%	0.00%	0.00%	0.00%	0.00%	-	0.19%	0.17%	0.00%	0.00%	0.11%	0.00%	0.19%	0.00%	0.00%	0.00%	0.00%	0.00%
C_4H_8	0.00%	0.00%	0.00%	0.00%	0.00%	0.00%	0.00%	0.00%	0.00%	0.00%	0.00%	-	0.28%	0.24%	0.00%	0.00%	0.17%	0.00%	1.09%	0.00%	0.00%	0.00%	0.00%	0.00%
C_4H_{10}	0.00%	0.11%	0.00%	0.00%	0.00%	0.00%	0.00%	0.00%	0.00%	0.00%	0.00%	-	0.14%	0.12%	0.00%	0.00%	0.09%	0.00%	0.64%	0.00%	0.00%	0.00%	0.00%	0.00%
C_5H_{12}	0.00%	0.00%	0.00%	0.00%	0.00%	0.00%	0.00%	0.00%	0.00%	0.00%	0.00%	-	0.20%	0.16%	0.00%	0.00%	0.14%	0.00%	3.53%	0.00%	0.00%	0.00%	0.00%	0.00%
C_6H_{14}	0.00%	0.00%	0.00%	0.00%	0.00%	0.00%	0.00%	0.00%	0.00%	0.00%	0.00%	-	0.12%	0.09%	0.00%	0.00%	0.13%	0.00%	7.23%	0.00%	0.00%	0.00%	0.00%	0.00%
C_7H_{16}	0.00%	0.00%	0.00%	0.00%	0.00%	0.00%	0.00%	0.00%	0.00%	0.00%	0.00%	-	0.05%	0.04%	0.00%	0.00%	0.12%	0.02%	9.95%	0.00%	0.00%	0.00%	0.00%	0.00%
C_8H_{18}	0.00%	0.00%	0.00%	0.00%	0.00%	0.00%	0.00%	0.00%	0.00%	0.00%	0.00%	-	0.02%	0.01%	0.00%	0.00%	0.11%	0.10%	25.15%	0.00%	0.00%	0.00%	0.00%	0.00%
C_9H_{20}	0.00%	0.00%	0.00%	0.00%	0.00%	0.00%	0.00%	0.00%	0.00%	0.00%	0.00%	-	0.00%	0.00%	0.00%	0.00%	0.10%	0.46%	30.48%	0.00%	0.00%	0.00%	0.00%	0.00%
$C_{10}H_{22}$	0.00%	0.00%	0.00%	0.00%	0.00%	0.00%	0.00%	0.00%	0.00%	0.00%	0.00%	-	0.00%	0.00%	0.00%	0.00%	0.10%	3.25%	19.47%	0.00%	0.00%	0.00%	0.00%	0.00%
$C_{11}H_{24}$	0.00%	0.00%	0.00%	0.00%	0.00%	0.00%	0.00%	0.00%	0.00%	0.00%	0.00%	-	0.00%	0.00%	0.00%	0.00%	0.09%	5.46%	0.38%	0.00%	0.00%	0.00%	0.00%	0.00%
$C_{12}H_{26}$	0.00%	0.00%	0.00%	0.00%	0.00%	0.00%	0.00%	0.00%	0.00%	0.00%	0.00%	-	0.00%	0.00%	0.00%	0.00%	0.08%	33.15%	0.01%	0.00%	0.00%	0.00%	0.00%	0.00%
$C_{13}H_{28}$	0.00%	0.00%	0.00%	0.00%	0.00%	0.00%	0.00%	0.00%	0.00%	0.00%	0.00%	-	0.00%	0.00%	0.00%	0.00%	0.07%	4.83%	0.00%	0.00%	0.00%	0.00%	0.00%	0.00%
$C_{14}H_{30}$	0.00%	0.00%	0.00%	0.00%	0.00%	0.00%	0.00%	0.00%	0.00%	0.00%	0.00%	-	0.00%	0.00%	0.00%	0.00%	0.07%	22.86%	0.00%	0.00%	0.00%	0.00%	0.00%	0.00%
$C_{15}H_{32}$	0.00%	0.00%	0.00%	0.00%	0.00%	0.00%	0.00%	0.00%	0.00%	0.00%	0.00%	-	0.00%	0.00%	0.00%	0.00%	0.06%	4.09%	0.00%	0.00%	0.00%	0.00%	0.00%	0.00%
$C_{16}H_{34}$	0.00%	0.00%	0.00%	0.00%	0.00%	0.00%	0.00%	0.00%	0.00%	0.00%	0.00%	-	0.00%	0.00%	0.00%	0.00%	0.06%	11.26%	0.00%	0.00%	0.00%	0.00%	0.00%	0.00%
$C_{17}H_{36}$	0.00%	0.00%	0.00%	0.00%	0.00%	0.00%	0.00%	0.00%	0.00%	0.00%	0.00%	-	0.00%	0.00%	0.00%	0.00%	0.05%	3.46%	0.00%	0.00%	0.00%	0.00%	0.00%	0.00%
$C_{18}H_{38}$	0.00%	0.00%	0.00%	0.00%	0.00%	0.00%	0.00%	0.00%	0.00%	0.00%	0.00%	-	0.00%	0.00%	0.00%	0.00%	0.05%	3.18%	0.00%	0.00%	0.00%	0.00%	0.00%	0.00%
$C_{19}H_{40}$	0.00%	0.00%	0.00%	0.00%	0.00%	0.00%	0.00%	0.00%	0.00%	0.00%	0.00%	-	0.00%	0.00%	0.00%	0.00%	0.04%	2.93%	0.00%	0.00%	0.00%	0.00%	0.00%	0.00%
$C_{20}H_{42}$	0.00%	0.00%	0.00%	0.00%	0.00%	0.00%	0.00%	0.00%	0.00%	0.00%	0.00%	-	0.00%	0.00%	0.00%	0.00%	0.04%	2.69%	0.00%	0.00%	0.00%	0.00%	0.00%	0.00%
$C_{24}H_{50}$	0.00%	0.00%	0.00%	0.00%	0.00%	0.00%	0.00%	0.00%	0.00%	0.00%	0.00%	-	0.00%	0.00%	0.00%	0.00%	0.13%	0.52%	0.00%	0.00%	0.00%	0.00%	0.00%	0.00%
$C_{28}+$	0.00%	0.00%	0.00%	0.00%	0.00%	0.00%	0.00%	0.00%	0.00%	0.00%	0.00%	-	0.00%	0.00%	0.00%	0.00%	0.33%	0.00%	0.00%	0.00%	0.00%	0.00%	0.00%	0.00%
Total	100.00%	100.00%	100.00%	100.00%	100.00%	100.00%	100.00%	100.00%	100.00%	100.00%	100.00%	0.00%	100.00%	100.00%	100.00%	100.00%	100.00%	100.00%	100.00%	100.00%	100.00%	100.00%	100.00%	100.00%

Notes:

* For CCS Enabled Cases Only

‡ For CCS Disabled Cases Only

Chapter 2

Supplementary Material for "Combining coal gasification, natural gas reforming, and external carbonless heat for efficient production of gasoline and diesel with CO_2 capture and sequestration"

by: Yaser Khojasteh Salkuyeh, Thomas A. Adams II

Case 2 **With Nuclear Heat**

Stream No.	1	2	3	4	5	6	7	8	9	10	11	12	13	14	15	16	17	18	19	20*	21*	22‡	23	24
Temperature (°C)	60.0	30.0	204.8	480.8	-	32.0	82.0	32.0	46.0	80.0	190.4	-	15.0	15.0	950.0	48.4	240.0	230.5	111.1	-7.0	68.9	-7.0	999.2	150.0
Pressure (bar)	72.4	30.0	55.0	29.5	-	10.0	67.6	10.0	2.1	54.3	1.8	-	32.0	32.0	39.0	35.9	35.0	2.3	2.8	1.0	153.0	1.0	2.2	1.5
Total Flow (kg/hr)	67201	49639	172824	77970	-	883	53179	30609	3561	105132	1683	-	25552	99846	159568	270018	270018	42307	15974	70378	70280	70378	229805	229805
Vapor Fraction	0.00	1.00	1.00	1.00	-	1.00	1.00	1.00	0.99	1.00	0.00	-	1.00	1.00	1.00	1.00	0.99	0.00	0.00	1.00	0.00	1.00	1.00	1.00
Mole Percent																								
Coal	100.00%	0.00%	0.00%	0.00%	-	0.00%	0.00%	0.00%	0.00%	0.00%	0.00%	-	0.00%	0.00%	0.00%	0.00%	0.00%	0.00%	0.00%	0.00%	0.00%	0.00%	0.00%	0.00%
CO	0.00%	0.00%	31.40%	0.13%	-	0.00%	0.00%	0.00%	0.00%	20.22%	0.00%	-	28.41%	28.48%	23.43%	31.47%	18.43%	0.00%	0.06%	3.82%	2.10%	3.82%	0.00%	0.00%
CO_2	0.00%	0.38%	8.42%	2.62%	-	0.00%	0.00%	0.00%	38.59%	3.33%	0.00%	-	3.90%	3.79%	6.97%	1.27%	2.47%	0.00%	0.27%	92.83%	96.39%	92.83%	10.28%	10.28%
H_2	0.00%	0.00%	23.75%	8.29%	-	0.00%	0.00%	0.00%	0.00%	72.89%	0.00%	-	56.37%	56.66%	47.00%	64.51%	36.65%	0.00%	0.05%	1.41%	0.77%	1.41%	0.00%	0.00%
H_2O	0.00%	0.00%	35.32%	27.80%	-	0.00%	0.00%	0.00%	5.35%	0.25%	7.36%	-	0.08%	0.06%	20.43%	0.08%	33.68%	1.72%	1.00%	0.61%	0.00%	0.61%	18.41%	18.41%
N_2	0.00%	0.47%	0.38%	0.29%	-	0.19%	0.19%	0.19%	1.41%	0.12%	0.00%	-	2.62%	2.63%	1.84%	1.02%	1.70%	0.00%	0.00%	0.02%	0.01%	0.02%	67.24%	67.24%
AR	0.00%	0.00%	0.06%	0.00%	-	0.32%	0.32%	0.32%	0.00%	0.00%	0.00%	-	0.42%	0.42%	0.31%	0.16%	0.27%	0.00%	0.00%	0.00%	0.00%	0.00%	1.01%	1.01%
NH_3	0.00%	0.00%	0.00%	0.00%	-	0.00%	0.00%	0.00%	0.00%	0.00%	0.00%	-	0.00%	0.00%	0.00%	0.00%	0.00%	0.00%	0.00%	0.00%	0.00%	0.00%	0.00%	0.00%
H_2S	0.00%	0.00%	0.57%	0.00%	-	0.00%	0.00%	0.00%	54.65%	0.00%	0.00%	-	0.00%	0.00%	0.00%	0.00%	0.00%	0.00%	0.00%	0.00%	0.00%	0.00%	0.00%	0.00%
O_2	0.00%	0.00%	0.00%	0.00%	-	0.00%	0.00%	0.00%	0.00%	0.00%	0.00%	-	0.00%	0.00%	0.00%	0.00%	0.00%	0.00%	0.00%	0.00%	0.00%	0.00%	3.04%	3.04%
SO_2	0.00%	0.00%	0.00%	0.00%	-	99.49%	99.49%	99.49%	0.00%	0.00%	0.00%	-	0.00%	0.00%	0.00%	0.00%	0.00%	0.00%	0.00%	0.00%	0.00%	0.00%	0.00%	0.00%
COS	0.00%	0.00%	0.03%	0.00%	-	0.00%	0.00%	0.00%	0.00%	0.00%	0.00%	-	0.00%	0.00%	0.00%	0.00%	0.00%	0.00%	0.00%	0.00%	0.00%	0.00%	0.00%	0.00%
Cl_2	0.00%	0.00%	0.00%	0.00%	-	0.00%	0.00%	0.00%	0.00%	0.00%	0.00%	-	0.00%	0.00%	0.00%	0.00%	0.00%	0.00%	0.00%	0.00%	0.00%	0.00%	0.00%	0.00%
HCl	0.00%	0.00%	0.06%	0.00%	-	0.00%	0.00%	0.00%	0.00%	0.00%	0.00%	-	0.03%	0.03%	0.02%	0.01%	0.02%	0.00%	0.00%	0.00%	0.00%	0.00%	0.01%	0.01%
Sulfur	0.00%	0.00%	0.00%	0.00%	-	0.00%	0.00%	0.00%	0.00%	0.00%	92.64%	-	0.00%	0.00%	0.00%	0.00%	0.00%	0.00%	0.00%	0.00%	0.00%	0.00%	0.00%	0.00%
CH_4	0.00%	97.01%	0.01%	60.86%	-	0.00%	0.00%	0.00%	0.00%	3.20%	0.00%	-	6.52%	6.48%	0.00%	1.49%	4.20%	0.00%	0.06%	1.32%	0.73%	1.32%	0.00%	0.00%
C_2H_4	0.00%	0.00%	0.00%	0.00%	-	0.00%	0.00%	0.00%	0.00%	0.00%	0.00%	-	0.01%	0.01%	0.00%	0.00%	0.01%	0.00%	0.00%	0.00%	0.00%	0.00%	0.00%	0.00%
C_2H_6	0.00%	1.76%	0.00%	0.00%	-	0.00%	0.00%	0.00%	0.00%	0.00%	0.00%	-	0.27%	0.26%	0.00%	0.00%	0.17%	0.00%	0.04%	0.00%	0.00%	0.00%	0.00%	0.00%
C_3H_6	0.00%	0.00%	0.00%	0.00%	-	0.00%	0.00%	0.00%	0.00%	0.00%	0.00%	-	0.37%	0.34%	0.00%	0.00%	0.23%	0.00%	0.31%	0.00%	0.00%	0.00%	0.00%	0.00%
C_3H_8	0.00%	0.26%	0.00%	0.00%	-	0.00%	0.00%	0.00%	0.00%	0.00%	0.00%	-	0.19%	0.17%	0.00%	0.00%	0.11%	0.00%	0.19%	0.00%	0.00%	0.00%	0.00%	0.00%
C_4H_8	0.00%	0.00%	0.00%	0.00%	-	0.00%	0.00%	0.00%	0.00%	0.00%	0.00%	-	0.28%	0.24%	0.00%	0.00%	0.17%	0.00%	1.09%	0.00%	0.00%	0.00%	0.00%	0.00%
C_4H_{10}	0.00%	0.11%	0.00%	0.00%	-	0.00%	0.00%	0.00%	0.00%	0.00%	0.00%	-	0.14%	0.12%	0.00%	0.00%	0.09%	0.00%	0.64%	0.00%	0.00%	0.00%	0.00%	0.00%
C_5H_{12}	0.00%	0.00%	0.00%	0.00%	-	0.00%	0.00%	0.00%	0.00%	0.00%	0.00%	-	0.20%	0.16%	0.00%	0.00%	0.14%	0.00%	3.53%	0.00%	0.00%	0.00%	0.00%	0.00%
C_6H_{14}	0.00%	0.00%	0.00%	0.00%	-	0.00%	0.00%	0.00%	0.00%	0.00%	0.00%	-	0.12%	0.09%	0.00%	0.00%	0.13%	0.00%	7.23%	0.00%	0.00%	0.00%	0.00%	0.00%
C_7H_{16}	0.00%	0.00%	0.00%	0.00%	-	0.00%	0.00%	0.00%	0.00%	0.00%	0.00%	-	0.05%	0.04%	0.00%	0.00%	0.12%	0.03%	9.95%	0.00%	0.00%	0.00%	0.00%	0.00%
C_8H_{18}	0.00%	0.00%	0.00%	0.00%	-	0.00%	0.00%	0.00%	0.00%	0.00%	0.00%	-	0.02%	0.01%	0.00%	0.00%	0.11%	0.10%	25.17%	0.00%	0.00%	0.00%	0.00%	0.00%
C_9H_{20}	0.00%	0.00%	0.00%	0.00%	-	0.00%	0.00%	0.00%	0.00%	0.00%	0.00%	-	0.00%	0.00%	0.00%	0.00%	0.10%	0.46%	30.51%	0.00%	0.00%	0.00%	0.00%	0.00%
$C_{10}H_{22}$	0.00%	0.00%	0.00%	0.00%	-	0.00%	0.00%	0.00%	0.00%	0.00%	0.00%	-	0.00%	0.00%	0.00%	0.00%	0.10%	3.25%	19.48%	0.00%	0.00%	0.00%	0.00%	0.00%
$C_{11}H_{24}$	0.00%	0.00%	0.00%	0.00%	-	0.00%	0.00%	0.00%	0.00%	0.00%	0.00%	-	0.00%	0.00%	0.00%	0.00%	0.09%	5.45%	0.38%	0.00%	0.00%	0.00%	0.00%	0.00%
$C_{12}H_{26}$	0.00%	0.00%	0.00%	0.00%	-	0.00%	0.00%	0.00%	0.00%	0.00%	0.00%	-	0.00%	0.00%	0.00%	0.00%	0.08%	33.48%	0.01%	0.00%	0.00%	0.00%	0.00%	0.00%
$C_{13}H_{28}$	0.00%	0.00%	0.00%	0.00%	-	0.00%	0.00%	0.00%	0.00%	0.00%	0.00%	-	0.00%	0.00%	0.00%	0.00%	0.07%	4.82%	0.00%	0.00%	0.00%	0.00%	0.00%	0.00%
$C_{14}H_{30}$	0.00%	0.00%	0.00%	0.00%	-	0.00%	0.00%	0.00%	0.00%	0.00%	0.00%	-	0.00%	0.00%	0.00%	0.00%	0.07%	22.82%	0.00%	0.00%	0.00%	0.00%	0.00%	0.00%
$C_{15}H_{32}$	0.00%	0.00%	0.00%	0.00%	-	0.00%	0.00%	0.00%	0.00%	0.00%	0.00%	-	0.00%	0.00%	0.00%	0.00%	0.06%	4.08%	0.00%	0.00%	0.00%	0.00%	0.00%	0.00%
$C_{16}H_{34}$	0.00%	0.00%	0.00%	0.00%	-	0.00%	0.00%	0.00%	0.00%	0.00%	0.00%	-	0.00%	0.00%	0.00%	0.00%	0.06%	11.24%	0.00%	0.00%	0.00%	0.00%	0.00%	0.00%
$C_{17}H_{36}$	0.00%	0.00%	0.00%	0.00%	-	0.00%	0.00%	0.00%	0.00%	0.00%	0.00%	-	0.00%	0.00%	0.00%	0.00%	0.05%	3.45%	0.00%	0.00%	0.00%	0.00%	0.00%	0.00%
$C_{18}H_{38}$	0.00%	0.00%	0.00%	0.00%	-	0.00%	0.00%	0.00%	0.00%	0.00%	0.00%	-	0.00%	0.00%	0.00%	0.00%	0.05%	3.18%	0.00%	0.00%	0.00%	0.00%	0.00%	0.00%
$C_{19}H_{40}$	0.00%	0.00%	0.00%	0.00%	-	0.00%	0.00%	0.00%	0.00%	0.00%	0.00%	-	0.00%	0.00%	0.00%	0.00%	0.04%	2.92%	0.00%	0.00%	0.00%	0.00%	0.00%	0.00%
$C_{20}H_{42}$	0.00%	0.00%	0.00%	0.00%	-	0.00%	0.00%	0.00%	0.00%	0.00%	0.00%	-	0.00%	0.00%	0.00%	0.00%	0.04%	2.69%	0.00%	0.00%	0.00%	0.00%	0.00%	0.00%
$C_{24}H_{50}$	0.00%	0.00%	0.00%	0.00%	-	0.00%	0.00%	0.00%	0.00%	0.00%	0.00%	-	0.00%	0.00%	0.00%	0.00%	0.13%	0.32%	0.00%	0.00%	0.00%	0.00%	0.00%	0.00%
C_{28}+	0.00%	0.00%	0.00%	0.00%	-	0.00%	0.00%	0.00%	0.00%	0.00%	0.00%	-	0.00%	0.00%	0.00%	0.00%	0.33%	0.00%	0.00%	0.00%	0.00%	0.00%	0.00%	0.00%
Total	100.00%	100.00%	100.00%	100.00%	0.00%	100.00%	100.00%	100.00%	100.00%	100.00%	100.00%	0.00%	100.00%	100.00%	100.00%	100.00%	100.00%	100.00%	100.00%	100.00%	100.00%	100.00%	100.00%	100.00%

Notes:

* For CCS Enabled Cases Only

‡ For CCS Disabled Cases Only

Chapter 2

Supplementary Material for "Combining coal gasification, natural gas reforming, and external carbonless heat for efficient production of gasoline and diesel with CO $_2$ capture and sequestration"

by: Yaser Khojasteh Salkuyeh, Thomas A. Adams II

Case 3 **Without Nuclear Heat**

Stream No.	1	2	3	4	5	6	7	8	9	10	11	12	13	14	15	16	17	18	19	20*	21*	22‡	23	24×
Temperature (°C)	60.0	30.0	204.8	534.8	32.2	32.0	82.0	32.0	46.0	80.0	188.9	15.0	-	15.0	950.0	40.8	240.0	229.3	119.0	-7.0	57.0	-7.0	-	15.0
Pressure (bar)	72.4	30.0	55.0	29.1	10.0	10.0	67.6	10.0	2.1	54.3	1.8	32.0	-	32.0	39.0	35.4	35.0	2.3	2.8	1.0	153.0	1.0	-	32.0
Total Flow (kg/hr)	61629	63757	158495	186074	68171	814	48770	38696	5610	210342	1544	61410	-	245642	328819	460420	460420	43991	16089	121737	121614	121737	-	3071
Vapor Fraction	0.00	1.00	1.00	1.00	1.00	1.00	1.00	1.00	0.99	1.00	0.00	1.00	-	1.00	1.00	1.00	0.99	0.00	0.00	1.00	0.00	1.00	-	1.00
Mole Percent																								
Coal	100.00%	0.00%	0.00%	0.00%	0.00%	0.00%	0.00%	0.00%	0.00%	0.00%	0.00%	0.00%	-	0.00%	0.00%	0.00%	0.00%	0.00%	0.00%	0.00%	0.00%	0.00%	-	0.00%
CO	0.00%	0.00%	31.40%	0.48%	0.00%	0.00%	0.00%	0.00%	0.00%	20.25%	0.00%	18.18%	-	18.18%	14.11%	25.81%	13.49%	0.00%	0.03%	2.37%	1.39%	2.37%	-	19.54%
CO_2	0.00%	0.38%	8.42%	5.43%	0.00%	0.00%	0.00%	0.00%	46.07%	9.11%	0.00%	4.04%	-	4.04%	7.29%	1.85%	3.01%	0.00%	0.29%	95.89%	97.84%	95.89%	-	2.84%
H_2	0.00%	0.00%	23.75%	10.97%	0.00%	0.00%	0.00%	0.00%	0.00%	62.68%	0.00%	36.64%	-	36.64%	28.40%	53.15%	27.18%	0.00%	0.03%	0.88%	0.51%	0.88%	-	39.08%
H_2O	0.00%	0.00%	35.32%	31.34%	0.00%	0.00%	0.00%	0.00%	4.26%	0.25%	4.61%	0.06%	-	0.06%	21.43%	0.09%	24.68%	1.75%	0.93%	0.42%	0.00%	0.42%	-	0.06%
N_2	0.00%	0.47%	0.38%	8.87%	0.19%	0.19%	0.19%	0.19%	17.77%	5.71%	0.00%	30.34%	-	30.34%	23.05%	15.08%	22.52%	0.00%	0.05%	0.17%	0.10%	0.17%	-	28.95%
AR	0.00%	0.00%	0.06%	2.10%	0.32%	0.32%	0.32%	0.32%	0.00%	1.39%	0.00%	7.35%	-	7.35%	5.60%	3.66%	5.46%	0.00%	0.03%	0.09%	0.05%	0.09%	-	4.59%
NH_3	0.00%	0.00%	0.00%	0.00%	0.00%	0.00%	0.00%	0.00%	0.00%	0.00%	0.00%	0.00%	-	0.00%	0.00%	0.00%	0.00%	0.00%	0.00%	0.00%	0.00%	0.00%	-	0.00%
H_2S	0.00%	0.00%	0.57%	0.00%	0.00%	0.00%	0.00%	0.00%	31.91%	0.00%	0.00%	0.00%	-	0.00%	0.00%	0.00%	0.00%	0.00%	0.00%	0.00%	0.00%	0.00%	-	0.00%
O_2	0.00%	0.00%	0.00%	0.00%	0.00%	0.00%	0.00%	0.00%	0.00%	0.00%	0.00%	0.00%	-	0.00%	0.00%	0.00%	0.00%	0.00%	0.00%	0.00%	0.00%	0.00%	-	0.00%
SO_2	0.00%	0.00%	0.00%	0.00%	99.49%	99.49%	99.49%	99.49%	0.00%	0.00%	0.00%	0.00%	-	0.00%	0.00%	0.00%	0.00%	0.00%	0.00%	0.00%	0.00%	0.00%	-	0.00%
COS	0.00%	0.00%	0.03%	0.00%	0.00%	0.00%	0.00%	0.00%	0.00%	0.00%	0.00%	0.00%	-	0.00%	0.00%	0.00%	0.00%	0.00%	0.00%	0.00%	0.00%	0.00%	-	0.00%
Cl_2	0.00%	0.00%	0.00%	0.00%	0.00%	0.00%	0.00%	0.00%	0.00%	0.00%	0.00%	0.00%	-	0.00%	0.00%	0.00%	0.00%	0.00%	0.00%	0.00%	0.00%	0.00%	-	0.00%
HCl	0.00%	0.00%	0.06%	0.04%	0.00%	0.00%	0.00%	0.00%	0.00%	0.03%	0.00%	0.15%	-	0.15%	0.11%	0.08%	0.11%	0.00%	0.02%	0.00%	0.00%	0.00%	-	0.18%
Sulfur	0.00%	0.00%	0.00%	0.00%	0.00%	0.00%	0.00%	0.00%	0.00%	0.00%	95.38%	0.00%	-	0.00%	0.00%	0.00%	0.00%	0.00%	0.00%	0.00%	0.00%	0.00%	-	0.00%
CH_4	0.00%	97.01%	0.01%	40.75%	0.00%	0.00%	0.00%	0.00%	0.00%	0.57%	0.00%	2.26%	-	2.26%	0.00%	0.29%	1.68%	0.00%	0.02%	0.18%	0.11%	0.18%	-	3.72%
C_2H_4	0.00%	0.00%	0.00%	0.00%	0.00%	0.00%	0.00%	0.00%	0.00%	0.00%	0.00%	0.01%	-	0.01%	0.00%	0.00%	0.01%	0.00%	0.00%	0.00%	0.00%	0.00%	-	0.01%
C_2H_6	0.00%	1.76%	0.00%	0.00%	0.00%	0.00%	0.00%	0.00%	0.00%	0.00%	0.00%	0.17%	-	0.17%	0.00%	0.00%	0.13%	0.00%	0.03%	0.00%	0.00%	0.00%	-	0.18%
C_3H_6	0.00%	0.00%	0.00%	0.00%	0.00%	0.00%	0.00%	0.00%	0.00%	0.00%	0.00%	0.22%	-	0.22%	0.00%	0.00%	0.17%	0.00%	0.20%	0.00%	0.00%	0.00%	-	0.24%
C_3H_8	0.00%	0.26%	0.00%	0.00%	0.00%	0.00%	0.00%	0.00%	0.00%	0.00%	0.00%	0.11%	-	0.11%	0.00%	0.00%	0.08%	0.00%	0.13%	0.00%	0.00%	0.00%	-	0.12%
C_4H_8	0.00%	0.00%	0.00%	0.00%	0.00%	0.00%	0.00%	0.00%	0.00%	0.00%	0.00%	0.16%	-	0.16%	0.00%	0.00%	0.13%	0.00%	0.75%	0.00%	0.00%	0.00%	-	0.17%
C_4H_{10}	0.00%	0.11%	0.00%	0.00%	0.00%	0.00%	0.00%	0.00%	0.00%	0.00%	0.00%	0.08%	-	0.08%	0.00%	0.00%	0.06%	0.00%	0.45%	0.00%	0.00%	0.00%	-	0.08%
C_5H_{12}	0.00%	0.00%	0.00%	0.00%	0.00%	0.00%	0.00%	0.00%	0.00%	0.00%	0.00%	0.12%	-	0.12%	0.00%	0.00%	0.11%	0.00%	2.66%	0.00%	0.00%	0.00%	-	0.12%
C_6H_{14}	0.00%	0.00%	0.00%	0.00%	0.00%	0.00%	0.00%	0.00%	0.00%	0.00%	0.00%	0.07%	-	0.07%	0.00%	0.00%	0.10%	0.00%	6.10%	0.00%	0.00%	0.00%	-	0.08%
C_7H_{16}	0.00%	0.00%	0.00%	0.00%	0.00%	0.00%	0.00%	0.00%	0.00%	0.00%	0.00%	0.04%	-	0.04%	0.00%	0.00%	0.09%	0.03%	9.40%	0.00%	0.00%	0.00%	-	0.04%
C_8H_{18}	0.00%	0.00%	0.00%	0.00%	0.00%	0.00%	0.00%	0.00%	0.00%	0.00%	0.00%	0.01%	-	0.01%	0.00%	0.00%	0.08%	0.12%	26.17%	0.00%	0.00%	0.00%	-	0.01%
C_9H_{20}	0.00%	0.00%	0.00%	0.00%	0.00%	0.00%	0.00%	0.00%	0.00%	0.00%	0.00%	0.00%	-	0.00%	0.00%	0.00%	0.08%	0.55%	32.24%	0.00%	0.00%	0.00%	-	0.00%
$C_{10}H_{22}$	0.00%	0.00%	0.00%	0.00%	0.00%	0.00%	0.00%	0.00%	0.00%	0.00%	0.00%	0.00%	-	0.00%	0.00%	0.00%	0.07%	3.60%	20.13%	0.00%	0.00%	0.00%	-	0.00%
$C_{11}H_{24}$	0.00%	0.00%	0.00%	0.00%	0.00%	0.00%	0.00%	0.00%	0.00%	0.00%	0.00%	0.00%	-	0.00%	0.00%	0.00%	0.06%	5.47%	0.33%	0.00%	0.00%	0.00%	-	0.00%
$C_{12}H_{26}$	0.00%	0.00%	0.00%	0.00%	0.00%	0.00%	0.00%	0.00%	0.00%	0.00%	0.00%	0.00%	-	0.00%	0.00%	0.00%	0.06%	32.97%	0.01%	0.00%	0.00%	0.00%	-	0.00%
$C_{13}H_{28}$	0.00%	0.00%	0.00%	0.00%	0.00%	0.00%	0.00%	0.00%	0.00%	0.00%	0.00%	0.00%	-	0.00%	0.00%	0.00%	0.05%	4.80%	0.00%	0.00%	0.00%	0.00%	-	0.00%
$C_{14}H_{30}$	0.00%	0.00%	0.00%	0.00%	0.00%	0.00%	0.00%	0.00%	0.00%	0.00%	0.00%	0.00%	-	0.00%	0.00%	0.00%	0.05%	22.74%	0.00%	0.00%	0.00%	0.00%	-	0.00%
$C_{15}H_{32}$	0.00%	0.00%	0.00%	0.00%	0.00%	0.00%	0.00%	0.00%	0.00%	0.00%	0.00%	0.00%	-	0.00%	0.00%	0.00%	0.05%	4.06%	0.00%	0.00%	0.00%	0.00%	-	0.00%
$C_{16}H_{34}$	0.00%	0.00%	0.00%	0.00%	0.00%	0.00%	0.00%	0.00%	0.00%	0.00%	0.00%	0.00%	-	0.00%	0.00%	0.00%	0.04%	11.20%	0.00%	0.00%	0.00%	0.00%	-	0.00%
$C_{17}H_{36}$	0.00%	0.00%	0.00%	0.00%	0.00%	0.00%	0.00%	0.00%	0.00%	0.00%	0.00%	0.00%	-	0.00%	0.00%	0.00%	0.04%	3.44%	0.00%	0.00%	0.00%	0.00%	-	0.00%
$C_{18}H_{38}$	0.00%	0.00%	0.00%	0.00%	0.00%	0.00%	0.00%	0.00%	0.00%	0.00%	0.00%	0.00%	-	0.00%	0.00%	0.00%	0.04%	3.16%	0.00%	0.00%	0.00%	0.00%	-	0.00%
$C_{19}H_{40}$	0.00%	0.00%	0.00%	0.00%	0.00%	0.00%	0.00%	0.00%	0.00%	0.00%	0.00%	0.00%	-	0.00%	0.00%	0.00%	0.03%	2.91%	0.00%	0.00%	0.00%	0.00%	-	0.00%
$C_{20}H_{42}$	0.00%	0.00%	0.00%	0.00%	0.00%	0.00%	0.00%	0.00%	0.00%	0.00%	0.00%	0.00%	-	0.00%	0.00%	0.00%	0.03%	2.68%	0.00%	0.00%	0.00%	0.00%	-	0.00%
$C_{24}H_{50}$	0.00%	0.00%	0.00%	0.00%	0.00%	0.00%	0.00%	0.00%	0.00%	0.00%	0.00%	0.00%	-	0.00%	0.00%	0.00%	0.10%	0.51%	0.00%	0.00%	0.00%	0.00%	-	0.00%
C_{28}+	0.00%	0.00%	0.00%	0.00%	0.00%	0.00%	0.00%	0.00%	0.00%	0.00%	0.00%	0.00%	-	0.00%	0.00%	0.00%	0.24%	0.00%	0.00%	0.00%	0.00%	0.00%	-	0.00%
Total	100.00%	100.00%	100.00%	100.00%	100.00%	100.00%	100.00%	100.00%	100.00%	100.00%	100.00%	100.00%	0.00%	100.00%	100.00%	100.00%	100.00%	100.00%	100.00%	100.00%	100.00%	100.00%	0.00%	100.00%

Notes:

* For CCS Enabled Cases Only

‡ For CCS Disabled Cases Only

× Purge stream of FT light gases, sent to the Flare

Chapter 2

Supplementary Material for "Combining coal gasification, natural gas reforming, and external carbonless heat for efficient production of gasoline and diesel with CO_2 capture and sequestration"

by: Yaser Khojasteh Salkuyeh, Thomas A. Adams II

Case 3 **With Nuclear Heat**

Stream No.	1	2	3	4	5	6	7	8	9	10	11	12	13	14	15	16	17	18	19	20*	21*	22‡	23	24×
Temperature (°C)	60.0	30.0	204.8	551.1	-	32.0	82.0	32.0	46.0	80.0	189.9	15.0	-	15.0	950.0	13.5	240.0	229.3	119.0	-7.0	65.8	-7.0	-	15.0
Pressure (bar)	72.4	30.0	55.0	29.1	-	10.0	67.6	10.0	2.1	54.3	1.8	32.0	-	32.0	39.0	35.9	35.0	2.3	2.8	1.0	153.0	1.0	-	32.0
Total Flow (kg/hr)	68696	43800	176668	144303	-	906	54362	38103	4495	149869	1723	52770	-	211079	284316	415590	415590	43475	16051	85354	85243	85354	-	2638
Vapor Fraction	0.00	1.00	1.00	1.00	-	1.00	1.00	1.00	1.00	1.00	0.00	1.00	-	1.00	1.00	1.00	0.99	0.00	0.00	1.00	0.00	1.00	-	1.00
Mole Percent																								
Coal	100.00%	0.00%	0.00%	0.00%	-	0.00%	0.00%	0.00%	0.00%	0.00%	0.00%	0.00%	-	0.00%	0.00%	0.00%	0.00%	0.00%	0.00%	0.00%	0.00%	0.00%	-	0.00%
CO	0.00%	0.00%	31.40%	0.63%	-	0.00%	0.00%	0.00%	0.00%	19.68%	0.00%	19.54%	-	19.54%	16.29%	26.74%	14.23%	0.00%	0.04%	3.62%	1.89%	3.62%	-	26.02%
CO_2	0.00%	0.38%	8.42%	5.83%	-	0.00%	0.00%	0.00%	33.87%	3.96%	0.00%	2.84%	-	2.84%	6.42%	1.19%	2.08%	0.00%	0.21%	93.25%	96.80%	93.25%	-	5.47%
H_2	0.00%	0.00%	23.75%	12.25%	-	0.00%	0.00%	0.00%	0.00%	67.37%	0.00%	39.08%	-	39.08%	32.84%	54.92%	28.43%	0.00%	0.03%	1.33%	0.69%	1.33%	-	52.15%
H_2O	0.00%	0.00%	35.32%	31.86%	-	0.00%	0.00%	0.00%	4.65%	0.25%	5.92%	0.06%	-	0.06%	18.91%	0.09%	26.03%	1.75%	0.95%	0.60%	0.00%	0.60%	-	0.06%
N_2	0.00%	0.47%	0.38%	9.97%	-	0.19%	0.19%	0.19%	18.76%	5.78%	0.00%	28.95%	-	28.95%	21.92%	13.86%	21.07%	0.00%	0.05%	0.24%	0.13%	0.24%	-	8.18%
AR	0.00%	0.00%	0.06%	1.55%	-	0.32%	0.32%	0.32%	0.00%	0.90%	0.00%	4.59%	-	4.59%	3.49%	2.20%	3.34%	0.00%	0.02%	0.08%	0.04%	0.08%	-	0.98%
NH_3	0.00%	0.00%	0.00%	0.00%	-	0.00%	0.00%	0.00%	0.00%	0.00%	0.00%	0.00%	-	0.00%	0.00%	0.00%	0.00%	0.00%	0.00%	0.00%	0.00%	0.00%	-	0.00%
H_2S	0.00%	0.00%	0.57%	0.00%	-	0.00%	0.00%	0.00%	42.72%	0.00%	0.00%	0.00%	-	0.00%	0.00%	0.00%	0.00%	0.00%	0.00%	0.00%	0.00%	0.00%	-	0.00%
O_2	0.00%	0.00%	0.00%	0.00%	-	0.00%	0.00%	0.00%	0.00%	0.00%	0.00%	0.00%	-	0.00%	0.00%	0.00%	0.00%	0.00%	0.00%	0.00%	0.00%	0.00%	-	0.00%
SO_2	0.00%	0.00%	0.00%	0.00%	-	99.49%	99.49%	99.49%	0.00%	0.00%	0.00%	0.00%	-	0.00%	0.00%	0.00%	0.00%	0.00%	0.00%	0.00%	0.00%	0.00%	-	0.00%
COS	0.00%	0.00%	0.03%	0.00%	-	0.00%	0.00%	0.00%	0.00%	0.00%	0.00%	0.00%	-	0.00%	0.00%	0.00%	0.00%	0.00%	0.00%	0.00%	0.00%	0.00%	-	0.00%
Cl_2	0.00%	0.00%	0.00%	0.00%	-	0.00%	0.00%	0.00%	0.00%	0.00%	0.00%	0.00%	-	0.00%	0.00%	0.00%	0.00%	0.00%	0.00%	0.00%	0.00%	0.00%	-	0.00%
HCl	0.00%	0.00%	0.06%	0.06%	-	0.00%	0.00%	0.00%	0.00%	0.03%	0.00%	0.18%	-	0.18%	0.13%	0.09%	0.13%	0.00%	0.03%	0.00%	0.00%	0.00%	-	0.09%
Sulfur	0.00%	0.00%	0.00%	0.00%	-	0.00%	0.00%	0.00%	0.00%	0.00%	94.08%	0.00%	-	0.00%	0.00%	0.00%	0.00%	0.00%	0.00%	0.00%	0.00%	0.00%	-	0.00%
CH_4	0.00%	97.01%	0.01%	37.84%	-	0.00%	0.00%	0.00%	0.00%	2.03%	0.00%	3.72%	-	3.72%	0.00%	0.91%	2.71%	0.00%	0.03%	0.88%	0.46%	0.88%	-	5.70%
C_2H_4	0.00%	0.00%	0.00%	0.00%	-	0.00%	0.00%	0.00%	0.00%	0.00%	0.00%	0.01%	-	0.01%	0.00%	0.00%	0.01%	0.00%	0.00%	0.00%	0.00%	0.00%	-	0.01%
C_2H_6	0.00%	1.76%	0.00%	0.00%	-	0.00%	0.00%	0.00%	0.00%	0.00%	0.00%	0.18%	-	0.18%	0.00%	0.00%	0.13%	0.00%	0.03%	0.00%	0.00%	0.00%	-	0.24%
C_3H_6	0.00%	0.00%	0.00%	0.00%	-	0.00%	0.00%	0.00%	0.00%	0.00%	0.00%	0.24%	-	0.24%	0.00%	0.00%	0.18%	0.00%	0.22%	0.00%	0.00%	0.00%	-	0.31%
C_3H_8	0.00%	0.26%	0.00%	0.00%	-	0.00%	0.00%	0.00%	0.00%	0.00%	0.00%	0.12%	-	0.12%	0.00%	0.00%	0.09%	0.00%	0.14%	0.00%	0.00%	0.00%	-	0.16%
C_4H_8	0.00%	0.00%	0.00%	0.00%	-	0.00%	0.00%	0.00%	0.00%	0.00%	0.00%	0.17%	-	0.17%	0.00%	0.00%	0.13%	0.00%	0.80%	0.00%	0.00%	0.00%	-	0.22%
C_4H_{10}	0.00%	0.11%	0.00%	0.00%	-	0.00%	0.00%	0.00%	0.00%	0.00%	0.00%	0.08%	-	0.08%	0.00%	0.00%	0.07%	0.00%	0.49%	0.00%	0.00%	0.00%	-	0.11%
C_5H_{12}	0.00%	0.00%	0.00%	0.00%	-	0.00%	0.00%	0.00%	0.00%	0.00%	0.00%	0.12%	-	0.12%	0.00%	0.00%	0.11%	0.00%	2.80%	0.00%	0.00%	0.00%	-	0.15%
C_6H_{14}	0.00%	0.00%	0.00%	0.00%	-	0.00%	0.00%	0.00%	0.00%	0.00%	0.00%	0.08%	-	0.08%	0.00%	0.00%	0.10%	0.00%	6.30%	0.00%	0.00%	0.00%	-	0.09%
C_7H_{16}	0.00%	0.00%	0.00%	0.00%	-	0.00%	0.00%	0.00%	0.00%	0.00%	0.00%	0.04%	-	0.04%	0.00%	0.00%	0.09%	0.03%	9.52%	0.00%	0.00%	0.00%	-	0.04%
C_8H_{18}	0.00%	0.00%	0.00%	0.00%	-	0.00%	0.00%	0.00%	0.00%	0.00%	0.00%	0.01%	-	0.01%	0.00%	0.00%	0.09%	0.11%	26.01%	0.00%	0.00%	0.00%	-	0.01%
C_9H_{20}	0.00%	0.00%	0.00%	0.00%	-	0.00%	0.00%	0.00%	0.00%	0.00%	0.00%	0.00%	-	0.00%	0.00%	0.00%	0.08%	0.53%	31.96%	0.00%	0.00%	0.00%	-	0.00%
$C_{10}H_{22}$	0.00%	0.00%	0.00%	0.00%	-	0.00%	0.00%	0.00%	0.00%	0.00%	0.00%	0.00%	-	0.00%	0.00%	0.00%	0.07%	3.54%	20.03%	0.00%	0.00%	0.00%	-	0.00%
$C_{11}H_{24}$	0.00%	0.00%	0.00%	0.00%	-	0.00%	0.00%	0.00%	0.00%	0.00%	0.00%	0.00%	-	0.00%	0.00%	0.00%	0.07%	5.47%	0.34%	0.00%	0.00%	0.00%	-	0.00%
$C_{12}H_{26}$	0.00%	0.00%	0.00%	0.00%	-	0.00%	0.00%	0.00%	0.00%	0.00%	0.00%	0.00%	-	0.00%	0.00%	0.00%	0.06%	33.00%	0.01%	0.00%	0.00%	0.00%	-	0.00%
$C_{13}H_{28}$	0.00%	0.00%	0.00%	0.00%	-	0.00%	0.00%	0.00%	0.00%	0.00%	0.00%	0.00%	-	0.00%	0.00%	0.00%	0.06%	4.81%	0.00%	0.00%	0.00%	0.00%	-	0.00%
$C_{14}H_{30}$	0.00%	0.00%	0.00%	0.00%	-	0.00%	0.00%	0.00%	0.00%	0.00%	0.00%	0.00%	-	0.00%	0.00%	0.00%	0.05%	22.76%	0.00%	0.00%	0.00%	0.00%	-	0.00%
$C_{15}H_{32}$	0.00%	0.00%	0.00%	0.00%	-	0.00%	0.00%	0.00%	0.00%	0.00%	0.00%	0.00%	-	0.00%	0.00%	0.00%	0.05%	4.07%	0.00%	0.00%	0.00%	0.00%	-	0.00%
$C_{16}H_{34}$	0.00%	0.00%	0.00%	0.00%	-	0.00%	0.00%	0.00%	0.00%	0.00%	0.00%	0.00%	-	0.00%	0.00%	0.00%	0.04%	11.21%	0.00%	0.00%	0.00%	0.00%	-	0.00%
$C_{17}H_{36}$	0.00%	0.00%	0.00%	0.00%	-	0.00%	0.00%	0.00%	0.00%	0.00%	0.00%	0.00%	-	0.00%	0.00%	0.00%	0.04%	3.44%	0.00%	0.00%	0.00%	0.00%	-	0.00%
$C_{18}H_{38}$	0.00%	0.00%	0.00%	0.00%	-	0.00%	0.00%	0.00%	0.00%	0.00%	0.00%	0.00%	-	0.00%	0.00%	0.00%	0.04%	3.17%	0.00%	0.00%	0.00%	0.00%	-	0.00%
$C_{19}H_{40}$	0.00%	0.00%	0.00%	0.00%	-	0.00%	0.00%	0.00%	0.00%	0.00%	0.00%	0.00%	-	0.00%	0.00%	0.00%	0.03%	2.91%	0.00%	0.00%	0.00%	0.00%	-	0.00%
$C_{20}H_{42}$	0.00%	0.00%	0.00%	0.00%	-	0.00%	0.00%	0.00%	0.00%	0.00%	0.00%	0.00%	-	0.00%	0.00%	0.00%	0.03%	2.68%	0.00%	0.00%	0.00%	0.00%	-	0.00%
$C_{24}H_{50}$	0.00%	0.00%	0.00%	0.00%	-	0.00%	0.00%	0.00%	0.00%	0.00%	0.00%	0.00%	-	0.00%	0.00%	0.00%	0.10%	0.51%	0.00%	0.00%	0.00%	0.00%	-	0.00%
C_{28}+	0.00%	0.00%	0.00%	0.00%	-	0.00%	0.00%	0.00%	0.00%	0.00%	0.00%	0.00%	-	0.00%	0.00%	0.00%	0.25%	0.00%	0.00%	0.00%	0.00%	0.00%	-	0.00%
Total	100.00%	100.00%	100.00%	100.00%	0.00%	100.00%	100.00%	100.00%	100.00%	100.00%	100.00%	100.00%	0.00%	100.00%	100.00%	100.00%	100.00%	100.00%	100.00%	100.00%	100.00%	100.00%	0.00%	100.00%

Notes:

* For CCS Enabled Cases Only

‡ For CCS Disabled Cases Only

× Purge stream of FT light gases, sent to the Flare

Chapter 2

Supplementary Material for "Combining coal gasification, natural gas reforming, and external carbonless heat for efficient production of gasoline and diesel with CO_2 capture and sequestration"

by: Yaser Khojasteh Salkuyeh, Thomas A. Adams II

Case 4 **Without Nuclear Heat**

Stream No.	1	2	3	4	5	6	7	8	9	10	11	12	13	14	15	16	17	18	19	20*	21*	22‡	23	24×
Temperature (°C)	60.0	30.0	204.8	631.8	32.2	32.0	82.0	-	46.0	80.0	188.9	15.0	-	-	-	32.8	240.0	229.2	108.7	-7.0	67.3	-7.0	-	14.6
Pressure (bar)	72.4	30.0	55.0	29.1	10.0	10.0	67.6	-	2.1	54.3	1.8	32.0	-	-	-	52.0	35.0	2.3	2.8	1.0	153.0	1.0	-	29.5
Total Flow (kg/hr)	61674	57684	158611	347917	84075	816	48806	-	7173	318404	1544	172347	-	-	-	318593	318593	42721	15910	104619	104456	104619	-	8617
Vapor Fraction	0.00	1.00	1.00	1.00	1.00	1.00	1.00	-	0.99	1.00	0.00	1.00	-	-	-	1.00	0.99	0.00	0.00	1.00	0.00	1.00	-	1.00
Mole Percent																								
Coal	100.00%	0.00%	0.00%	0.00%	0.00%	0.00%	0.00%	-	0.00%	0.00%	0.00%	0.00%	-	-	-	0.00%	0.00%	0.00%	0.00%	0.00%	0.00%	0.00%	-	0.00%
CO	0.00%	0.00%	31.40%	2.68%	0.00%	0.00%	0.00%	-	0.00%	22.74%	0.00%	25.49%	-	-	-	30.12%	17.15%	0.00%	0.04%	2.13%	2.14%	2.13%	-	25.49%
CO_2	0.00%	0.38%	8.42%	11.21%	0.00%	0.00%	0.00%	-	55.25%	11.04%	0.00%	8.41%	-	-	-	3.31%	5.70%	0.00%	0.54%	96.38%	96.74%	96.38%	-	8.41%
H_2	0.00%	0.00%	23.75%	18.39%	0.00%	0.00%	0.00%	-	0.00%	60.34%	0.00%	49.90%	-	-	-	61.41%	33.56%	0.00%	0.04%	0.77%	0.78%	0.77%	-	49.90%
H_2O	0.00%	0.00%	35.32%	34.54%	0.00%	0.00%	0.00%	-	4.53%	0.25%	3.93%	0.06%	-	-	-	0.01%	31.23%	1.74%	0.99%	0.37%	0.00%	0.37%	-	0.06%
N_2	0.00%	0.47%	0.38%	4.85%	0.19%	0.19%	0.19%	-	14.48%	4.08%	0.00%	9.07%	-	-	-	3.75%	6.10%	0.00%	0.01%	0.12%	0.12%	0.12%	-	9.07%
AR	0.00%	0.00%	0.06%	1.14%	0.32%	0.32%	0.32%	-	0.00%	0.99%	0.00%	2.17%	-	-	-	0.90%	1.46%	0.00%	0.01%	0.06%	0.06%	0.06%	-	2.17%
NH_3	0.00%	0.00%	0.00%	0.00%	0.00%	0.00%	0.00%	-	0.00%	0.00%	0.00%	0.00%	-	-	-	0.00%	0.00%	0.00%	0.00%	0.00%	0.00%	0.00%	-	0.00%
H_2S	0.00%	0.00%	0.57%	0.00%	0.00%	0.00%	0.00%	-	25.74%	0.00%	0.00%	0.00%	-	-	-	0.00%	0.00%	0.00%	0.00%	0.00%	0.00%	0.00%	-	0.00%
O_2	0.00%	0.00%	0.00%	0.00%	0.00%	0.00%	0.00%	-	0.00%	0.00%	0.00%	0.00%	-	-	-	0.00%	0.00%	0.00%	0.00%	0.00%	0.00%	0.00%	-	0.00%
SO_2	0.00%	0.00%	0.00%	0.00%	99.49%	99.49%	99.49%	-	0.00%	0.00%	0.00%	0.00%	-	-	-	0.00%	0.00%	0.00%	0.00%	0.00%	0.00%	0.00%	-	0.00%
COS	0.00%	0.00%	0.03%	0.00%	0.00%	0.00%	0.00%	-	0.00%	0.00%	0.00%	0.00%	-	-	-	0.00%	0.00%	0.00%	0.00%	0.00%	0.00%	0.00%	-	0.00%
Cl_2	0.00%	0.00%	0.00%	0.00%	0.00%	0.00%	0.00%	-	0.00%	0.00%	0.00%	0.00%	-	-	-	0.00%	0.00%	0.00%	0.00%	0.00%	0.00%	0.00%	-	0.00%
HCl	0.00%	0.00%	0.06%	0.04%	0.00%	0.00%	0.00%	-	0.00%	0.03%	0.00%	0.07%	-	-	-	0.03%	0.05%	0.00%	0.01%	0.00%	0.00%	0.00%	-	0.07%
Sulfur	0.00%	0.00%	0.00%	0.00%	0.00%	0.00%	0.00%	-	0.00%	0.00%	96.06%	0.00%	-	-	-	0.00%	0.00%	0.00%	0.00%	0.00%	0.00%	0.00%	-	0.00%
CH_4	0.00%	97.01%	0.01%	27.15%	0.00%	0.00%	0.00%	-	0.00%	0.53%	0.00%	3.50%	-	-	-	0.47%	2.36%	0.00%	0.03%	0.16%	0.16%	0.16%	-	3.50%
C_2H_4	0.00%	0.00%	0.00%	0.00%	0.00%	0.00%	0.00%	-	0.00%	0.00%	0.00%	0.01%	-	-	-	0.00%	0.01%	0.00%	0.00%	0.00%	0.00%	0.00%	-	0.01%
C_2H_6	0.00%	1.76%	0.00%	0.00%	0.00%	0.00%	0.00%	-	0.00%	0.00%	0.00%	0.23%	-	-	-	0.00%	0.16%	0.00%	0.04%	0.00%	0.00%	0.00%	-	0.23%
C_3H_6	0.00%	0.00%	0.00%	0.00%	0.00%	0.00%	0.00%	-	0.00%	0.00%	0.00%	0.31%	-	-	-	0.00%	0.21%	0.00%	0.26%	0.00%	0.00%	0.00%	-	0.31%
C_3H_8	0.00%	0.26%	0.00%	0.00%	0.00%	0.00%	0.00%	-	0.00%	0.00%	0.00%	0.15%	-	-	-	0.00%	0.11%	0.00%	0.16%	0.00%	0.00%	0.00%	-	0.15%
C_4H_8	0.00%	0.00%	0.00%	0.00%	0.00%	0.00%	0.00%	-	0.00%	0.00%	0.00%	0.22%	-	-	-	0.00%	0.16%	0.00%	0.96%	0.00%	0.00%	0.00%	-	0.22%
C_4H_{10}	0.00%	0.11%	0.00%	0.00%	0.00%	0.00%	0.00%	-	0.00%	0.00%	0.00%	0.11%	-	-	-	0.00%	0.08%	0.00%	0.57%	0.00%	0.00%	0.00%	-	0.11%
C_5H_{12}	0.00%	0.00%	0.00%	0.00%	0.00%	0.00%	0.00%	-	0.00%	0.00%	0.00%	0.15%	-	-	-	0.00%	0.13%	0.00%	3.25%	0.00%	0.00%	0.00%	-	0.15%
C_6H_{14}	0.00%	0.00%	0.00%	0.00%	0.00%	0.00%	0.00%	-	0.00%	0.00%	0.00%	0.09%	-	-	-	0.00%	0.12%	0.00%	6.92%	0.00%	0.00%	0.00%	-	0.09%
C_7H_{16}	0.00%	0.00%	0.00%	0.00%	0.00%	0.00%	0.00%	-	0.00%	0.00%	0.00%	0.04%	-	-	-	0.00%	0.11%	0.03%	9.81%	0.00%	0.00%	0.00%	-	0.04%
C_8H_{18}	0.00%	0.00%	0.00%	0.00%	0.00%	0.00%	0.00%	-	0.00%	0.00%	0.00%	0.01%	-	-	-	0.00%	0.10%	0.11%	25.43%	0.00%	0.00%	0.00%	-	0.01%
C_9H_{20}	0.00%	0.00%	0.00%	0.00%	0.00%	0.00%	0.00%	-	0.00%	0.00%	0.00%	0.00%	-	-	-	0.00%	0.10%	0.48%	30.93%	0.00%	0.00%	0.00%	-	0.00%
$C_{10}H_{22}$	0.00%	0.00%	0.00%	0.00%	0.00%	0.00%	0.00%	-	0.00%	0.00%	0.00%	0.00%	-	-	-	0.00%	0.09%	3.35%	19.63%	0.00%	0.00%	0.00%	-	0.00%
$C_{11}H_{24}$	0.00%	0.00%	0.00%	0.00%	0.00%	0.00%	0.00%	-	0.00%	0.00%	0.00%	0.00%	-	-	-	0.00%	0.08%	5.47%	0.36%	0.00%	0.00%	0.00%	-	0.00%
$C_{12}H_{26}$	0.00%	0.00%	0.00%	0.00%	0.00%	0.00%	0.00%	-	0.00%	0.00%	0.00%	0.00%	-	-	-	0.00%	0.07%	33.10%	0.01%	0.00%	0.00%	0.00%	-	0.00%
$C_{13}H_{28}$	0.00%	0.00%	0.00%	0.00%	0.00%	0.00%	0.00%	-	0.00%	0.00%	0.00%	0.00%	-	-	-	0.00%	0.07%	4.82%	0.00%	0.00%	0.00%	0.00%	-	0.00%
$C_{14}H_{30}$	0.00%	0.00%	0.00%	0.00%	0.00%	0.00%	0.00%	-	0.00%	0.00%	0.00%	0.00%	-	-	-	0.00%	0.06%	22.83%	0.00%	0.00%	0.00%	0.00%	-	0.00%
$C_{15}H_{32}$	0.00%	0.00%	0.00%	0.00%	0.00%	0.00%	0.00%	-	0.00%	0.00%	0.00%	0.00%	-	-	-	0.00%	0.06%	4.08%	0.00%	0.00%	0.00%	0.00%	-	0.00%
$C_{16}H_{34}$	0.00%	0.00%	0.00%	0.00%	0.00%	0.00%	0.00%	-	0.00%	0.00%	0.00%	0.00%	-	-	-	0.00%	0.05%	11.25%	0.00%	0.00%	0.00%	0.00%	-	0.00%
$C_{17}H_{36}$	0.00%	0.00%	0.00%	0.00%	0.00%	0.00%	0.00%	-	0.00%	0.00%	0.00%	0.00%	-	-	-	0.00%	0.05%	3.45%	0.00%	0.00%	0.00%	0.00%	-	0.00%
$C_{18}H_{38}$	0.00%	0.00%	0.00%	0.00%	0.00%	0.00%	0.00%	-	0.00%	0.00%	0.00%	0.00%	-	-	-	0.00%	0.05%	3.18%	0.00%	0.00%	0.00%	0.00%	-	0.00%
$C_{19}H_{40}$	0.00%	0.00%	0.00%	0.00%	0.00%	0.00%	0.00%	-	0.00%	0.00%	0.00%	0.00%	-	-	-	0.00%	0.04%	2.92%	0.00%	0.00%	0.00%	0.00%	-	0.00%
$C_{20}H_{42}$	0.00%	0.00%	0.00%	0.00%	0.00%	0.00%	0.00%	-	0.00%	0.00%	0.00%	0.00%	-	-	-	0.00%	0.04%	2.69%	0.00%	0.00%	0.00%	0.00%	-	0.00%
$C_{24}H_{50}$	0.00%	0.00%	0.00%	0.00%	0.00%	0.00%	0.00%	-	0.00%	0.00%	0.00%	0.00%	-	-	-	0.00%	0.13%	0.52%	0.00%	0.00%	0.00%	0.00%	-	0.00%
C_{28}+	0.00%	0.00%	0.00%	0.00%	0.00%	0.00%	0.00%	-	0.00%	0.00%	0.00%	0.00%	-	-	-	0.00%	0.31%	0.00%	0.00%	0.00%	0.00%	0.00%	-	0.00%
Total	100.00%	100.00%	100.00%	100.00%	100.00%	100.00%	100.00%	0.00%	100.00%	100.00%	100.00%	100.00%	0.00%	0.00%	0.00%	100.00%	100.00%	100.00%	100.00%	100.00%	100.00%	100.00%	0.00%	100.00%

Notes:

* For CCS Enabled Cases Only

‡ For CCS Disabled Cases Only

× Purge stream of FT light gases, sent to the Flare

Chapter 2

Supplementary Material for "Combining coal gasification, natural gas reforming, and external carbonless heat for efficient production of gasoline and diesel with CO_2 capture and sequestration"

by: Yaser Khojasteh Salkuyeh, Thomas A. Adams II

Case 4 **With Nuclear Heat**

Stream No.	1	2	3	4	5	6	7	8	9	10	11	12	13	14	15	16	17	18	19	20*	21*	22‡	23	24×
Temperature (°C)	60.0	30.0	204.8	606.0	-	32.0	82.0	-	46.0	80.0	188.9	15.0	-	-	-	33.3	240.0	229.3	37.8	-7.0	73.3	-7.0	-	14.6
Pressure (bar)	72.4	30.0	55.0	29.1	-	10.0	67.6	-	2.1	54.3	1.8	32.0	-	-	-	52.0	35.0	2.3	2.8	1.0	153.0	1.0	-	29.5
Total Flow (kg/hr)	73339	33027	188609	289109	-	969	58036	-	5607	239327	1838	153519	-	-	-	299208	299208	42577	15904	65002	64849	65002	-	7676
Vapor Fraction	0.00	1.00	1.00	1.00	-	1.00	1.00	-	0.99	1.00	0.00	1.00	-	-	-	1.00	0.99	0.00	0.00	1.00	0.00	1.00	-	1.00
Mole Percent																								
Coal	100.00%	0.00%	0.00%	0.00%	-	0.00%	0.00%	-	0.00%	0.00%	0.00%	0.00%	-	-	-	0.00%	0.00%	0.00%	0.00%	3.37%	3.39%	3.37%	-	0.00%
CO	0.00%	0.00%	31.40%	1.78%	-	0.00%	0.00%	-	0.00%	22.70%	0.00%	26.02%	-	-	-	30.38%	17.39%	0.00%	0.10%	93.90%	94.42%	93.90%	-	26.02%
CO_2	0.00%	0.38%	8.42%	10.90%	-	0.00%	0.00%	-	41.64%	5.57%	0.00%	5.47%	-	-	-	2.05%	3.68%	0.00%	0.77%	1.23%	1.24%	1.23%	-	5.47%
H_2	0.00%	0.00%	23.75%	16.21%	-	0.00%	0.00%	-	0.00%	65.36%	0.00%	52.15%	-	-	-	62.43%	34.84%	0.00%	0.09%	0.55%	0.00%	0.55%	-	52.15%
H_2O	0.00%	0.00%	35.32%	38.78%	-	0.00%	0.00%	-	5.22%	0.25%	5.39%	0.06%	-	-	-	0.01%	31.66%	1.73%	2.01%	0.17%	0.17%	0.17%	-	0.06%
N_2	0.00%	0.47%	0.38%	5.13%	-	0.19%	0.19%	-	15.65%	3.92%	0.00%	8.18%	-	-	-	3.34%	5.46%	0.00%	0.03%	0.04%	0.04%	0.04%	-	8.18%
AR	0.00%	0.00%	0.06%	0.61%	-	0.32%	0.32%	-	0.00%	0.46%	0.00%	0.98%	-	-	-	0.40%	0.66%	0.00%	0.01%	0.00%	0.00%	0.00%	-	0.98%
NH_3	0.00%	0.00%	0.00%	0.00%	-	0.00%	0.00%	-	0.00%	0.00%	0.00%	0.00%	-	-	-	0.00%	0.00%	0.00%	0.00%	0.00%	0.00%	0.00%	-	0.00%
H_2S	0.00%	0.00%	0.57%	0.00%	-	0.00%	0.00%	-	37.50%	0.00%	0.00%	0.00%	-	-	-	0.00%	0.00%	0.00%	0.00%	0.00%	0.00%	0.00%	-	0.00%
O_2	0.00%	0.00%	0.00%	0.00%	-	0.00%	0.00%	-	0.00%	0.00%	0.00%	0.00%	-	-	-	0.00%	0.00%	0.00%	0.00%	0.00%	0.00%	0.00%	-	0.00%
SO_2	0.00%	0.00%	0.00%	0.00%	-	99.49%	99.49%	-	0.00%	0.00%	0.00%	0.00%	-	-	-	0.00%	0.00%	0.00%	0.00%	0.00%	0.00%	0.00%	-	0.00%
COS	0.00%	0.00%	0.03%	0.00%	-	0.00%	0.00%	-	0.00%	0.00%	0.00%	0.00%	-	-	-	0.00%	0.00%	0.00%	0.00%	0.00%	0.00%	0.00%	-	0.00%
Cl_2	0.00%	0.00%	0.00%	0.00%	-	0.00%	0.00%	-	0.00%	0.00%	0.00%	0.00%	-	-	-	0.00%	0.00%	0.00%	0.00%	0.00%	0.00%	0.00%	-	0.00%
HCl	0.00%	0.00%	0.06%	0.06%	-	0.00%	0.00%	-	0.00%	0.04%	0.00%	0.09%	-	-	-	0.04%	0.06%	0.00%	0.03%	0.00%	0.00%	0.00%	-	0.09%
Sulfur	0.00%	0.00%	0.00%	0.00%	-	0.00%	0.00%	-	0.00%	0.00%	94.61%	0.00%	-	-	-	0.00%	0.00%	0.00%	0.00%	0.00%	0.00%	0.00%	-	0.00%
CH_4	0.00%	97.01%	0.01%	26.53%	-	0.00%	0.00%	-	0.00%	1.69%	0.00%	5.70%	-	-	-	1.35%	3.82%	0.00%	0.10%	0.73%	0.74%	0.73%	-	5.70%
C_2H_4	0.00%	0.00%	0.00%	0.00%	-	0.00%	0.00%	-	0.00%	0.00%	0.00%	0.01%	-	-	-	0.00%	0.01%	0.00%	0.00%	0.00%	0.00%	0.00%	-	0.01%
C_2H_6	0.00%	1.76%	0.00%	0.00%	-	0.00%	0.00%	-	0.00%	0.00%	0.00%	0.24%	-	-	-	0.00%	0.16%	0.00%	0.08%	0.00%	0.00%	0.00%	-	0.24%
C_3H_6	0.00%	0.00%	0.00%	0.00%	-	0.00%	0.00%	-	0.00%	0.00%	0.00%	0.31%	-	-	-	0.00%	0.22%	0.00%	0.56%	0.00%	0.00%	0.00%	-	0.31%
C_3H_8	0.00%	0.26%	0.00%	0.00%	-	0.00%	0.00%	-	0.00%	0.00%	0.00%	0.16%	-	-	-	0.00%	0.11%	0.00%	0.35%	0.00%	0.00%	0.00%	-	0.16%
C_4H_8	0.00%	0.00%	0.00%	0.00%	-	0.00%	0.00%	-	0.00%	0.00%	0.00%	0.22%	-	-	-	0.00%	0.16%	0.00%	2.03%	0.00%	0.00%	0.00%	-	0.22%
C_4H_{10}	0.00%	0.11%	0.00%	0.00%	-	0.00%	0.00%	-	0.00%	0.00%	0.00%	0.11%	-	-	-	0.00%	0.08%	0.00%	1.20%	0.00%	0.00%	0.00%	-	0.11%
C_5H_{12}	0.00%	0.00%	0.00%	0.00%	-	0.00%	0.00%	-	0.00%	0.00%	0.00%	0.15%	-	-	-	0.00%	0.14%	0.00%	6.75%	0.00%	0.00%	0.00%	-	0.15%
C_6H_{14}	0.00%	0.00%	0.00%	0.00%	-	0.00%	0.00%	-	0.00%	0.00%	0.00%	0.09%	-	-	-	0.00%	0.13%	0.00%	14.20%	0.00%	0.00%	0.00%	-	0.09%
C_7H_{16}	0.00%	0.00%	0.00%	0.00%	-	0.00%	0.00%	-	0.00%	0.00%	0.00%	0.04%	-	-	-	0.00%	0.12%	0.03%	19.99%	0.00%	0.00%	0.00%	-	0.04%
C_8H_{18}	0.00%	0.00%	0.00%	0.00%	-	0.00%	0.00%	-	0.00%	0.00%	0.00%	0.01%	-	-	-	0.00%	0.11%	0.11%	21.83%	0.00%	0.00%	0.00%	-	0.01%
C_9H_{20}	0.00%	0.00%	0.00%	0.00%	-	0.00%	0.00%	-	0.00%	0.00%	0.00%	0.00%	-	-	-	0.00%	0.10%	0.48%	20.06%	0.00%	0.00%	0.00%	-	0.00%
$C_{10}H_{22}$	0.00%	0.00%	0.00%	0.00%	-	0.00%	0.00%	-	0.00%	0.00%	0.00%	0.00%	-	-	-	0.00%	0.09%	3.33%	9.23%	0.00%	0.00%	0.00%	-	0.00%
$C_{11}H_{24}$	0.00%	0.00%	0.00%	0.00%	-	0.00%	0.00%	-	0.00%	0.00%	0.00%	0.00%	-	-	-	0.00%	0.08%	5.46%	0.56%	0.00%	0.00%	0.00%	-	0.00%
$C_{12}H_{26}$	0.00%	0.00%	0.00%	0.00%	-	0.00%	0.00%	-	0.00%	0.00%	0.00%	0.00%	-	-	-	0.00%	0.08%	33.11%	0.02%	0.00%	0.00%	0.00%	-	0.00%
$C_{13}H_{28}$	0.00%	0.00%	0.00%	0.00%	-	0.00%	0.00%	-	0.00%	0.00%	0.00%	0.00%	-	-	-	0.00%	0.07%	4.82%	0.00%	0.00%	0.00%	0.00%	-	0.00%
$C_{14}H_{30}$	0.00%	0.00%	0.00%	0.00%	-	0.00%	0.00%	-	0.00%	0.00%	0.00%	0.00%	-	-	-	0.00%	0.06%	22.84%	0.00%	0.00%	0.00%	0.00%	-	0.00%
$C_{15}H_{32}$	0.00%	0.00%	0.00%	0.00%	-	0.00%	0.00%	-	0.00%	0.00%	0.00%	0.00%	-	-	-	0.00%	0.06%	4.08%	0.00%	0.00%	0.00%	0.00%	-	0.00%
$C_{16}H_{34}$	0.00%	0.00%	0.00%	0.00%	-	0.00%	0.00%	-	0.00%	0.00%	0.00%	0.00%	-	-	-	0.00%	0.05%	11.25%	0.00%	0.00%	0.00%	0.00%	-	0.00%
$C_{17}H_{36}$	0.00%	0.00%	0.00%	0.00%	-	0.00%	0.00%	-	0.00%	0.00%	0.00%	0.00%	-	-	-	0.00%	0.05%	3.45%	0.00%	0.00%	0.00%	0.00%	-	0.00%
$C_{18}H_{38}$	0.00%	0.00%	0.00%	0.00%	-	0.00%	0.00%	-	0.00%	0.00%	0.00%	0.00%	-	-	-	0.00%	0.05%	3.18%	0.00%	0.00%	0.00%	0.00%	-	0.00%
$C_{19}H_{40}$	0.00%	0.00%	0.00%	0.00%	-	0.00%	0.00%	-	0.00%	0.00%	0.00%	0.00%	-	-	-	0.00%	0.04%	2.92%	0.00%	0.00%	0.00%	0.00%	-	0.00%
$C_{20}H_{42}$	0.00%	0.00%	0.00%	0.00%	-	0.00%	0.00%	-	0.00%	0.00%	0.00%	0.00%	-	-	-	0.00%	0.04%	2.69%	0.00%	0.00%	0.00%	0.00%	-	0.00%
$C_{24}H_{50}$	0.00%	0.00%	0.00%	0.00%	-	0.00%	0.00%	-	0.00%	0.00%	0.00%	0.00%	-	-	-	0.00%	0.13%	0.52%	0.00%	0.00%	0.00%	0.00%	-	0.00%
C_{28}+	0.00%	0.00%	0.00%	0.00%	-	0.00%	0.00%	-	0.00%	0.00%	0.00%	0.00%	-	-	-	0.00%	0.31%	0.00%	0.00%	0.00%	0.00%	0.00%	-	0.00%
Total	100.00%	100.00%	100.00%	100.00%	0.00%	100.00%	100.00%	0.00%	100.00%	100.00%	100.00%	100.00%	0.00%	0.00%	0.00%	100.00%	100.00%	100.00%	100.00%	100.00%	100.00%	100.00%	0.00%	100.00%

Notes:

* For CCS Enabled Cases Only

‡ For CCS Disabled Cases Only

× Purge stream of FT light gases, sent to the Flare

Chapter 2

Supplementary Material for "Combining coal gasification, natural gas reforming, and external carbonless heat for efficient production of gasoline and diesel with CO_2 capture and sequestration"

by: Yaser Khojasteh Salkuyeh, Thomas A. Adams II

	Case 1				Case 2				Case 3				Case 4				CTL	
Scenario	CGTL with CCS	CGNTL with CCS	CGTL without CCS	CGNTL without CCS	CGTL with CCS	CGNTL with CCS	CGTL without CCS	CGNTL without CCS	CGTL with CCS	CGNTL with CCS	CGTL without CCS	CGNTL without CCS	CGTL with CCS	CGNTL with CCS	CGTL without CCS	CGNTL without CCS	with CCS	without CCS
Total Thermal Input (MW)	1351	1156	1351	1156	1401	1238	1402	1238	1419	1169	1419	1169	1328	1345	1328	1345	1711	1711
Solids Handling																		
Total Coal Handling	$ 17,894	$ 19,654	$ 17,894	$ 19,654	$ 16,660	$ 17,941	$ 16,664	$ 17,941	$ 16,967	$ 18,306	$ 16,967	$ 18,306	$ 16,975	$ 19,164	$ 16,975	$ 19,164	$ 42,197	$ 42,197
Total Coal & Sorbent Preparation	28,251	31,030	28,251	31,030	26,302	28,325	26,309	28,325	26,787	28,902	26,787	28,902	26,801	30,255	26,801	30,255	66,621	66,621
Ash, Slag, & Spent Sorbent Handling	$ 22,192	$ 24,374	$ 22,192	$ 24,374	$ 20,661	$ 22,250	$ 20,666	$ 22,250	$ 21,041	$ 22,703	$ 21,041	$ 22,703	$ 21,052	$ 23,766	$ 21,052	$ 23,766	$ 52,332	$ 52,332
Total Coal Input (tonne/hr)	66.6	76.2	66.6	76.2	60.2	66.9	60.2	66.9	61.8	68.8	61.8	68.8	61.8	73.5	61.8	73.5	227.0	227.0
Subtotal Solids	$ 68,337	$ 75,058	$ 68,337	$ 75,058	$ 63,623	$ 68,516	$ 63,640	$ 68,516	$ 64,795	$ 69,910	$ 64,795	$ 69,910	$ 64,828	$ 73,185	$ 64,828	$ 73,185	$ 161,150	$ 161,150
Water Systems																		
Total Feedwater	$ 30,108	$ 30,214	$ 29,894	$ 30,064	$ 34,845	$ 34,611	$ 33,228	$ 33,956	$ 33,071	$ 31,982	$ 30,793	$ 31,114	$ 27,977	$ 27,205	$ 26,030	$ 26,996	$ 24,170	$ 24,170
Total Boiler Plant & Water	$ 13,310	$ 13,357	$ 13,216	$ 13,291	$ 15,405	$ 15,301	$ 14,690	$ 15,012	$ 14,621	$ 14,139	$ 13,613	$ 13,755	$ 12,368	$ 12,027	$ 11,508	$ 11,935	$ 10,685	$ 10,685
Total Cooling System (Towers, &c)	$ 31,009	$ 31,118	$ 30,788	$ 30,963	$ 35,887	$ 35,647	$ 34,222	$ 34,971	$ 34,060	$ 32,939	$ 31,714	$ 32,044	$ 28,813	$ 28,018	$ 26,809	$ 27,803	$ 24,893	$ 24,893
Total Cooling Duty (MW)	426.7	428.9	422.4	425.8	525.8	520.8	491.3	506.7	488.0	465.2	440.7	447.2	384.2	369.2	346.6	365.1	311.8	311.8
Subtotal Water	$ 74,427	$ 74,689	$ 73,897	$ 74,319	$ 86,137	$ 85,559	$ 82,139	$ 83,939	$ 81,752	$ 79,060	$ 76,121	$ 76,913	$ 69,158	$ 67,250	$ 64,346	$ 66,734	$ 59,748	$ 59,748
Gasifier																		
Gasifier	$ 121,588	$ 133,545	$ 121,588	$ 133,545	$ 113,200	$ 121,906	$ 113,230	$ 121,906	$ 115,284	$ 124,386	$ 115,284	$ 124,386	$ 115,344	$ 130,213	$ 115,344	$ 130,213	$ 286,721	$ 286,721
Subtotal Gasification	$ 121,588	$ 133,545	$ 121,588	$ 133,545	$ 113,200	$ 121,906	$ 113,230	$ 121,906	$ 115,284	$ 124,386	$ 115,284	$ 124,386	$ 115,344	$ 130,213	$ 115,344	$ 130,213	$ 286,721	$ 286,721
Air Separation Unit																		
Air Separation Unit	$ 150,901	$ 94,232	$ 85,222	$ 94,232	$ 165,768	$ 119,646	$ 110,546	$ 119,646	$ 190,574	$ 129,402	$ 119,285	$ 129,402	$ 169,384	$ 91,717	$ 80,543	$ 91,717	$ 234,884	$ 234,884
Air Intake Rate (tonne/hr)	498.9	266.3	232.9	266.3	565.5	366.1	329.5	366.1	681.1	406.5	364.7	406.5	582.0	256.9	216.0	256.9	900.0	900.0
Subtotal Air Separation	$ 150,901	$ 94,232	$ 85,222	$ 94,232	$ 165,768	$ 119,646	$ 110,546	$ 119,646	$ 190,574	$ 129,402	$ 119,285	$ 129,402	$ 169,384	$ 91,717	$ 80,543	$ 91,717	$ 234,884	$ 234,884
Gas Cleaning																		
Syngas Scrubbing & Cooling	$ 16,358	$ 17,967	$ 16,358	$ 17,967	$ 15,230	$ 16,401	$ 15,234	$ 16,401	$ 15,510	$ 16,735	$ 15,510	$ 16,735	$ 15,518	$ 17,519	$ 15,518	$ 17,519	$ 38,576	$ 38,576
Elemental Sulfur Plant (Claus)	$ 16,334	$ 17,941	$ 16,334	$ 17,941	$ 15,208	$ 16,377	$ 15,212	$ 16,377	$ 15,488	$ 16,710	$ 15,488	$ 16,710	$ 15,496	$ 17,493	$ 15,496	$ 17,493	$ 38,519	$ 38,519
Mercury Removal	1119.2	1279.7	1119.2	1279.7	1010.6	1123.4	1010.9	1123.4	1037.2	1156.2	1037.2	1156.2	1038.0	1234.3	1038.0	1234.3	3812.0	3812.0
H_2S Removal (Section 2)	$ 12,797	$ 14,041	$ 12,797	$ 14,041	$ 11,880	$ 12,783	$ 11,883	$ 12,783	$ 12,132	$ 13,076	$ 12,132	$ 13,076	$ 12,153	$ 13,699	$ 12,153	$ 13,699	$ 29,690	$ 29,690
H_2S to 2 Stage Selexol (kmol/hr)	53	60	53	60	47	52	47	52	49	54	49	54	49	58	49	58	175	175
CO_2 Removal (Section 2)	$ 24,872	$ 19,256	$ 24,872	$ 19,256	$ 24,193	$ 19,341	$ 24,199	$ 19,341	$ 28,931	$ 22,127	$ 28,931	$ 22,127	$ 28,319	$ 20,126	$ 28,319	$ 20,126	$ 45,093	$ 45,093
CO_2 Input to Selexol (kmol/hr)	2,726	1,891	2,726	1,891	2,620	1,903	2,621	1,903	3,383	2,307	3,383	2,307	3,281	2,014	3,281	2,014	6,378	6,378
Other Cleaning	$ 2,321	$ 2,653	$ 2,321	$ 2,653	$ 2,095	$ 2,329	$ 2,096	$ 2,329	$ 2,151	$ 2,397	$ 2,151	$ 2,397	$ 2,152	$ 2,559	$ 2,152	$ 2,559	$ 7,904	$ 7,904
Subtotal Gas Cleaning	$ 73,801	$ 73,138	$ 73,801	$ 73,138	$ 69,616	$ 68,355	$ 69,635	$ 68,355	$ 75,249	$ 72,202	$ 75,249	$ 72,202	$ 74,676	$ 72,630	$ 74,676	$ 72,630	$ 163,594	$ 163,594
CO_2 Compression																		
CO_2 Compression	$ 9,746	$ 6,911	$ -	$ -	$ 10,326	$ 8,081	$ -	$ -	$ 12,622	$ 9,293	$ -	$ -	$ 11,039	$ 7,292	$ -	$ -	$ 28,497	-
CO_2 Sequestered (kmol/hr)	2,021	1,349	-	-	2,163	1,621	-	-	2,740	1,911	-	-	2,340	1,437	-	-	7,141	-
Subtotal CO_2 Compression	$ 9,746	$ 6,911	$ -	$ -	$ 10,326	$ 8,081	$ -	$ -	$ 12,622	$ 9,293	$ -	$ -	$ 11,039	$ 7,292	$ -	$ -	$ 28,497	-
Reforming and Reforming Auxiliaries																		
NG Feed (kmol/hr)	3,438	2,378	3,438	2,378	3,831	2,981	3,832	2,981	3,855	2,648	3,855	2,648	3,488	1,997	3,488	1,997		
Prereformer Preheating	$ 392	$ 317	$ 392	$ 317	$ 409	$ 369	$ 410	$ 369	$ 411	$ 340	$ 411	$ 340	$ 394	$ 284	$ 394	$ 284		
Pre-reformer	$ 95	$ 89	$ 95	$ 89	$ 95	$ 94	$ 95	$ 94	$ 95	$ 91	$ 95	$ 91	$ 95	$ 86	$ 95	$ 86		
Intermediate Heat	$ 1,745	$ 1,247	$ 1,745	$ 1,247	$ 1,923	$ 1,536	$ 1,924	$ 1,536	$ 1,934	$ 1,377	$ 1,934	$ 1,377	$ 1,767	$ 1,065	$ 1,767	$ 1,065		
Reformer	$ 5,155	$ 3,726	$ 5,155	$ 3,726	$ 5,667	$ 4,554	$ 5,669	$ 4,554	$ 5,698	$ 4,097	$ 5,698	$ 4,097	$ 5,219	$ 3,203	$ 5,219	$ 3,203		
O_2 Boost Compressor	$ 1,332	$ 1,269	$ 1,332	$ 1,269	$ 1,350	$ 1,310	$ 1,350	$ 1,310	$ 1,351	$ 1,287	$ 1,351	$ 1,287	$ 1,335	$ 1,243	$ 1,335	$ 1,243		
Steam Generators	$ 316	$ 256	$ 316	$ 256	$ 338	$ 290	$ 338	$ 290	$ 340	$ 271	$ 340	$ 271	$ 319	$ 234	$ 319	$ 234		
Condenser	$ 211	$ 178	$ 211	$ 178	$ 223	$ 197	$ 224	$ 197	$ 224	$ 186	$ 224	$ 186	$ 213	$ 166	$ 213	$ 166		
Condenser Drum	$ 158	$ 149	$ 158	$ 149	$ 160	$ 156	$ 160	$ 156	$ 160	$ 152	$ 160	$ 152	$ 158	$ 145	$ 158	$ 145		
4:1 Syngas Compression	$ 2,159	$ 1,969	$ 2,159	$ 1,969	$ 2,278	$ 2,034	$ 2,278	$ 2,034	$ 2,285	$ 1,998	$ 2,285	$ 1,998	$ 2,174	$ 1,928	$ 2,174	$ 1,928		
Reformer Water Preheater	$ 254	$ 212	$ 254	$ 212	$ 270	$ 236	$ 270	$ 236	$ 271	$ 223	$ 271	$ 223	$ 256	$ 196	$ 256	$ 196		
Subtotal Reforming	$ 11,817	$ 9,412	$ 11,817	$ 9,412	$ 12,714	$ 10,776	$ 12,718	$ 10,776	$ 12,769	$ 10,023	$ 12,769	$ 10,023	$ 11,931	$ 8,551	$ 11,931	$ 8,551		
Gas Shifting																		
COS Hyrolysis	$ 5,913	$ 6,451	$ 5,913	$ 6,451	$ 12,255	$ 13,125	$ 12,258	$ 13,125	$ 5,628	$ 6,039	$ 5,628	$ 6,039	$ 5,631	$ 6,302	$ 5,631	$ 6,302	$ 7,996	$ 7,996
COS fed to first reactor (kmol/hr)	2.9	3.3	2.9	3.3	8.8	9.8	8.8	9.8	2.7	3.0	2.7	3.0	2.7	3.2	2.7	3.2	4.6	4.6
Water Gas Shift Units																	$ 5,937	$ 5,937
CO feed to first reactor (kmol/hr)																	4954.8	4954.8
Subtotal Gas Shifting	$ 5,913	$ 6,451	$ 5,913	$ 6,451	$ 12,255	$ 13,125	$ 12,258	$ 13,125	$ 5,628	$ 6,039	$ 5,628	$ 6,039	$ 5,631	$ 6,302	$ 5,631	$ 6,302	$ 13,933	$ 13,933
Power Generation																		
F7 Turb,Air Comp,Combust Chmbr	-	-	-	-	-	-	-	-	-	-	-	-	-	-	-	-	37,190	37,190
Gas Turbine Power Out (MW)	0	0	0	0	0	0	0	0	0	0	0	0	0	0	0	0	60.3	60.3
Steam Turbine Generator & Accessor.	$ 12,667	$ 13,407	$ 12,667	$ 13,407	$ 19,064	$ 19,361	$ 19,069	$ 19,361	$ 15,291	$ 15,555	$ 15,291	$ 15,555	$ 9,543	$ 10,134	$ 9,543	$ 10,134	$ 34,819	$ 34,819
Power Produced (MW)	$ 26	$ 28	$ 26	$ 28	$ 47	$ 48	$ 47	$ 48	$ 34	$ 35	$ 34	$ 35	$ 17	$ 19	$ 17	$ 19	$ 110	$ 110
Condenser and Acessories	$ 8,785	$ 8,811	$ 8,731	$ 8,774	$ 9,957	$ 9,900	$ 9,560	$ 9,739	$ 9,521	$ 9,252	$ 8,956	$ 9,036	$ 8,249	$ 8,054	$ 7,755	$ 8,001	$ 7,277	$ 7,277
Feedwater Steam Generator (HRSG)	$ 11,360	$ 12,024	$ 11,360	$ 12,024	$ 17,098	$ 17,364	$ 17,102	$ 17,364	$ 13,714	$ 13,950	$ 13,714	$ 13,950	$ 8,559	$ 9,089	$ 8,559	$ 9,089	$ 31,228	$ 31,228
Stack	$ 3,797	$ 3,797	$ 3,797	$ 3,797	$ 3,797	$ 3,797	$ 3,797	$ 3,797	$ 3,797	$ 3,797	$ 3,797	$ 3,797	$ 3,797	$ 3,797	$ 3,797	$ 3,797	$ 3,797	$ 3,797
Subtotal Power Generation	$ 38,167	$ 41,524	$ 41,258	$ 44,829	$ 53,319	$ 55,546	$ 55,801	$ 58,320	$ 45,793	$ 47,778	$ 48,165	$ 50,582	$ 31,682	$ 34,489	$ 34,126	$ 37,660	$ 117,778	$ 117,778
Fischer Tropsch Synthesis																		
Cost of Fischer-Tropsch Section	$ 284,979	$ 284,373	$ 284,979	$ 284,373	$ 295,139	$ 295,692	$ 295,221	$ 295,692	$ 363,433	$ 350,683	$ 363,433	$ 350,683	$ 294,014	$ 291,562	$ 294,014	$ 291,562	$ 277,073	$ 277,073
Flow Rate of Syngas (kmol/hr)	24,208	24,136	24,208	24,136	23,766	23,825	23,775	23,825	30,987	29,583	30,987	29,583	25,280	24,988	25,280	24,988	23,280	23,280
Subtotal Fischer-Tropsch	$ 284,979	$ 284,373	$ 284,979	$ 284,373	$ 295,139	$ 295,692	$ 295,221	$ 295,692	$ 363,433	$ 350,683	$ 363,433	$ 350,683	$ 294,014	$ 291,562	$ 294,014	$ 291,562	$ 277,073	$ 277,073
Accessories																		
Txformers, Condiuts, Switchgears, &c	$ 21,703	$ 13,240	$ 12,792	$ 11,165	$ 15,733	$ 6,083	$ 5,770	$ 7,765	$ 23,655	$ 14,583	$ 9,548	$ 6,859	$ 25,853	$ 16,479	$ 15,345	$ 14,605	$ 15,390	$ 21,548
Control Systems and Instrumentation	$ 23,142	$ 21,077	$ 23,142	$ 21,077	$ 23,659	$ 21,965	$ 23,664	$ 21,965	$ 23,837	$ 21,224	$ 23,837	$ 21,224	$ 22,903	$ 23,085	$ 22,903	$ 23,085	$ 26,667	$ 26,667
Site Improvements & Facilities	$ 19,137	$ 17,429	$ 19,137	$ 17,429	$ 19,564	$ 18,164	$ 19,569	$ 18,164	$ 19,712	$ 17,551	$ 19,712	$ 17,551	$ 18,939	$ 19,090	$ 18,939	$ 19,090	$ 22,052	$ 22,052
Structures & Various Buildings	$ 16,887	$ 15,380	$ 16,887	$ 15,380	$ 17,264	$ 16,028	$ 17,268	$ 16,028	$ 17,394	$ 15,487	$ 17,394	$ 15,487	$ 16,712	$ 16,845	$ 16,712	$ 16,845	$ 19,459	$ 19,459
Subtotal Accessories	$ 80,868	$ 67,126	$ 71,957	$ 65,050	$ 76,219	$ 62,240	$ 66,270	$ 63,922	$ 84,599	$ 68,844	$ 70,492	$ 61,120	$ 84,408	$ 75,499	$ 73,899	$ 73,625	$ 83,568	$ 89,727
Solvents, Catalysts, &c																		
All Catalysts	$ 397	$ 396	$ 397	$ 396	$ 85	$ 75	$ 85	$ 75	$ 104	$ 90	$ 104	$ 90	$ 294	$ 198	$ 294	$ 198	$ 2,224	$ 2,224
Carbon for Hg Removal	$ 79	$ 67	$ 79	$ 67	$ 82	$ 72	$ 82	$ 72	$ 83	$ 68	$ 83	$ 68	$ 77	$ 78	$ 77	$ 78	$ 100	$ 100
Water Gas Shift catalyst	$ 318	$ 329	$ 318	$ 329	$ 4	$ 3	$ 4	$ 3	$ 21	$ 21	$ 21	$ 21	$ 217	$ 119	$ 217	$ 119	$ 2,124	$ 2,124
Selexol	$ 2	$ 2	$ 2	$ 2	$ 2	$ 2	$ 2	$ 2	$ 2	$ 2	$ 2	$ 2	$ 2	$ 2	$ 2	$ 2	$ 7	$ 7
Initial Charge for H_2S Sections	$ 2	$ 2	$ 2	$ 2	$ 2	$ 2	$ 2	$ 2	$ 2	$ 2	$ 2	$ 2	$ 2	$ 2	$ 2	$ 2	$ 6	$ 6
Initial Charge for CO_2 Section	$ 0	$ 0	$ -	$ -	$ 0	$ 0	$ -	$ -	$ 0	$ 0	$ -	$ -	$ 0	$ 0	$ -	$ -	$ 1	$ 1
Subtotal Solvents & Catalysts	$ 399	$ 399	$ 399	$ 399	$ 87	$ 77	$ 87	$ 77	$ 106	$ 92	$ 105	$ 91	$ 297	$ 200	$ 296	$ 200	$ 2,231	$ 2,231
Annual Operating and Maintenance Costs ($1000s/yr) - At 100% Capacity																		
All Labor	$ 27,767	$ 27,767	$ 27,767	$ 27,767	$ 27,767	$ 27,767	$ 27,767	$ 27,767	$ 27,767	$ 27,767	$ 27,767	$ 27,767	$ 27,767	$ 27,767	$ 27,767	$ 27,767	$ 27,767	$ 27,767
Maintenance Materials	$ 27,734	$ 23,733	$ 27,734	$ 23,733	$ 28,775	$ 25,424	$ 28,785	$ 25,424	$ 29,138	$ 24,010	$ 29,138	$ 24,010	$ 27,259	$ 27,621	$ 27,259	$ 27,621	$ 35,128	$ 35,128
All Catalysts	$ 1,369	$ 1,558	$ 1,369	$ 1,558	$ 1,175	$ 1,306	$ 1,176	$ 1,306	$ 1,210	$ 1,349	$ 1,210	$ 1,349	$ 1,253	$ 1,460	$ 1,253	$ 1,460	$ 4,886	$ 4,886
Carbon for Hg Removal	$ 14	$ 16	$ 14	$ 16	$ 13	$ 14	$ 13	$ 14	$ 13	$ 15	$ 13	$ 15	$ 13	$ 16	$ 13	$ 16	$ 48	$ 48
Claus Replacement Catalyst	$ 34	$ 39	$ 34	$ 39	$ 31	$ 35	$ 31	$ 35	$ 32	$ 36	$ 32	$ 36	$ 32	$ 38	$ 32	$ 38	$ 117	$ 117
Water Gas Shift catalyst	$ 68	$ 70	$ 68	$ 70	$ 1	$ 1	$ 1	$ 1	$ 5	$ 5	$ 5	$ 5	$ 46	$ 26	$ 46	$ 26	$ 455	$ 455
Solid Waste Disposal	$ 1,252	$ 1,432	$ 1,252	$ 1,432	$ 1,131	$ 1,257	$ 1,131	$ 1,257	$ 1,161	$ 1,294	$ 1,161	$ 1,294	$ 1,161	$ 1,381	$ 1,161	$ 1,381	$ 4,265	$ 4,265
Selexol	$ 111	$ 118	$ 111	$ 118	$ 101	$ 105	$ 101	$ 105	$ 110	$ 111	$ 110	$ 111	$ 109	$ 115	$ 109	$ 115	$ 350	$ 350
Replacement for H_2S Removal	$ 90	$ 103	$ 90	$ 103	$ 81	$ 90	$ 81	$ 90	$ 84	$ 93	$ 84	$ 93	$ 84	$ 99	$ 84	$ 99	$ 300	$ 300
Replacement for CO_2 Removal	$ 21	$ 15	$ 21	$ 15	$ 20	$ 15	$ 20	$ 15	$ 26	$ 18	$ 26	$ 18	$ 25	$ 16	$ 25	$ 16	$ 49	$ 49
CO_2 Transport and Sequestration	$ 7,792	$ 5,200	$ -	$ -	$ 8,340	$ 6,251	$ -	$ -	$ 10,562	$ 7,368	$ -	$ -	$ 9,022	$ 5,539	$ -	$ -	$ 27,532	$ -
SUMMARY AT 100% CAPACITY																		
Total Capital Cost ($1000s)	$ 915,032	$ 860,405	$ 833,256	$ 854,354	$ 946,148	$ 896,396	$ 869,287	$ 891,149	$ 1,046,976	$ 961,675	$ 945,698	$ 945,314	$ 926,760	$ 852,588	$ 814,003	$ 846,077	$ 1,415,245	$ 1,392,904
Total Labor Costs ($1000s/yr)	$ 27,767	$ 27,767	$ 27,767	$ 27,767	$ 27,767	$ 27,767	$ 27,767	$ 27,767	$ 27,767	$ 27,767	$ 27,767	$ 27,767	$ 27,767	$ 27,767	$ 27,767	$ 27,767	$ 27,767	$ 27,767
Nuclear Section Cost ($1000s/yr)	$ -	$ 46,461	$ -	$ 46,461	$ -	$ 39,207	$ -	$ 39,207	$ -	$ 53,232	$ -	$ 53,232	$ -	$ 73,289	$ -	$ 73,289		
Total Operating Cost ($1000s/yr)	$ 38,258	$ 78,501	$ 30,467	$ 73,301	$ 39,522	$ 73,550	$ 31,194	$ 67,300	$ 42,180	$ 87,363	$ 31,618	$ 79,996	$ 38,804	$ 109,405	$ 29,782	$ 103,866	$ 82,626	$ 55,094
Total Fuel Costs ($1000s/yr)	$ 135,042	$ 107,329	$ 135,042	$ 107,329	$ 143,962	$ 121,306	$ 144,016	$ 121,306	$ 145,423	$ 112,121	$ 145,423	$ 112,121	$ 134,314	$ 94,528	$ 134,314	$ 94,528	$ 104,981	$ 104,981
Total Coal Consumed (tonne/hr)	583,748	667,453	583,748	667,453	527,083	585,935	527,282	585,935	541,000	603,034	541,000	603,034	541,398	643,793	541,398	643,793	1,988,241	1,988,241
Total Natural Gas Consum. (Mmol/yr)	30,117	20,831	30,117	20,831	33,559	26,114	33,571	26,114	33,769	23,199	33,769	23,199	30,552	17,493	30,552	17,493	-	-
Total Electricity Required (MWhr/yr)	461,228	202,398	191,109	152,335	269,801	55,365	50,694	83,157	532,407	237,744	117,369	67,629	617,402	291,459	258,816	238,349	260,071	455,745
Total Diesel Prod. (tonne/yr)	364,021	363,915	364,021	363,915	361,896	363,178	362,032	363,178	388,759	384,186	388,759	384,186	368,699	367,418	368,699	367,418	359,739	359,739
Total Naphtha Prod. (tonne/yr)	137,526	137,541	137,526	137,541	137,544	137,598	137,596	137,598	137,560	137,522	137,560	137,522	137,549	137,552	137,549	137,552	137,537	137,537
Total Sulfur Produced (tonne/yr)	1,192	1,383	1,192	1,383	1,086	1,225	1,086	1,225	1,101	1,245	1,101	1,245	1,094	1,321	1,094	1,321	3,862	3,862
Profitability Assessment - Capacity Factor of 85%																		

Total Coal Consumed (tonne/yr)	496,186	567,335	496,186	567,335	448,020	498,045	448,189	498,045	459,850	512,579	459,850	512,579	460,188	547,224	460,188	547,224	1,690,005	1,690,005
Total Natural Gas Comsumed (GJ/yr)	23,366,077	16,161,866	23,366,077	16,161,866	26,036,626	20,260,553	26,046,447	20,260,553	26,199,447	17,998,769	26,199,447	17,998,769	23,704,109	13,571,905	23,704,109	13,571,905	-	-
Total Diesel Prod. (tonne/yr)	309,418	309,328	309,418	309,328	307,612	308,701	307,728	308,701	330,445	326,558	330,445	326,558	313,394	312,305	313,394	312,305	305,778	305,778
Total Naphtha Prod. (tonne/yr)	116,897	116,910	116,897	116,910	116,913	116,958	116,957	116,958	116,926	116,894	116,926	116,894	116,917	116,919	116,917	116,919	116,907	116,907
Total Sulfur Produced (tonne/yr)	1,014	1,175	1,014	1,175	923	1,042	923	1,042	936	1,058	936	1,058	930	1,123	930	1,123	3,283	3,283
Total CO_2 Sequestered (tonne/yr)	662,291	441,975	-	-	708,874	531,316	-	-	897,749	626,240	-	-	766,829	470,773	-	-	6,070	-
Total CO_2 Emitted (tonne/yr)	529,756	290,936	1,052,032	732,910	409,223	274,763	978,615	806,079	278,006	1,315	960,622	627,555	334,409	9,135	915,366	479,908	242,366	2,582,583
Total Capital Cost ($1000s)	915,032	860,405	833,256	854,354	$ 946,148	$ 896,396	$ 869,287	$ 891,149	$ 1,046,976	$ 961,675	$ 945,698	$ 945,314	926,760	852,588	814,003	846,077	1,415,245	1,392,904
Cash Reserves ($1000s)	17,751	16,861	15,344	16,149	$ 17,158	$ 16,490	$ 14,719	$ 15,667	$ 19,253	$ 18,070	$ 15,655	$ 16,380	18,811	18,754	15,709	17,997	15,596	13,647
Inventory ($1000s/yr)	9,369	9,368	9,369	9,368	$ 9,330	$ 9,355	$ 9,333	$ 9,355	$ 9,830	$ 9,744	$ 9,830	$ 9,744	9,456	9,433	9,456	9,433	9,294	9,294
Accounts Receivable ($1000s)	$ 40,648	$ 40,642	$ 40,648	$ 40,642	$ 40,478	$ 40,586	$ 40,841	$ 41,158	$ 42,648	$ 42,277	$ 42,648	$ 42,277	$ 41,027	$ 40,926	$ 41,027	$ 40,926	42,109	43,453
Accounts Payable ($1000s)	$ 9,562	$ 7,599	$ 9,562	$ 7,599	$ 10,193	$ 8,589	$ 10,197	$ 8,589	$ 10,297	$ 7,939	$ 10,297	$ 7,939	$ 9,510	$ 6,693	$ 9,510	$ 6,693	7,433	7,433
Working Capital ($1000s)	$ 58,207	$ 59,272	$ 55,800	$ 58,560	$ 56,772	$ 57,842	$ 54,696	$ 57,591	$ 61,434	$ 62,153	$ 57,836	$ 60,463	$ 59,785	$ 62,420	$ 56,683	$ 61,663	59,566	58,961
Total Capital Investment ($1000s)	$ 973,239	$ 919,677	$ 889,056	$ 912,913	$ 1,002,920	$ 954,238	$ 923,983	$ 948,739	$ 1,108,410	$ 1,023,828	$ 1,003,533	$ 1,005,777	$ 986,544	$ 915,008	$ 870,686	$ 907,740	$ 1,474,811	$ 1,451,865
Total Capital Investment ($Billion)	$ 0.97	$ 0.92	$ 0.89	$ 0.91	$ 1.00	$ 0.95	$ 0.92	$ 0.95	$ 1.11	$ 1.02	$ 1.00	$ 1.01	$ 0.99	$ 0.92	$ 0.87	$ 0.91	$ 1.47	$ 1.45
Debt Taken ($1000s)	$ 486,619	$ 459,838	$ 444,528	$ 456,457	$ 501,460	$ 477,119	$ 461,992	$ 474,370	$ 554,205	$ 511,914	$ 501,767	$ 502,888	$ 493,272	$ 457,504	$ 435,343	$ 453,870	$ 737,405	725932.5174
Equity Expended ($1000s)	$ 486,619	$ 459,838	$ 444,528	$ 456,457	$ 501,460	$ 477,119	$ 461,992	$ 474,370	$ 554,205	$ 511,914	$ 501,767	$ 502,888	$ 493,272	$ 457,504	$ 435,343	$ 453,870	$ 737,405	$ 725,933
Annual Payment on Loan ($1000s)	$ 49,480	$ 46,757	$ 45,200	$ 46,413	$ 50,989	$ 48,514	$ 46,976	$ 48,234	$ 56,352	$ 52,052	$ 51,020	$ 51,134	$ 50,156	$ 46,519	$ 44,266	$ 46,150	$ 74,980	$ 73,813
Total Annual Expense ($1000s/yr)	$ 213,101	$ 202,411	$ 184,207	$ 193,863	$ 205,974	$ 197,960	$ 176,696	$ 188,082	$ 231,127	$ 216,931	$ 187,930	$ 196,642	$ 225,822	$ 225,141	$ 188,589	$ 216,054	$ 187,233	$ 163,830
Labor Costs ($1000s/yr)	$ 27,767	$ 27,767	$ 27,767	$ 27,767	$ 27,767	$ 27,767	$ 27,767	$ 27,767	$ 27,767	$ 27,767	$ 27,767	$ 27,767	$ 27,767	$ 27,767	$ 27,767	$ 27,767	$ 27,767	$ 27,767
Operating Cost ($1000s/yr)	$ 32,520	$ 66,726	$ 25,897	$ 62,306	$ 33,593	$ 62,518	$ 26,515	$ 57,205	$ 35,853	$ 74,259	$ 26,876	$ 67,996	$ 32,983	$ 92,994	$ 25,315	$ 88,286	$ 70,232	$ 46,830
Fuel Costs ($1000s/yr)	$ 114,786	$ 91,230	$ 114,786	$ 91,230	$ 122,368	$ 103,110	$ 122,414	$ 103,110	$ 123,610	$ 95,303	$ 123,610	$ 95,303	$ 114,167	$ 80,349	$ 114,167	$ 80,349	$ 89,233	$ 89,233
Total Revenue ($1000s/yr)	$ 487,977	$ 487,904	$ 487,977	$ 487,904	$ 485,925	$ 487,232	$ 490,288	$ 494,089	$ 511,980	$ 507,523	$ 511,980	$ 507,523	$ 492,525	$ 491,305	$ 492,525	$ 491,305	$ 505,507	$ 521,640
Distillate ($1000s/yr)	$ 352,839	$ 352,736	$ 352,839	$ 352,736	$ 350,779	$ 352,022	$ 350,911	$ 352,022	$ 376,817	$ 372,385	$ 376,817	$ 372,385	$ 357,373	$ 356,131	$ 357,373	$ 356,131	$ 348,688	$ 348,688
Naphtha ($1000s/yr)	$ 135,036	$ 135,051	$ 135,036	$ 135,051	$ 135,054	$ 135,107	$ 135,105	$ 135,107	$ 135,069	$ 135,032	$ 135,069	$ 135,032	$ 135,059	$ 135,061	$ 135,059	$ 135,061	$ 135,047	$ 135,047
Sulfur ($1000s/yr)	$ 101	$ 118	$ 101	$ 118	$ 92	$ 104	$ 92	$ 104	$ 94	$ 106	$ 94	$ 106	$ 93	$ 112	$ 93	$ 112	$ 328	$ 328
Gross Earnings ($1000s/yr)	$ 274,876	$ 285,494	$ 303,770	$ 294,041	$ 279,952	$ 289,272	$ 313,592	$ 306,006	$ 280,853	$ 290,592	$ 324,050	$ 310,881	$ 266,702	$ 266,164	$ 303,936	$ 275,251	$ 318,274	$ 357,809
CO_2 Emissions Taxes ($1000s/yr)	$ -	$ -	$ -	$ -	$ -	$ -	$ -	$ -	$ -	$ -	$ -	$ -	$ -	$ -	$ -	$ -	$ -	-
CASH FLOW - Depreciation																		
2011	$ 91,503	$ 86,041	$ 83,326	$ 85,435	$ 94,615	$ 89,640	$ 86,929	$ 89,115	$ 104,698	$ 96,167	$ 94,570	$ 94,531	$ 92,676	$ 85,259	$ 81,400	$ 84,608	$ 141,524	$ 139,290
2012	$ 164,706	$ 154,873	$ 149,986	$ 153,784	$ 170,307	$ 161,351	$ 156,472	$ 160,407	$ 188,456	$ 173,101	$ 170,226	$ 170,157	$ 166,817	$ 153,466	$ 146,521	$ 152,294	$ 254,744	$ 250,723
2013	$ 131,765	$ 123,898	$ 119,989	$ 123,027	$ 136,245	$ 129,081	$ 125,177	$ 128,325	$ 150,764	$ 138,481	$ 136,180	$ 136,125	$ 133,453	$ 122,773	$ 117,216	$ 121,835	$ 203,795	$ 200,578
2014	$ 105,412	$ 99,119	$ 95,991	$ 98,422	$ 108,996	$ 103,265	$ 100,142	$ 102,660	$ 120,612	$ 110,785	$ 108,944	$ 108,900	$ 106,763	$ 98,218	$ 93,773	$ 97,468	$ 163,036	$ 160,463
2015	$ 84,366	$ 79,329	$ 76,826	$ 78,771	$ 87,235	$ 82,648	$ 80,148	$ 82,164	$ 96,531	$ 88,666	$ 87,193	$ 87,158	$ 85,447	$ 78,609	$ 75,051	$ 78,008	$ 130,486	$ 128,426
2016	$ 67,438	$ 63,412	$ 61,411	$ 62,966	$ 69,731	$ 66,064	$ 64,066	$ 65,678	$ 77,162	$ 70,875	$ 69,698	$ 69,670	$ 68,302	$ 62,836	$ 59,992	$ 62,356	$ 104,304	$ 102,657
2017	$ 59,935	$ 56,357	$ 54,578	$ 55,960	$ 61,973	$ 58,714	$ 56,938	$ 58,370	$ 68,577	$ 62,990	$ 61,943	$ 61,918	$ 60,703	$ 55,844	$ 53,317	$ 55,418	$ 92,699	$ 91,235
2018	$ 59,935	$ 56,357	$ 54,578	$ 55,960	$ 61,973	$ 58,714	$ 56,938	$ 58,370	$ 68,577	$ 62,990	$ 61,943	$ 61,918	$ 60,703	$ 55,844	$ 53,317	$ 55,418	$ 92,699	$ 91,235
2019	$ 60,026	$ 56,443	$ 54,662	$ 56,046	$ 62,067	$ 58,804	$ 57,025	$ 58,459	$ 68,682	$ 63,086	$ 62,038	$ 62,013	$ 60,795	$ 55,930	$ 53,399	$ 55,503	$ 92,840	$ 91,375
2020	$ 59,935	$ 56,357	$ 54,578	$ 55,960	$ 61,973	$ 58,714	$ 56,938	$ 58,370	$ 68,577	$ 62,990	$ 61,943	$ 61,918	$ 60,703	$ 55,844	$ 53,317	$ 55,418	$ 92,699	$ 91,235
2021	$ 30,013	$ 28,221	$ 27,331	$ 28,023	$ 31,034	$ 29,402	$ 28,513	$ 29,230	$ 34,341	$ 31,543	$ 31,019	$ 31,006	$ 30,398	$ 27,965	$ 26,699	$ 27,751	$ 46,420	$ 45,687
Loan Principal Balance at start of																		
2011	$ 486,619	$ 459,838	$ 444,528	$ 456,457	$ 501,460	$ 477,119	$ 461,992	$ 474,370	$ 554,205	$ 511,914	$ 501,767	$ 502,888	$ 493,272	$ 457,504	$ 435,343	$ 453,870	$ 737,405	$ 725,933
2012	$ 483,369	$ 456,766	$ 441,558	$ 453,407	$ 498,110	$ 473,932	$ 458,905	$ 471,201	$ 550,502	$ 508,494	$ 498,415	$ 499,529	$ 489,977	$ 454,447	$ 432,435	$ 450,838	$ 732,479	$ 721,083
2013	$ 479,809	$ 453,403	$ 438,306	$ 450,068	$ 494,442	$ 470,442	$ 455,526	$ 467,731	$ 546,448	$ 504,749	$ 494,744	$ 495,850	$ 486,368	$ 451,101	$ 429,250	$ 447,518	$ 727,085	$ 715,772
2014	$ 475,911	$ 449,719	$ 434,746	$ 446,412	$ 490,425	$ 466,620	$ 451,825	$ 463,931	$ 542,009	$ 500,649	$ 490,725	$ 491,822	$ 482,417	$ 447,436	$ 425,763	$ 443,882	$ 721,178	$ 709,958
2015	$ 471,643	$ 445,686	$ 430,847	$ 442,408	$ 486,027	$ 462,435	$ 447,773	$ 459,770	$ 537,148	$ 496,159	$ 486,324	$ 487,411	$ 478,091	$ 443,423	$ 421,945	$ 439,901	$ 714,710	$ 703,590
2016	$ 466,969	$ 441,269	$ 426,577	$ 438,024	$ 481,210	$ 457,852	$ 443,336	$ 455,214	$ 531,825	$ 491,242	$ 481,505	$ 482,581	$ 473,353	$ 439,029	$ 417,763	$ 435,542	$ 707,628	$ 696,618
2017	$ 461,851	$ 436,433	$ 421,902	$ 433,224	$ 475,937	$ 452,835	$ 438,477	$ 450,225	$ 525,997	$ 485,858	$ 476,228	$ 477,292	$ 468,165	$ 434,218	$ 413,185	$ 430,769	$ 699,873	$ 688,984
2018	$ 456,247	$ 431,138	$ 416,783	$ 427,967	$ 470,162	$ 447,340	$ 433,157	$ 444,762	$ 519,614	$ 479,963	$ 470,449	$ 471,501	$ 462,485	$ 428,949	$ 408,172	$ 425,542	$ 691,381	$ 680,624
2019	$ 450,111	$ 425,339	$ 411,178	$ 422,211	$ 463,838	$ 441,324	$ 427,331	$ 438,780	$ 512,626	$ 473,508	$ 464,122	$ 465,160	$ 456,265	$ 423,180	$ 402,682	$ 419,819	$ 682,082	$ 671,470
2020	$ 443,392	$ 418,990	$ 405,040	$ 415,909	$ 456,914	$ 434,736	$ 420,952	$ 432,230	$ 504,974	$ 466,439	$ 457,194	$ 458,216	$ 449,454	$ 416,863	$ 396,671	$ 413,552	$ 671,900	$ 661,446
2021	$ 436,034	$ 412,037	$ 398,318	$ 409,007	$ 449,332	$ 427,522	$ 413,967	$ 425,058	$ 496,594	$ 458,699	$ 449,607	$ 450,612	$ 441,996	$ 409,945	$ 390,088	$ 406,690	$ 660,751	$ 650,470
2022	$ 427,978	$ 404,424	$ 390,959	$ 401,450	$ 441,030	$ 419,623	$ 406,318	$ 417,204	$ 487,419	$ 450,224	$ 441,300	$ 442,286	$ 433,829	$ 402,371	$ 382,881	$ 399,175	$ 648,542	$ 638,452
2023	$ 419,156	$ 396,088	$ 382,900	$ 393,175	$ 431,939	$ 410,973	$ 397,943	$ 408,605	$ 477,372	$ 440,944	$ 432,203	$ 433,170	$ 424,887	$ 394,077	$ 374,989	$ 390,947	$ 635,174	$ 625,292
2024	$ 409,496	$ 386,960	$ 374,076	$ 384,114	$ 421,985	$ 401,502	$ 388,772	$ 399,188	$ 466,370	$ 430,782	$ 422,243	$ 423,187	$ 415,095	$ 384,995	$ 366,347	$ 381,937	$ 620,536	$ 610,881
2025	$ 398,919	$ 376,964	$ 364,413	$ 374,192	$ 411,085	$ 391,131	$ 378,729	$ 388,877	$ 454,323	$ 419,654	$ 411,336	$ 412,256	$ 404,372	$ 375,050	$ 356,884	$ 372,072	$ 604,507	$ 595,102
2026	$ 387,336	$ 366,019	$ 353,832	$ 363,327	$ 399,149	$ 379,774	$ 367,733	$ 377,586	$ 441,132	$ 407,470	$ 399,393	$ 400,286	$ 392,632	$ 364,161	$ 346,522	$ 361,269	$ 586,955	$ 577,823
2027	$ 374,653	$ 354,034	$ 342,247	$ 351,431	$ 386,079	$ 367,339	$ 355,692	$ 365,222	$ 426,688	$ 394,128	$ 386,315	$ 387,179	$ 379,775	$ 352,237	$ 335,175	$ 349,439	$ 567,736	$ 558,903
2028	$ 360,766	$ 340,911	$ 329,560	$ 338,404	$ 371,768	$ 353,722	$ 342,507	$ 351,684	$ 410,871	$ 379,518	$ 371,995	$ 372,827	$ 365,698	$ 339,180	$ 322,751	$ 336,486	$ 546,691	$ 538,185
2029	$ 345,559	$ 326,541	$ 315,669	$ 324,139	$ 356,097	$ 338,812	$ 328,070	$ 336,860	$ 393,552	$ 363,521	$ 356,315	$ 357,112	$ 350,283	$ 324,883	$ 309,146	$ 322,303	$ 523,647	$ 515,500
2030	$ 328,907	$ 310,806	$ 300,457	$ 308,520	$ 338,938	$ 322,486	$ 312,261	$ 320,627	$ 374,588	$ 346,003	$ 339,145	$ 339,903	$ 333,404	$ 309,228	$ 294,249	$ 306,772	$ 498,414	$ 490,659
2031	$ 310,673	$ 293,575	$ 283,801	$ 291,416	$ 320,148	$ 304,608	$ 294,950	$ 302,853	$ 353,822	$ 326,822	$ 320,344	$ 321,060	$ 314,921	$ 292,085	$ 277,937	$ 289,765	$ 470,783	$ 463,458
2032	$ 290,708	$ 274,709	$ 265,562	$ 272,688	$ 299,573	$ 285,032	$ 275,995	$ 283,390	$ 331,083	$ 305,819	$ 299,757	$ 300,427	$ 294,682	$ 273,314	$ 260,075	$ 271,143	$ 440,528	$ 433,674
2033	$ 268,845	$ 254,049	$ 245,591	$ 252,181	$ 277,044	$ 263,596	$ 255,239	$ 262,077	$ 306,184	$ 282,820	$ 277,214	$ 277,833	$ 272,521	$ 252,759	$ 240,516	$ 250,752	$ 407,398	$ 401,060
2034	$ 244,906	$ 231,427	$ 223,722	$ 229,725	$ 252,375	$ 240,124	$ 232,511	$ 238,741	$ 278,920	$ 257,636	$ 252,529	$ 253,093	$ 248,254	$ 230,252	$ 219,099	$ 228,424	$ 371,121	$ 365,347
2035	$ 218,692	$ 206,656	$ 199,776	$ 205,136	$ 225,361	$ 214,422	$ 207,624	$ 213,187	$ 249,065	$ 230,059	$ 225,499	$ 226,003	$ 221,682	$ 205,607	$ 195,648	$ 203,974	$ 331,398	$ 326,242
2036	$ 189,988	$ 179,532	$ 173,554	$ 178,212	$ 195,782	$ 186,279	$ 180,372	$ 185,205	$ 216,375	$ 199,863	$ 195,902	$ 196,340	$ 192,585	$ 178,620	$ 169,968	$ 177,202	$ 287,901	$ 283,421
2037	$ 158,557	$ 149,831	$ 144,842	$ 148,729	$ 163,392	$ 155,461	$ 150,532	$ 154,566	$ 180,579	$ 166,799	$ 163,492	$ 163,858	$ 160,725	$ 149,070	$ 141,849	$ 147,886	$ 240,271	$ 236,533
2038	$ 124,140	$ 117,308	$ 113,402	$ 116,445	$ 127,926	$ 121,717	$ 117,857	$ 121,015	$ 141,382	$ 130,593	$ 128,004	$ 128,290	$ 125,837	$ 116,712	$ 111,059	$ 115,785	$ 188,117	$ 185,191
2039	$ 86,454	$ 81,696	$ 78,976	$ 81,095	$ 89,090	$ 84,766	$ 82,078	$ 84,277	$ 98,461	$ 90,947	$ 89,145	$ 89,344	$ 87,636	$ 81,281	$ 77,344	$ 80,635	$ 131,009	$ 128,970
2040	$ 45,187	$ 42,700	$ 41,278	$ 42,386	$ 46,565	$ 44,305	$ 42,900	$ 44,049	$ 51,463	$ 47,536	$ 46,594	$ 46,698	$ 45,805	$ 42,483	$ 40,426	$ 42,146	$ 68,475	$ 67,409
Interest Payed During																		
2011	$ 46,229	$ 43,685	$ 42,230	$ 43,363	$ 47,639	$ 45,326	$ 43,889	$ 45,065	$ 52,649	$ 48,632	$ 47,668	$ 47,774	$ 46,861	$ 43,463	$ 41,358	$ 43,118	$ 70,054	$ 68,964
2012	$ 45,920	$ 43,393	$ 41,948	$ 43,074	$ 47,320	$ 45,024	$ 43,596	$ 44,764	$ 52,298	$ 48,307	$ 47,349	$ 47,455	$ 46,548	$ 43,173	$ 41,081	$ 42,830	$ 69,586	$ 68,503
2013	$ 45,582	$ 43,073	$ 41,639	$ 42,756	$ 46,972	$ 44,692	$ 43,275	$ 44,434	$ 51,913	$ 47,951	$ 47,001	$ 47,106	$ 46,205	$ 42,855	$ 40,779	$ 42,514	$ 69,073	$ 67,998
2014	$ 45,212	$ 42,723	$ 41,301	$ 42,409	$ 46,590	$ 44,329	$ 42,923	$ 44,073	$ 51,491	$ 47,562	$ 46,619	$ 46,723	$ 45,830	$ 42,506	$ 40,447	$ 42,169	$ 68,512	$ 67,446
2015	$ 44,806	$ 42,340	$ 40,930	$ 42,029	$ 46,173	$ 43,931	$ 42,538	$ 43,678	$ 51,029	$ 47,135	$ 46,201	$ 46,304	$ 45,419	$ 42,125	$ 40,085	$ 41,791	$ 67,897	$ 66,841
2016	$ 44,362	$ 41,921	$ 40,525	$ 41,612	$ 45,715	$ 43,496	$ 42,117	$ 43,245	$ 50,523	$ 46,668	$ 45,743	$ 45,845	$ 44,969	$ 41,708	$ 39,688	$ 41,377	$ 67,225	$ 66,179
2017	$ 43,876	$ 41,461	$ 40,081	$ 41,156	$ 45,214	$ 43,019	$ 41,655	$ 42,771	$ 49,970	$ 46,157	$ 45,242	$ 45,343	$ 44,476	$ 41,251	$ 39,253	$ 40,923	$ 66,488	$ 65,453
2018	$ 43,344	$ 40,958	$ 39,594	$ 40,657	$ 44,665	$ 42,497	$ 41,150	$ 42,252	$ 49,363	$ 45,596	$ 44,693	$ 44,793	$ 43,936	$ 40,750	$ 38,776	$ 40,427	$ 65,681	$ 64,659
2019	$ 42,761	$ 40,407	$ 39,062	$ 40,110	$ 44,065	$ 41,926	$ 40,596	$ 41,684	$ 48,699	$ 44,983	$ 44,092	$ 44,190	$ 43,345	$ 40,202	$ 38,255	$ 39,883	$ 64,798	$ 63,790
2020	$ 42,122	$ 39,804	$ 38,479	$ 39,511	$ 43,407	$ 41,300	$ 39,990	$ 41,062	$ 47,972	$ 44,312	$ 43,433	$ 43,531	$ 42,698	$ 39,602	$ 37,684	$ 39,287	$ 63,831	$ 62,837
2021	$ 41,423	$ 39,144	$ 37,840	$ 38,856	$ 42,687	$ 40,615	$ 39,327	$ 40,381	$ 47,176	$ 43,576	$ 42,713	$ 42,808	$ 41,990	$ 38,945	$ 37,058	$ 38,636	$ 62,771	$ 61,795
2022	$ 40,658	$ 38,420	$ 37,141	$ 38,138	$ 41,898	$ 39,864	$ 38,600	$ 39,634	$ 46,305	$ 42,771	$ 41,923	$ 42,017	$ 41,214	$ 38,225	$ 36,374	$ 37,922	$ 61,612	$ 60,653
2023	$ 39,820	$ 37,628	$ 36,376	$ 37,352	$ 41,034	$ 39,042	$ 37,805	$ 38,817	$ 45,350	$ 41,890	$ 41,059	$ 41,151	$ 40,364	$ 37,437	$ 35,624	$ 37,140	$ 60,342	$ 59,403
2024	$ 38,902	$ 36,761	$ 35,537	$ 36,491	$ 40,089	$ 38,143	$ 36,933	$ 37,923	$ 44,305	$ 40,924	$ 40,113	$ 40,203	$ 39,434	$ 36,575	$ 34,803	$ 36,284	$ 58,951	$ 58,034
2025	$ 37,897	$ 35,812	$ 34,619	$ 35,548	$ 39,053	$ 37,157	$ 35,979	$ 36,943	$ 43,161	$ 39,867	$ 39,077	$ 39,164	$ 38,415	$ 35,630	$ 33,904	$ 35,347	$ 57,428	$ 56,535
2026	$ 36,797	$ 34,772	$ 33,614	$ 34,516	$ 37,919	$ 36,079	$ 34,935	$ 35,871	$ 41,908	$ 38,710	$ 37,942	$ 38,027	$ 37,300	$ 34,595	$ 32,920	$ 34,321	$ 55,761	$ 54,893
2027	$ 35,592	$ 33,633	$ 32,513	$ 33,386	$ 36,678	$ 34,897	$ 33,791	$ 34,696	$ 40,535	$ 37,442	$ 36,700	$ 36,782	$ 36,079	$ 33,463	$ 31,842	$ 33,197	$ 53,935	$ 53,096
2028	$ 34,273	$ 32,387	$ 31,308	$ 32,148	$ 35,318	$ 33,604	$ 32,538	$ 33,410	$ 39,033	$ 36,054	$ 35,340	$ 35,419	$ 34,741	$ 32,222	$ 30,661	$ 31,966	$ 51,936	$ 51,128
2029	$ 32,828	$ 31,021	$ 29,989	$ 30,793	$ 33,829	$ 32,187	$ 31,167	$ 32,002	$ 37,387	$ 34,534	$ 33,850	$ 33,926	$ 33,277	$ 30,864	$ 29,369	$ 30,619	$ 49,746	$ 48,972
2030	$ 31,246	$ 29,527	$ 28,543	$ 29,309	$ 32,199	$ 30,636	$ 29,665	$ 30,460	$ 35,586	$ 32,870	$ 32,219	$ 32,291	$ 31,673	$ 29,377	$ 27,954	$ 29,143	$ 47,349	$ 46,613
2031	$ 29,514	$ 27,890	$ 26,961	$ 27,685	$ 30,414	$ 28,938	$ 28,020	$ 28,771	$ 33,613	$ 31,048	$ 30,433	$ 30,501	$ 29,917	$ 27,748	$ 26,404	$ 27,528	$ 44,724	$ 44,029
2032	$ 27,617	$ 26,097	$ 25,228	$ 25,905	$ 28,459	$ 27,078	$ 26,220	$ 26,922	$ 31,453	$ 29,053	$ 28,477	$ 28,541	$ 27,995	$ 25,965	$ 24,707	$ 25,759	$ 41,850	$ 41,199
2033	$ 25,540	$ 24,135	$ 23,331	$ 23,957	$ 26,319	$ 25,042	$ 24,248	$ 24,897	$ 29,088	$ 26,868	$ 26,335	$ 26,394	$ 25,889	$ 24,012	$ 22,849	$ 23,821	$ 38,703	$ 38,101
2034	$ 23,266	$ 21,986	$ 21,254	$ 21,824	$ 23,976	$ 22,812	$ 22,089	$ 22,680	$ 26,497	$ 24,475	$ 23,990	$ 24,044	$ 23,584	$ 21,874	$ 20,814	$ 21,700	$ 35,256	$ 34,708
2035	$ 20,776	$ 19,632	$ 18,979	$ 19,488	$ 21,409	$ 20,370	$ 19,724	$ 20,253	$ 23,661	$ 21,856	$ 21,422	$ 21,470	$ 21,060	$ 19,533	$ 18,587	$ 19,378	$ 31,483	$ 30,993
2036	$ 18,049	$ 17,056	$ 16,488	$ 16,930	$ 18,599	$ 17,696	$ 17,135	$ 17,594	$ 20,556	$ 18,987	$ 18,611	$ 18,652	$ 18,296	$ 16,969	$ 16,147	$ 16,834	$ 27,351	$ 26,925
2037	$ 15,063	$ 14,234	$ 13,760	$ 14,129	$ 15,522	$ 14,769	$ 14,301	$ 14,684	$ 17,155	$ 15,846	$ 15,532	$ 15,567	$ 15,269	$ 14,162	$ 13,476	$ 14,049	$ 22,826	$ 22,471
2038	$ 11,793	$ 11,144	$ 10,773	$ 11,062	$ 12,153	$ 11,563	$ 11,196	$ 11,496	$ 13,431	$ 12,406	$ 12,160	$ 12,188	$ 11,955	$ 11,088	$ 10,551	$ 11,000	$ 17,871	$ 17,593
2039	$ 8,213	$ 7,761	$ 7,503	$ 7,704	$ 8,464	$ 8,053	$ 7,797	$ 8,006	$ 9,354	$ 8,640	$ 8,469	$ 8,488	$ 8,325	$ 7,722	$ 7,348	$ 7,660	$ 12,446	$ 12,252
2040	$ 4,293	$ 4,057	$ 3,921	$ 4,027	$ 4,424	$ 4,209	$ 4,076	$ 4,185	$ 4,889	$ 4,516	$ 4,426	$ 4,436	$ 4,351	$ 4,036	$ 3,840	$ 4,004	$ 6,505	$ 6,404
CASH FLOW - Taxable Earnings																		
2011	$ 137,144	$ 155,769	$ 178,214	$ 165,242	$ 137,698	$ 154,306	$ 182,775	$ 171,826	$ 123,506	$ 145,793	$ 181,812	$ 168,575	$ 127,165	$ 137,442	$ 181,178	$ 147,525	$ 106,696	$ 149,555
2012	$ 71,908	$ 95,182	$ 120,299	$ 105,376	$ 70,124	$ 90,956	$ 122,261	$ 109,361	$ 47,924	$ 77,280	$ 115,503	$ 101,930	$ 60,768	$ 76,941	$ 124,802	$ 87,796	$ 2,811	$ 48,552
2013	$ 113,059	$ 134,651	$ 159,304	$ 144,870	$ 112,551	$ 131,842	$ 162,857	$ 150,535	$ 94,042	$ 120,577	$ 159,176	$ 145,213	$ 102,111	$ 115,574	$ 163,112	$ 126,452	$ 63,387	$ 109,448
2014	$ 147,873	$ 168,184	$ 192,581	$ 178,477	$ 148,421	$ 166,535	$ 197,474	$ 185,567	$ 132,884	$ 157,216	$ 196,332	$ 181,971	$ 137,028	$ 148,311	$ 195,832	$ 159,266	$ 114,075	$ 160,647
2015	$ 177,640	$ 196,994	$ 221,307	$ 207,404	$ 179,070	$ 196,302	$ 227,340	$ 215,717	$ 165,923	$ 188,553	$ 228,305	$ 213,538	$ 166,823	$ 176,354	$ 224,112	$ 187,431	$ 156,869	$ 204,114
2016	$ 203,560	$ 222,209	$ 246,574	$ 232,769	$ 205,737	$ 222,316	$ 253,595	$ 242,152	$ 194,531	$ 215,847	$ 256,335	$ 241,152	$ 192,712	$ 200,821	$ 249,020	$ 212,057	$ 193,621	$ 241,672
2017	$ 220,335	$ 238,849	$ 263,560	$ 249,630	$ 222,944	$ 239,389	$ 271,208	$ 259,714	$ 212,647	$ 233,532	$ 274,949	$ 259,343	$ 209,328	$ 216,777	$ 265,845	$ 228,246	$ 216,136	$ 265,256
2018	$ 229,898	$ 248,731	$ 274,026	$ 259,789	$ 232,690	$ 249,414	$ 282,016	$ 270,286	$ 222,480	$ 243,639	$ 286,144	$ 270,107	$ 218,630	$ 226,022	$ 276,306	$ 237,786	$ 227,399	$ 277,805
2019	$ 239,672	$ 258,837	$ 284,733	$ 270,180	$ 242,650	$ 259,665	$ 293,072	$ 281,099	$ 232,523	$ 253,969	$ 297,593	$ 281,112	$ 228,135	$ 235,473	$ 287,010	$ 247,540	$ 238,889	$ 290,618
2020	$ 249,942	$ 269,436	$ 295,943	$ 281,070	$ 253,120	$ 270,421	$ 304,650	$ 292,432	$ 243,103	$ 264,823	$ 309,594	$ 292,657	$ 238,131	$ 245,396	$ 298,212	$ 257,774	$ 251,045	$ 304,129
2021	$ 290,370	$ 308,417	$ 334,667	$ 320,154	$ 294,767	$ 310,738	$ 344,927	$ 333,171	$ 288,155	$ 307,373	$ 352,800	$ 335,382	$ 278,660	$ 283,429	$ 336,298	$ 295,912	$ 309,737	$ 363,485
2022	$ 331,228	$ 347,830	$ 373,836	$ 359,677	$ 336,855	$ 351,498	$ 385,666	$ 374,368	$ 333,667	$ 350,377	$ 396,491	$ 378,580	$ 319,614	$ 321,874	$ 374,828	$ 334,471	$ 368,988	$ 423,435
2023	$ 342,427	$ 359,383	$ 386,052	$ 371,546	$ 348,271	$ 363,223	$ 398,282	$ 386,719	$ 345,207	$ 362,212	$ 409,569	$ 391,164	$ 330,516	$ 332,694	$ 387,034	$ 345,627	$ 382,255	$ 438,172
2024	$ 353,994	$ 371,311	$ 398,659	$ 383,799	$ 360,062	$ 375,330	$ 411,302	$ 399,469	$ 357,133	$ 374,435	$ 423,070	$ 404,156	$ 341,779	$ 343,869	$ 399,630	$ 357,147	$ 395,976	$ 453,404

	2025	$ 365,944	$ 383,630	$ 411,673	$ 396,451	$ 372,246	$ 387,835	$ 424,744	$ 412,634	$ 369,462	$ 387,064	$ 437,010	$ 417,575	$ 353,418	$ 355,412	$ 412,632	$ 369,045	$ 410,173	$ 469,151
	2026	$ 378,296	$ 396,355	$ 425,112	$ 409,518	$ 384,839	$ 400,754	$ 438,624	$ 426,232	$ 382,210	$ 400,116	$ 451,408	$ 431,436	$ 365,450	$ 367,341	$ 426,057	$ 381,338	$ 424,868	$ 485,438
	2027	$ 391,065	$ 409,505	$ 438,993	$ 423,019	$ 397,858	$ 414,105	$ 452,961	$ 440,281	$ 395,399	$ 413,609	$ 466,284	$ 445,761	$ 377,891	$ 379,672	$ 439,922	$ 394,042	$ 440,084	$ 502,289
	2028	$ 404,271	$ 423,097	$ 453,334	$ 436,972	$ 411,324	$ 427,908	$ 467,775	$ 454,800	$ 409,046	$ 427,563	$ 481,657	$ 460,568	$ 390,762	$ 392,422	$ 454,245	$ 407,175	$ 455,846	$ 519,730
	2029	$ 417,933	$ 437,152	$ 468,156	$ 451,397	$ 425,256	$ 442,182	$ 483,085	$ 469,810	$ 423,175	$ 441,999	$ 497,551	$ 475,879	$ 404,081	$ 405,611	$ 469,047	$ 420,757	$ 472,182	$ 537,789
	2030	$ 432,073	$ 451,690	$ 483,479	$ 466,314	$ 439,676	$ 456,949	$ 498,914	$ 485,332	$ 437,808	$ 456,940	$ 513,986	$ 491,717	$ 417,869	$ 419,258	$ 484,348	$ 434,808	$ 489,120	$ 556,496
	2031	$ 446,714	$ 466,733	$ 499,326	$ 481,747	$ 454,607	$ 472,231	$ 515,284	$ 501,390	$ 452,969	$ 472,408	$ 530,990	$ 508,105	$ 432,149	$ 433,386	$ 500,171	$ 449,349	$ 506,691	$ 575,883
	2032	$ 461,878	$ 482,306	$ 515,721	$ 497,719	$ 470,075	$ 488,053	$ 532,221	$ 518,010	$ 468,685	$ 488,430	$ 548,587	$ 525,071	$ 446,945	$ 448,016	$ 516,538	$ 464,404	$ 524,928	$ 595,983
	2033	$ 477,592	$ 498,433	$ 532,689	$ 514,255	$ 486,104	$ 504,441	$ 549,751	$ 535,216	$ 484,985	$ 505,031	$ 566,805	$ 542,641	$ 462,282	$ 463,174	$ 533,475	$ 479,997	$ 543,865	$ 616,833
	2034	$ 493,884	$ 515,140	$ 550,257	$ 531,383	$ 502,724	$ 521,422	$ 567,902	$ 553,038	$ 501,897	$ 522,242	$ 585,675	$ 560,844	$ 478,188	$ 478,885	$ 551,009	$ 496,154	$ 563,542	$ 638,472
	2035	$ 510,782	$ 532,458	$ 568,455	$ 549,131	$ 519,964	$ 539,026	$ 586,703	$ 571,505	$ 519,454	$ 540,094	$ 605,228	$ 579,713	$ 494,691	$ 495,177	$ 569,167	$ 512,904	$ 583,998	$ 660,942
	2036	$ 528,318	$ 550,416	$ 587,311	$ 567,531	$ 537,856	$ 557,285	$ 606,187	$ 590,649	$ 537,690	$ 558,618	$ 625,498	$ 599,280	$ 511,824	$ 512,081	$ 587,982	$ 530,277	$ 605,277	$ 684,287
	2037	$ 546,525	$ 569,047	$ 606,861	$ 586,615	$ 556,436	$ 576,231	$ 626,388	$ 610,505	$ 556,644	$ 577,851	$ 646,522	$ 619,581	$ 529,620	$ 529,627	$ 607,484	$ 548,304	$ 627,427	$ 708,556
	2038	$ 565,440	$ 588,387	$ 627,138	$ 606,418	$ 575,740	$ 595,902	$ 647,341	$ 631,110	$ 576,353	$ 597,831	$ 668,338	$ 640,655	$ 548,115	$ 547,851	$ 627,709	$ 567,021	$ 650,497	$ 733,799
	2039	$ 585,102	$ 608,473	$ 648,180	$ 626,979	$ 595,808	$ 616,336	$ 669,087	$ 652,503	$ 596,862	$ 618,598	$ 690,988	$ 662,543	$ 567,347	$ 566,789	$ 648,693	$ 586,464	$ 674,543	$ 760,074
	2040	$ 605,552	$ 629,345	$ 670,029	$ 648,339	$ 616,683	$ 637,575	$ 691,667	$ 674,727	$ 618,216	$ 640,197	$ 714,517	$ 685,289	$ 587,359	$ 586,481	$ 670,478	$ 606,673	$ 699,624	$ 787,439
CASH FLOW - Net Earnings - Includes carbon taxes applied AFTER state&fed taxes are applied																			
	2011	$ (407,584)	$ (369,449)	$ (340,569)	$ (360,361)	$ (422,191)	$ (387,723)	$ (355,413)	$ (374,443)	$ (483,804)	$ (427,858)	$ (396,031)	$ (405,103)	$ (420,268)	$ (378,095)	$ (329,545)	$ (368,387)	$ (678,314)	$ (641,049)
	2012	$ 39,585	$ 53,745	$ 68,928	$ 59,886	$ 38,406	$ 51,083	$ 69,977	$ 62,146	$ 24,700	$ 42,623	$ 65,631	$ 57,479	$ 32,852	$ 42,818	$ 71,696	$ 49,357	$ (3,707)	$ 23,821
	2013	$ 63,937	$ 77,107	$ 92,022	$ 83,266	$ 63,514	$ 75,283	$ 94,013	$ 86,521	$ 51,986	$ 68,246	$ 91,487	$ 83,100	$ 57,316	$ 65,680	$ 94,380	$ 72,235	$ 32,125	$ 59,854
	2014	$ 84,455	$ 96,877	$ 111,650	$ 103,083	$ 84,654	$ 95,736	$ 114,432	$ 107,180	$ 74,869	$ 89,840	$ 113,398	$ 104,772	$ 77,890	$ 84,974	$ 113,681	$ 91,579	$ 61,977	$ 90,021
	2015	$ 101,910	$ 113,780	$ 128,515	$ 120,058	$ 102,626	$ 113,198	$ 131,967	$ 124,874	$ 94,231	$ 108,215	$ 132,164	$ 123,293	$ 95,356	$ 101,418	$ 130,286	$ 108,100	$ 87,039	$ 115,496
	2016	$ 117,018	$ 128,489	$ 143,269	$ 134,861	$ 118,168	$ 128,372	$ 147,298	$ 140,302	$ 110,890	$ 124,125	$ 148,524	$ 139,402	$ 110,439	$ 115,681	$ 144,834	$ 122,461	$ 108,418	$ 137,369
	2017	$ 126,597	$ 138,014	$ 153,017	$ 144,521	$ 127,992	$ 138,139	$ 157,405	$ 150,366	$ 121,206	$ 134,224	$ 159,191	$ 149,814	$ 119,917	$ 124,797	$ 154,493	$ 131,721	$ 121,190	$ 150,794
	2018	$ 131,803	$ 143,440	$ 158,810	$ 150,118	$ 133,291	$ 143,632	$ 163,384	$ 156,190	$ 126,500	$ 139,728	$ 165,359	$ 155,723	$ 124,958	$ 129,844	$ 160,294	$ 136,948	$ 127,141	$ 157,529
	2019	$ 137,084	$ 148,953	$ 164,702	$ 155,805	$ 138,666	$ 149,211	$ 169,464	$ 162,109	$ 131,862	$ 145,313	$ 171,628	$ 161,724	$ 130,070	$ 134,966	$ 166,195	$ 142,257	$ 133,151	$ 164,347
	2020	$ 142,608	$ 154,709	$ 170,845	$ 161,741	$ 144,290	$ 155,038	$ 175,805	$ 168,287	$ 137,483	$ 151,154	$ 178,170	$ 167,991	$ 135,421	$ 140,321	$ 172,345	$ 147,802	$ 139,477	$ 171,502
	2021	$ 166,165	$ 177,437	$ 193,441	$ 184,535	$ 168,558	$ 178,544	$ 199,308	$ 192,049	$ 163,718	$ 175,948	$ 203,373	$ 192,904	$ 159,029	$ 162,483	$ 194,572	$ 170,033	$ 173,634	$ 206,073
	2022	$ 189,915	$ 200,362	$ 216,243	$ 207,531	$ 193,022	$ 202,249	$ 223,024	$ 216,021	$ 190,153	$ 200,946	$ 228,798	$ 218,031	$ 182,826	$ 184,830	$ 217,005	$ 192,454	$ 208,025	$ 240,901
	2023	$ 195,796	$ 206,502	$ 222,807	$ 213,867	$ 199,008	$ 208,463	$ 229,798	$ 222,615	$ 196,123	$ 207,165	$ 235,781	$ 224,715	$ 188,517	$ 190,534	$ 223,578	$ 198,367	$ 214,715	$ 248,493
	2024	$ 201,819	$ 212,791	$ 229,533	$ 220,357	$ 205,137	$ 214,827	$ 236,739	$ 229,370	$ 202,233	$ 213,534	$ 242,935	$ 231,563	$ 194,345	$ 196,376	$ 230,315	$ 204,423	$ 221,557	$ 256,263
	2025	$ 207,984	$ 219,233	$ 236,423	$ 227,006	$ 211,412	$ 221,344	$ 243,850	$ 236,290	$ 208,486	$ 220,054	$ 250,263	$ 238,575	$ 200,310	$ 202,358	$ 237,217	$ 210,624	$ 228,552	$ 264,212
	2026	$ 214,295	$ 225,828	$ 243,481	$ 233,814	$ 217,834	$ 228,017	$ 251,134	$ 243,376	$ 214,882	$ 226,728	$ 257,767	$ 245,755	$ 206,414	$ 208,481	$ 244,288	$ 216,974	$ 235,701	$ 272,343
	2027	$ 220,751	$ 232,579	$ 250,709	$ 240,785	$ 224,404	$ 234,847	$ 258,592	$ 250,630	$ 221,423	$ 233,556	$ 265,450	$ 253,104	$ 212,657	$ 214,746	$ 251,529	$ 223,472	$ 243,005	$ 280,656
	2028	$ 227,356	$ 239,488	$ 258,109	$ 247,919	$ 231,123	$ 241,835	$ 266,227	$ 258,056	$ 228,109	$ 240,541	$ 273,314	$ 260,625	$ 219,042	$ 221,156	$ 258,943	$ 230,122	$ 250,464	$ 289,152
	2029	$ 234,108	$ 246,556	$ 265,682	$ 255,219	$ 237,994	$ 248,983	$ 274,042	$ 265,653	$ 234,941	$ 247,682	$ 281,360	$ 268,319	$ 225,569	$ 227,711	$ 266,531	$ 236,923	$ 258,076	$ 297,833
	2030	$ 241,010	$ 253,784	$ 273,431	$ 262,685	$ 245,016	$ 256,292	$ 282,037	$ 273,425	$ 241,919	$ 254,982	$ 289,591	$ 276,187	$ 232,239	$ 234,412	$ 274,297	$ 243,878	$ 265,842	$ 306,697
	2031	$ 248,062	$ 261,173	$ 281,357	$ 270,320	$ 252,190	$ 263,763	$ 290,215	$ 281,371	$ 249,043	$ 262,441	$ 298,007	$ 284,230	$ 239,051	$ 241,260	$ 282,240	$ 250,987	$ 273,759	$ 315,745
	2032	$ 255,264	$ 268,724	$ 289,461	$ 278,124	$ 259,515	$ 271,396	$ 298,577	$ 289,494	$ 256,312	$ 270,059	$ 306,609	$ 292,449	$ 246,006	$ 248,255	$ 290,364	$ 258,251	$ 281,827	$ 324,976
	2033	$ 262,616	$ 276,438	$ 297,745	$ 286,098	$ 266,993	$ 279,193	$ 307,123	$ 297,793	$ 263,726	$ 277,835	$ 315,398	$ 300,845	$ 253,102	$ 255,397	$ 298,668	$ 265,670	$ 290,042	$ 334,387
	2034	$ 270,116	$ 284,313	$ 306,208	$ 294,241	$ 274,621	$ 287,151	$ 315,854	$ 306,269	$ 271,283	$ 285,769	$ 324,375	$ 309,417	$ 260,341	$ 262,686	$ 307,154	$ 273,243	$ 298,402	$ 343,978
	2035	$ 277,765	$ 292,350	$ 314,852	$ 302,554	$ 282,399	$ 295,272	$ 324,771	$ 314,921	$ 278,982	$ 293,860	$ 333,539	$ 318,164	$ 267,718	$ 270,120	$ 315,821	$ 280,970	$ 306,902	$ 353,745
	2036	$ 285,560	$ 300,548	$ 323,675	$ 311,036	$ 290,324	$ 303,554	$ 333,872	$ 323,750	$ 286,818	$ 302,106	$ 342,890	$ 327,086	$ 275,234	$ 277,698	$ 324,670	$ 288,851	$ 315,537	$ 363,684
	2037	$ 293,498	$ 308,905	$ 332,677	$ 319,685	$ 298,395	$ 311,994	$ 343,158	$ 332,753	$ 294,789	$ 310,505	$ 352,425	$ 336,181	$ 282,885	$ 285,419	$ 333,700	$ 296,882	$ 324,302	$ 373,791
	2038	$ 301,578	$ 317,420	$ 341,856	$ 328,500	$ 306,608	$ 320,591	$ 352,626	$ 341,928	$ 302,891	$ 319,053	$ 362,143	$ 345,447	$ 290,667	$ 293,279	$ 342,910	$ 305,062	$ 333,190	$ 384,059
	2039	$ 309,795	$ 326,088	$ 351,211	$ 337,479	$ 314,960	$ 329,341	$ 362,274	$ 351,274	$ 311,119	$ 327,747	$ 372,042	$ 354,880	$ 298,578	$ 301,276	$ 352,298	$ 313,389	$ 342,192	$ 394,483
	2040	$ 318,144	$ 334,907	$ 360,739	$ 346,617	$ 323,445	$ 338,240	$ 372,100	$ 360,787	$ 319,467	$ 336,583	$ 382,117	$ 364,476	$ 306,611	$ 309,405	$ 361,861	$ 321,858	$ 351,299	$ 405,054
CASH FLOW - Discounted Cash Flow																			
	2011	$ (316,081)	$ (283,409)	$ (257,243)	$ (274,925)	$ (327,576)	$ (298,083)	$ (268,484)	$ (285,328)	$ (379,106)	$ (331,691)	$ (301,462)	$ (310,572)	$ (327,592)	$ (292,836)	$ (248,144)	$ (283,779)	$ (536,790)	$ (501,758)
	2012	$ 204,291	$ 208,618	$ 218,914	$ 213,670	$ 208,713	$ 212,435	$ 226,449	$ 222,553	$ 213,156	$ 215,724	$ 235,857	$ 227,636	$ 199,669	$ 196,284	$ 218,217	$ 201,651	$ 251,037	$ 274,544
	2013	$ 195,702	$ 201,006	$ 212,010	$ 206,293	$ 199,759	$ 204,364	$ 219,191	$ 214,846	$ 202,751	$ 206,727	$ 227,667	$ 219,225	$ 190,769	$ 188,452	$ 211,596	$ 194,071	$ 235,921	$ 260,432
	2014	$ 189,867	$ 195,996	$ 207,641	$ 201,504	$ 193,651	$ 199,001	$ 214,574	$ 209,840	$ 195,481	$ 200,624	$ 222,343	$ 213,672	$ 184,653	$ 183,192	$ 207,454	$ 189,047	$ 225,013	$ 250,484
	2015	$ 186,276	$ 193,109	$ 205,341	$ 198,830	$ 189,861	$ 195,846	$ 212,115	$ 207,038	$ 190,762	$ 196,881	$ 219,357	$ 210,451	$ 180,803	$ 180,027	$ 205,337	$ 186,108	$ 217,525	$ 243,922
	2016	$ 184,456	$ 191,901	$ 204,680	$ 197,827	$ 187,900	$ 194,436	$ 211,365	$ 205,980	$ 188,052	$ 195,000	$ 218,222	$ 209,072	$ 178,741	$ 178,517	$ 204,826	$ 184,817	$ 212,721	$ 240,026
	2017	$ 186,532	$ 194,370	$ 207,595	$ 200,481	$ 189,965	$ 196,853	$ 214,343	$ 208,736	$ 189,783	$ 197,214	$ 221,134	$ 211,733	$ 180,619	$ 180,642	$ 207,811	$ 187,139	$ 213,888	$ 242,029
	2018	$ 191,737	$ 199,797	$ 213,388	$ 206,078	$ 195,264	$ 202,346	$ 220,322	$ 214,560	$ 195,076	$ 202,718	$ 227,302	$ 217,641	$ 185,661	$ 185,688	$ 213,611	$ 192,366	$ 219,839	$ 248,764
	2019	$ 197,110	$ 205,395	$ 219,364	$ 211,851	$ 200,733	$ 208,014	$ 226,489	$ 220,569	$ 200,543	$ 208,399	$ 233,665	$ 223,736	$ 190,865	$ 190,896	$ 219,593	$ 197,760	$ 225,991	$ 255,722
	2020	$ 202,543	$ 211,065	$ 225,423	$ 217,701	$ 206,263	$ 213,752	$ 232,743	$ 226,657	$ 206,060	$ 214,144	$ 240,113	$ 229,909	$ 196,124	$ 196,165	$ 225,662	$ 203,220	$ 232,176	$ 262,737
	2021	$ 196,178	$ 205,658	$ 220,771	$ 212,558	$ 199,591	$ 207,946	$ 227,820	$ 221,279	$ 198,059	$ 207,491	$ 234,391	$ 223,910	$ 189,427	$ 190,448	$ 221,271	$ 197,784	$ 220,054	$ 251,760
	2022	$ 189,915	$ 200,362	$ 216,243	$ 207,531	$ 193,022	$ 202,249	$ 223,024	$ 216,021	$ 190,153	$ 200,946	$ 228,798	$ 218,031	$ 182,826	$ 184,830	$ 217,005	$ 192,454	$ 208,025	$ 240,901
	2023	$ 195,796	$ 206,502	$ 222,807	$ 213,867	$ 199,008	$ 208,463	$ 229,798	$ 222,615	$ 196,123	$ 207,165	$ 235,781	$ 224,715	$ 188,517	$ 190,534	$ 223,578	$ 198,367	$ 214,715	$ 248,493
	2024	$ 201,819	$ 212,791	$ 229,533	$ 220,357	$ 205,137	$ 214,827	$ 236,739	$ 229,370	$ 202,233	$ 213,534	$ 242,935	$ 231,563	$ 194,345	$ 196,376	$ 230,315	$ 204,423	$ 221,557	$ 256,263
	2025	$ 207,984	$ 219,233	$ 236,423	$ 227,006	$ 211,412	$ 221,344	$ 243,850	$ 236,290	$ 208,486	$ 220,054	$ 250,263	$ 238,575	$ 200,310	$ 202,358	$ 237,217	$ 210,624	$ 228,552	$ 264,212
	2026	$ 214,295	$ 225,828	$ 243,481	$ 233,814	$ 217,834	$ 228,017	$ 251,134	$ 243,376	$ 214,882	$ 226,728	$ 257,767	$ 245,755	$ 206,414	$ 208,481	$ 244,288	$ 216,974	$ 235,701	$ 272,343
	2027	$ 220,751	$ 232,579	$ 250,709	$ 240,785	$ 224,404	$ 234,847	$ 258,592	$ 250,630	$ 221,423	$ 233,556	$ 265,450	$ 253,104	$ 212,657	$ 214,746	$ 251,529	$ 223,472	$ 243,005	$ 280,656
	2028	$ 227,356	$ 239,488	$ 258,109	$ 247,919	$ 231,123	$ 241,835	$ 266,227	$ 258,056	$ 228,109	$ 240,541	$ 273,314	$ 260,625	$ 219,042	$ 221,156	$ 258,943	$ 230,122	$ 250,464	$ 289,152
	2029	$ 234,108	$ 246,556	$ 265,682	$ 255,219	$ 237,994	$ 248,983	$ 274,042	$ 265,653	$ 234,941	$ 247,682	$ 281,360	$ 268,319	$ 225,569	$ 227,711	$ 266,531	$ 236,923	$ 258,076	$ 297,833
	2030	$ 241,010	$ 253,784	$ 273,431	$ 262,685	$ 245,016	$ 256,292	$ 282,037	$ 273,425	$ 241,919	$ 254,982	$ 289,591	$ 276,187	$ 232,239	$ 234,412	$ 274,297	$ 243,878	$ 265,842	$ 306,697
	2031	$ 248,062	$ 261,173	$ 281,357	$ 270,320	$ 252,190	$ 263,763	$ 290,215	$ 281,371	$ 249,043	$ 262,441	$ 298,007	$ 284,230	$ 239,051	$ 241,260	$ 282,240	$ 250,987	$ 273,759	$ 315,745
	2032	$ 255,264	$ 268,724	$ 289,461	$ 278,124	$ 259,515	$ 271,396	$ 298,577	$ 289,494	$ 256,312	$ 270,059	$ 306,609	$ 292,449	$ 246,006	$ 248,255	$ 290,364	$ 258,251	$ 281,827	$ 324,976
	2033	$ 262,616	$ 276,438	$ 297,745	$ 286,098	$ 266,993	$ 279,193	$ 307,123	$ 297,793	$ 263,726	$ 277,835	$ 315,398	$ 300,845	$ 253,102	$ 255,397	$ 298,668	$ 265,670	$ 290,042	$ 334,387
	2034	$ 270,116	$ 284,313	$ 306,208	$ 294,241	$ 274,621	$ 287,151	$ 315,854	$ 306,269	$ 271,283	$ 285,769	$ 324,375	$ 309,417	$ 260,341	$ 262,686	$ 307,154	$ 273,243	$ 298,402	$ 343,978
	2035	$ 277,765	$ 292,350	$ 314,852	$ 302,554	$ 282,399	$ 295,272	$ 324,771	$ 314,921	$ 278,982	$ 293,860	$ 333,539	$ 318,164	$ 267,718	$ 270,120	$ 315,821	$ 280,970	$ 306,902	$ 353,745
	2036	$ 285,560	$ 300,548	$ 323,675	$ 311,036	$ 290,324	$ 303,554	$ 333,872	$ 323,750	$ 286,818	$ 302,106	$ 342,890	$ 327,086	$ 275,234	$ 277,698	$ 324,670	$ 288,851	$ 315,537	$ 363,684
	2037	$ 293,498	$ 308,905	$ 332,677	$ 319,685	$ 298,395	$ 311,994	$ 343,158	$ 332,753	$ 294,789	$ 310,505	$ 352,425	$ 336,181	$ 282,885	$ 285,419	$ 333,700	$ 296,882	$ 324,302	$ 373,791
	2038	$ 301,578	$ 317,420	$ 341,856	$ 328,500	$ 306,608	$ 320,591	$ 352,626	$ 341,928	$ 302,891	$ 319,053	$ 362,143	$ 345,447	$ 290,667	$ 293,279	$ 342,910	$ 305,062	$ 333,190	$ 384,059
	2039	$ 309,795	$ 326,088	$ 351,211	$ 337,479	$ 314,960	$ 329,341	$ 362,274	$ 351,274	$ 311,119	$ 327,747	$ 372,042	$ 354,880	$ 298,578	$ 301,276	$ 352,298	$ 313,389	$ 342,192	$ 394,483
	2040	$ 318,144	$ 334,907	$ 360,739	$ 346,617	$ 323,445	$ 338,240	$ 372,100	$ 360,787	$ 319,467	$ 336,583	$ 382,117	$ 364,476	$ 306,611	$ 309,405	$ 361,861	$ 321,858	$ 351,299	$ 405,054
CASH FLOW - Cumulative Cash Flow (PV)																			
	2011	$ (316,081)	$ (283,409)	$ (257,243)	$ (274,925)	$ (327,576)	$ (298,083)	$ (268,484)	$ (285,328)	$ (379,106)	$ (331,691)	$ (301,462)	$ (310,572)	$ (327,592)	$ (292,836)	$ (248,144)	$ (283,779)	$ (536,790)	$ (501,758)
	2012	$ (145,838)	$ (109,560)	$ (74,815)	$ (96,867)	$ (153,649)	$ (121,054)	$ (79,777)	$ (99,867)	$ (201,477)	$ (151,920)	$ (104,914)	$ (120,875)	$ (161,201)	$ (129,266)	$ (66,297)	$ (115,737)	$ (327,592)	$ (272,972)
	2013	$ (9,934)	$ 30,027	$ 72,414	$ 46,392	$ (14,928)	$ 20,865	$ 72,439	$ 49,332	$ (60,678)	$ (8,360)	$ 53,188	$ 31,364	$ (28,723)	$ 1,603	$ 80,645	$ 19,034	$ (163,759)	$ (92,116)
	2014	$ 99,942	$ 143,451	$ 192,576	$ 163,003	$ 97,139	$ 136,028	$ 196,614	$ 170,767	$ 52,448	$ 107,742	$ 181,858	$ 155,017	$ 78,136	$ 107,617	$ 200,700	$ 128,436	$ (33,543)	$ 52,839
	2015	$ 189,775	$ 236,578	$ 291,603	$ 258,889	$ 188,700	$ 230,475	$ 298,907	$ 270,612	$ 144,443	$ 202,689	$ 287,644	$ 256,507	$ 165,329	$ 194,435	$ 299,724	$ 218,188	$ 71,359	$ 170,472
	2016	$ 263,903	$ 313,699	$ 373,859	$ 338,392	$ 264,212	$ 308,615	$ 383,850	$ 353,390	$ 220,017	$ 281,055	$ 375,342	$ 340,529	$ 237,162	$ 266,177	$ 382,039	$ 292,461	$ 156,847	$ 266,932
	2017	$ 326,373	$ 378,793	$ 443,382	$ 405,532	$ 327,831	$ 374,540	$ 455,633	$ 423,296	$ 283,575	$ 347,102	$ 449,400	$ 411,437	$ 297,651	$ 326,674	$ 451,634	$ 355,134	$ 228,478	$ 347,987
	2018	$ 379,883	$ 434,553	$ 502,935	$ 463,045	$ 382,326	$ 431,011	$ 517,120	$ 483,175	$ 338,018	$ 403,676	$ 512,836	$ 472,177	$ 349,465	$ 378,496	$ 511,249	$ 408,820	$ 289,831	$ 417,413
	2019	$ 425,724	$ 482,321	$ 553,952	$ 512,315	$ 429,010	$ 479,389	$ 569,795	$ 534,473	$ 384,658	$ 452,143	$ 567,179	$ 524,211	$ 393,854	$ 422,893	$ 562,320	$ 454,812	$ 342,389	$ 476,886
	2020	$ 464,978	$ 523,227	$ 597,640	$ 554,507	$ 468,985	$ 520,816	$ 614,902	$ 578,400	$ 424,593	$ 493,646	$ 613,714	$ 568,769	$ 431,864	$ 460,911	$ 606,055	$ 494,198	$ 387,386	$ 527,806
	2021	$ 496,662	$ 556,442	$ 633,296	$ 588,836	$ 501,220	$ 554,400	$ 651,696	$ 614,138	$ 456,581	$ 527,157	$ 651,570	$ 604,931	$ 462,458	$ 491,669	$ 641,791	$ 526,141	$ 422,926	$ 568,467
	2022	$ 522,223	$ 583,408	$ 662,400	$ 616,767	$ 527,198	$ 581,620	$ 681,712	$ 643,212	$ 482,173	$ 554,202	$ 682,363	$ 634,276	$ 487,064	$ 516,545	$ 670,997	$ 552,043	$ 450,924	$ 600,889
	2023	$ 544,182	$ 606,569	$ 687,389	$ 640,754	$ 549,518	$ 605,001	$ 707,486	$ 668,180	$ 504,170	$ 577,437	$ 708,808	$ 659,479	$ 508,207	$ 537,915	$ 696,073	$ 574,291	$ 475,006	$ 628,759
	2024	$ 563,045	$ 626,457	$ 708,842	$ 661,349	$ 568,691	$ 625,079	$ 729,612	$ 689,617	$ 523,071	$ 597,395	$ 731,513	$ 681,122	$ 526,372	$ 556,269	$ 717,599	$ 593,397	$ 495,713	$ 652,710
	2025	$ 579,244	$ 643,532	$ 727,256	$ 679,030	$ 585,158	$ 642,319	$ 748,605	$ 708,021	$ 539,309	$ 614,534	$ 751,005	$ 699,704	$ 541,973	$ 572,030	$ 736,075	$ 609,802	$ 513,514	$ 673,289
	2026	$ 593,153	$ 658,190	$ 743,060	$ 694,206	$ 599,296	$ 657,119	$ 764,905	$ 723,818	$ 553,256	$ 629,250	$ 767,736	$ 715,654	$ 555,370	$ 585,561	$ 751,931	$ 623,885	$ 528,813	$ 690,965
	2027	$ 605,093	$ 670,770	$ 756,620	$ 707,229	$ 611,434	$ 669,821	$ 778,892	$ 737,374	$ 565,233	$ 641,882	$ 782,094	$ 729,344	$ 566,873	$ 597,177	$ 765,535	$ 635,972	$ 541,956	$ 706,146
	2028	$ 615,341	$ 681,564	$ 768,254	$ 718,404	$ 621,851	$ 680,721	$ 790,891	$ 749,005	$ 575,514	$ 652,724	$ 794,413	$ 741,092	$ 576,746	$ 607,145	$ 777,207	$ 646,344	$ 553,245	$ 719,179
	2029	$ 624,134	$ 690,825	$ 778,233	$ 727,990	$ 630,790	$ 690,073	$ 801,185	$ 758,983	$ 584,339	$ 662,027	$ 804,981	$ 751,170	$ 585,218	$ 615,698	$ 787,218	$ 655,243	$ 562,939	$ 730,366
	2030	$ 631,678	$ 698,769	$ 786,792	$ 736,212	$ 638,460	$ 698,095	$ 810,013	$ 767,542	$ 591,911	$ 670,009	$ 814,045	$ 759,815	$ 592,488	$ 623,035	$ 795,804	$ 662,877	$ 571,260	$ 739,965
	2031	$ 638,149	$ 705,581	$ 794,131	$ 743,263	$ 645,038	$ 704,975	$ 817,583	$ 774,881	$ 598,407	$ 676,854	$ 821,819	$ 767,229	$ 598,723	$ 629,328	$ 803,166	$ 669,424	$ 578,401	$ 748,201
	2032	$ 643,697	$ 711,422	$ 800,423	$ 749,309	$ 650,679	$ 710,875	$ 824,073	$ 781,174	$ 603,979	$ 682,724	$ 828,483	$ 773,586	$ 604,070	$ 634,724	$ 809,477	$ 675,037	$ 584,527	$ 755,265
	2033	$ 648,454	$ 716,430	$ 805,816	$ 754,491	$ 655,515	$ 715,932	$ 829,636	$ 786,568	$ 608,756	$ 687,757	$ 834,196	$ 779,035	$ 608,655	$ 639,351	$ 814,887	$ 679,850	$ 589,781	$ 761,322
	2034	$ 652,532	$ 720,721	$ 810,438	$ 758,933	$ 659,660	$ 720,266	$ 834,404	$ 791,191	$ 612,851	$ 692,071	$ 839,093	$ 783,706	$ 612,585	$ 643,316	$ 819,524	$ 683,974	$ 594,285	$ 766,515
	2035	$ 656,026	$ 724,399	$ 814,399	$ 762,739	$ 663,213	$ 723,981	$ 838,489	$ 795,152	$ 616,360	$ 695,767	$ 843,288	$ 787,708	$ 615,952	$ 646,714	$ 823,497	$ 687,508	$ 598,146	$ 770,964
	2036	$ 659,019	$ 727,549	$ 817,792	$ 765,999	$ 666,256	$ 727,163	$ 841,989	$ 798,546	$ 619,367	$ 698,934	$ 846,883	$ 791,137	$ 618,838	$ 649,625	$ 826,900	$ 690,536	$ 601,453	$ 774,777
	2037	$ 661,583	$ 730,248	$ 820,698	$ 768,792	$ 668,863	$ 729,888	$ 844,987	$ 801,453	$ 621,942	$ 701,646	$ 849,961	$ 794,073	$ 621,309	$ 652,118	$ 829,815	$ 693,130	$ 604,286	$ 778,042
	2038	$ 663,778	$ 732,558	$ 823,186	$ 771,183	$ 671,095	$ 732,222	$ 847,553	$ 803,942	$ 624,147	$ 703,969	$ 852,598	$ 796,588	$ 623,425	$ 654,253	$ 832,311	$ 695,351	$ 606,712	$ 780,838
	2039	$ 665,657	$ 734,537	$ 825,317	$ 773,230	$ 673,005	$ 734,220	$ 849,751	$ 806,073	$ 626,034	$ 705,957	$ 854,855	$ 798,741	$ 625,236	$ 656,081	$ 834,448	$ 697,252	$ 608,787	$ 783,231
NPV	2040	$ 667,266	$ 736,230	$ 827,140	$ 774,983	$ 674,640	$ 735,930	$ 851,632	$ 807,897	$ 627,649	$ 707,659	$ 856,786	$ 800,583	$ 626,786	$ 657,645	$ 836,278	$ 698,879	$ 610,563	$ 785,278
NPV (Millions)		$ 667	$ 736	$ 827	$ 775	$ 675	$ 736	$ 852	$ 808	$ 628	$ 708	$ 857	$ 801	$ 627	$ 658	$ 836	$ 699	$ 611	$ 785
Coal Price	47.90																		
CO_2 Tax	0.00																		
NG Price	4.00																		
Gasoline	3.40																		
SELECT PROPERTIES																			
Total Efficiency (%HHV)		46.4%	50.8%	50.9%	51.6%	47.6%	51.2%	52.4%	52.8%	45.5%	50.8%	52.2%	53.6%	45.0%	49.8%	51.2%	50.7%	44.2%	45.5%
Total Thermal Output (MW)		679	708	710	714	698	724	734	740	707	734	754	753	668	703	709	709	756	778

CO_2 Emitted (tonne CO2/MWh Out)	0.06	0.06	0.19	0.14	0.05	0.05	0.18	0.15	0.00	0.00	0.16	0.11	0.00	0.00	0.15	0.09	0.04	0.46
CO_2 Sequestered (tonne CO2/MWh Out)	0.14	0.09	0.00	0.00	0.14	0.10	0.00	0.00	0.19	0.12	0.00	0.00	0.17	0.09	0.00	0.00	0.42	0.00
CO_2 Emitted (tonne CO2/MWh In)	0.03	0.03	0.10	0.09	0.03	0.03	0.09	0.09	0.00	0.00	0.09	0.07	0.00	0.00	0.08	0.05	0.02	0.20
CO_2 Sequestered (tonne CO2/MWh In)	0.07	0.05	0.00	0.00	0.07	0.06	0.00	0.00	0.09	0.07	0.00	0.00	0.09	0.05	0.00	0.00	0.18	0.00
CO_2 Emitted (tonne CO2/GJ Out)	0.22	0.21	0.67	0.51	0.20	0.19	0.64	0.53	0.00	0.00	0.59	0.41	0.01	0.01	0.56	0.34	0.16	1.65
CO_2 Sequestered (tonne CO2/GJ Out)	0.51	0.31	0.00	0.00	0.51	0.36	0.00	0.00	0.67	0.43	0.00	0.00	0.62	0.34	0.00	0.00	1.50	0.00

Power and Heat duty of units

Power Required, MWh/ton of Products																		
Air Separation Unit	2819.3	1606.8	2819.3	1606.8	3170.0	2120.5	3170.0	2120.5	3589.5	2238.6	3589.5	2238.6	3218.0	1538.5	3218.0	1538.5	5841.0	5841.0
Reformer	1071.7	865.0	1071.7	865.0	706.7	514.5	706.7	514.5	844.4	601.5	844.4	601.5	1017.5	928.1	1017.5	928.1	0.0	0.0
CO_2 Removal	7.6	5.5	7.6	5.5	7.3	5.4	7.3	5.4	9.3	6.5	9.3	6.5	9.0	5.8	9.0	5.8	18.2	18.2
CO_2 Compression	493.6	353.6	-	-	377.1	275.4	-	-	452.3	309.2	-	-	580.6	372.4	580.6	372.4	1416.6	0.0
CLAUS	26.0	19.6	26.0	19.6	16.4	12.0	16.4	12.0	25.5	18.7	25.5	18.7	35.1	24.8	35.1	24.8	28.6	28.6
Fischer-Tropsch (FT)	11.6	11.6	11.6	11.6	105.5	103.9	105.5	103.9	160.3	148.0	160.3	148.0	11.7	11.7	11.7	11.7	109.3	109.3
Steam turbines power generation, MWh/to	1609.8	1746.2	1609.8	1746.2	2898.9	2960.1	2898.9	2960.1	2002.5	2070.8	2002.5	2070.8	1063.8	1162.1	1063.8	1162.1	6913.7	6913.7
Nuclear Heat Duty requirement, MJ/tonne c	0	10.3	0	10.3	0	8.8	0	8.8	0.0	11.4	0.0	11.4	0.0	16.2	0.0	16.2	0	0

Chapter 3

A New Power, Methanol, and DME Polygeneration Process Using Integrated Chemical Looping Systems

Energy Conversion and Management 88 (2014) 411–425

Contents lists available at ScienceDirect

Energy Conversion and Management

journal homepage: www.elsevier.com/locate/enconman

A new power, methanol, and DME polygeneration process using integrated chemical looping systems

Yaser Khojasteh Salkuyeh, Thomas A. Adams II *

Department of Chemical Engineering, McMaster University, 1280 Main St. W, Hamilton, Ontario L8S 4L7, Canada

ARTICLE INFO

Article history:
Received 13 June 2014
Accepted 18 August 2014
Available online 16 September 2014

Keywords:
Coal gasification
Natural gas reforming
Chemical looping
Helium-heated steam reformer
Polygeneration

ABSTRACT

In this work, a novel polygeneration process has been proposed which combines coal gasification and natural gas reforming with either one or two chemical looping systems to produce electricity, methanol, and dimethyl ether (DME). Optionally, a modular helium reactor (MHR) is used to provide the heat required for the natural gas reforming step, which minimizes the amount of fossil fuels used for heating purposes. The process is fully integrated such that essentially 100% of all CO_2 produced by the process can be captured and sequestered. Techno-economic analysis of different design strategies are presented, considering three options for coal gasification, incorporation of various ratios of natural gas input, utilization of carbonless energy from MHR, power generation using chemical looping combustion and also CO_2 sequestration based on liquefaction or hydration technologies. Moreover, the impact of varying the proportions of products on the thermal efficiency and profitability of the plant is investigated.

1. Introduction

Global energy demand is increasing in all forms, including electrical power, liquid fuels (e.g. gasoline, diesel) and hydrogen. Coal is still a relatively inexpensive and reliable resource for most industrialized countries (50% of electricity in the United States comes from coal [1]). Most research in this area focuses on advanced concepts such as: (1) decreasing the carbon capture cost by switching from traditional pulverized coal combustion plants to the integrated gasification combined cycle process (IGCC) as an approach to replace the low-concentration CO_2 absorption processes with more effective techniques [2]; (2) improving the efficiency and flexibility of power plants by using multi-product processes [3]; and (3) integrating existing techniques with alternative energy sources such as natural gas [4–6] and biomass [7].

By use of the Fischer–Tropsch (FT) process, coal can be converted to synthesis gas (CO and H_2) which is then converted into diesel and gasoline. CO_2 emissions can be captured from this process using amine solvents with a moderate energy penalty. However, the carbon emissions of FT processes are still relatively high, generating more than 15 kg per gallon of fuel product [8], which accounts for as much as 18% of the total inlet carbon in even the most novel designs [9]. Natural gas is another attractive feedstock that can be used to produce liquid fuels or other chemical products instead of coal. Considering the low price and abundance of natural gas, it is a practical option to supply the growing demands for liquid fuels (gasoline and diesel are projected to grow 29% and 50% respectively by 2035 compared to 2010 [10]). In addition to the FT process, the conversion of natural gas to other chemicals such as methanol and dimethyl ether (DME) is another attractive research area [11]. DME can be used as a fuel with lower soot, CO, and NO_x emissions than diesel [12] and also as a blending component for liquefied petroleum gas (LPG) and diesel fuels [13].

Creating liquid fuels from natural gas instead of coal can result in a higher efficiency, although the potential for carbon emissions remains because of unreacted tail-gas losses from the liquid production unit and the limited capability of CO_2 removal in commercial CO_2 absorption units. In fact, the CO_2 absorption section has a very strong impact on both the net thermal efficiency [14] and the

Abbreviations: ASU, air separation unit; C_i, concentration of component i, kmol/m^3; DME, dimethyl ether; FT, Fischer–Tropsch; GTL, gas-to-liquids; HHV, higher heating value; HP, high pressure steam; HRSG, heat recovery steam generation; IGCC, integrated gasification combined cycle; IP, intermediate pressure steam; $K_{eq,i}$, equilibrium constant of reaction i; k_i, rate constant of reaction i, kmol/kg$_{cat}$ s; K_i, adsorption constant of component i; LHV, lower heating value; LP, low pressure steam; LPG, liquefied petroleum gas; MHR, modular helium reactor; NG, natural gas; NPV, net present value; p_i, partial pressure of component i, bar; r_i, rate of reaction i, kmol/kg$_{cat}$ s; R, gas constant, 8.314 kj/kmol K; SCL, syngas chemical looping; T, temperature, K; TAC, total annualized cost; WGS, water gas shift; η_{therm}, thermal efficiency of plant.

* Corresponding author. Tel.: +1 (905) 525 9140x24782.
E-mail address: tadams@mcmaster.ca (T.A. Adams II).

http://dx.doi.org/10.1016/j.enconman.2014.08.039
0196-8904/

capital investment [15] of such a plant. In terms of incorporation of new feedstocks, using carbonless resources is a promising possibility. For example, the integration of a modular helium reactor (MHR) unit with a hydrogen production plant based on a Sulfur–Iodine cycle as well as high-temperature electrolysis have been studied with promising results [16]. Considering these processes, a similar approach can be used with natural-gas-to-liquids (GTL) plants where energy from a MHR can be introduced to supply some of the heat demand without any additional carbon emissions. Demonstration plants that coupled the steam reformer with a simulated helium reactor were constructed and tested successfully in Japan [17] and China [18]. Because this carbonless energy displaces fossil fuel combustion for heat production, the production of CO_2 can be significantly reduced [19].

Furthermore, the implementation of large-scale polygeneration plants which use multiple feeds (coal, natural gas, etc.) and produce multiple products (power, liquid fuels, chemicals, etc.) has received particular interest over recent years [20,21]. The purpose of a polygeneration system is twofold. First, efficiency gains can be achieved by tightly integrating multiple processes together into one chemical system in order to take advantage of synergies between them (for example, exothermic heat from one process drives an endothermic reaction in another). Second, profitability gains can be achieved by operating the plant flexibly enough to change the proportions of feedstocks used and the proportions of products produced in response to fluctuating market prices [5,22]. Previous studies of polygeneration systems have mostly focused on design and simulation, thermal optimization and economic analyses. Although the multi-in/multi-out configuration has a much higher efficiency than using a single feedstock (e.g. coal only) [5,23,24], CO_2 emissions for previously published polygeneration plants remain a concern due to the way tail gas is handled—e.g. combustion in a gas turbine and subsequent venting of the CO_2 to the atmosphere. Therefore, the purpose of this work is to design and analyze a polygeneration plant using a different approach which has both high efficiency and near-zero CO_2 emissions. In this work, electricity and liquid fuels are produced in a polygeneration facility using chemical looping technologies integrated with MHR.

Although polygeneration processes have the capability of producing electricity and fuel, most polygeneration processes proposed to date have used the water gas shift reaction (WGS) to increase the H_2 content of syngas. However, this reaction is one of the major contributors to energy losses that can potentially be avoided. Not only is energy lost in the form of low grade heat from the exothermic water gas shift reaction, but additional CO_2 is produced, which increases downstream CO_2 capture requirements. In addition, there are significant energy losses in the CO_2 removal section, which is required to remove CO_2 both from the syngas before FT synthesis, as well as from flue exhausts, if desired. Together, these have a significant impact on efficiency, which in turn has a negative environmental impact.

The syngas chemical looping (SCL) process is one such process which can be used to alleviate both of these problems for plants which rely on coal as a major carbon and energy source [25]. The SCL process (Fig. 1) first oxidizes syngas generated by a coal gasifier by reducing metal oxides, producing hot combustion products (from which the heat can be recovered for electricity generation or other purposes) and hot reduced metal particles. The hot reduced metal particles are then partially oxidized using steam, which produces useful H_2 for sale or for upgrading the H_2 content of syngas for use in liquid fuel production downstream. The partially oxidized metals are then fully oxidized in a combustion step using air, generating a hot exhaust gas (spent air with useful waste heat) and fully oxidized metals, which are recycled to the reducer. Overall, the net reaction is to take energy originating in the coal syngas and produce two useful hot exhaust streams (one containing primarily CO_2 and H_2O, the other containing primarily N_2 and O_2) and one high-purity H_2 product stream. In addition to the useful H_2 and heat products, all carbon in the feed syngas ends up in the CO_2/H_2O waste stream, from which essentially 100% can be captured by techniques such as simply condensing the H_2O, or by the formation of CO_2 hydrates for sequestration. As a result, the SCL process addresses both of the current polygeneration challenges by producing H_2 without the losses associated with the water gas shift reaction and by capturing up to 100% of the CO_2 without the losses associated with CO_2 absorption processes.

After comparing various metal oxides (Fe_2O_3, NiO, CuO, Mn_3O_4 and CoO), Li et al. determined that iron oxide was the best choice for SCL with the right balance of conversion, the ability of the solid pellets to resists against crushing, and price [26]. A hybrid iron oxide chemical looping/solid oxide fuel cell system based on coal as the inlet fuel was developed by Chen et al. [27] with a net plant electrical efficiency of 43.5% by lower heating value (LHV). In addition, a 25 kW moving bed SCL sub-pilot plant for hydrogen production from syngas, based on iron-oxide chemical looping, was tested by Tong to demonstrate the operability of technology [28]. The reactivity tests of a bench scale chemical looping system using iron-oxide shows promising results for long term continuous operation [29]. The reactions are given as follows [30,31]:

Reduction (750–900 °C):

$$Fe_2O_3 + H_2 \rightleftharpoons 2FeO + H_2O \quad (1\text{-}1)$$

$$3Fe_2O_3 + H_2 \rightleftharpoons 2Fe_3O_4 + H_2O \quad (1\text{-}2)$$

$$Fe_2O_3 + CO \rightleftharpoons 2FeO + CO_2 \quad (2\text{-}1)$$

$$3Fe_2O_3 + CO \rightleftharpoons 2Fe_3O_4 + CO_2 \quad (2\text{-}2)$$

Oxidization (500–750 °C):

$$3FeO + 4H_2O \rightleftharpoons Fe_3O_4 + 4H_2 \quad (3)$$

Combustion (900–1150 °C):

$$4Fe_3O_4 + O_2 \rightleftharpoons 6Fe_2O_3 \quad (4)$$

Note that some other reaction mechanisms have been reported [28,32]. However, in all works chemical and phase equilibria are assumed for all moving bed/fluidized bed reactor models, and thus the kinetic mechanisms and rates are not considered for modeling purposes (see the proposed models by Fan [33] for more details on the simulation of chemical looping systems).

In addition, a novel chemical looping system is designed by Jin et al. for hydrogen-fuelled gas turbine combustion [34,35]. This loop is based on the reduction of nickel oxide (NiO), supported on inert $NiAl_2O_4$ [36] or $MgAl_2O_4$ [37] with hydrogen, and then oxidization of the reduced metal with air. This can avoid NO_x completely because N_2 is not present in the fuel oxidizing section. The simplified process flow diagram of this method is presented in Fig. 2 [38,39]. Note that, in theory, any fuel can be used instead of H_2 with similar benefits. The reduction and oxidization reactions of this system are as follows:

$$\text{Reducer}: NiO + H_2 \rightleftharpoons H_2O + Ni \quad (5)$$

$$\text{Oxidizer}: 2Ni + O_2 \rightleftharpoons 2NiO \quad (6)$$

This work introduces a new integrated polygeneration process based on the incorporation of the two chemical looping systems mentioned above, and using a combination of coal, natural gas and nuclear energy in various proportions. It also co-produces power, DME and methanol, and can be altered to produce FT liquids if desired (although FT liquids are not considered for this particular study). The main advantage of this process is that the carbon emissions of the power and liquid production units can

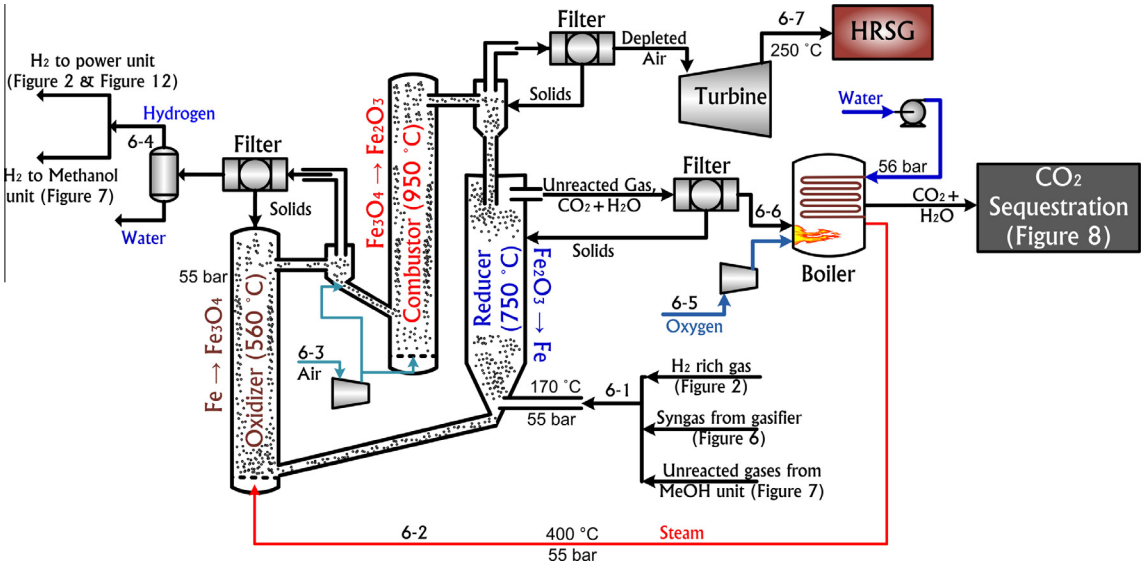

Fig. 1. Simplified SCL process, based on experimental results of a sub-pilot plant constructed by Tong et al. [28]. The first digit of each stream (6) represents the unit number shown in Fig. 3.

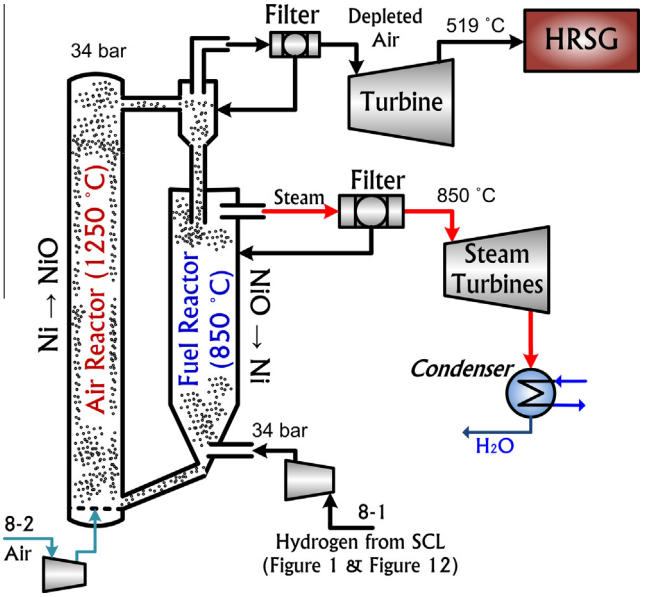

Fig. 2. Hydrogen fuelled chemical looping power plant, based on experimental set-up proposed by Ishida et al. [34,40].

be completely captured in an efficient manner. A techno-economic analysis of this novel system is performed for eleven different system configuration options. These options consider various combinations of the use of natural gas in variant amounts, the optional use of nuclear energy, the strategy for CO_2 capture (liquefaction or hydration), the strategy for gasification (dry gasification, slurry gasification, or both), and the strategy for power generation (traditional gas turbines or nickel oxide chemical looping combustion), all with 100% CO_2 capture and no heat or electricity imports. The results include the thermal efficiencies and profitability of each case as well as a sensitivity analysis that examines the effects of changes in key economic parameters and changes in desired product portfolios.

Both gasifiers are modeled based on heat and material balance data published in previous works [5,22,41–43]. The MHR reactor and also both chemical looping systems are also simulated based on operating conditions reported by Yin et al. [18], Tong et al. [28], and Ishida et al. [34,40]. In addition, the natural gas reforming as well as the methanol and DME production models are adopted from our prior works and updated for this new integrated system [44,45].

2. Polygeneration system integrated with chemical looping and MHR reactor

Our proposed process, shown in Fig. 3, produces methanol, DME, and power while capturing up to 100% of the CO_2 directly produced by the process. In this configuration, coal gasification is used in conjunction with iron oxide and nickel oxide chemical looping systems to produce pure hydrogen and electrical power, respectively. A methanol/DME production section is coupled with the chemical looping sections to complete the polygeneration system. In the base-case configuration, coal is the only fuel. However, two optional modifications have been considered. In Option A, auto-thermal natural gas reforming is used to increase the H_2/CO ratio at the inlet of the iron-oxide loop (see Fig. 4), thus creating a system fuelled by both coal and natural gas. In Option B, natural gas reforming is also used to increase the H_2/CO ratio, except that the required heat for the reaction is provided not by combusting natural gas, but via integration with a modular helium reactor (MHR) system (see Fig. 5) [19]. In this option, helium is used as a heat carrier which transports heat produced by the MHR to the reformer to supply the required heat (see [46] for more details). The components of these systems are described next.

2.1. Coal gasifiers

Two different coal gasifiers are investigated for synthesis gas production and hydrogen production. One is a slurry-type gasifier (downward entrained flow slagging-type) which operates at high pressures (>5 MPa) and results in higher H_2 concentrations (Table 1) [8] and easier CO_2 separation at this high pressure (Fig. 6a). The second option is dry gasification technology which results in a higher molar syngas ratio ((H_2 + CO)/other gases) of 0.95 compared to 0.85 for the slurry gasifier. Furthermore, the syngas from both gasifiers is exposed to calcium oxide to remove some portion of the impurities (H_2S, COS and HCl) as follows [33]:

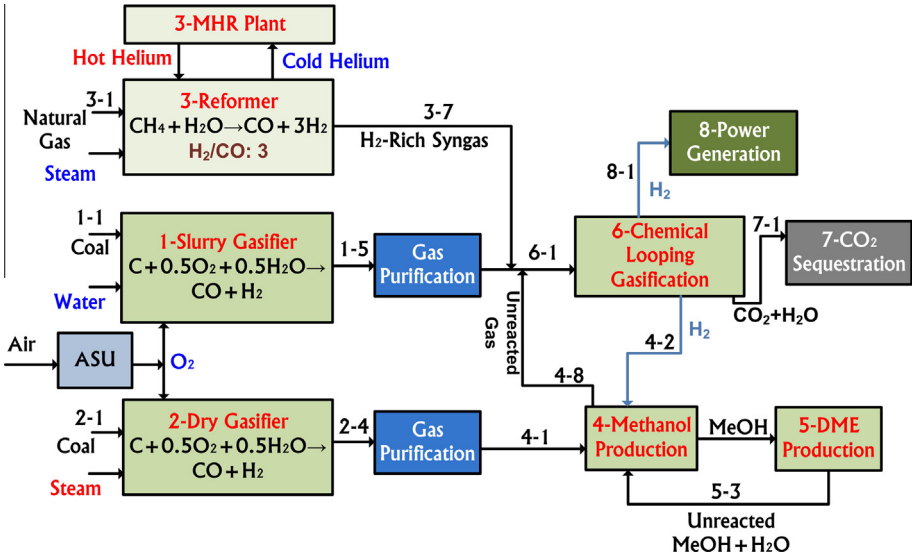

Fig. 3. Simplified polygeneration process, integrated with natural gas reformer and MHR.

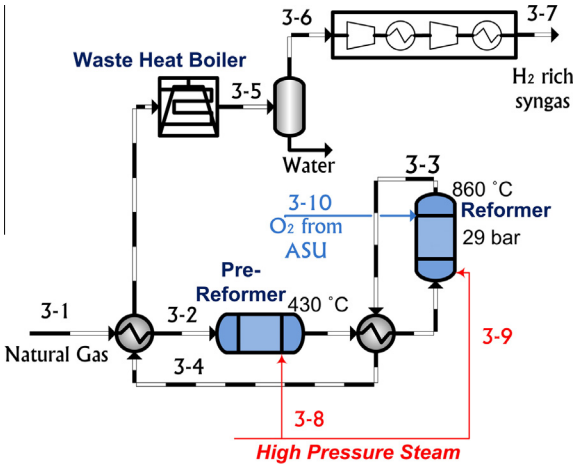

Fig. 4. Option A, natural gas reformer.

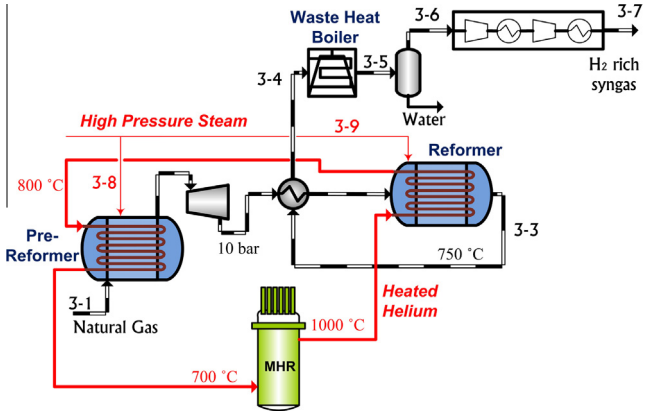

Fig. 5. Option B, MHR plant to supply the required heat of reformer. Simulation is based on pilot plant constructed by Institute of Nuclear and New Energy Technology (INET) [18].

Table 1
Syngas composition of both gasifiers (dry basis).

Syngas mole fraction	Slurry gasifier	Dry gasifier
CO	0.48	0.60
CO_2	0.14	0.04
H_2	0.37	0.35
CH_4	1.7×10^{-4}	4.4×10^{-4}

$$CaO + H_2S \rightleftharpoons CaS + H_2O \quad (7)$$

$$CaO + COS \rightleftharpoons CaS + CO_2 \quad (8)$$

$$CaO + 2HCl \rightleftharpoons CaCl_2 + H_2O \quad (9)$$

2.2. DME/methanol production

As shown in Fig. 7, DME is made from syngas by use of a two-step reaction sequence in the presence of catalyst: (1) methanol synthesis (with side reactions of ethanol and methyl methanoate formation), and (2) methanol dehydration. The syngas composition going into the methanol reactor can vary significantly depending on the gasification technology, the unreacted gas recycle ratio to the reactor (see Fig. 7), and whether or not the natural gas reformer and MHR coupling system is employed. Since these changes directly affect the yield and conversion rate of the methanol reactor, a kinetic model for the reactors is required. A detailed study on the kinetics of the methanol synthesis was performed by Vanden bussche and Froment [48]. Based on their results, CO_2 is the main source of carbon (instead of CO) and the actual reaction mechanism is:

$$CO + H_2O \leftrightarrow CO_2 + H_2 \overset{2H_2}{\leftrightarrow} CH_3OH + H_2O$$

Therefore, the methanol synthesis reactions on $Cu/ZnO/Al_2O_3$ catalyst are simulated in Aspen Plus based on their work as follows [48]:

$$\text{Methanol synthesis}: CO_2 + 3H_2 \rightleftharpoons CH_3OH + H_2O \quad \Delta H_{25} = -49.51\ \text{kJ/mol} \quad (10)$$

$$CO_2 + H_2 \rightleftharpoons CO + H_2O \quad \Delta H_{25} = 41\ \text{kJ/mol} \quad (11)$$

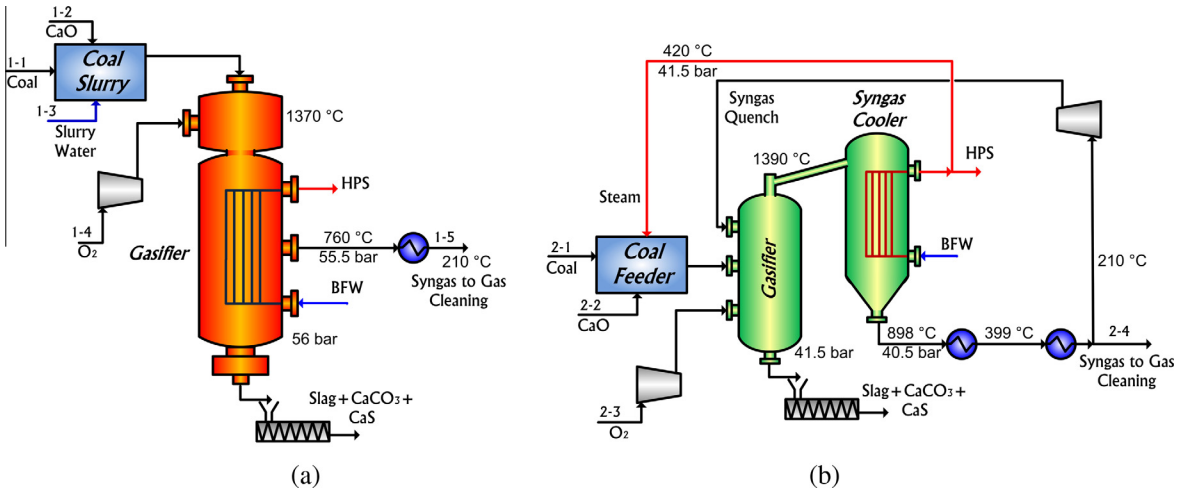

Fig. 6. Gasification technology: (a) Slurry gasifier; (b) dry gasifier. The simulation results are in agreement with the results reported by Haslbeck et al. [47].

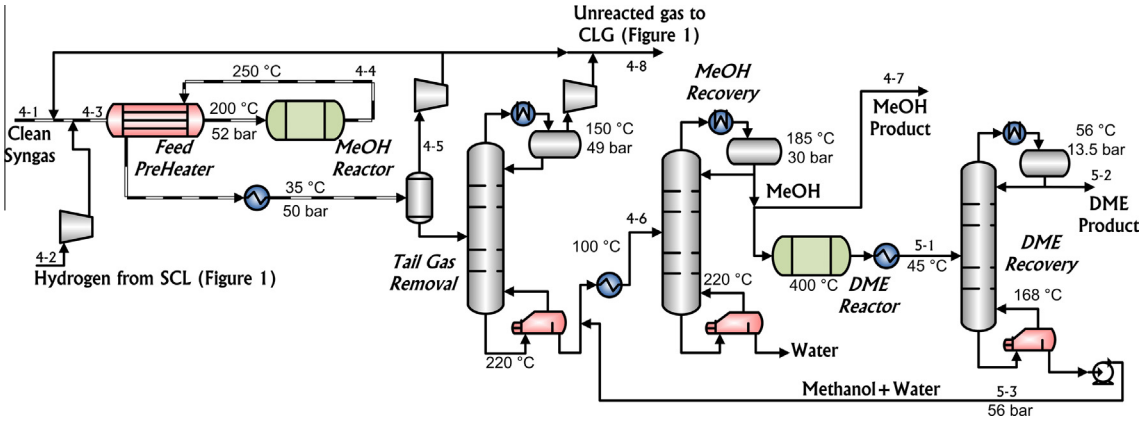

Fig. 7. Methanol and DME production unit; picture was adapted from [45].

$$r_{11} = \frac{k_{11} p_{CO_2} p_{H_2} [1 - (1/K_{eq,11})(p_{H_2O} p_{CH_3OH} / p_{H_2}^3 p_{CO_2})]}{(1 + K_1(p_{H_2O}/p_{H_2}) + K_2\sqrt{p_{H_2}} + K_3 p_{H_2O})^3}, \frac{kmol}{kg_{cat}\ s}$$

$$r_{12} = \frac{k_{12} p_{CO_2} [1 - (1/K_{eq,12})(p_{H_2O} p_{CO} / p_{CO_2} p_{H_2})]}{(1 + K_1(p_{H_2O}/p_{H_2}) + K_2\sqrt{p_{H_2}} + K_3 p_{H_2O})}, \frac{kmol}{kg_{cat}\ s}$$

$$K_1 = 3453.38$$

$$K_2 = 0.499 \exp\left(\frac{17197}{RT}\right)$$

$$K_3 = 6.62 \times 10^{-11} \exp\left(\frac{124119}{RT}\right)$$

$$k_{11} = 1.07 \times 10^{-3} \exp\left(\frac{36696}{RT}\right)$$

$$k_{12} = 1.22 \times 10^{7} \exp\left(\frac{-94765}{RT}\right)$$

The equilibrium constants are [49]:

$$\ln(K_{eq,11}) = -24.389 + 7059.726/T$$

$$\ln(K_{eq,12}) = 4.4724 - 4400/T$$

The DME synthesis reaction (Eq. (12)) is modeled based on the kinetic parameters of methanol dehydration on a γ-Al_2O_3 catalyst [50], and the thermodynamic equilibrium constant parameters [51]:

$$\text{Methanol dehydration}: 2CH_3OH \rightleftharpoons CH_3OCH_3 + H_2O$$
$$\Delta H_{25} = -24\ kJ/mol \quad (12)$$

$$r_{13} = \frac{k_{13} K_4^2 [C_{CH_3OH}^2 - (1/K_{eq,13}) C_{H_2O} C_{CH_3OCH_3}]}{(1 + 2\sqrt{K_4 C_{CH_3OH}} + K_5 C_{H_2O})^4}, \frac{kmol}{kg_{cat}\ s}$$

$$K_4 = 5.39 \times 10^{-4} \exp\left(\frac{8487}{T}\right)$$

$$K_5 = 8.47 \times 10^{-2} \exp\left(\frac{5070}{T}\right)$$

$$K_{13} = 1.49 \times 10^{10} \exp\left(\frac{-17280}{T}\right)$$

$$\ln(K_{eq,13}) = \frac{2835.2}{T} + 1.675 \ln(T) - 2.39 \times 10^{-4} T - 0.21 \times 10^{-6} T^2 - 13.36$$

In the proposed process, methanol is produced via reaction (10) using syngas produced by the gasifier mixed with hydrogen produced by the Fe_2O_3 loop and unreacted syngas recycled from downstream. The hydrogen is used to ensure that the molar ratio of H_2:CO is 2:1 to meet the stoichiometry of reaction (10). The recycled unreacted syngas is recovered in the vapor product of a distillation column immediately downstream of the methanol synthesis reactor. Traditionally, a purge stream is required for this recycle stream in order to avoid the accumulation of N_2, CO_2 and unreacted CH_4 [52,53]. The purge stream is typically sent to the combustion chamber of a gas turbine or flared to the atmosphere, resulting in unwanted CO_2 emissions. However, in our process, the purge stream (10% of the unreacted gas) is sent to the Fe_2O_3 loop. This innovation prevents both the buildup of N_2 but also prevents CO_2 emissions from flaring or combustion.

Methanol is purified in a second distillation column by removing water. A portion of the methanol is collected for sale (stream 4–7 in Fig. 8) and the rest is sent to the methanol dehydration reactor to produce DME. The DME product is purified and collected in stream 5–2. It should be noted that instead of using this two-step approach to produce DME, a single step approach [54] may be utilized in which DME is synthesized directly from syngas in a dual catalyzed reactor. However, this is beyond the scope of this paper.

2.3. Fe_2O_3 loop

In general, the required H_2/CO ratio for methanol production is around 2:1, but the H_2 content of coal-derived syngas is generally too low (around 0.75). One possible strategy for increasing the H_2 content includes using the water gas shift reaction to convert H_2O and CO in the coal-derived syngas into H_2 and CO_2 [5]. However, as discussed in Section 1, additional CO_2 removal steps would be required to extract the newly added CO_2, which is expensive and energy intensive. Another alternative is to produce syngas rich in H_2 by reforming natural gas (H_2/CO ratio around 3:1). One could then mix this H_2-rich syngas directly with the H_2-lean coal-derived syngas. However, this would also require CO_2 and water removal steps due to the CO_2 generated during the reforming process and the use of excess steam. Instead, the iron-oxide chemical looping process can be used to produce H_2 from natural gas-derived syngas without a large CO_2 content with costs and energy consumption potentially lower than using a CO_2 separation process. In fact, both coal-derived and gas-derived syngas can be used in the iron-oxide chemical looping process. The H_2 produced by the iron-oxide loop can then be blended directly into the coal-derived syngas to achieve the desired H_2/CO ratio. The loop used in this work follows the three-stage design described in Section 1.

2.4. Natural gas reformer (Option A or B)

The optional natural gas reformer (Fig. 4) can be used to improve the ability of the Fe_2O_3 loop to produce H_2, or simply to increase the amount of H_2 that is produced. Excess H_2 not needed for mixing into coal-derived syngas is used for power generation. The process can thus be fine-tuned to produce more or less power (for the same amount of liquid fuel production) by changing the amount of natural gas that is reformed.

The reformer process of Option A needs mostly pure oxygen from an air separation unit (ASU) in order to oxidize or combust some of the natural gas to provide the rather large heat requirement for reforming. This approach is chosen for this process because the CO_2 produced by oxidation will remain mixed with the syngas and never mix with air (nitrogen). It will thus pass through the iron oxide loop (leaving through stream 6–6 in Fig. 1), and then be captured downstream with minimal energy losses since the CO_2 is never mixed with nitrogen. An alternative could be a more traditional approach in which heat is provided to the reformer by the burning of natural gas in air. However, this approach produces CO_2 emissions since the CO_2 cannot easily be removed from the air.

In Option B, heat is provided to the reformer from a carbonless heat source, thus eliminating the need for the burner as well as the production of high-purity oxygen. In the proposed process, high-temperature helium from a modular helium reactor (MHR) is used as the source of carbonless heat [19]. In this system, helium flows through the reactor and removes the heat generated by nuclear elements that contain coated uranium oxy-carbide micro spheres. The temperature of helium outlet can be 1000 °C or higher, which is very suitable for gas turbine plants or other high temperature processes [55]. Details of the structure of this system is described by Şahin and Akbayir [56].

2.5. MHR unit (Option B)

This system is based on the integration of a gas turbine and modular helium reactor that can operate at higher temperatures than conventional nuclear power plants [56]. In Option B, helium cools the MHR, exits up to 1000 °C (see Fig. 5), is used to heat the natural gas reforming reactor, and is finally returned to the MHR.

2.6. CO_2 sequestration

The proposed process is designed such that all carbon atoms originating in the natural gas and coal feeds end up in either the

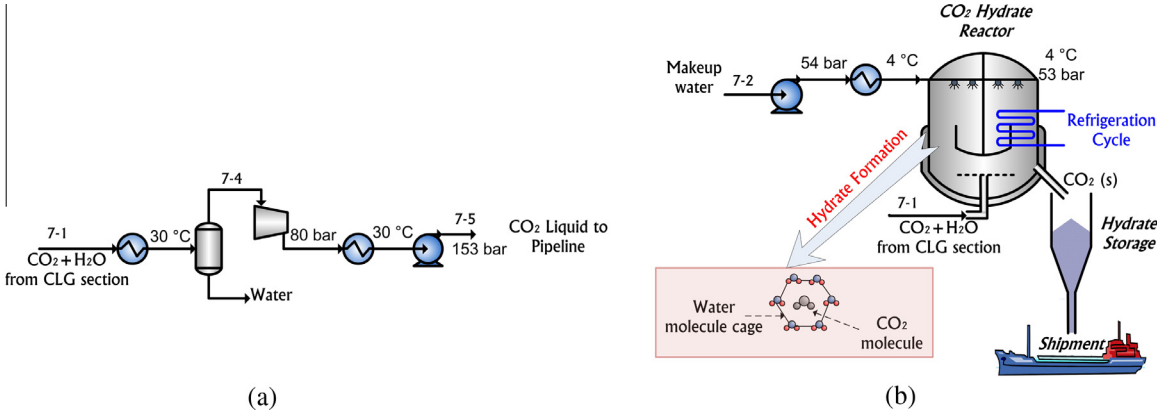

Fig. 8. CO_2 sequestration options.

liquid products or the reducer exhaust (Fig. 1, stream 6–6). Any CO or hydrocarbons remaining in the reducer exhaust is oxidized in an oxidizer, resulting in a stream consisting of essentially H_2O and CO_2 at 54 bar. At this point, there are two options for CO_2 sequestration. One could cool and condense out the water, leaving a CO_2 stream at high purity and pressure suitable for supercritical CO_2 pipeline transportation and sequestration, as shown in Fig. 8 [41]. However, in this process, we also investigate a different carbon capture strategy using gas hydrate formations [57,58] for the purpose of comparing its performance with the liquefaction approach. The gas hydrate approach involves the crystalline formation of CO_2 (as the guest molecule) trapped in water (as the host molecule) at high pressure [59]. The main reaction can be expressed as [60]:

$$CO_2\ (g) + nH_2O\ (\text{liq. to solid}) \rightleftharpoons CO_2 \cdot nH_2O\ (\text{solid})\ (n \geq 6)$$

By using this sequestration method the CO_2 compression can be avoided. The outlet stream from the CO oxidizer is around 54 bar, and contains mostly CO_2 (97–99 mol% dry basis with some N_2 and argon impurities) plus some excess water by-product from the methanol synthesis section (Fig. 7, water stream). As shown in Fig. 8, CO_2 hydration occurs by spraying liquid water into the gas CO_2 at the hydrate formation temperature and pressure in a stirred tank reactor. It should be noted that the hydration pressure could be reduced significantly by using hydrate promoters such as Tetrahydrofuran (THF) [58]. The temperature of the reactor is adjusted by a refrigeration cycle. The cost analysis results of this system is described in Section 4.2 and compared with the liquefaction approach. The solid CO_2 can also be converted to powder or pellet forms and then transported [61].

2.7. Gas turbines and the NiO loop

In the proposed process, power is produced in several places: the HRSG bottoming cycle (see Section 3.2), a Brayton cycle turbine which recovers waste energy in the compressed air exhaust leaving the iron-oxide section, a conventional gas combustion turbine, and the gas turbine in the nickel oxide loop. The conventional gas turbine section combusts a portion of the H_2 produced in the iron oxide loop to produce electricity, with excess air and waste N_2 from the ASU section used as a diluent. This is analogous to a gas turbine system commonly found in integrated gasification combined cycles with CO_2 capture [47]. The nickel oxide loop uses the configuration introduced by Jin et al. [34,35] and is discussed in Section 1 and shown in Fig. 2. The amount of H_2 sent to either the conventional gas combustion turbine or the nickel oxide loop is taken as a parameter and discussed in Sections 4.3 and 4.4.

3. Methodology

To compute mass flows, energy uses, and operating parameters of the three design cases (the base case, Option A, and Option B), steady-state simulations in Advanced System for Process Engineering (ASPEN Plus 2006.5) software were performed. The properties of coal and natural gas feedstock streams used in this study are listed in Table 2. In addition, the main design parameters and cost analysis assumptions are listed in Tables 3 and 4 respectively.

The operating conditions of the chemical looping systems were determined by sensitivity analysis as described in Section 3.1. Water-only unit operations were simulated with the NBS/NRC physical property package, and the Peng–Robinson Boston–Mathias equation of state was used for the remaining units, which was determined in prior work to be a good choice for this application [41]. The simulation of the slurry gasifier, natural gas reformer and also the ASU plant is based on models described in other works [5,22,41,42]. Furthermore, the dry gasifier is modeled based on the work of Cormos [43]. The ambient heat losses of the reformer to the environment were not modeled throughout the flowsheet. There are various commercial sulfur removal processes that can be used to remove H_2S from syngas. Aqueous phase processes like LOCAT [62], or non-aqueous such as CrystaSulf [63] and Clauspol [64] technologies can be used to remove the H_2S impurities. Sulfur recovery is not modeled in this work, but its steam and power requirement is considered in thermal calculations based on the Clauspol process [64].

The thermal efficiency of the plant is calculated for each case as [3,47]:

$$\eta_{\text{therm}} = \frac{\text{HHV of fuels produced} + \text{power generated}}{\text{HHV of all fossil fuel consumed} + \text{helium stream energy consumed}}$$

The power generated is the total power produced minus the power consumption of all auxiliary equipment (pumps and compressors), the ASU section, the refrigeration system and the cooling system.

A summary of market prices and cost analysis parameters is listed in Table 4. To incorporate the risk of investment on this innovative technology, some conservative values for the debt-to-equity ratio and shareholder investment rate are used which are recommended by the NETL for high risk projects in the coal-to-liquids area [66]. The economic analysis of the gasifiers, steam reforming unit, CO_2 compression and power generation part was performed using calculated values from [47] and [5]. In addition, Aspen Icarus was used for the capital costs estimation of the rest of the plant, for which no published data could be found in the literature for this application.

3.1. Iron-oxide reduction/oxidization reactors

There are three main parameters of the iron-oxide loop that can affect the performance of system: the temperature, the metal-oxide circulation rate, and the steam consumption in the oxidizer. The circulation rate and steam consumption must be minimized to decrease the size of the reactors and also the power loss due to high pressure steam consumption in the oxidizer. Fe_2O_3 is an inexpensive metal oxide with relatively high activity compared to other oxygen carriers [28,74,75]. The simulation results show that around 92% of Fe_2O_3 is converted to FeO (reaction (1-1)) and the rest is reduced to Fe_3O_4 (reaction (1-2)). The effect of the inlet $Fe_2O_3/(H_2 + CO)$ ratio on the carbon monoxide and hydrogen conversion in the reducer for the coal-only (base) case is shown in Fig. 9. It can be seen that, at the same iron-oxide/syngas ratio, although higher CO conversion (exothermic) is achievable at a lower temperature, a higher temperature is needed to reach the highest achievable H_2 conversion (endothermic). The ratio of 0.8–0.9 is enough to get around 90% CO conversion for this case; however this ratio is revised upward for Options A and B which use syngas coming from the natural gas reformer. In general, this ratio and also the operating temperature of the reducer is specified such that both the reducer and combustor must be exothermic (cooling is provided by raising steam, see Section 3.2). The $Fe_2O_3/(H_2 + CO)$ ratio is between 0.9 and 1 for coal-only and between 1.1 and 1.45 for Options A and B. The combustor temperature varies between 900 and 960 °C for coal-only and 920–1000 °C for Options A and B.

The minimum steam requirement for Fe/FeO conversion to Fe_3O_4 is shown in Fig. 10. It can be seen that at lower temperatures, this exothermic reaction needs less inlet steam to achieve the same conversion. However, the operating temperature of the oxidizer and reducer are restricted by the minimum reported operating temperature to achieve sufficiently fast gas–solid reactions, which is 500 °C for the oxidizer and 750 °C for the reducer [43,75].

Table 2
Properties of feedstock streams [47].

Coal: illinois bituminous # 6					
13126 Btu/lb (HHV); moisture content: 11.12% weight					
Dry basis analysis (wt.%)					
Ash	10.91	Nitrogen	1.41	Oxygen	7.75
Carbon	71.72	Chlorine	0.33		
Hydrogen	5.06	Sulfur	2.82		
Natural gas composition (mol.%)					
Methane	93.9	Propane	0.7	CO_2	1
Ethane	3.2	n-Butane	0.4	N_2	0.8

Table 3
Main process design parameters.

Air separation unit	Cryogenic Process [65]; Oxygen purity: 99.5% molar Delivery condition: 32 °C and 10 bar
Slurry gasifier	Temperature: 1370 °C, pressure: 55 bar Oxygen/coal ratio (kg/kg): 0.80
Dry gasifier	Temperature: 1400 °C, pressure: 40 bar Oxygen/coal ratio (kg/kg): 0.7 Inlet steam/coal ratio (kg/kg): 0.1 RGIBBS reactor model for both gasifiers
Iron-oxide loop	Reducer temperature: 750 °C, pressure: 55 bar Fe_2O_3/syngas molar ratio: 0.83–1.4 Oxidizer temperature: 560 °C, pressure: 55 bar Steam/FeO molar ratio: 1.4–1.51 Combustor temperature: 950 °C, pressure: 55 bar RGIBBS reactor model for all reactors
Sulfur removal	Steam demand: 0.48 kg/kg sulfur Power demand: 24 kw h/kg sulfur
Methanol/DME	Methanol reactor temperature: 250 °C, pressure: 51 bar DME reactor temperature: 400 °C, Pressure: 15 bar RPlug reactor model for both reactors Syngas column-condenser: 151 °C, 49 bar; reboiler: 218 °C, 50.9 bar Methanol mass recovery: 98% Methanol column-condenser: 185 °C, 30 bar; reboiler: 219 °C, 33.9 bar Methanol mass recovery: 95%, methanol mole purity: 99.8% DME column-condenser: 56.7 °C, 13.5 bar; reboiler: 160 °C, 16.4 bar DME mass recovery: 99.9%, DME mole purity: 99.6%
NiO loop	Reducer temperature: 860 °C, pressure: 34.5 bar Oxidizer temperature: 1250 °C, pressure: 34 bar RGIBBS reactor model for both reactors
Gas turbine	Temperature: 1260 °C, inlet pressure: 35 bar, outlet pressure: 1.05 Isentropic efficiency: 0.898, mechanical efficiency: 0.988
Steam turbines	High pressure steam: 420 °C, 40.5 bar Turbine outlet pressure (HP, IP, LP): 17/5.8/0.1 bar Turbine outlet temperature: 308/193/46 °C Isentropic efficiency: 0.875, mechanical efficiency: 0.983

3.2. Power generation and HRSG

The Heat Recovery Steam Generator (HRSG) section is integrated with other sections and its design consists of a heat exchanger network which uses all available heat sources to produce high pressure steam (HP). The HRSG and turbines are based on standard closed loop steam cycle using typical heuristics. Some of the steam is used to supply the required HPS for the gasifier, pre-reformer, reformer and the Fe_2O_3 loop, and the remaining steam is used to produce electricity in the first steam turbine. The effluent from the first turbine is medium pressure steam (MPS), which is used for the reboilers in the distillation columns and for electricity in subsequent intermediate (IP) and low pressure (LP) steam turbines. The operating conditions of steam levels are decided by the process requirements, except for the LPS pressure (the outlet of the second turbine), which is selected to achieve the maximum total power from the IP and LP turbines. The operating conditions of the power generation section were determined based upon previous works [5,22] as well as the steam requirements for the other process units.

4. Results and discussion

Example stream tables and the line-item details for the net present value (NPV) analysis are provided in supplementary material for the base case. Sensitivity analyses of the key design parameters are discussed in the following sections.

4.1. Gasification technology

As shown in Fig. 11, a sensitivity analysis was performed on the thermal efficiency and profitability of the whole plant for the coal-only scenario and for three different gasification options: (1) combination of dry/slurry gasification technology based on the schematic shown in Fig. 3; (2) slurry gasifier only, which is similar to first option with the exception that the dry gasification unit is removed and the syngas coming from the slurry gasifier is split between the chemical looping gasification and methanol/DME production units; (3) dry gasifier only, with the syngas coming from the dry gasifier is split between two downstream units. As far as efficiency is concerned, it can be seen from Fig. 11a that the dry technology is more efficient than the two other gasification systems. However, in terms of plant profitability, Fig. 11b shows that the slurry gasification technology has higher NPV when the net power output percentage is more than 40%. This result occurs because there is no high pressure steam requirement in the slurry gasifier, thus all of the generated steam is used for power generation. Due to these results, the slurry gasification configuration is chosen as the candidate case for the remaining discussion.

4.2. CO_2 sequestration

Using the reported value for the temperature required for hydrate formation at 54 bar [76,77], the power consumption, capital and total annualized costs of both CO_2 capture variants for the sequestration rate of 537 tonne CO_2/day (the CO_2 rate of the base case) are shown in Table 5. It can be seen that although the hydration approach has lower capital cost, the power requirement cost, mostly because of the refrigeration cycle, plays very important role in the total annual cost of hydration technology. Therefore, the liquefaction technique is chosen as the sequestration approach for the remainder of this paper.

4.3. NiO loop or conventional hydrogen combustion gas turbine

In this section, the two primary power production options (the nickel oxide loop versus conventional hydrogen combustion

Table 4
Cost analysis elements and assumptions.

Natural gas price, $/MMBtu	4.26 [67]
Coal price, $/ton	46 [68]
Electricity, ¢/kW h	10.04 [69]
Iron-oxide (commercial grade, 96 wt.%), $/kg	0.8 [70]
Iron-oxide disposal cost, $/kg	1
MHR capital investment, $/MW	0.4575 [71]
MHR reactor fuel and operating cost, $/yr MW	0.04 [71]
Chemical Engineering Plant Cost Index (CEPCI), July 2013	582.2
Design scale for the economic analysis of each case	4000 MW of input (coal, natural gas and helium)
Economic assumptions [5,72]	
Chemical Engineering Plant Cost Index (CEPCI), July 2013	582.2
Operation time (h/year)	8760
Capacity factor	85%
Plant/loan lifetimes (year)	30
Interest rate on loan	9.5%
Debt percentage	50%
Inflation	2.79%
Federal + state tax rate	40%
Equity return rate	20%
Cost elements [73]	
Indirect cost	20% Fixed capital cost
Working capital cost	15% Total investment
Operating labor	10% Total production cost
Laboratory charges, direct supervisory and clerical labor	20% Operating labor
Utilities	10% Total product cost
Maintenance and repairs	5% Fixed capital investment
Operating supplies	10% Maintenance and repair
Administrative and plant-overhead costs	65% Cost for operating labor, supervision, and maintenance
R&D, distribution and selling costs	4% of total product cost

turbine) are compared. To do this, two parameters were varied: the proportion of H_2 produced by the Fe_2O_3 loop which has been diverted to either the nickel oxide loop (stream 8–1 in Fig. 12) or the combustion turbine (stream 8–3 in Fig. 12), and the inlet temperatures to the NiO gas turbine (labelled "Gas Turbine" in Fig. 2) and combustion turbine (stream 8–5 in Fig. 12). In each case, both turbines were specified to have the same turbine inlet temperature by changing the amount of air sent to either the combustion chamber (stream 8–4 in Fig. 12) or the NiO loop (stream 8–2 in Fig. 2), since air acts as a diluent. All other design variables were held constant throughout the procedure.

As shown in Fig. 13, higher gas turbine inlet temperatures generally translate to higher total plant power outputs (which is preferred) except for the cases where 80% or more of the H_2 is used in the NiO loop. In those cases, an optimum turbine inlet temperature exists between 1250 and 1325 °C. This is because the negative effects on electricity conversion efficiency in the gas turbine at lower temperatures are offset by higher mass flow rates to the gas turbine (noting that the inlet stream to the gas turbine in the NiO case is depleted air which has similar properties with diluent air). For the conventional combustion strategy, the effect of heat capacity reduction is more dominant than increasing the mass rate to the gas turbine. It should be noted that, although both strategies have the same total power production at temperatures between 1350 and 1375 °C, because of the low melting temperature of NiO (around 1450 °C [26]) it is impractical to increase the NiO turbine inlet temperature to these high temperatures. Furthermore, the NiO loop is more complex and expensive to construct, and since its highest achievable power (about 108.2 MJ/mol inlet H_2) is similar to that of combustion turbines, there is no incentive to use it. Therefore, for the remainder of this paper, conventional fuel gas combustion is selected for the power island and the NiO loop is not used. However, NiO loops will be reconsidered in a future work wherein the consideration of more details such as blade-cooling system design may result in very different results due to the trade-off between turbine inlet temperature and cooling system design [78–80].

4.4. Nitrogen injection to the gas turbine from ASU

Instead of (or in addition to) increasing the excess air used for dilution purposes, it is possible to inject waste nitrogen from the ASU plant instead. In the analysis described in the previous section, the waste nitrogen produced by the ASU is at high pressure and thus some power is recovered by expansion through a gas turbine after preheating with available waste heat (not shown in Fig. 3, although it is factored into the total power calculations, see [41] for an example). As shown in Fig. 14, diverting some or all of this waste ASU nitrogen into the combustion turbine instead (thereby reducing the hydrogen concentration) can increase the net power output of the system for all possible turbine inlet temperatures within the ranges of interest considered. This is because using waste nitrogen at the much higher temperatures of the gas combustion turbine creates more power (due to higher efficiency) than is lost by diverting it away from the Brayton expansion turbines in the ASU. It should be noted that for a given amount of nitrogen diverted from the ASU (or hydrogen composition), higher turbine inlet temperatures are still preferable. To draw the isotherms in Fig. 14, the diversion rate of ASU was varied, and for each case, the flow rate of excess air (stream 8–4 in Fig. 12) was adjusted to achieve the desired turbine inlet temperature.

It is therefore possible to dilute and decrease the inlet temperature by using N_2 while still achieving a higher net power output. In addition, lower hydrogen purities in the feed stream are more desirable from a maintenance and operational safety perspective. For the investigations herein, all available N_2 from the ASU was used, and the air flow rate was adjusted accordingly to obtain the maximum achievable turbine inlet temperature. However, this temperature reduction is limited by $\Delta T_{approach}$ between the hot exhaust gases of the turbine for high pressure steam generation in the HRSG unit. Assuming 50 °C for this temperature approach in HRSG, the maximum nitrogen ratio and minimum acceptable TIT are 1.4 and 1260 °C respectively, which are selected as the final design conditions as indicated in Fig. 14.

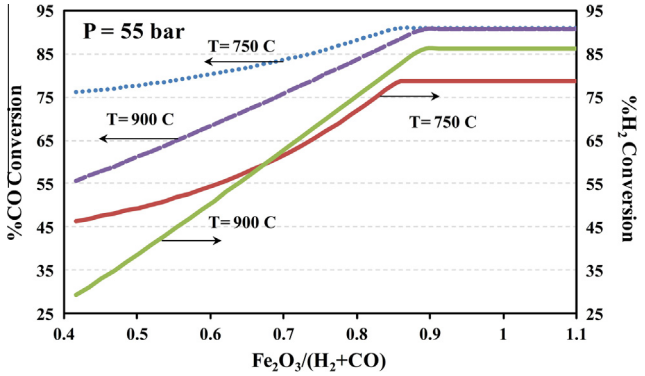

Fig. 9. Effect of iron-oxide to syngas molar ratio on CO conversion in the reducer for two different temperatures.

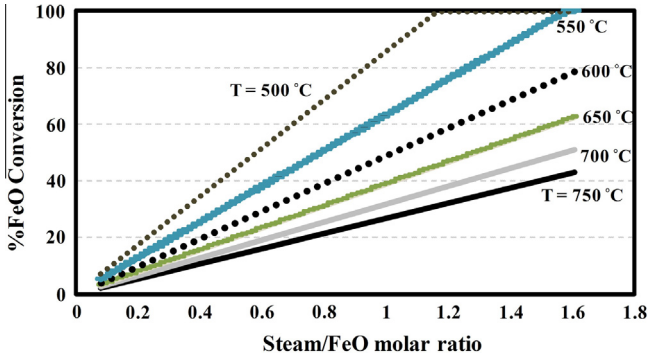

Fig. 10. Minimum steam requirement in the oxidizer.

4.5. Liquid fuels production

The product portfolio can be changed by varying the ratio of syngas (coming from coal or natural gas) that is sent to the CLG and Methanol/DME units. As presented in Figs. 15a and 16a, liquid fuel production has a higher net thermal efficiency and net profit than power production, and thus polygeneration processes that produce a greater portion of liquid fuels will have a greater net thermal efficiency. This is consistent with other polygeneration processes [5,22]. For example, as shown in Fig. 15a, a coal-only polygeneration system in which 80% of the energy content in the products is power has an efficiency of 36.3 HHV% (or 41.8% by LHV), but if only 30% of the products are power the efficiency increases to 49.5 HHV% (or 53.4% by LHV). Similar results for the net profit of the plant can be seen in Fig. 16a. The typical thermal efficiency of coal-only polygeneration processes is around 41% (HHV) when 50% of the output is electricity [5]. It should be noted that the CO_2 emissions of that system was around 250 kg CO_2/GJ of output, while in our proposed model the CO_2 emissions is essentially zero. In addition, Yu et al. investigated new synergies for a coal-based polygeneration system that co-produces liquid fuels and electricity [81]. The thermal efficiency of their proposed system was around 44.9% (LHV) when 30% of output was electricity.

Table 5
Cost parameters of both CO_2 sequestration options (power consumption of the refrigeration is included in the hydration part).

	Liquefaction	Hydration
Power consumption, kJ/kg CO_2	37.3	55.4
Capital cost, $/(kg/h CO_2)	87.2	79.3
Total Annual Cost (TAC), $/tonne CO_2	2.02	2.41

4.6. Utilization of natural gas and helium heated streams

For this novel design, the incorporation of natural gas and helium-heated stream from MHR is studied to determine the effect of Options A and B on the total thermal efficiency. The inlet natural gas/coal ratio (MJ/MJ) is 20% for this case. As shown in Fig. 15a (see the "20% NG" line and the "Coal Only" line), at the same power generation percentage, it is possible to obtain a higher efficiency when using natural gas when compared to a coal-only system. For example, at a power generation percentage of 80%, the net efficiency of the coal/NG case is 37.5% (1.2 percentage points more than coal-only). This value can also be increased by supplying the required heat for natural gas reforming with helium stream from the MHR (Fig. 15b). Therefore, for the same operating condition of plant, the net efficiency of coal/natural gas/helium plant is 38.8 HHV%. As another example, when 40% of the net output is power, the efficiency of coal-only, coal/NG and coal/NG/MHR are 46.2%, 48.1% and 49.3% respectively.

4.7. Natural gas to coal ratio

As shown in Figs. 15 and 16, increasing the percentage of inlet natural gas from 20% to 40% (compared to coal) can improve the net efficiency and NPV of plant whether MHR is used or not. In addition, using an integrated MHR/reformer instead of an autothermal reformer increases the total efficiency by approximately 1 percentage point (on average) for each case, noting that this carbonless energy stream is 3.9%/5.7%/7.2% of the total input for cases 20%/30%/40% NG respectively. This means that around 4–7.2% of the energy in the liquid fuel and power comes from this nuclear energy source. Note that although using more natural gas yields higher efficiencies, there is a limit to how much natural gas can

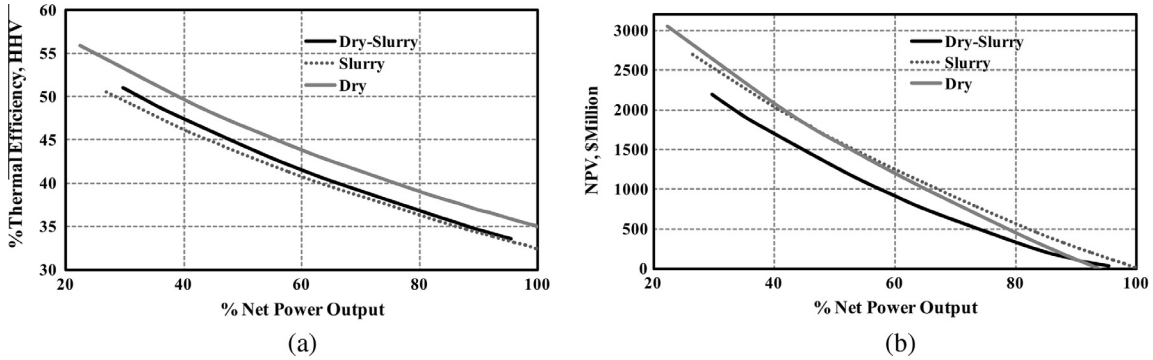

Fig. 11. Illustration of the gasification technology effect on the (a) performance and (b) NPV of the system.

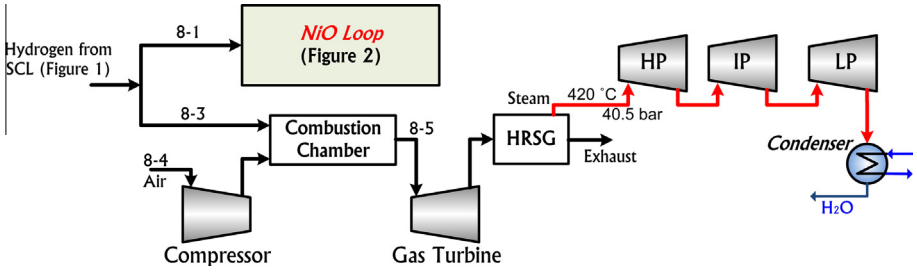

Fig. 12. Power generation island.

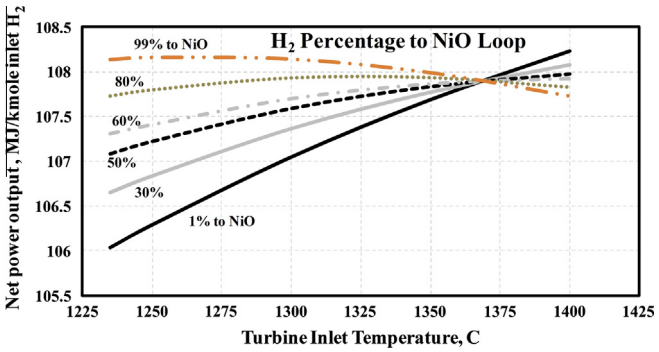

Fig. 13. Effect of gas turbine inlet temperature on the net power output of plant for different hydrogen fuel percentage to the NiO loop.

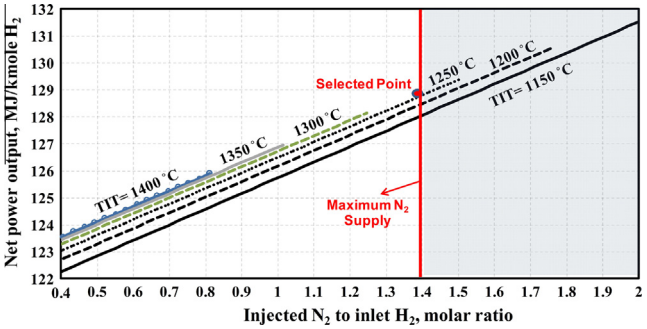

Fig. 14. Net power output of gas turbine varying with nitrogen injection ratio. All cases with inlet N_2/H_2 molar ratios utilize 100% of the available nitrogen in the plant.

be used for different product portfolios. This limit is due to the desired H_2/CO ratio for methanol synthesis of about 2.0, and using too much natural gas results in too much H_2 production and thus ratios which are too high.

In addition, the efficiency of selected cases of the new proposed zero-carbon-emissions process (coal-only, coal-natural gas, coal-natural gas-helium) for power-only configurations is compared to other processes and shown in Fig. 17. It should be noted that the efficiency of other processes are based on 90% carbon capture for General Electric Energy IGCC (GEE, 93.4 kg CO_2 emission/MW h_{net}) and Shell IGCC (98.9 kg/MW h_{net}), subcritical (120.7 kg/MW h_{net}) and supercritical (110.7 kg/MW h_{net}) pulverized coal, and natural gas combined cycle (NGCC, 42.6 kg/MW h_{net}) cases [47]. It can be seen that the proposed processes produce power with zero CO_2 emissions at higher efficiencies than the other coal-based processes. Fig. 18 summarizes the net efficiency of different cases where 50% of the net output is electricity. It can be seen that the maximum net achievable efficiency is around 48.5% (HHV).

4.8. MHR cost

The influence of MHR capital and operating cost changes on the net present value is shown in Fig. 19 for two scenarios: Power-only and 50%-Power. In general, the Coal-40% NG design is more sensitive to the MHR cost, because it uses the most helium of all options. In addition, changing the power output ratio to 50% decreases the difference between the NPVs of Coal-NG and Coal-NG-Helium systems. This is because the total electricity production is smaller in this case.

5. Future challenges

Although the proposed process is promising, more work remains before implementation is possible. Chemical looping has not been commercialized yet [82], and its integration into systems of this type requires additional experimentation. In addition, although supercritical CO_2 sequestration has been demonstrated, there are several regulatory and financial barriers before its use will be widespread. Sequestration in hydrate form is more futuristic. Furthermore, carbon taxes (and sequestration regulations) are not developed enough at present to incentivize CO_2 sequestration on the large scale, and therefore it is unlikely that it will be implemented within the next few years. If not, the process could be constructed to be "CO_2 Capture Ready" in which the waste CO_2/H_2O stream leaving the CO oxidizer is vented to the atmosphere. Then, the CO_2 capture section (either supercritical pipeline or CO_2 hydrate) can be retrofitted to the process at relatively low expense since the rest of the process would remain unchanged.

In addition, if Option B were to be exercised, a MHR would have to be integrated for this purpose. Although MHR prototypes have been demonstrated a half-century ago, new versions are still in development and are unlikely to come online for at least a decade, and nuclear regulatory issues are always a challenge. Therefore, it is likely that the first commercial versions of the proposed process will exercise Option A (not using the MHR) and use a "Capture Ready" strategy in which the CO_2 capture and sequestration portions are retrofitted to the process as the regulatory framework changes or sale for use in enhanced oil recovery is profitable.

Other process variants are possible without substantial modification to the system. For example, biomass could be used in place of some or all of the coal, either by replacing one or both of the coal gasifiers with biomass variants or by mixing biomass into the coal in appropriate proportions. The addition of biomass is likely to reduce the profitability of the plant due to its higher cost than coal, although there is potential for a substantial environmental benefit to using a "carbon neutral" fuel. For example, although our process has 100% CO_2 emissions, there will be CO_2 emissions downstream from combustion of the methanol or DME. It may be possible to integrate enough biomass into the process to counteract these emissions (since biomass removes CO_2 from the atmosphere) to make not only a process that has zero direct CO_2 emissions, but a product that is net zero lifecycle CO_2.

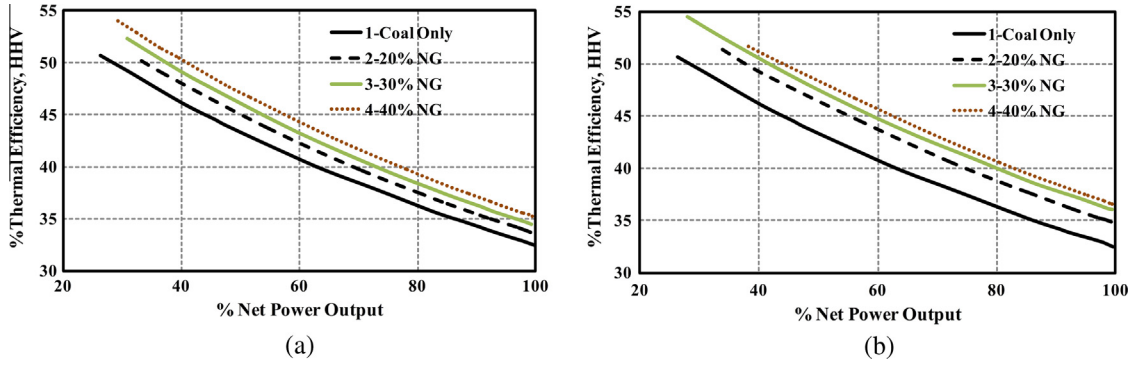

Fig. 15. Thermal efficiency versus net power output for different cases (a) natural gas/coal; (b) natural gas/coal/MHR.

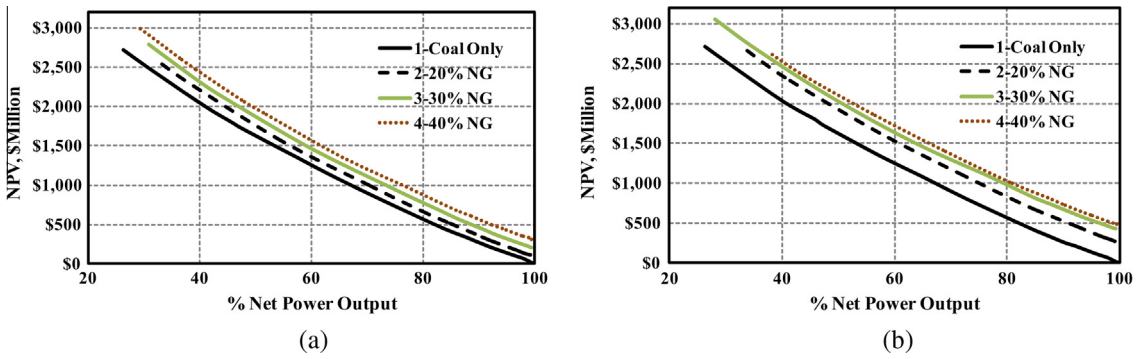

Fig. 16. Net present value versus net power output for different cases (a) natural gas/coal; (b) natural gas/coal/MHR.

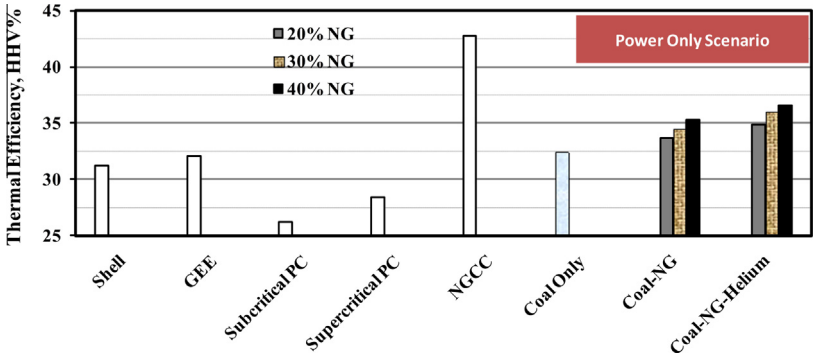

Fig. 17. Thermal efficiency of different cases of the proposed process with 100% CO_2 capture for power-only scenario compared to other power generation processes with only 90% CO_2 capture.

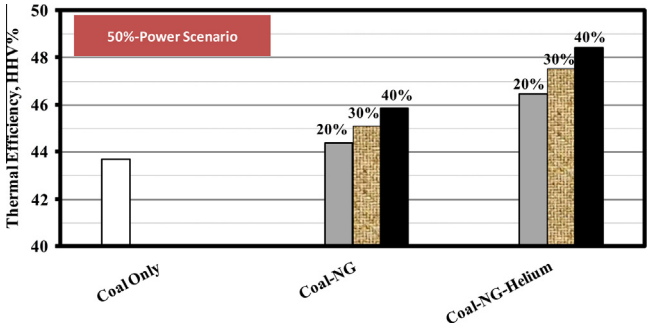

Fig. 18. Thermal efficiency of different cases of new process for 50%-power scenario.

Syngas produced by this process could be used for other purposes with similar effect. For example, some or all of the 2:1 syngas can be used to produce Fischer–Tropsch liquids such as diesel and gasoline. The process itself would be very similar; most of the unreacted syngas captured after downstream separation of the Fischer–Tropsch synthesis reaction could be recycled to the reactor and the rest sent to the iron-oxide chemical loop for hydrogen production, which avoids CO_2 emissions from purging or flaring. The remainder of the process would be the same. This is a subject of future work.

Finally, it is important to note that each design case studied in this work is a "static" design, meaning that once it has been constructed, only small changes to the product throughputs are likely to be possible. However, prior work by Chen et al. has shown that there is a significant potential for economic gain if polygeneration plants (in general) are operated flexibly, where product through-

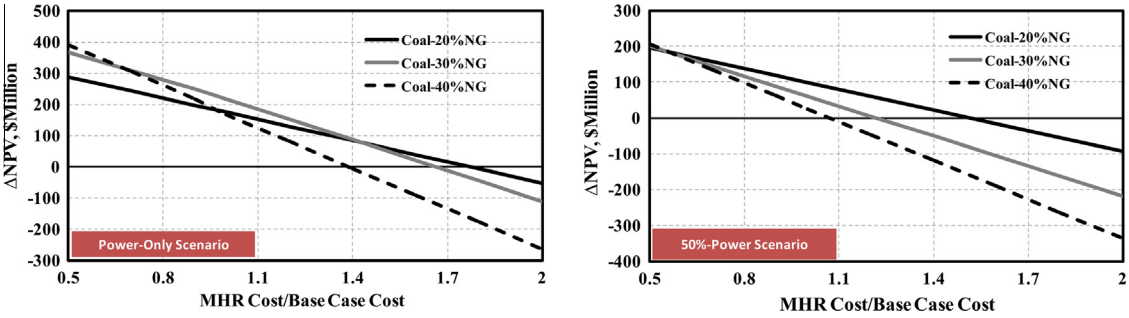

Fig. 19. Difference between the NPV of Coal-NG and Coal-NG-Helium as a function of MHR capital-operating cost.

puts are changed seasonally, weekly, or even daily in response to market conditions [24]. This concept is called "flexible polygeneration" or "agile processing", which is a subject of future work.

6. Concluding remarks

In this work, a new polygeneration system is introduced which produces methanol, dimethyl ether, and power from coal without any process CO_2 emissions. The novel system uses either one or two forms of coal gasification and either one or two separate chemical looping systems for hydrogen production and power generation. The product portfolios can be chosen according to market demand or optimal economics with minimal effect on system design. Several design options were explored using a sensitivity analysis to determine the optimal configuration. Some of the conclusions from the sensitivity analysis include: (1) there was no significant benefit to using a nickel-oxide chemical loop for power production when a traditional combustion turbine using H_2 produced by an iron-oxide chemical loop was available; (2) the net efficiency of the plant can be improved by routing waste N_2 (at pressure) from the ASU plant to the gas combustion turbine, rather than using a separate expander as was done in previous studies; and (3) at current market prices and for our particular polygeneration plant, the slurry gasification technology can achieve higher profit than the dry-gasification system when the power output ratio is more than 50%.

In addition, the process can be augmented to incorporate natural gas as a source of both carbon and energy by integrating autothermal natural gas reforming into the process (we call this Option A). With Option A, the amounts of natural gas used can be adjusted as desired (within some upper limit depending on the product portfolio), typically in the range of 20–40% of the total energy input. Furthermore, another design option is introduced (which we call Option B) where a modular helium reactor (MHR) is integrated into the process to yield a higher efficiency. The high-temperature heat from the MHR is used to drive the endothermic natural gas reformer, eliminating the need to oxidize or combust natural gas for this purpose. As a result, approximately 4–7.2% of the energy of the products originates from carbonless nuclear energy.

Moreover, we proposed the use of a hydrate-based CO_2 sequestration approach as opposed to using compression and condensation at supercritical pressure (around 150 bar). The goal of this process is to eliminate the requirement for CO_2 transportation by pipeline by using special CO_2 hydrate trucks which make the transportation and sequestration steps easier. However, the polygeneration process can be altered with little modification to use the supercritical CO_2 pipeline transport method and generally meet purity specifications for CO_2 pipeline transport for either sequestration or enhanced oil recovery. The supercritical CO_2 pipeline transport method was determined to be the lower cost option using current technology. In either case, effectively 100% of the CO_2 directly produced by the process (and all of its variants and product portfolios) can be captured with minimal impacts on efficiency.

As a result, this effective and innovative polygeneration system offers a novel alternative to coal-based traditional methods and increases the performance of the polygeneration system significantly. For example, the thermal efficiency of the proposed system for a power-only product portfolio is 32.5% HHV (38.3% LHV), which is around 0.5–6.3 percentage points greater than other coal-based processes. In addition, integrating natural gas into the process (option A) can increase the efficiency by 1.3–2.8 percentage points, and integrating both natural gas and MHR (option B) can yield an additional 2.4–4.1 percentage point increase over the coal-only case. However, the profitability of option B is very sensitive to the MHR capital-operating costs, as shown in Fig. 19.

Appendix A. Supplementary material

Supplementary data associated with this article can be found, in the online version, at http://dx.doi.org/10.1016/j.enconman.2014.08.039.

References

[1] Ansolabehere S, Beer J, Deutch J, Ellerman AD, Friedmann SJ, Herzog H, et al. The future of coal-options for a carbon-constrained world. An Interdisciplinary MIT Study; 2007.
[2] Falcke TJ, Hoadley AFA, Brennan DJ, Sinclair SE. The sustainability of clean coal technology: IGCC with/without CCS. Process Saf Environ Prot 2011;89:41–52.
[3] Zhang X, Gundersen T, Roussanaly S, Brunsvold AL, Zhang S. Carbon chain analysis on a coal IGCC—CCS system with flexible multi-products. Fuel Process Technol 2012;108:146–53.
[4] Floudas CA, Elia JA, Baliban RC. Hybrid and single feedstock energy processes for liquid transportation fuels: a critical review. Comput Chem Eng 2012;41:24–51.
[5] Adams II TA, Barton PI. Combining coal gasification and natural gas reforming for efficient polygeneration. Fuel Process Technol 2011;92:639–55.
[6] Gangadharan P, Zanwar A, Zheng K, Gossage J, Lou HH. Sustainability assessment of polygeneration processes based on syngas derived from coal and natural gas. Comput Chem Eng 2012;39:105–17.
[7] Liu G, Larson ED, Williams RH, Kreutz TG, Guo X. Making Fischer–Tropsch fuels and electricity from coal and biomass: performance and cost analysis. Energy Fuels 2011;25:415–37.
[8] Mantripragada HC, Rubin ES. CO_2 reduction potential of coal-to-liquids (CTL) process: effect of gasification technology. Energy Proc 2011;4:2700–7.
[9] Lu X, Norbeck JM, Park CS. Production of Fischer–Tropsch fuels and electricity from bituminous coal based on steam hydrogasification. Energy 2012;48:525–31.
[10] Wood DA, Nwaoha C, Towler BF. Gas-to-liquids (GTL): a review of an industry offering several routes for monetizing natural gas. J Nat Gas Sci Eng 2012;9:196–208.
[11] Gradassi MJ, Wayne Green N. Economics of natural gas conversion processes. Fuel Process Technol 1995;42:65–83.
[12] Semelsberger TA, Borup RL. Thermodynamic equilibrium calculations of hydrogen production from the combined processes of dimethyl ether steam reforming and partial oxidation. J Power Sources 2006;155:340–52.

[13] Semelsberger TA, Borup RL, Greene HL. Dimethyl ether (DME) as an alternative fuel. J Power Sources 2006;156:497–511.
[14] Bracht M, Alderliesten PT, Kloster R, Pruschek R, Haupt G, Xue E, et al. Water gas shift membrane reactor for CO_2 control in IGCC systems: techno-economic feasibility study. Energy Convers Manage 1997;38(Supplement):S159–64.
[15] Hoffmann BS, Szklo A. Integrated gasification combined cycle and carbon capture: a risky option to mitigate CO_2 emissions of coal-fired power plants. Appl Energy 2011;88:3917–29.
[16] Richards M, Shenoy A. H_2-MHR pre-conceptual design summary for hydrogen production. Nucl Eng Technol 2007;39:1–8.
[17] Yoshiyuki I, Karl V. Nuclear steam reforming of methane. Nuclear hydrogen production handbook. CRC Press; 2011.
[18] Yin H, Jiang S, Zhang Y, JU H. Modeling of the helium-heated steam reformer for HTR-10. J Nucl Sci Technol 2007;44:977–84.
[19] Salkuyeh Y Khojasteh, Adams II TA. Combining coal, natural gas, and nuclear heat for liquid fuels production with reduced CO_2 emissions. In: Ian David Lockhart B, Michael F, editors. Computer aided chemical engineering. Elsevier; 2012. p. 247–51.
[20] Baliban RC, Elia JA, Weekman V, Floudas CA. Process synthesis of hybrid coal, biomass, and natural gas to liquids via Fischer–Tropsch synthesis, ZSM-5 catalytic conversion, methanol synthesis, methanol-to-gasoline, and methanol-to-olefins/distillate technologies. Comput Chem Eng 2012;47:29–56.
[21] Soltanieh M, Azar KM, Saber M. Development of a zero emission integrated system for co-production of electricity and methanol through renewable hydrogen and CO_2 capture. Int J Greenhouse Gas Control 2012;7:145–52.
[22] Adams II TA, Barton PI. Combining coal gasification, natural gas reforming, and solid oxide fuel cells for efficient polygeneration with CO_2 capture and sequestration. Fuel Process Technol 2011;92:2105–15.
[23] Chen Y, Adams TA, Barton PI. Optimal design and operation of static energy polygeneration systems. Ind Eng Chem Res 2010;50:5099–113.
[24] Chen Y, Adams TA, Barton PI. Optimal design and operation of flexible energy polygeneration systems. Ind Eng Chem Res 2011;50:4553–66.
[25] Fan L, Li F, Ramkumar S. Utilization of chemical looping strategy in coal gasification processes. Particuology 2008;6:131–42.
[26] Li F, Kim HR, Sridhar D, Wang F, Zeng L, Chen J, et al. Syngas chemical looping gasification process: oxygen carrier particle selection and performance. Energy Fuels 2009;23:4182–9.
[27] Chen S, Xue Z, Wang D, Xiang W. An integrated system combining chemical looping hydrogen generation process and solid oxide fuel cell/gas turbine cycle for power production with CO_2 capture. J Power Sources 2012;215:89–98.
[28] Tong A, Sridhar D, Sun Z, Kim HR, Zeng L, Wang F, et al. Continuous high purity hydrogen generation from a syngas chemical looping 25 kW_{th} sub-pilot unit with 100% carbon capture. Fuel 2013;103:495–505.
[29] Chiu P-C, Ku Y. Chemical looping process – a novel technology for inherent CO_2 capture. Aerosol Air Qual Res 2012;12:1421–32.
[30] Tong A, Bayham S, Kathe MV, Zeng L, Luo S, Fan L-S. Iron-based syngas chemical looping process and coal-direct chemical looping process development at Ohio State University. Appl Energy 2014;113:1836–45.
[31] Xiang W, Chen S, Xue Z, Sun X. Investigation of coal gasification hydrogen and electricity co-production plant with three-reactors chemical looping process. Int J Hydrogen Energy 2010;35:8580–91.
[32] Cleeton JPE, Bohn CD, Müller CR, Dennis JS, Scott SA. Clean hydrogen production and electricity from coal via chemical looping: identifying a suitable operating regime. Int J Hydrogen Energy 2009;34:1–12.
[33] Fan LS. Chemical looping systems for fossil energy conversions. John Wiley & Sons, Inc.; 2010.
[34] Jin H, Ishida M. A novel gas turbine cycle with hydrogen-fueled chemical-looping combustion. Int J Hydrogen Energy 2000;25:1209–15.
[35] Ishida M, Jin H. A new advanced power-generation system using chemical-looping combustion. Energy 1994;19:415–22.
[36] Linderholm C, Abad A, Mattisson T, Lyngfelt A. 160 h of chemical-looping combustion in a 10 kW reactor system with a NiO-based oxygen carrier. Int J Greenhouse Gas Control 2008;2:520–30.
[37] Linderholm C, Jerndal E, Mattisson T, Lyngfelt A. Investigation of NiO-based mixed oxides in a 300-W chemical-looping combustor. Chem Eng Res Des 2010;88:661–72.
[38] Mattisson T, Johansson M, Lyngfelt A. The use of NiO as an oxygen carrier in chemical-looping combustion. Fuel 2006;85:736–47.
[39] Mattisson T, Lyngfelt A, Leion H. Chemical-looping with oxygen uncoupling for combustion of solid fuels. Int J Greenhouse Gas Control 2009;3:11–9.
[40] Ishida M, Yamamoto M, Ohba T. Experimental results of chemical-looping combustion with $NiO/NiAl_2O_4$ particle circulation at 1200 °C. Energy Convers Manage 2002;43:1469–78.
[41] Adams II TA, Barton PI. High-efficiency power production from coal with carbon capture. AIChE J 2010;56:3120–36.
[42] Adams II TA, Barton PI. High-efficiency power production from natural gas with carbon capture. J Power Sources 2010;195:1971–83.
[43] Cormos C-C. Evaluation of energy integration aspects for IGCC-based hydrogen and electricity co-production with carbon capture and storage. Int J Hydrogen Energy 2010;35:7485–97.
[44] Salkuyeh YK, Adams TA. Combining coal gasification, natural gas reforming, and external carbonless heat for efficient production of gasoline and diesel with CO_2 capture and sequestration. Energy Convers Manage 2013;74:492–504.
[45] Salkuyeh Y. Khojasteh, Adams II TA. Shale gas for the petrochemical industry: incorporation of novel technologies. Proceedings of the 8th international conference on foundations of computer-aided process design – FOCAPD, Washington (USA); 2014.
[46] Salkuyeh Y Khojasteh, Adams II TA. Combining coal gasification, natural gas reforming, and external carbonless heat for efficient production of gasoline and diesel with CO_2 capture and sequestration. Energy Convers Manage 2013;74:492–504.
[47] Haslbeck JL, Kuehn NJ, Lewis EG, Pinkerton LL, Simpson J, Turner MJ, et al. Cost and performance baseline for fossil energy plants volume 1: bituminous coal and natural gas to electricity, DOE. National Energy Technology Laboratory (NETL); 2010.
[48] Vanden bussche KM, Froment GF. A steady-state kinetic model for methanol synthesis and the water gas shift reaction on a commercial $Cu/ZnO/Al_2O_3$ catalyst. J Catal 1996;161:1–10.
[49] Pedersen TH, Schultz RH, Kær SK, Hoffmann PFJ. Technical and economic assessment of methanol production from biogas. Masters thesis within thermal energy and process engineering. Denmark: University of Aalborg; 2012.
[50] Bercic G, Levec J. Catalytic dehydration of methanol to dimethyl ether. Kinetic investigation and reactor simulation. Ind Eng Chem Res 1993;32:2478–84.
[51] Diep BT, Wainwright MS. Thermodynamic equilibrium constants for the methanol–dimethyl ether–water system. J Chem Eng Data 1987;32:330–3.
[52] Larson ED, Jin H, Celik FE. Large-scale gasification-based coproduction of fuels and electricity from switchgrass. Biofuels, Bioprod Biorefin 2009;3:174–94.
[53] Peng XD, Wang AW, Toseland BA, Tijm PJA. Single-step syngas-to-dimethyl ether processes for optimal productivity, minimal emissions, and natural gas-derived syngas. Ind Eng Chem Res 1999;38:4381–8.
[54] Ogawa T, Inoue N, Shikada T, Ohno Y. Direct dimethyl ether synthesis. J Nat Gas Chem 2003;12:219–27.
[55] Gat GB, Ornl SB, Ornl TB, Ornl BC, Ineel TF, Gat ML, et al. Very high temperature reactor (VHTR) survey of materials research and development needs to support early deployment; 2003.
[56] Şahin HM, Akbayir Ö. Alternative operating conditions for the modular helium reactor. Energy Convers Manage 2012;63:31–7.
[57] Seo Y-T, Moudrakovski IL, Ripmeester JA, Lee J-W, Lee H. Efficient recovery of CO_2 from flue gas by clathrate hydrate formation in porous silica gels. Environ Sci Technol 2005;39:2315–9.
[58] Kang S-P, Lee H. Recovery of CO_2 from flue gas using gas hydrate: thermodynamic verification through phase equilibrium measurements. Environ Sci Technol 2000;34:4397–400.
[59] Belandria V, Eslamimanesh A, Mohammadi AH, Richon D. Study of gas hydrate formation in the carbon dioxide + hydrogen + water systems: compositional analysis of the gas phase. Ind Eng Chem Res 2011;50:6455–9.
[60] Circone S, Stern LA, Kirby SH, Durham WB, Chakoumakos BC, Rawn CJ, et al. CO_2 hydrate: synthesis, composition, structure, dissociation behavior, and a comparison to structure I CH_4 hydrate. J Phys Chem B 2003;107:5529–39.
[61] Tanaka S, Maruyama F, Takano O, Uchida K, Oya N. Experimental study on CO_2 storage and sequestration in form of hydrate pellets. Proceedings of the 5th international conference on gas hydrates, Norway; 2005.
[62] de Angelis A. Natural gas removal of hydrogen sulphide and mercaptans. Appl Catal B 2012;113–114:37–42.
[63] Srinivas G, Gebhard SC, DeBerry DW. Hybrid sulfur recovery process for natural gas upgrading. National Energy Technology Lab., Pittsburgh, PA (US); National Energy Technology Lab., Morgantown, WV (US); 2001.
[64] Barrere-Tricca C, Smith D, Margotin J. Thirty years of operating experience with the Clauspol process. Oil Gas Sci Technol 2001;56:199–206.
[65] Smith AR, Klosek J. A review of air separation technologies and their integration with energy conversion processes. Fuel Process Technol 2001;70:115–34.
[66] Worhach P, Haslbeck J. Recommended project finance structures for the economic analysis of fossil-based energy projects. DOE/NETL-401/090808; 2008.
[67] EIA. US Energy information administration, natural gas weekly update. Henry Hub spot price. <http://wwweiagov/naturalgas/weekly/>; [18.12.13].
[68] EIA-Coal. US energy information administration, coal news and markets report: average weekly coal commodity spot prices. <http://www.eia.gov/coal/news_markets/>; [29.11.13].
[69] EIA. U.S. Energy information administration (EIA), Table 5.3. Average retail price of electricity to ultimate customers, all sectors. Electric power monthly. <http://wwweiagov/electricity/monthly/>; (Average 2013).
[70] Fe_2O_3. Factory price of iron oxide (Fe_2O_3), CAS No.: 1309-37-1. <http://www.alibaba.com/product-gs/814503142/factory_price_of_iron_oxide_fe2o3_.html?s=p>; 2013.
[71] Schultz K, Atomics G. Use of the modular helium reactor for hydrogen production. Nucl Eng 2004;45:37–41.
[72] CEPCI. Chemical engineering plant cost index. Chem Eng 2013; 120: 176.
[73] Peters MS, Timmerhaus KD. Plant design and economics for chemical engineers. 4th ed. 1991.
[74] Corbella BM, Palacios JM. Titania-supported iron oxide as oxygen carrier for chemical-looping combustion of methane. Fuel 2007;86:113–22.
[75] Gupta P, Vargas LGV, Fan L-S. Syngas redox (SGR) process to produce hydrogen from coal derived syngas. Energy Fuels 2007;21:2900–8.
[76] Szymcek P, McCallum SD, Taboada-Serrano P, Tsouris C. A pilot-scale continuous-jet hydrate reactor. Chem Eng J 2008;135:71–7.

[77] Taboada-Serrano P, Szymcek P, McCallum Scott D, Tsouris C. A novel continuous-flow reactor for gas hydrate production. 6th International conference on gas hydrates (ICGH 2008), Vancouver, British Columbia, Canada; 2008.
[78] Bolland O, Stadaas JF. Comparative evaluation of combined cycles and gas turbine systems with water injection, steam injection, and recuperation. ASME J Eng Gas Turbines Power 1995;117:138–45.
[79] Sanjay OS, Prasad BN. Influence of different means of turbine blade cooling on the thermodynamic performance of combined cycle. Appl Therm Eng 2008;28:2315–26.
[80] Sanjay OS, Prasad BN. Comparative performance analysis of cogeneration gas turbine cycle for different blade cooling means. Int J Therm Sci 2009;48:1432–40.
[81] Yu GW, Xu YY, Hao X, Li YW, Liu GQ. Process analysis for polygeneration of Fischer–Tropsch liquids and power with CO_2 capture based on coal gasification. Fuel 2010;89:1070–6.
[82] Moghtaderi B. Review of the recent chemical looping process developments for novel energy and fuel applications. Energy Fuels 2011;26:15–40.

Chapter 3

Supplementary Material 1

Process Flowsheet

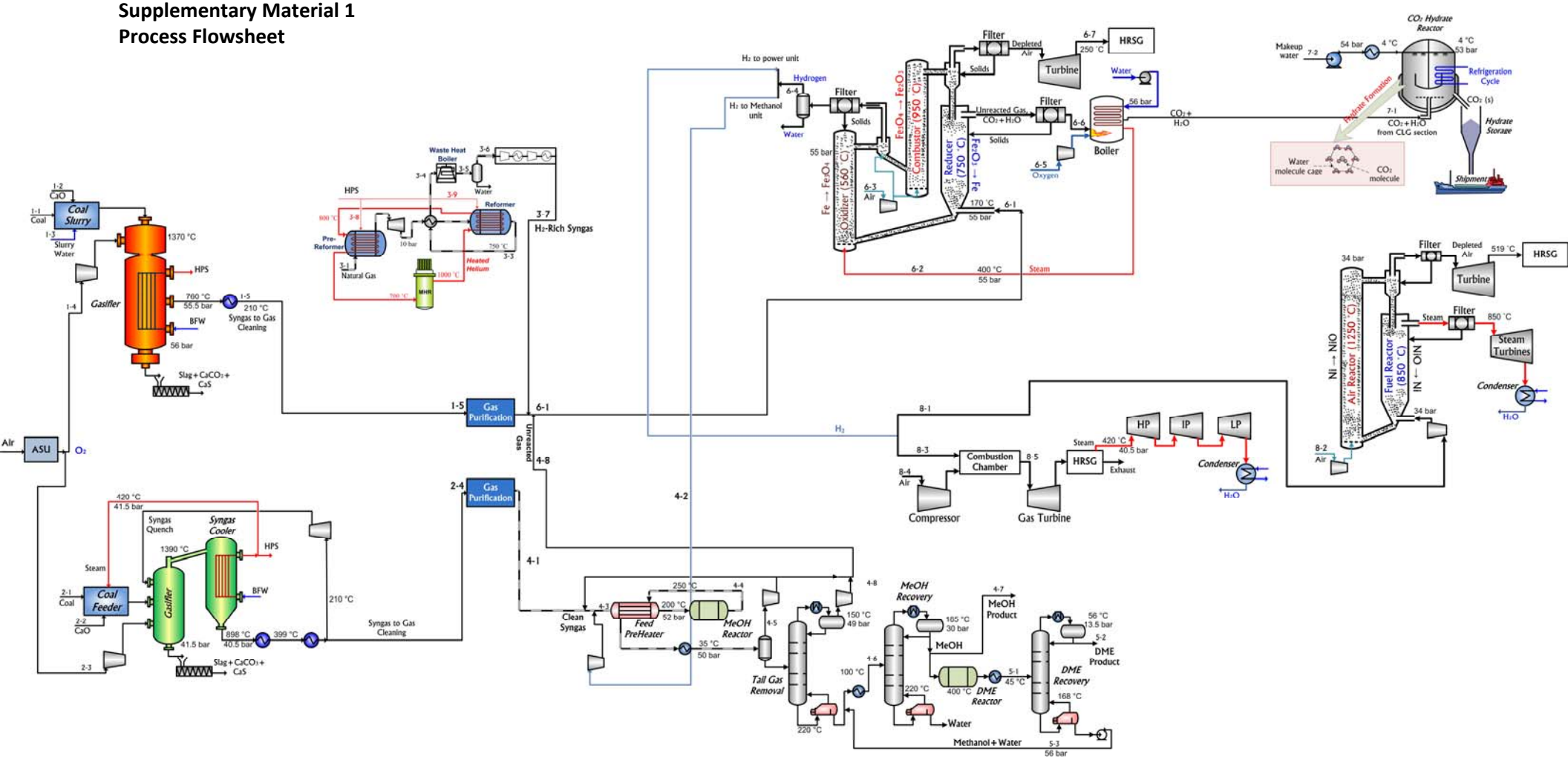

Chapter 3

Supplementary Material 2

Slurry Gasifier

Design Basis: 80% of the net output is Electricity

Stream No.	**1-1**	**1-2**	**1-3**	**1-4**	**1-5**
Description	**Coal**	**CaO**	**Slurry Water**	**Oxygen**	**Syngas**
Temperature (°C)	60.0	60.0	60.0	31.0	210.0
Pressure (bar)	56.0	56.0	60.0	57.0	55.0
Total Flow (kg/hr)	583633	24819	239757	476698	1508694
Total Flow (kmole/hr)		443	13309	14889	76153
Mass Vapor Fraction	0.00	0.00	0.00	1.00	1.00
Mole Percent					
Coal	100.00%	0.00%	0.00%	0.00%	0.00%
H_2O	0.00%	0.00%	100.00%	0.00%	36.30%
N_2	0.00%	0.00%	0.00%	0.19%	0.38%
O_2	0.00%	0.00%	0.00%	99.49%	0.00%
AR	0.00%	0.00%	0.00%	0.32%	0.06%
H_2	0.00%	0.00%	0.00%	0.00%	23.31%
CO	0.00%	0.00%	0.00%	0.00%	30.61%
CO_2	0.00%	0.00%	0.00%	0.00%	9.23%
H_2S	0.00%	0.00%	0.00%	0.00%	0.02%
CH_4	0.00%	0.00%	0.00%	0.00%	0.01%
NH_3	0.00%	0.00%	0.00%	0.00%	2.19E-05
HCl	0.00%	0.00%	0.00%	0.00%	6.34E-04
CaO	0.00%	100.00%	0.00%	0.00%	0.00%
Total	100.00%	100.00%	100.00%	100.00%	100.00%

Chapter 3

Supplementary Material 2

Dry Gasifier

Design Basis: 80% of the net output is Electricity

Stream No.	**2-1**	**2-2**	**2-3**	**2-4**
Description	**Coal**	**CaO**	**Oxygen**	**Syngas**
Temperature (°C)	60.0	60.0	31.0	210.0
Pressure (bar)	41.5	41.5	41.5	40.5
Total Flow (kg/hr)	58363.3	2531	41015	98086
Total Flow (kmole/hr)		45	1281	5052
Mass Vapor Fraction	0.00	0.00	1.00	1.00
Mole Percent				
Coal	100.00%	0.00%	0.00%	0.00%
H_2O	0.00%	0.00%	0.00%	5.83%
N_2	0.00%	0.00%	0.19%	0.56%
O_2	0.00%	0.00%	99.49%	0.00%
AR	0.00%	0.00%	0.32%	0.08%
H_2	0.00%	0.00%	0.00%	33.34%
CO	0.00%	0.00%	0.00%	56.04%
CO_2	0.00%	0.00%	0.00%	3.99%
H_2S	0.00%	0.00%	0.00%	9.66E-05
CH_4	0.00%	0.00%	0.00%	0.04%
NH_3	0.00%	0.00%	0.00%	2.40E-05
HCl	0.00%	0.00%	0.00%	9.56E-04
CaO	0.00%	100.00%	0.00%	0.00%
Total	100.00%	100.00%	100.00%	100.00%

Chapter 3

Supplementary Material 2

MeOH-DME

Design Basis: 80% of the net output is Electricity

Stream No.	**4-1**	**4-2**	**4-3**	**4-4**	**4-5**	**4-6**	**4-7**	**5-1**	**5-2**	**5-3**
Description	**an Syngas**	**Hydrogen**								
Temperature (°C)	200.0	65.5	103.0	250.0	35.0	100.0	150.0	45.0	56.6	167.8
Pressure (bar)	52.0	51.0	52.0	51.0	50.0	33.0	30.0	28.5	13.5	16.4
Total Flow (kg/hr)	101500	6383	384241	384241	307064	71346	57476	6386	2589	3798
Total Flow (kmole/hr)	5252.2	3048	23993	19853	17437	2323	1794	199	56	143
Mass Vapor Fraction	1.00	1.00	1.00	1.00	1.00	0.00	0.00	0.00	0.00	0.00
Mole Percent										
H_2O	9.59%	0.49%	2.19%	0.89%	0.05%	9.67%	0.10%	28.22%	0.00%	39.32%
N_2	0.54%		1.18%	1.42%	1.62%					
O_2	0.00%									
H_2	32.07%	99.51%	54.39%	46.67%	53.10%					
CO	53.91%		26.96%	20.37%	23.17%					
CO_2	3.84%		14.71%	19.55%	21.20%	0.04%	0.05%	0.05%	0.19%	0.00%
H_2S	0.00%									
CH_4	0.04%		0.09%	0.10%	0.12%					
NH_3			0.00%		0.00%					
MeOH			0.48%	10.96%	0.73%	90.13%	99.80%	43.56%	0.23%	60.58%
EtOH				0.02%	0.00%	0.14%	0.04%	0.04%	0.00%	0.06%
Methanoate				0.01%	0.00%	0.00%	0.00%	0.00%	0.00%	0.00%
DME						0.00%	0.00%	28.13%	99.59%	0.04%
HCl										
Total	100.00%	100.00%	100.00%	100.00%	100.00%	100.00%	100.00%	100.00%	100.00%	100.00%

Chapter 3

Supplementary Material 2

SCL

Design Basis: 80% of the net output is Electricity

Stream No.	**6-1**	**6-2**	**6-3**	**6-4**	**6-5**	**6-6**	**6-7**
Description	**Fuel Gas**	**Steam**	**Air**	**Hydrogen**	**Oxygen**		
Temperature (°C)	198.4	400.0	45.0	63.5	179.6	749.8	250.0
Pressure (bar)	55.0	55.0	2.0	52.5	54.5	55.0	1.1
Total Flow (kg/hr)	1510041	1766809	1259791	40117	100605	2318855	975365
Total Flow (kmole/hr)	76089	98073	43667	19158	3142	76153	34597
Mass Vapor Fraction	0.97	1.00	1.00	1.00	1.00	1.00	1.00
Mole Percent							
H_2O	33.79%	100.00%	1.08%	0.49%		53.24%	0.16%
N_2	0.42%		77.19%		0.19%	0.42%	97.43%
O_2	0.00%		20.76%		99.49%		1.19%
H_2	24.56%			99.51%		5.14%	
CO	31.17%					2.87%	
CO_2	9.97%		0.03%			38.28%	0.04%
H_2S	0.00%						
CH_4	0.02%					0.05%	
NH_3	0.00%					0.00%	
MeOH	0.07%						
EtOH							
Methanoate							
DME							
AR			0.94%		0.32%		1.19%
HCl							
Total	100.00%	100.00%	100.00%	100.00%	100.00%	100.00%	100.00%

Chapter 3

Supplementary Material 2

Sequestration

Design Basis: 80% of the net output is Electricity

Stream No.	**7-1**	**7-2 ***	**7-3**	**7-4**
Description				
Temperature (°C)	100.0	35.0	45.0	48.5
Pressure (bar)	53.5	2.0	53.0	153.0
Total Flow (kg/hr)	2192611	2589143	1383424	1383424
Total Flow (kmole/hr)	76244.2	143719	31507	31507
Mass Vapor Fraction	1.00	0.00	1.00	0.00
Mole Percent				
H_2O	58.49%	100.00%	0.38%	0.38%
N_2				
O_2				
H_2				
CO				
CO_2	41.49%		99.58%	99.58%
H_2S				
CH_4				
NH_3				
MeOH				
EtOH				
Methanoate				
DME				
AR	0.01%		0.03%	0.03%
HCl				
Total	100.00%	100.00%	100.00%	100.00%

* Make-up water is only used in the Hydration option.

Chapter 3

Supplementary Material 2

Power Generation

Design Basis: 80% of the net output is Electricity

Stream No.	**8-3**	**8-4**	**8-5**
Description	**Hydrogen**	**Air**	
Temperature (°C)	65.5	65.0	1260.0
Pressure (bar)	52.5	2.0	51.9
Total Flow (kg/hr)	33734.6	3480601	4146832
Total Flow (kmole/hr)	16109.5	120645	151293
Mass Vapor Fraction	1.00	1.00	1.00
Mole Percent			
H_2O	0.49%	1.08%	11.51%
N_2		77.19%	76.42%
O_2		20.76%	11.26%
H_2	99.51%		
CO			
CO_2		0.03%	0.02%
H_2S			
CH_4			
NH_3			
MeOH			
EtOH			
Methanoate			
DME			
AR		0.94%	0.79%
HCl			
Total	100.00%	100.00%	100.00%

Chapter 3

Supplementary Material 3

Slurry Gasifier

Design Basis: 37% of the net output is Electricity

Stream No.	**1-1**	**1-2**	**1-3**	**1-4**	**1-5**
Description	**Coal**	**CaO**	**Slurry Water**	**Oxygen**	**Syngas**
Temperature (°C)	60.0	60.0	60.0	31.0	210.0
Pressure (bar)	56.0	56.0	60.0	57.0	55.0
Total Flow (kg/hr)	509184	21653	209173	415890	1316242
Total Flow (kmole/hr)		386	11611	12990	66439
Mass Vapor Fraction	0.00	0.00	0.00	1.00	1.00
Mole Percent					
Coal	100.00%	0.00%	0.00%	0.00%	0.00%
H_2O	0.00%	0.00%	100.00%	0.00%	36.30%
N_2	0.00%	0.00%	0.00%	0.19%	0.38%
O_2	0.00%	0.00%	0.00%	99.49%	0.00%
AR	0.00%	0.00%	0.00%	0.32%	0.06%
H_2	0.00%	0.00%	0.00%	0.00%	23.31%
CO	0.00%	0.00%	0.00%	0.00%	30.61%
CO_2	0.00%	0.00%	0.00%	0.00%	9.23%
H_2S	0.00%	0.00%	0.00%	0.00%	0.02%
CH_4	0.00%	0.00%	0.00%	0.00%	0.01%
NH_3	0.00%	0.00%	0.00%	0.00%	2.19E-05
HCl	0.00%	0.00%	0.00%	0.00%	6.34E-04
CaO	0.00%	100.00%	0.00%	0.00%	0.00%
Total	100.00%	100.00%	100.00%	100.00%	100.00%

Chapter 3

Supplementary Material 3

Reformer

Design Basis: 37% of the net output is Electricity

Stream No.	**3-1**	**3-2**	**3-3**	**3-4**	**3-5**	**3-6**	**3-7**	**3-8**	**3-9**	**3-10**
Description	**NG**									
Temperature (°C)	30.0	500.0	860.3	639.0	40.0	40.0	80.0	420.0	420.0	15.0
Pressure (bar)	30.0	29.7	28.9	28.7	28.4	28.2	55.0	40.5	40.5	12.9
Total Flow (kg/hr)	62087	62087	230506	230506	230506	134700	134700	35435	83210	49774
Total Flow (kmole/hr)	3746	3746	16588	16588	16588	11272	11272	1967	4619	1555
Mass Vapor Fraction	1.00	1.00	1.00	1.00	0.58	1.00	1.00	1.00	1.00	1.00
Mole Percent										
H_2O			32.22%	32.22%	32.22%	0.27%	0.27%	100.00%	100.00%	
N_2	0.47%	0.47%	0.12%	0.12%	0.12%	0.18%	0.18%			0.19%
O_2										99.49%
AR			0.03%	0.03%	0.03%	0.04%	0.04%			0.32%
H_2			44.55%	44.55%	44.55%	65.57%	65.57%			
CO			11.54%	11.54%	11.54%	16.98%	16.98%			
CO_2	0.38%	0.38%	7.38%	7.38%	7.38%	10.85%	10.85%			
H_2S										
CH_4	97.01%	97.01%	4.15%	4.15%	4.15%	6.11%	6.11%			
C_2H_6	1.76%	1.76%								
C_3H_8	0.26%	0.26%								
C_4H_{10}	0.11%	0.11%								
NH_3										
HCl										
CaO										
Total	100.00%	100.00%	100.00%	100.00%	100.00%	100.00%	100.00%	100.00%	100.00%	100.00%

Chapter 3

Supplementary Material 3

MeOH-DME

Design Basis: 37% of the net output is Electricity

Stream No.	**4-1**	**4-2**	**4-3**	**4-4**	**4-5**	**4-6**	**4-7**	**5-1**	**5-2**	**5-3**
Description	**ın Syngas**	**Hydrogen**								
Temperature (°C)	200.0	65.5	53.2	250.0	35.0	100.0	150.0	45.0	56.6	173.0
Pressure (bar)	55.0	52.5	52.0	51.0	50.0	33.0	30.0	28.5	13.5	33.0
Total Flow (kg/hr)	560378	26822	1746573	1746573	1439568	279120	224094	24899	10235	14664
Total Flow (kmole/hr)	28005.1	12808	100696	84529	74938	9110	6994	777	222	555
Mass Vapor Fraction	1.00	1.00	1.00	1.00	1.00	0.00	0.00	0.00	0.00	0.00
Mole Percent										
H_2O	28.29%	0.49%	0.45%	0.88%	0.05%	10.19%	0.10%	28.62%	1.49E-10	40.10%
N_2	0.43%		1.18%	1.40%	1.58%					
O_2	0.00%									
H_2	26.31%	99.51%	52.66%	43.29%	48.80%					
CO	34.54%		26.10%	21.85%	24.62%					
CO_2	10.42%		19.07%	22.40%	24.15%	0.04%	0.05%	0.05%	0.17%	0.00%
H_2S	0.00%									
CH_4	0.02%		0.04%	0.05%	0.05%					
NH_3	0.00%		0.00%			0.01%				
MeOH			0.49%	10.11%	0.74%	89.61%	99.80%	42.76%	0.24%	59.80%
EtOH			0.00%	0.02%	0.00%	0.14%	0.04%	0.04%	0.00%	0.06%
Methanoate				0.01%	0.00%	0.00%	0.00%	0.00%	0.00%	0.00%
DME						0.00%	0.00%	28.52%	99.59%	0.04%
HCl										
Total	100.00%	100.00%	100.00%	100.00%	100.00%	100.00%	100.00%	100.00%	100.00%	100.00%

Chapter 3

Supplementary Material 3

SCL

Design Basis: 37% of the net output is Electricity

Stream No.	**6-1**	**6-2**	**6-3**	**6-4**	**6-5**	**6-6**	**6-7**
Description	**Fuel Gas**	**Steam**	**Air**	**Hydrogen**	**Oxygen**		
Temperature (°C)	167.9	400.0	45.0	63.5	179.6	550.0	250.0
Pressure (bar)	55.0	54.5	2.0	52.5	54.5	54.5	1.1
Total Flow (kg/hr)	939043	1626851	1154046	36940	69020	1532984	903129
Total Flow (kmole/hr)	50677.7	90304	40002	17640	2156	52473.25	31994
Mass Vapor Fraction	0.98	1.00	1.00	1.00	1.00	1.00	1.00
Mole Percent							
H_2O	17.30%	100.00%	1.08%	0.49%	0.00%	56.72%	0.16%
N_2	0.54%	0.00%	77.19%	0.00%	0.19%	0.53%	96.51%
O_2	0.00%	0.00%	20.76%	0.00%	99.49%	0.00%	2.12%
H_2	37.87%	0.00%	0.00%	99.51%	0.00%	0.00%	0.00%
CO	28.49%	0.00%	0.00%	0.00%	0.00%	0.00%	0.00%
CO_2	13.97%	0.00%	0.03%	0.00%	0.00%	42.73%	0.04%
H_2S							
CH_4	1.38%	0.00%	0.00%	0.00%	0.00%	0.00%	0.00%
NH_3							
MeOH	0.42%						
EtOH							
Methanoate	0.01%						
DME							
AR	0.01%	0.00%	0.94%	0.00%	0.32%	0.02%	1.18%
HCl							
Total	100.00%	100.00%	100.00%	100.00%	100.00%	100.00%	100.00%

Chapter 3

Supplementary Material 3

Sequestration

Design Basis: 37% of the net output is Electricity

Stream No.	**7-1**	**7-2***	**7-3**	**7-4**
Description				
Temperature (°C)	100.0		45.0	48.5
Pressure (bar)	53.5		53.0	153.0
Total Flow (kg/hr)	1532984		989938	989938
Total Flow (kmole/hr)	52536.4		22546	22546
Mass Vapor Fraction	0.65		1.00	0.00
Mole Percent				
H_2O	56.75%		0.38%	0.38%
N_2				
O_2			0.01%	0.01%
H_2				
CO				
CO_2	43.23%		99.56%	99.56%
H_2S				
CH_4				
NH_3				
MeOH				
EtOH				
Methanoate				
DME				
AR	0.02%		0.05%	0.05%
HCl				
Total	100.00%		100.00%	100.00%

* The Hydration option is not used here.

Chapter 3

Supplementary Material 3

Power Generation

Design Basis: 37% of the net output is Electricity

Stream No.	**8-3**	**8-4**	**8-5**
Description	**Hydrogen**	**Air**	
Temperature (°C)	65.5	65.0	1260.0
Pressure (bar)	52.5	2.0	51.9
Total Flow (kg/hr)	10117.6	1043899	1243715
Total Flow (kmole/hr)	4831.56	36184	45377
Mass Vapor Fraction	1.00	1.00	1.00
Mole Percent			
H_2O	0.49%	1.08%	11.51%
N_2		77.19%	76.42%
O_2		20.76%	11.26%
H_2	99.51%		
CO			
CO_2		0.03%	0.02%
H_2S			
CH_4			
NH_3			
MeOH			
EtOH			
Methanoate			
DME			
AR		0.94%	0.79%
HCl			
Total	100.00%	100.00%	100.00%

Chapter 3

Supplementary Material 4

Slurry Gasifier

Design Basis: 50% of the net output is Electricity

Stream No.	**1-1**	**1-2**	**1-3**	**1-4**	**1-5**
Description	**Coal**	**CaO**	**Slurry Water**	**Oxygen**	**Syngas**
Temperature (°C)	60.0	60.0	60.0	31.0	210.0
Pressure (bar)	56.0	56.0	60.0	57.0	55.0
Total Flow (kg/hr)	484017	20583	198834	395334	1251185
Total Flow (kmole/hr)		367	11037	12348	63155
Mass Vapor Fraction	0.00	0.00	0.00	1.00	1.00
Mole Percent					
Coal	100.00%	0.00%	0.00%	0.00%	0.00%
H_2O	0.00%	0.00%	100.00%	0.00%	36.30%
N_2	0.00%	0.00%	0.00%	0.19%	0.38%
O_2	0.00%	0.00%	0.00%	99.49%	0.00%
AR	0.00%	0.00%	0.00%	0.32%	0.06%
H_2	0.00%	0.00%	0.00%	0.00%	23.31%
CO	0.00%	0.00%	0.00%	0.00%	30.61%
CO_2	0.00%	0.00%	0.00%	0.00%	9.23%
H_2S	0.00%	0.00%	0.00%	0.00%	0.02%
CH4	0.00%	0.00%	0.00%	0.00%	0.01%
NH3	0.00%	0.00%	0.00%	0.00%	2.19E-05
HCl	0.00%	0.00%	0.00%	0.00%	6.34E-04
CaO	0.00%	100.00%	0.00%	0.00%	0.00%
Total	100.00%	100.00%	100.00%	100.00%	100.00%

Chapter 3

Supplementary Material 4

Reformer

Design Basis: 50% of the net output is Electricity

Stream No.	**3-1**	**3-2**	**3-3**	**3-4**	**3-5**	**3-6**	**3-7**	**3-8**	**3-9**
Description	**NG**								
Temperature (°C)	30.0	30.0	750.0	719.3	40.0	40.0	80.0	420.0	420.0
Pressure (bar)	30.0	30.0	9.4	9.0	8.9	8.9	55.0	40.5	40.5
Total Flow (kg/hr)	59018	59018	171799	171799	171799	114256	114256	33683	79098
Total Flow (kmole/hr)	3561	3561	14183	14183	14183	10989	10989	1870	4391
Mass Vapor Fraction	1.00	1.00	1.00	1.00	0.67	1.00	1.00	1.00	1.00
Mole Percent									
H_2O			23.11%	23.11%	23.11%	0.76%	0.76%	100.00%	100.00%
N_2	0.47%	0.47%	0.12%	0.12%	0.12%	0.15%	0.15%		
O_2									
AR									
H_2			51.12%	51.12%	51.12%	65.98%	65.98%		
CO			9.72%	9.72%	9.72%	12.54%	12.54%		
CO_2	0.38%	0.38%	5.75%	5.75%	5.75%	7.42%	7.42%		
H_2S									
CH_4	97.01%	97.01%	10.18%	10.18%	10.18%	13.14%	13.14%		
C_2H_6	1.76%	1.76%							
C_3H_8	0.26%	0.26%							
C_4H_{10}	0.11%	0.11%							
NH_3									
HCl									
CaO									
Total	100.00%	100.00%	100.00%	100.00%	100.00%	100.00%	100.00%	100.00%	100.00%

Chapter 3

Supplementary Material 4

MeOH-DME

Design Basis: 50% of the net output is Electricity

Stream No.	**4-1**	**4-2**	**4-3**	**4-4**	**4-5**	**4-6**	**4-7**	**5-1**	**5-2**	**5-3**
Temperature (°C)	200.0	65.5	53.2	250.0	35.0	100.0	150.0	45.0	56.6	173.0
Pressure (bar)	55.0	52.5	52.0	51.0	50.0	33.0	30.0	28.5	13.5	33.0
Total Flow (kg/hr)	417789	19995	1302117	1302117	1073232	208097	167073	18564	7631	10933
Total Flow (kmole/hr)	20879.1	9549	75072	63019	55869	6792	5214	579	166	414
Mass Vapor Fraction	1.00	1.00	1.00	1.00	1.00	0.00	0.00	0.00	0.00	0.00
Mole Percent										
H_2O	28.29%	0.49%	0.45%	0.88%	0.05%	10.19%	0.10%	28.62%	0.00%	40.10%
N_2	0.43%		1.18%	1.40%	1.58%	0.00%				
O_2										
H_2	26.31%	99.51%	52.66%	43.29%	48.80%					
CO	34.54%		26.10%	21.85%	24.62%					
CO_2	10.42%		19.07%	22.40%	24.15%	0.04%	0.05%	0.05%	0.17%	0.00%
H_2S										
CH_4	0.02%		0.04%	0.05%	0.05%					
NH_3						0.01%				
MeOH			0.49%	10.11%	0.74%	89.61%	99.80%	42.76%	0.24%	59.80%
EtOH			0.00%	0.02%	0.00%	0.14%	0.04%	0.04%	0.00%	0.06%
Methanoate				0.01%	0.00%	0.00%	0.00%	0.00%	0.00%	0.00%
DME						0.00%	0.00%	28.52%	99.59%	0.04%
HCl										
Total	100.00%	100.00%	100.00%	100.00%	100.00%	100.00%	100.00%	100.00%	100.00%	100.00%

Chapter 3

Supplementary Material 4

SCL

Design Basis: 50% of the net output is Electricity

Stream No.	**6-1**	**6-2**	**6-3**	**6-4**	**6-5**	**6-6**	**6-7**
Description	**Fuel Gas**	**Steam**	**Air**	**Hydrogen**	**Oxygen**		
Temperature (°C)	173.1	400.0	45.0	63.5	179.6	550.0	250.0
Pressure (bar)	55.0	54.5	2.0	52.5	54.5	54.5	1.1
Total Flow (kg/hr)	955493	1905656	1150920	42119	73464	1529220	890632
Total Flow (kmole/hr)	52439.8	105780	39893	20115	2295	55625.96	31594
Mass Vapor Fraction	0.98	1.00	1.00	1.00	1.00	1.00	1.00
Mole Percent							
H_2O	19.10%	100.00%	1.08%	0.49%	0.00%	53.15%	0.16%
N_2	0.49%		77.19%		0.19%	0.46%	97.47%
O_2	0.00%		20.76%		99.49%	5.25E-20	1.14%
H_2	36.66%			99.51%	0.00%	5.13%	0.00%
CO	28.39%					2.87%	
CO_2	12.28%		0.03%	0.00%	0.00%	38.33%	0.04%
H_2S							
CH_4	2.77%		0.00%	0.00%	0.00%	0.05%	0.00%
NH_3							
MeOH	0.31%						
EtOH							
Methanoate	0.01%						
DME							
AR		0.00%	0.94%	0.00%	0.32%	0.00%	1.19%
HCl							
Total	100.00%	100.00%	100.00%	100.00%	100.00%	100.00%	100.00%

Chapter 3

Supplementary Material 4

Sequestration

Design Basis: 50% of the net output is Electricity

Stream No.	**7-1**	**7-2***	**7-3**	**7-4**
Description				
Temperature (°C)	100.0		45.0	48.5
Pressure (bar)	53.5		53.0	153.0
Total Flow (kg/hr)	1602684		1011936	1011936
Total Flow (kmole/hr)	55693.5		23047	23047
Mass Vapor Fraction	0.64		1.00	0.00
Mole Percent				
H_2O	58.71%		0.38%	0.38%
N_2				
O_2			0.00%	0.00%
H_2				
CO				
CO_2	41.28%		99.58%	99.58%
H_2S				
CH_4				
NH_3				
MeOH				
EtOH				
Methanoate				
DME				
AR	0.01%		0.03%	0.03%
HCl				
Total	100.00%		100.00%	100.00%

* The Hydration option is not used here.

Chapter 3

Supplementary Material 4

Power Generation

Design Basis: 50% of the net output is Electricity

Stream No.	**8-3**	**8-4**	**8-5**
Description	**Hydrogen**	**Air**	
Temperature (°C)	65.5	65.0	1260.0
Pressure (bar)	52.5	2.0	51.9
Total Flow (kg/hr)	22123.8	2282960	2719928
Total Flow (kmole/hr)	10566	79132	99234
Mass Vapor Fraction	1.00	1.00	1.00
Mole Percent			
H_2O	0.49%	1.08%	11.51%
N_2		77.19%	76.42%
O_2		20.76%	11.26%
H_2	99.51%		
CO			
CO_2		0.03%	0.02%
H_2S			
CH_4			
NH_3			
MeOH			
EtOH			
Methanoate			
DME			
AR		0.94%	0.79%
HCl			
Total	100.00%	100.00%	100.00%

Chapter 3
Supplementary Material 5
Coal Only (Dry-Slurry)
Design Basis: 80% of the net output is Electricity

Final Results		
%Thermal Efficiency	36.7	HHV
	42.3	LHV
NPV	$324	$Million
Capital Investment	$2,736	$Million
% Output		
DME	1.2	
MeOH	18.8	
Power	80.0	

Dry Gasifier		
Coal Rate	58.4	tonne/hr
Shell Gasifier Sub-Total	$308,157	$1,000
	$0.31	$Billion
Slurry Gasifier		
Coal Rate	583.6	tonne/hr
GE Gasifier Sub-Total	$1,116,651	$1,000
	$1.12	$Billion
Air Separation Unit		
Air intake rate	2686.4	tonne/hr
ASU Sub-Total	514302.72	$100
	$0.51	$Billion
Sulfur Removal		
H2S rate	5.4	tonne/day
Sulfur Removal Cost	658.6	$1,000
	$0.00	$Billion

Methanol		
Syngas	23993.2	kmole/hr
Synthesi Cost	$90,116	$1,000
Methanol Production	559428.9	tonne/yr
Separation Cost	$6,504	$1,000
Methanl Sub-Total	$96,620	$1,000
	$0.10	$Billion

DME		
DME Sub-Total	$514	$1,000
	$0.00	$Billion

CO2 Compression		
CO2 compression Sub-T	$102,445	$1,000
	$0.10	$Billion

Power Generation		
Power Generation Sub-T	$457,064	$1,000
	$0.46	$Billion

Chemical Looping		
Solid Inventory	564328	kg
Solid Annual Refill	56	kg/hr
CaO Solid Solid		
Inventory	488	kg/hr
Capital	138207	$1,000

Reforming and Reforming Auxiliaries		
NG Feed (kmol/hr)	0	
Subtotal Reforming	0	$1,000

MHR		
Capital Cost	$0	$
Operating Cost	$0	$

Total Capital Investment	4,023,054,952
Direct Cost, $	2,735,677,367
Indirect Cost, $	683,919,342
Fixed Capital Ir	3,419,596,709
Working Capit	603,458,243
Total Capital In	4,023,054,952
Feed and Product Prices	
Natural Gas Pr	4.26
Ethylene Price,	1384.72
Ethane Price, $	0.21
Electricity, cen	10.04
Methanol Price	632.00
DME Price, $/t	651.30
Propylene, $/t	1485.92
C4+, $/MJ	0.02
Solid, $/kg	1.88
CaO, $/kg	0.08
Coal Price, $/t	50.87
Total Annual Expense, $/	705,422,067
Feed Cost, $/y	244,261,789
Operating Labo	48,852,358
Direct supervis	4,885,236
Utilities, $/yr	48,852,358
Maintenance a	170,979,835
Operating sup	17,097,984
Laboratory cha	4,885,236
Plant-overhead	112,358,714
Administrative	33,707,614
Distribution an	9,770,472
Research and d	9,770,472
Total Revenue, $/yr	1,293,878,911
Ethylene Sale,	0
Ethane Sale, $/	0
Power, $/yr	1,010,852,358
Methanol Sale	270,472,688
DME Sale, $/yr	12,553,864
Propylene, $/y	0
C4+, $/yr	0
Gross Earning,	588,456,845
Debt Taken, $	2,011,527,476
Equity Expend	2,011,527,476
Annual Payme	204,533,289
Carbon Taxes,	0

CASH FLOW - Depreciation

2013	341,959,671
2014	615,527,408
2015	492,421,926
2016	393,937,541
2017	315,286,817
2018	252,024,277
2019	223,983,584
2020	223,983,584
2021	224,325,544
2022	223,983,584
2023	112,162,772

Loan Principal Balance at start of

2013	2,011,527,476
2014	1,998,089,297
2015	1,983,374,490
2016	1,967,261,778
2017	1,949,618,357
2018	1,930,298,812
2019	1,909,143,909
2020	1,885,979,291
2021	1,860,614,035
2022	1,832,839,079
2023	1,802,425,502
2024	1,769,122,635
2025	1,732,655,996
2026	1,692,725,026
2027	1,649,000,614
2028	1,601,122,383
2029	1,548,695,720
2030	1,491,288,524
2031	1,428,427,645
2032	1,359,594,982
2033	1,284,223,215
2034	1,201,691,131
2035	1,111,318,500
2036	1,012,360,468
2037	904,001,423
2038	785,348,268
2039	655,423,065
2040	513,154,966
2041	357,371,399
2042	186,788,392

Interest Payed During

2013	191,095,110
2014	189,818,483
2015	188,420,577
2016	186,889,869
2017	185,213,744
2018	183,378,387
2019	181,368,671
2020	179,168,033
2021	176,758,333
2022	174,119,712
2023	171,230,423
2024	168,066,650
2025	164,602,320
2026	160,808,877
2027	156,655,058
2028	152,106,626
2029	147,126,093
2030	141,672,410
2031	135,700,626
2032	129,161,523
2033	122,001,205
2034	114,160,657
2035	105,575,257
2036	96,174,244
2037	85,880,135
2038	74,608,085
2039	62,265,191
2040	48,749,722
2041	33,950,283
2042	17,744,897

CASH FLOW - Taxable Earnings

2013	55,402,063
2014	-200,494,744
2015	-59,140,311
2016	58,195,294
2017	156,325,202
2018	239,722,147
2019	288,581,412
2020	310,114,919
2021	332,054,137
2022	355,459,811
2023	491,164,047
2024	628,069,618
2025	653,714,163
2026	680,305,756
2027	707,892,879
2028	736,527,462
2029	766,265,182
2030	797,165,783
2031	829,293,431
2032	862,717,096
2033	897,510,976
2034	933,754,951
2035	971,535,093
2036	1,010,944,208
2037	1,052,082,439
2038	1,095,057,923
2039	1,139,987,503
2040	1,186,997,518
2041	1,236,224,655
2042	1,287,816,887

CASH FLOW - Net Earnings - Includes carbon taxes applied AFTER state&fed taxes are applied

2013	-1,991,724,417
2014	-215,209,550
2015	-75,253,023
2016	17,273,756
2017	74,475,576
2018	122,678,386
2019	149,984,229
2020	160,703,695
2021	171,457,526
2022	182,862,310
2023	261,395,562
2024	340,375,132
2025	352,297,528
2026	364,459,042
2027	376,857,496
2028	389,489,814
2029	402,351,913
2030	415,438,590
2031	428,743,396
2032	442,258,492
2033	455,974,501
2034	469,880,339
2035	483,963,024
2036	498,207,480
2037	512,596,309
2038	527,109,550
2039	541,724,404
2040	556,414,943
2041	571,151,786
2042	585,901,740

CASH FLOW - Discounted Cash Flow

2013	-1,649,764,746
2014	400,317,858
2015	417,168,903
2016	411,211,297
2017	389,762,392
2018	374,702,663
2019	373,967,814
2020	384,687,279
2021	395,783,070
2022	406,845,894
2023	373,558,334
2024	340,375,132
2025	352,297,528
2026	364,459,042
2027	376,857,496
2028	389,489,814
2029	402,351,913
2030	415,438,590
2031	428,743,396
2032	442,258,492
2033	455,974,501
2034	469,880,339
2035	483,963,024
2036	498,207,480
2037	512,596,309
2038	527,109,550
2039	541,724,404
2040	556,414,943
2041	571,151,786
2042	585,901,740

CASH FLOW - Cumulative Cash Flow (PV)

2013	-1,649,764,746
2014	-1,316,166,531
2015	-1,026,465,904
2016	-788,496,404
2017	-600,532,287
2018	-449,947,691
2019	-324,706,626
2020	-217,347,467
2021	-125,300,974
2022	-46,451,514
2023	13,880,242
2024	59,690,645
2025	99,203,158
2026	133,266,913
2027	162,619,050
2028	187,899,070
2029	209,661,437
2030	228,386,602
2031	244,490,648
2032	258,333,721
2033	270,227,384
2034	280,441,038
2035	289,207,508
2036	296,727,919
2037	303,175,927
2038	308,701,404
2039	313,433,635
2040	317,484,103
2041	320,948,891
2042	323,910,779
NPV, $Milli	324

Chapter 3

Supplementary Material 5

Option A (Coal-NG)

Design Basis: 37% of the net output is Electricity

Final Results		
%Thermal Efficiency	48.9	HHV
	52.6	LHV
NPV	$2,334	$Million
Capital Investment	$2,273	$Million
% Output		
DME	3.9	
MeOH	58.8	
Power	37.3	

Dry Gasifier		
Coal Rate	0.0	tonne/hr
Shell Gasifier Sub-Total	$0	$1,000
	$0.00	$Billion
Slurry Gasifier		
Coal Rate	509.2	tonne/hr
GE Gasifier Sub-Total	$1,021,903	$1,000
	$1.02	$Billion
Air Separation Unit		
Air intake rate	2323.0	tonne/hr
ASU Sub-Total	$461,192	$1,000
	$0.46	$Billion
Sulfur Removal		
H2S rate	4.6	tonne/day
Sulfur Removal Cost	$584	$1,000
	$0.00	$Billion

Methanol		
Syngas	100695.8	kmole/hr
Synthesi Cost	$228,930	$1,000
Methanol Production	2181184.8	tonne/yr
Separation Cost	$9,651	$1,000
Methanl Sub-Total	$238,581	$1,000
	$0.24	$Billion

DME		
DME Sub-Total	$2,179	$1,000
	$0.00	$Billion

CO2 Compression		
CO2 compression Sub-T	$77,083	$1,000
	$0.08	$Billion

Power Generation		
Power Generation Sub-T	$307,652	$1,000
	$0.31	$Billion

Chemical Looping		
Solid Inventory	492319	kg
Solid Annual Refill	49	kg/hr
CaO Solid Solid		
Inventory	386	kg/hr
Capital	150923	$1,000

Reforming and Reforming Auxiliaries			
NG Feed (kmol/hr)	3746.1		
Subtotal Reforming		12,022	$1,000

MHR		
Capital Cost	$0	$
Operating Cost	$0	$

Total Capital Investment	3,342,708,298
Direct Cost, $	2,273,041,643
Indirect Cost, $	568,260,411
Fixed Capital Ir	2,841,302,054
Working Capit	501,406,245
Total Capital Ir	3,342,708,298
Feed and Product Prices	
Natural Gas Pr	4.26
Ethylene Price,	1384.72
Ethane Price, $	0.21
Electricity, cen	10.04
Methanol Pric	632.00
DME Price, $/t	651.36
Propylene, $/t	1485.92
C4+, $/MJ	0.02
Solid, $/kg	1.88
CaO, $/kg	0.08
Coal Price, $/t	50.87
Total Annual Expense, $/	719,718,174
Feed Cost, $/y	283,285,776
Operating Lab	56,657,155
Direct supervis	5,665,716
Utilities, $/yr	56,657,155
Maintenance a	142,065,103
Operating sup	14,206,510
Laboratory cha	5,665,716
Plant-overhea	102,193,987
Administrative	30,658,196
Distribution an	11,331,431
Research and	11,331,431
Total Revenue, $/yr	1,690,524,611
Ethylene Sale,	0
Ethane Sale, $/	0
Power, $/yr	586,323,986
Methanol Sale	1,054,559,211
DME Sale, $/yr	49,641,415
Propylene, $/y	0
C4+, $/yr	0
Gross Earning,	970,806,437
Debt Taken, $	1,671,354,149
Equity Expend	1,671,354,149
Annual Payme	169,944,267
Carbon Taxes,	0

CASH FLOW - Depreciation

2013	284,130,205
2014	511,434,370
2015	409,147,496
2016	327,317,997
2017	261,968,049
2018	209,403,961
2019	186,105,285
2020	186,105,285
2021	186,389,415
2022	186,105,285
2023	93,194,707

Loan Principal Balance at start of

2013	1,671,354,149
2014	1,660,188,527
2015	1,647,962,170
2016	1,634,574,309
2017	1,619,914,602
2018	1,603,862,223
2019	1,586,284,867
2020	1,567,037,663
2021	1,545,961,974
2022	1,522,884,095
2023	1,497,613,817
2024	1,469,942,863
2025	1,439,643,168
2026	1,406,465,002
2027	1,370,134,911
2028	1,330,353,461
2029	1,286,792,773
2030	1,239,093,819
2031	1,186,863,465
2032	1,129,671,228
2033	1,067,045,728
2034	998,470,805
2035	923,381,265
2036	841,158,218
2037	751,123,983
2038	652,536,494
2039	544,583,194
2040	426,374,331
2041	296,935,626
2042	155,200,244

Interest Payed During

2013	158,778,644
2014	157,717,910
2015	156,556,406
2016	155,284,559
2017	153,891,887
2018	152,366,911
2019	150,697,062
2020	148,868,578
2021	146,866,388
2022	144,673,989
2023	142,273,313
2024	139,644,572
2025	136,766,101
2026	133,614,175
2027	130,162,817
2028	126,383,579
2029	122,245,313
2030	117,713,913
2031	112,752,029
2032	107,318,767
2033	101,369,344
2034	94,854,726
2035	87,721,220
2036	79,910,031
2037	71,356,778
2038	61,990,967
2039	51,735,403
2040	40,505,561
2041	28,208,884
2042	14,744,023

CASH FLOW - Taxable Earnings

2013	527,897,587
2014	328,700,651
2015	459,949,033
2016	571,624,887
2017	667,738,095
2018	752,016,006
2019	808,014,435
2020	841,737,311
2021	876,238,334
2022	912,411,154
2023	1,042,357,471
2024	1,173,780,909
2025	1,213,251,179
2026	1,254,014,345
2027	1,296,124,787
2028	1,339,640,142
2029	1,384,621,567
2030	1,431,134,009
2031	1,479,246,520
2032	1,529,032,577
2033	1,580,570,456
2034	1,633,943,616
2035	1,689,241,136
2036	1,746,558,179
2037	1,805,996,510
2038	1,867,665,048
2039	1,931,680,484
2040	1,998,167,938
2041	2,067,261,695
2042	2,139,105,993

CASH FLOW - Net Earnings - Includes carbon taxes applied AFTER state&fed taxes are applied

2013	-1,365,781,219
2014	184,994,034
2015	262,581,559
2016	328,315,225
2017	384,590,477
2018	433,632,248
2019	465,561,457
2020	483,966,698
2021	502,665,121
2022	522,176,415
2023	597,743,528
2024	673,968,850
2025	694,772,542
2026	716,078,516
2027	737,893,422
2028	760,223,397
2029	783,073,987
2030	806,450,052
2031	830,355,674
2032	854,794,046
2033	879,767,351
2034	905,276,630
2035	931,321,635
2036	957,900,672
2037	985,010,417
2038	1,012,645,729
2039	1,040,799,427
2040	1,069,462,058
2041	1,098,621,635
2042	1,128,263,352

CASH FLOW - Discounted Cash Flow

2013	-1,081,651,014
2014	696,428,404
2015	671,729,055
2016	655,633,221
2017	646,558,527
2018	643,036,210
2019	651,666,741
2020	670,071,982
2021	689,054,536
2022	708,281,699
2023	690,938,236
2024	673,968,850
2025	694,772,542
2026	716,078,516
2027	737,893,422
2028	760,223,397
2029	783,073,987
2030	806,450,052
2031	830,355,674
2032	854,794,046
2033	879,767,351
2034	905,276,630
2035	931,321,635
2036	957,900,672
2037	985,010,417
2038	1,012,645,729
2039	1,040,799,427
2040	1,069,462,058
2041	1,098,621,635
2042	1,128,263,352

CASH FLOW - Cumulative Cash Flow (PV)

2013	-1,081,651,014
2014	-501,294,011
2015	-34,815,500
2016	344,601,873
2017	656,406,718
2018	914,828,549
2019	1,133,070,422
2020	1,320,075,214
2021	1,480,327,277
2022	1,617,597,015
2023	1,729,187,398
2024	1,819,895,508
2025	1,897,818,872
2026	1,964,746,348
2027	2,022,218,332
2028	2,071,560,990
2029	2,113,915,812
2030	2,150,265,132
2031	2,181,454,152
2032	2,208,209,944
2033	2,231,157,843
2034	2,250,835,579
2035	2,267,705,471
2036	2,282,164,922
2037	2,294,555,482
2038	2,305,170,638
2039	2,314,262,538
2040	2,322,047,773
2041	2,328,712,360
2042	2,334,416,030
NPV, $Milli	2,334

Chapter 3
Supplementary Material 5
Option B (Coal-NG-He)
Design Basis: 50% of the net output is Electricity

Final Results		
%Thermal Efficiency	46.0	HHV
	50.0	LHV
NPV	$1,867	$Million
Capital Investment	$2,332	$Million
% Output		
DME	3.1	
MeOH	46.2	
Power	50.7	

Dry Gasifier		
Coal Rate	0.00	tonne/hr
Shell Gasifier Sub-Total	$0	$1,000
	$0.00	$Billion
Slurry Gasifier		
Coal Rate	484.02	tonne/hr
GE Gasifier Sub-Total	$984,719	$1,000
	$0.98	$Billion
Air Separation Unit		
Air intake rate	2036.76	tonne/hr
ASU Sub-Total	417877.55	$1,000
	$0.42	$Billion
Sulfur Removal		
H2S rate	4.33	tonne/day
Sulfur Removal Cost	563.69	$1,000
	$0.00	$Billion

Methanol		
Syngas	75072.16	kmole/hr
Synthesi Cost	189150.0946	$1,000
Methanol Production	1626176.018	tonne/yr
Separation Cost	8862.91392	$1,000
Methanl Sub-Total	198013.0085	$1,000
	$0.20	$Billion

DME		
DME Sub-Total	1624.30721	$1,000
	$0.00	$Billion

CO2 Compression		
CO2 compression Sub-Tc	78535.02697	$1,000
	$0.08	$Billion

Power Generation		
Power Generation Sub-T	368237.3711	$1,000
	$0.37	$Billion

Chemical Looping		
Solid Inventory	499345	kg
Solid Annual Refill	50	kg/hr
CaO Solid Solid		
Inventory	367	kg/hr
Capital	143414	$1,000

Reforming and Reforming Auxiliaries		
NG Feed (kmol/hr)	737.6824439	
Subtotal Reforming	5,521	$1,000

MHR		
Capital Cost	$127	$Million
Operating Cost	$10	$Million

Total Capital Investment	3,430,057,464
Direct Cost, $	2,332,439,075
Indirect Cost, $	583,109,769
Fixed Capital Ir	2,915,548,844
Working Capit	514,508,620
Total Capital In	3,430,057,464
Feed and Product Prices	
Natural Gas Pr	4.26
Ethylene Price,	1384.72
Ethane Price, $	0.21
Electricity, cen	10.04
Methanol Price	632.00
DME Price, $/t	651.36
Propylene, $/t	1485.92
C4+, $/MJ	0.02
Solid, $/kg	1.88
CaO, $/kg	0.08
Coal Price, $/tc	50.87
Total Annual Expense, $/	712,541,551
Feed Cost, $/y	269,327,807
Operating Labo	53,865,561
Direct supervis	5,386,556
Utilities, $/yr	53,865,561
Maintenance a	145,777,442
Operating supp	14,577,744
Laboratory cha	5,386,556
Plant-overheac	102,514,780
Administrative	30,754,434
Distribution an	10,773,112
Research and d	10,773,112
Total Revenue, $/yr	1,581,040,448
Ethylene Sale,	0
Ethane Sale, $/	0
Power, $/yr	757,806,849
Methanol Sale	786,223,581
DME Sale, $/yr	37,010,019
Propylene, $/y	0
C4+, $/yr	0
Gross Earning,	868,498,898
Debt Taken, $	1,715,028,732
Equity Expend	1,715,028,732
Annual Payme	174,385,124
Carbon Taxes,	0

CASH FLOW - Depreciation

2013	291,554,884
2014	524,798,792
2015	419,839,034
2016	335,871,227
2017	268,813,603
2018	214,875,950
2019	190,968,449
2020	190,968,449
2021	191,260,004
2022	190,968,449
2023	95,630,002

Loan Principal Balance at start of

2013	1,715,028,732
2014	1,703,571,338
2015	1,691,025,491
2016	1,677,287,789
2017	1,662,245,005
2018	1,645,773,156
2019	1,627,736,482
2020	1,607,986,324
2021	1,586,359,901
2022	1,562,678,968
2023	1,536,748,347
2024	1,508,354,316
2025	1,477,262,852
2026	1,443,217,699
2027	1,405,938,256
2028	1,365,117,267
2029	1,320,418,284
2030	1,271,472,897
2031	1,217,877,698
2032	1,159,190,956
2033	1,094,928,973
2034	1,024,562,101
2035	947,510,377
2036	863,138,739
2037	770,751,795
2038	669,588,092
2039	558,813,837
2040	437,516,028
2041	304,694,927
2042	159,255,821

Interest Payed During

2013	162,927,730
2014	161,839,277
2015	160,647,422
2016	159,342,340
2017	157,913,275
2018	156,348,450
2019	154,634,966
2020	152,758,701
2021	150,704,191
2022	148,454,502
2023	145,991,093
2024	143,293,660
2025	140,339,971
2026	137,105,681
2027	133,564,134
2028	129,686,140
2029	125,439,737
2030	120,789,925
2031	115,698,381
2032	110,123,141
2033	104,018,252
2034	97,333,400
2035	90,013,486
2036	81,998,180
2037	73,221,421
2038	63,610,869
2039	53,087,315
2040	41,564,023
2041	28,946,018
2042	15,129,303

CASH FLOW - Taxable Earnings

2013	414,016,284
2014	206,057,053
2015	337,078,993
2016	447,915,091
2017	542,677,175
2018	625,187,078
2019	678,567,909
2020	708,977,404
2021	740,068,520
2022	772,755,002
2023	901,541,937
2024	1,031,717,690
2025	1,067,406,986
2026	1,104,288,890
2027	1,142,415,468
2028	1,181,842,026
2029	1,222,627,370
2030	1,264,834,090
2031	1,308,528,872
2032	1,353,782,829
2033	1,400,671,876
2034	1,449,277,128
2035	1,499,685,334
2036	1,551,989,365
2037	1,606,288,726
2038	1,662,690,131
2039	1,721,308,123
2040	1,782,265,755
2041	1,845,695,331
2042	1,911,739,219

CASH FLOW - Net Earnings - Includes carbon taxes applied AFTER state&fed taxes are applied

2013	-1,478,076,356
2014	111,088,385
2015	188,509,694
2016	253,706,271
2017	309,134,457
2018	357,075,573
2019	387,390,587
2020	403,760,019
2021	420,360,179
2022	437,722,379
2023	512,531,131
2024	587,939,150
2025	606,399,038
2026	625,293,891
2027	644,628,291
2028	664,406,232
2029	684,631,035
2030	705,305,256
2031	726,430,581
2032	748,007,714
2033	770,036,254
2034	792,514,552
2035	815,439,563
2036	838,806,676
2037	862,609,532
2038	886,839,823
2039	911,487,064
2040	936,538,352
2041	961,978,093
2042	987,787,711

CASH FLOW - Discounted Cash Flow

2013	-1,186,521,472
2014	635,887,177
2015	608,348,727
2016	589,577,498
2017	577,948,060
2018	571,951,523
2019	578,359,036
2020	594,728,469
2021	611,620,183
2022	628,690,829
2023	608,161,134
2024	587,939,150
2025	606,399,038
2026	625,293,891
2027	644,628,291
2028	664,406,232
2029	684,631,035
2030	705,305,256
2031	726,430,581
2032	748,007,714
2033	770,036,254
2034	792,514,552
2035	815,439,563
2036	838,806,676
2037	862,609,532
2038	886,839,823
2039	911,487,064
2040	936,538,352
2041	961,978,093
2042	987,787,711

CASH FLOW - Cumulative Cash Flow (PV)

2013	-1,186,521,472
2014	-656,615,491
2015	-234,151,097
2016	107,039,585
2017	385,756,821
2018	615,611,310
2019	809,302,581
2020	975,280,382
2021	1,117,523,689
2022	1,239,368,183
2023	1,337,589,601
2024	1,416,719,147
2025	1,484,730,835
2026	1,543,173,228
2027	1,593,381,111
2028	1,636,504,711
2029	1,673,534,961
2030	1,705,325,357
2031	1,732,610,843
2032	1,756,024,131
2033	1,776,109,797
2034	1,793,336,457
2035	1,808,107,269
2036	1,820,769,004
2037	1,831,619,869
2038	1,840,916,252
2039	1,848,878,545
2040	1,855,696,151
2041	1,861,531,815
2042	1,866,525,343

NPV, $Million 1,867

Chapter 4

A Novel Polygeneration Process to Co-Produce Ethylene and Electricity from Shale Gas with Zero CO_2 Emissions via Methane Oxidative Coupling

Energy Conversion and Management 92 (2015) 406–420

Contents lists available at ScienceDirect

Energy Conversion and Management

journal homepage: www.elsevier.com/locate/enconman

A novel polygeneration process to co-produce ethylene and electricity from shale gas with zero CO_2 emissions via methane oxidative coupling

Yaser Khojasteh Salkuyeh, Thomas A. Adams II *

Department of Chemical Engineering, McMaster University, 1280 Main St W, Hamilton, Ontario L8S 4L7, Canada

ARTICLE INFO

Article history:
Received 29 September 2014
Accepted 25 December 2014
Available online 13 January 2015

Keywords:
Shale gas
Polygeneration
Optimization
Methane oxidative coupling
CO_2 capture

ABSTRACT

A techno-economic analysis of a novel process to co-produce ethylene and electricity using a recently developed methane oxidative coupling catalyst is presented. Several design variants are considered, featuring the use of traditional gas turbines, chemical looping combustion, and 100% carbon dioxide capture. Mass and energy balance simulations were carried out using Aspen Plus simulations, and particle swarm optimization was used to determine the optimal process design under a variety of market scenarios. A custom model for the gas turbine section was used to ensure that the negative impacts of various cooling strategies were factored into the analysis. The results show that by synergistically co-producing power and ethylene using this catalyst, ethylene can be produced at costs close to traditional steam cracking methods with nearly zero carbon dioxide emissions, even when factoring in the relatively poor conversion and selectivity of the chosen catalyst.

1. Introduction

Olefins such as ethylene and propylene are among the most important feedstocks of petrochemical plants [1] since they are fundamental materials for many applications in the polymers and plastics industries. Globally, annual ethylene production was about 143.4 million tonne of ethylene in January 2013 [2], and it has been predicted that the worldwide demand for olefins such as ethylene will grow steadily by around 1.5–4.1% per year [2,3] regardless of the crude oil price. Traditionally, olefins are produced through different types of steam cracking processes depending on the industry. For example, in the oil industry naphtha is produced from petroleum, which can then be converted to olefins via a naphtha cracking process, while in the natural gas industry, ethane is recovered from natural gas and then converted to olefins via the ethane cracking process. In either type of steam cracker, the feedstock (naphtha or ethane) is "cracked" by reacting it with high pressure steam in a series of endothermic reactions at 600–900 °C [1].

However, recent shifts in environmental attitudes and energy markets have brought to light some new challenges and some new opportunities for the olefins industry. First, these processes rely heavily on the combustion of fossil fuels to supply the heat requirement in the cracking furnace of olefin plants which is extremely energy intensive and results in as many 200 million tons of CO_2 emitted per year worldwide [4]. The life cycle analysis results show that the greenhouse gas emissions of the typical oil to olefin plants is more than 4 tonne $CO_{2,eq.}$ per tonne olefins [5]. This is a significant amount of emissions which, if prevented, would be equivalent to taking about 42 million passenger cars off the road [6]. Unfortunately, there has been very little effort to reduce the CO_2 emissions from this process.

Second, from a North American economic perspective, the primary raw material for ethylene production (crude oil) is becoming increasingly difficult to use. Though North American markets continue to have access to plentiful oil, the reserves of lighter crudes suitable for naphtha production (and therefore for ethylene production) are depleting. Heavier crudes may be used instead, but these are more expensive to convert into the light products for ethylene production. A more attractive alternative is natural gas, which due to the shale gas boom beginning in 2009 experienced a major decline in price compared to oil [7] and coal [8]. In fact, oil currently costs more than 3 times as much per joule of energy than natural gas [9].

Therefore, because of the low price of natural gas and shale gas it makes economic sense to use a different route to convert the plentiful methane contained in the gas into olefins. Two processes using methane are possible, namely methanol-to-olefins (MTO) and oxidative coupling of methane (OCM). In the MTO process, feeds like natural gas [10–12], coal [13] or biomass [14] are firstly converted to synthesis gas, which is then converted to methanol

* Corresponding author. Tel.: +1 (905) 525 9140x24782.
E-mail address: tadams@mcmaster.ca (T.A. Adams II).

http://dx.doi.org/10.1016/j.enconman.2014.12.081
0196-8904/

Nomenclature

ASU	air separation unit
CLC	chemical looping combustion
DGA	diglycolamine
DME	dimethyl ether
$E_{Ethylene}$	yield of ethylene production over ethane
Eth.	ethylene (price)
Eth. base	ethylene (price), base case
F_i	molar flow rate of component *i*
GA	genetic algorithm
GCT	gas combustion turbine
HHV	higher heating value
HRSG	heat recovery steam generator
NPV	net present value
OCM	oxidative coupling of methane
PSO	particle swarm optimization
R-50	methane refrigerant
R-1150	ethylene refrigerant
R-1270	propylene refrigerant
SG	shale gas (price)
SGB	shale gas (price), base case
S_i	selectivity of component *i*
X_i	% conversion of component *i*

and then dimethyl ether (DME). Then, olefin gases are produced through DME conversion to ethylene, propylene, butene and pentene along with carbon dioxide, H_2O and saturated hydrocarbons (ethane, propane and butane), in the presence of catalyst. The MTO process was developed at Mobil Oil in 1977 [15] and is offered for commercialization by several companies such as UOP, ExxonMobil [4] and Total [11]. Selectivity and product distribution of MTO over different catalysts such as SAPO-34 [16–20], KCl–$LnCl_3$ [21] and ZSM-5 [22,23] are an area of active development.

The OCM process has been studied and developed since 1980 [24] based on catalytic oxidative dimerization of methane to convert methane directly to ethylene [4] and ethane (by-product) [24–26]. In this method, methyl radicals are formed as a product of methane partial oxidization. After ethane formation from these methyl radicals, it is dehydrogenated into ethylene. The gas conversion, which can be adjusted by changing the relative amount of oxygen used, affects the selectivity of desired components in the product stream. Various reaction kinetics, reactor design, and operating conditions are described by Keller and Bhasin [24], Sinev et al. [27], Mleczko and Baerns [28], and Zaman [29]. Huff et al. [30] designed a pilot plant based on British Petroleum patent [26], and other catalysts. Taken together, their results indicate that poor methane conversion and product selectivity are a major drawback of this process due to the relatively stable properties of methane itself [24].

However, recent developments of newer and more effective catalysts have made the OCM process attractive again. For example, a La_2O_3/CaO catalyst has exhibited significant promise for converting gas to olefins with relatively high activity and selectivity compared to other catalysts [31,32]. This catalyst shows promise both as use in a traditional packed bed reactor design, as well as a membrane reactor design [33,34]. However, to the best of our knowledge, there have been no processes proposed at the industrial scale using this catalyst for high-methane shale gas feeds. In addition, there have been no processes of this type designed for near-zero CO_2 emissions.

Therefore, we present in this work the first process using this OCM catalyst for high-methane shale gas and feature an optional 100% CO_2 capture system. In this process electricity, ethane and in some scenarios propane are produced as important co-products, classifying it as a "polygeneration" process. Two different electricity production technologies are considered, namely gas combustion turbines (a traditional approach) and chemical looping combustion (an advanced approach). Aspen Plus simulations, custom models (for certain key unit operations), and derivative-free optimization techniques were used to create a collection of suitable design possibilities, each of which might be chosen depending on different business priorities, market conditions, or regulatory scenarios. A net present value approach was used to determine the economic feasibility of the proposed designs, and a sensitivity analysis was used to explore the effect of uncertainties in market conditions.

2. Process description

The simplified schematic of this process is shown in Fig. 1. It consists mainly of six sub-sections: direct ethylene synthesis from shale gas using an OCM reactor, compression, CO_2 removal, product recovery (a demethanizer and C_2 splitter), power generation, and CO_2 compression (optional). The OCM reactor is a gaseous fluidized bed reactor that uses a La_2O_3 (27 wt.%)/CaO (73 wt.%) catalyst at about 800 °C. The contact time (mass of catalyst divided by volumetric gas flow rate) should be also less than 250 kg s/m^3) [32]. The operating conditions and outlet composition of the reactor is based on a model derived from the experimental work of Godini et al. [35] and described in Section 3.3. The main OCM reactions and side reactions over the La_2O_3/CaO catalyst at 750–900 °C are as follows, noting that the primary products are ethane (C_2H_6) and ethylene (C_2H_4) [35,36]:

$$2CH_4 + 0.5O_2 \rightarrow C_2H_6 + H_2O$$

$$C_2H_6 + 0.5O_2 \rightarrow C_2H_4 + H_2O$$

$$C_2H_6 \rightarrow C_2H_4 + H_2$$

$$CH_4 + 1.5O_2 \rightarrow CO + 2H_2O$$

$$CH_4 + 2O_2 \rightarrow CO_2 + 2H_2O$$

$$CO + H_2O \rightarrow CO_2 + H_2$$

The most important property that affects the selectivity and conversion in the reactor is the ratio of inlet methane to oxygen. Raising the CH_4/O_2 ratio increases the catalyst selectivity in favor of ethylene production but reduces the conversion rate. Therefore, this ratio should be determined such that the maximum NPV can be achieved (see Section 4.1 for more detail).

Then, the product stream is compressed and sent to the amine unit (diglycolamine) to remove CO_2. After CO_2 removal, the ethylene and ethane products are separated from unreacted gases by using two separation columns with condenser temperatures so cold such that a refrigeration cycle is required to provide cooling (Fig. 2).

The unreacted gas can be either recycled to the OCM reactor (as in the traditional version of this process) [29,37], used as fuel for power generation, or a mix of both. Many options for power generation are available. A classic gas combustion turbine can be used, in which the fuel is combusted in air to spin a turbine and produce

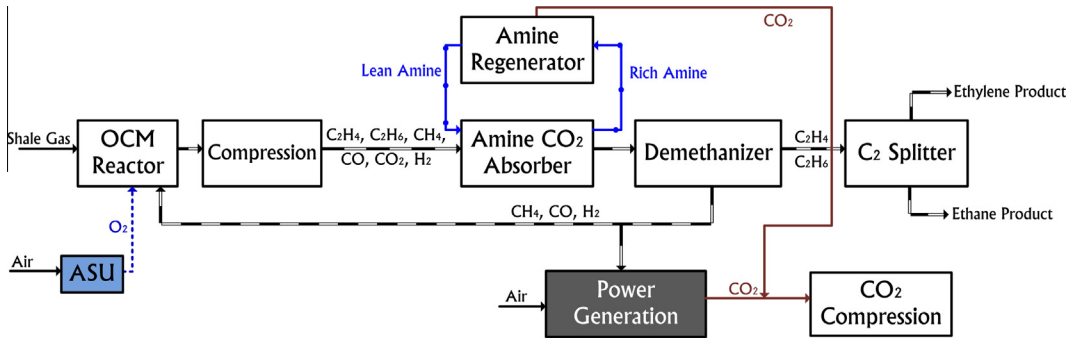

Fig. 1. OCM polygeneration process.

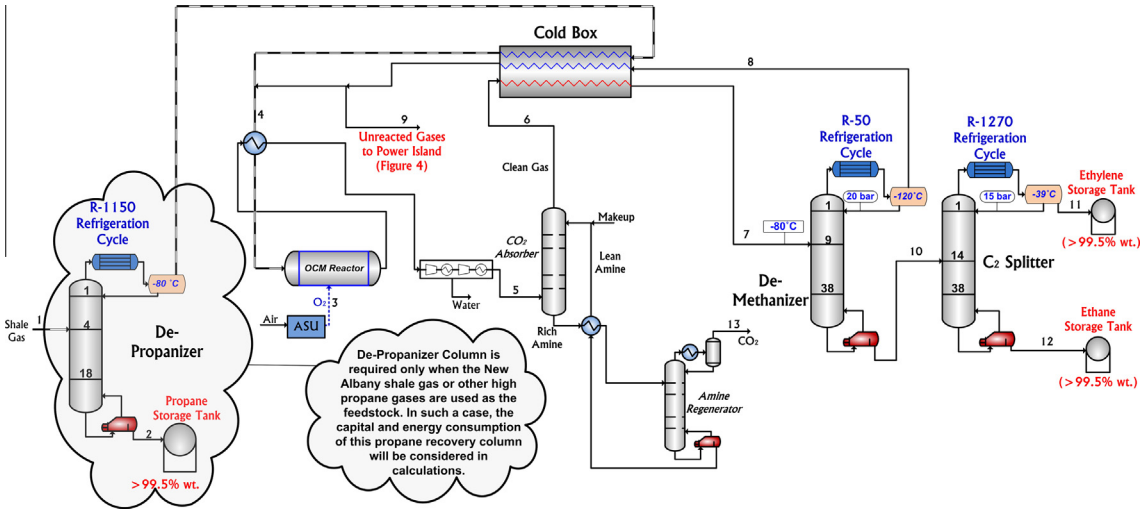

Fig. 2. Ethylene and ethane synthesis and recovery process.

electricity. However, the CO_2 produced by combustion is very expensive to capture because it is present in dilute amounts due to the large amount of N_2 present. Thus, this option typically would not employ CO_2 capture technology using amines without significant environmental legislation or incentives [38].

Three advanced power generation alternatives for combustion are designed to make CO_2 capture easier. These technologies avoid the mixing of N_2 with the fuel and are oxyfuel combustion, solid oxide fuel cells, and chemical looping combustion. In all three approaches, the waste product is a mixture of CO_2 and H_2O without N_2, which can be separated with nearly 100% CO_2 capture with a low energy penalty by essentially condensing out the water [39]. In oxyfuel combustion, high purity oxygen is used for combustion instead of air, preventing the mixing of N_2 with the fuel. However, one major downside is that the air separation unit for oxygen production would have to be significantly increased in size, which increases the production cost [40]. Solid oxide fuel cell systems work by employing an electrolyte which transmits oxygen ions from an air stream to the fuel stream, thus allowing the fuel to be oxidized electrochemically without the introduction of nitrogen [41]. One primary downside is the high cost and short lifetime of the cells. Chemical looping combustion works by combusting fuel using metal oxides as the oxygen source, rather than air. Metal oxides are regenerated using air in a separate unit and recycled [42]. The primary downsides relate to the costs of regenerating the metal particles and other difficulties with solids handling. In this work, we have selected chemical looping combustion because it is a very economical approach for CO_2 capture from a variety of fuels and can be integrated with other techniques readily [43]. However, all three processes could be used for the power generation section with similar effects.

3. Modeling and methodology

3.1. Shale gas basis

Although the composition of shale gas is usually similar to conventional gases, they are not the same and vary not only from area to area but also between different wells in the same area. The typical composition ranges of 6 shale gas reservoirs are shown in Table 1 [44]. The Fayetteville shale is the most suitable for this process since it has the highest methane content. The Haynesville, Marcellus, and New Albany shale gases have high ethane contents, but could still be suitable for the OCM process. However, shale gas with a high N_2 content, like Antrim, poses additional difficulties since presence of N_2 will limit the amount of unreacted gases recycled to the OCM reactor, reducing its potential yield. In addition, the N_2 present in the fuel for power generation cannot be easily separated, thus hindering the ability of the CO_2 capture section to produce high purity CO_2. In this work, the Fayetteville shale gas composition was chosen for the base case because it has a composition closest to the composition used in the development of the catalyst selected for this work [35] and because it is also the one of the least suitable for the traditional ethane cracking process due to its low ethane content. In addition, the effect of using different

Table 1
Compositions (in mol%) of various shale gas and conventional natural gas sources [44].

	C_1	C_2	C_3	C_4	CO_2	N_2
Barnett	80–94	3–8	0–2	0	1–3	1–8
Marcellus	79–96	3–16	1–4	0	0.1–0.9	0.2–0.4
Fayetteville	97	1	0	0	1	0.7
New Albany	88–93	1–2	0.6–3	0	6–10	0
Antrim	28–86	3.5–5	1–2	0	3–9	0.7–65
Haynesville	95	0.1	0	0	5	0.1
Conventional natural gas [45]	93.9	3.2	0.7	0.4	1	0.8
Liquefied natural gas (LNG), high ethane [46]	92	6	1	0	0	1

types of shale gas was studied by replacing the feedstock with the New Albany shale gas as a methane-lean feedstock.

3.2. Simulation strategy

The unit operations for all processes considered in this work were modeled in the Aspen Plus simulation software version 2006.5. The Peng–Robinson with Boston–Matthias (PR–BM) model was used in all physical property calculations except for the Amine unit where the Elec-NRTL physical property package was used as suggested by Chen and Mathias [47], and pure water streams where the STEAMNBS package was used [47]. The validity of the physical property models were verified by confirming that the vapor-liquid equilibria predicted by the model for each thermal separations used in the software closely match experimental data. Similarly, the Ethylene property package, an alternative property package provided with Aspen Plus commonly used in the ethylene industry, was considered. However, in comparison to the PR–BM model it was found to be less accurate at predicting the experimental data, and thus was not used. A more detailed comparison of these two models against experimental data can be found in Section 1 of the Supplementary material.

The process models accounted for all utilities consumed by the process as well as the heat integration of all relevant streams. All suitable waste heat was used to produce steam for either internal process steam needs or for power generation using a steam cycle, which was also simulated for each case and is included in all cost and balance calculations. The reactor was validated against experimental data as described in Section 3.3. The remaining process units are quite mature and thus the first-principle models contained in the Aspen Plus software were used since they are generally well-accepted and accurate given the validity of the chosen physical property models. The cost analysis used estimates for individual unit operations or processes published in the literature and Aspen Icarus to estimate any costs which could not be found in the literature at industrial scales. The completed models are available in the Section 2 of the Supplementary material and freely available for non-commercial use.

A summary of the major design parameters for the process are listed in Table 2. Details of each section of the plant are given in the following sections. Additional material balance tables related to selected optimization scenarios are listed in Section 2 of the Supplementary material.

3.3. Reactor model

The first step of this work was to identify a suitable model for the OCM reactor. Because the simulation results using the Gibbs or Equilibrium reactor models in Aspen Plus did not give results sufficiently close to the experimental results reported in the literature, a reduced model was developed for this reactor based on experimental data from [35]. The selectivity and reactivity of the

Table 2
Main design parameters of each process unit.

Unit	Parameters
OCM reactor	Temperature: 800 °C, pressure: 6 bar Compression outlet pressure: 27.2 bar
Amine CO_2 removal	Lean amine DGA wt.%: 68–70 Rich amine CO_2 loading: 0.36–0.47 (mole/mole DGA) CO_2 absorber: 10 stages, 25 bar Amine regenerator: 20 stages, 1.5 bar
Power consumption of refrigeration cycles	R-1150: 1.07 MW/MW refrigeration duty [48] R-50: 5.04 MW/MW refrigeration duty (simulation results) R-1270: 0.7 MW/MW refrigeration duty [48]
NiO loop	NiO to fuel reactor/fuel gas: 2.97 M (23.32 mass) Air to air reactor/Ni to air reactor: 2.39 M Operating pressure of air and fuel reactors: 45 bar
Gas turbine	Model: Siemens V94.3A [49] Temperature: 1250 °C, outlet pressure: 1.1 bar Polytropic efficiency: 0.92, mechanical efficiency: 0.983 Number of stages: 4 (see the Appendix A) Maximum metal surface temperature ($T_{m,external}$): 850 °C (see Section 3.5 and Appendix A)
Steam turbines	High pressure steam: 420 °C, 40.5 bar Turbine outlet pressure (HP/IP/LP): 17/5.8/0.1 bar Turbine outlet temperature (HP/IP/LP): 308/193/46 °C Isentropic efficiency: 0.875, mechanical efficiency: 0.983 [50]
CO_2 compression	Compressor outlet pressure: 80 bar CO_2 pump outlet condition: temperature: 44 °C, pressure: 153 bar [39]

Table 3
The reduced model for using experimental results [35] of an OCM reactor based on a La_2O_3/CaO catalyst in a fluidized bed reactor; (X: percent conversion, S: selectivity, $M_R = F_{CH_4,in}/F_{O_2,in}$, C_{2+}: $C_2H_6 + C_2H_4$ and ethylene yield ($E_{Ethylene}$) as $E_{Ethylene} = F_{C_2H_4,out}/F_{C_2H_6,out}$.

Parameter	Function	Residual sum of squares
X_{CH_4}	$0.0928M_R^4 - 2.089M_R^3 + 16.97M_R^2 - 60.83M_R + 108.01$	1
X_{O_2}	$359.51 - 25.50M_R + 0.00825\exp(M_R) - 723.82/M_R + 1111.96\exp(-M_R)$	0.9953
$S_{C_{2+}}$	$-0.0365M_R^4 + 1.38M_R^3 - 15.51M_R^2 + 68.49M_R - 47.41$	1
S_{CO_2}	$-0.122M_R^4 + 2.277M_R^3 - 13.12M_R^2 + 18.58M_R + 50.62$	0.9991
$E_{Ethylene}$	$-0.0027M_R^5 + 0.0773M_R^4 - 0.851M_R^3 + 4.432M_R^2 - 11.19M_R + 14.30$	0.993

OCM catalyst is a function of temperature and methane/oxygen ratio [35]. However, since the reactor is designed to operate isothermally at 800 °C, the same temperature at which experimental data was collected. The reduced model used for the reactor is listed in Table 3. The model equations compute intermediate reaction properties such as the percent conversion of certain reagents and the selectivity of the products. Using a Fortran Calculator block the equations are applied to the mass balance equations in Table 4 to achieve the reaction product flow rates by setting the appropriate values in an RYIELD block in Aspen Plus. The model was regressed from the experimental data of Godini et al. [35], in which an isothermal reactor configuration was maintained at T = 800 °C in the presence of La_2O_3/CaO catalyst.

The reactor can be cooled by using an internal gas cooling system that uses boiling feed water for steam generation. The model used in this work accounts for overall mass and energy balances associated with this cooling step, but does not consider a detailed design (number and type of internal cooling tubes, etc.). As an option, excess methane can be used as a diluent to help prevent high temperatures [51]. However, exploration of this concept is outside the scope of this work.

The model was used for interpolative purposes only: all inputs used in the simulation were within the bounds of the experimental data. In addition, a detailed comparison of the reduced model and experimental results showed that the model predicts all available experimental data very well, as shown in Table 3. Detailed comparisons of model results to experimental results are provided in Section 2 of the supplementary material.

3.4. Product recovery

As shown in Fig. 2, the first product recovery step is an optional De-Propanizer column that is located upstream of the OCM reactor. This column can be used in cases where propane exists in the shale gas in even small amounts, such as New Albany shale gas. The propane fraction can be recovered before sending the gas to the OCM reactor. The ethylene refrigeration cycle (R-1150) was utilized to supply the refrigeration duty required for separating propane from other lighter components [52]. Prior to being fed to the OCM reactor, the top stream is sent to an integrated cold box system to transfer its refrigeration duty and decrease the refrigeration load of the condenser of de-methanizer. This prevents propane from mixing with the ethane product downstream, which causes both a reduction in value of the ethane product, and an increased load on the condenser of the C_2 splitter. As an alternative, it is also possible to position a fractionation tower right after the C_2 splitter column to remove propane contained in the ethane product. However, our economic analysis results showed that the latter configuration would increase the size, energy consumption and capital investment cost of other equipment throughout the process resulting in a significantly lower NPV. Therefore, only the first configuration (shown in Fig. 2) is reported in this paper.

Diglycolamine (DGA) solvent (with 30 wt.% water) has been used for CO_2 removal from the OCM product gas [53]. The simulation results show that the reboiler duty is around 3.35 MJ/kg-CO_2 with 99.9% CO_2 removal and about 0.03% amine loss (although small, the costs of replacement solvent were considered in the analysis). Methyl-diethanol amine (MDEA) solvent mixture (with 30 wt.% water) was also considered as an alternative to DGA. However, at the same operating conditions, the MDEA solvent performed poorly compared to DGA. It was found that the reboiler duty for the MDEA solvent case was around 8.72 MJ/kg-CO_2 with just 93.8% CO_2 removal. This is because unlike DGA, MDEA is a tertiary amine that does not react directly with CO_2, but instead reacts with hydrogen ions produced from CO_2 hydrolysis reactions in water [54]. As a result, MDEA is more selective of H_2S acid gas, and is more commonly used when both H_2S and CO_2 removal is required simultaneously. On the other hand, primary amines like DGA are generally the better choice when acid gas has a relatively low CO_2 partial pressure, as found to be the case in this work [53,55].

The simulation results show that a very low temperature methane refrigeration cycle (R-50) is required to recover ethylene and ethane from unreacted gases. The R-50 refrigeration cycle is the most common industrial approach to provide that extremely low temperature (around −120 °C) [56]. For the C_2 splitter a propylene refrigeration cycle (R-1270) was used to provide around −39 °C for its condenser. The power consumption of each cycle has been shown in Table 2 and considered in the analysis as a utility. Although the selected refrigerants are suitable to deliver the required temperatures, other cycles may be more optimal, but an exhaustive comparison is outside the scope of our work.

Table 4
OCM reactor outlet molar flow rate of each component as a function of parameters mentioned in Table 3.

$$F_{O_2,out} = (1 - X_{O_2})F_{O_2,in}$$
$$F_{CH_4,out} = (1 - X_{CH_4})M_R F_{O_2,in}$$
$$F_{CO,out} = (1 - S_{CO_2} - S_{C_{2+}})X_{CH_4} M_R F_{O_2,in}$$
$$F_{CO_2,out} = S_{CO_2} X_{CH_4} M_R F_{O_2,in}$$
$$F_{C_2H_4,out} = S_{C_{2+}}\left(\frac{E}{E+1}\right)\left(\frac{X_{CH_4} M_R F_{O_2,in}}{2}\right)$$
$$F_{C_2H_6,out} = S_{C_{2+}}\left(\frac{1}{E+1}\right)\left(\frac{X_{CH_4} M_R F_{O_2,in}}{2}\right)$$
$$F_{H_2O,out} = 2F_{O_2,in}X_{O_2} - (F_{CO,out} + 2F_{CO_2,out})$$
$$F_{H_2,out} = 0.5\left[4M_R F_{O_2,in} X_{CH_4} - (4F_{CH_4,out} + 4F_{C_2H_4,out} + 6F_{C_2H_6,out})\right]$$

3.5. Gas turbine model

For natural gas power generation plants, higher temperatures in the combustion chamber typically result in higher performance of the turbine. However, the working temperature of the turbine blades must be below a safe value [57]. Existing commercial technologies for blade cooling generally use either air [58,59] from the primary compressor or steam [60] from waste heat boilers as a coolant. The cooling technique affects both the turbine power as well as the parasitic load of the balance of plant in significant ways

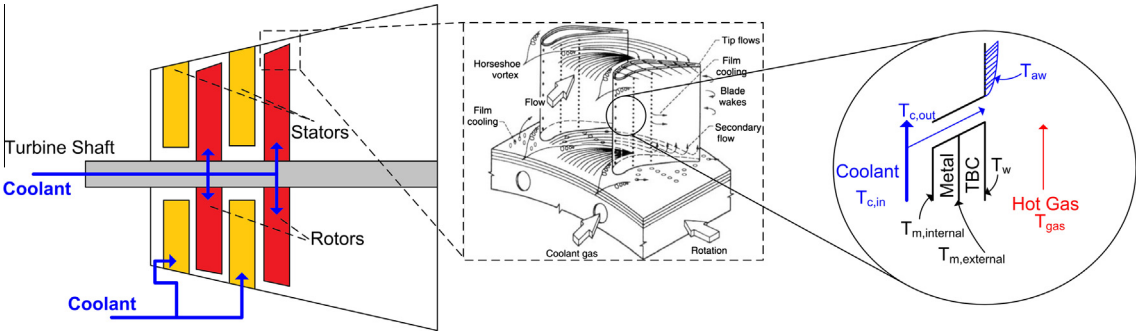

Fig. 3. Schematic of gas turbine blade film cooling strategy. The middle image was adapted from [65].

[61,62]. Therefore, depending on the cooling technology, there is some optimal turbine inlet temperature (TIT) which maximizes the net plant efficiency [57]. Common cooling technologies can be divided into three different approaches, using either steam or air in each [61]: (1) closed-loop cooling; the coolant is not contacted with hot fuel gas after cooling. (2) Internal convection; the coolant is mixed with hot fuel gas after cooling each stage [63]. (3) Open-loop film cooling; an insulation layer is formed by injecting the coolant onto the blade surface from holes in the airfoils. This film reduces the required coolant rate compared to other technologies. The exiting coolant mixes with the fuel gas in this case [64]. In this work, all three strategies were examined and it was found that open-loop film cooling strategy (shown in Fig. 3) generally resulted in the highest plant efficiencies. The strategy, which had the highest net power as produced by the Power Island, was selected as the best approach. Therefore, only the results using the film cooling strategy are presented herein.

Because the default turbine models in Aspen Plus do not directly account for the nuances of film cooling, the models are not suitable for use because they over-predict the performance of the turbine. Instead, a more accurate (and more conservative) model developed by Zhang et al. [49] was used to calculate the cooling requirement of the blade surfaces as a function of the composition and temperature of the hot gas and coolant. The film-cooling turbine model was implemented in Visual Basic (described in the Appendix A), and integrated with Aspen Plus. Aspen Plus results from the combustor model were used as input for the Visual Basic model, including the flow rates, pressure, and temperature of the hot gas and coolant inlets to the turbine. Then, using the user-specified turbine outlet pressure, mechanical efficiency and polytropic efficiency, the Visual Basic model computes the required flow rate of the coolant, the exhaust gas temperature, and work generated by the turbine. These results are returned to Aspen Plus, which incorporates the information as input to downstream models which simulate the balance of the power island, such as compressors and heat exchangers. The strategy is described in more detail in the Appendix A.

3.6. Chemical looping model with optional CO_2 capture

The CLC simulations used in this work employ nickel-oxide (NiO) as the oxygen carrier [66], as shown in Fig. 4. In this approach, metal-oxide is used to transfer oxygen from the air to the fuel combustion reactor. Although different types or combinations of metal oxides can be used for chemical looping combustion [67], NiO-based processes have been experimentally demonstrated to have a very good CO_2 capture efficiency (up to 99%) during a relatively long testing time (>1000 h [68]) with a high melting point (1452 °C) and long lifetime [69]. The main reactions for the fuel reactor [42] are as follows:

$$C_mH_n + [(4m+n)/2]NiO \rightarrow mCO_2 + n/2H_2O + [(4m+n)/2]Ni$$

$$CO + NiO \rightarrow CO_2 + Ni$$

$$H_2 + NiO \rightarrow H_2O + Ni$$

The main reaction for the air reactor is:

$$Ni + 1/2O_2 \rightarrow NiO$$

Due to lack of published kinetic data, the air and fuel reactors were modeled in Aspen Plus using standard RGIBBS reactor models as described by Fan [42]. No external heat requirement was required for either these reactors. The gas expansion turbine was modeled using the proposed model described in Section 3.5.

The CO_2 compression and liquefaction section is designed based on proposed process by Adams and Barton [39] that uses a multistage compression and a series of cascading flash drums to separate water, condense CO_2 and pump it to 153 bar (supercritical pressure). Simulations were performed using standard Aspen Plus models for those process units and the reader is referred to the source reference for details.

3.7. Heat Recovery and Steam Generation

In the Heat Recovery and Steam Generation Section (HRSG), all useable waste heat in the process is used to generate steam at three different pressure levels. Some of the steam is used for process needs such as distillation or gas combustion turbine cooling, and the rest is used to produce electricity in steam turbines. These unit operations are modeled in Aspen Plus using standard models for heat exchangers, pumps, and steam turbines. All process heat streams and utilities are fully accounted for in the analysis. See Table 2 for details concerning pressure levels and turbine efficiencies.

3.8. Cost analysis

The cost evaluation follows the commonly used discounted cash flow analysis method described by Peters and Timmerhaus [70] in order to determine the net present value (NPV) of the plant. The general cost parameters and key market data are listed in Table 5. The capital cost of the air separation unit (ASU) was obtained from Haslbeck et al. [45]. The investment cost of the OCM reactor was estimated based on the value provided by Godini et al. [35], scaled to the appropriate throughput using the six-tenths rule. The capital costs of the remaining equipment were estimated by using Aspen Capital Cost Estimator 2006.5 with appropriate scale-ups to July US$2012 using chemical engineering cost indices. Feedstock and utility prices were based on market prices on July 2012. For ethane, it was assumed that its price was 50% more than the average natural gas price [71]. Historical data

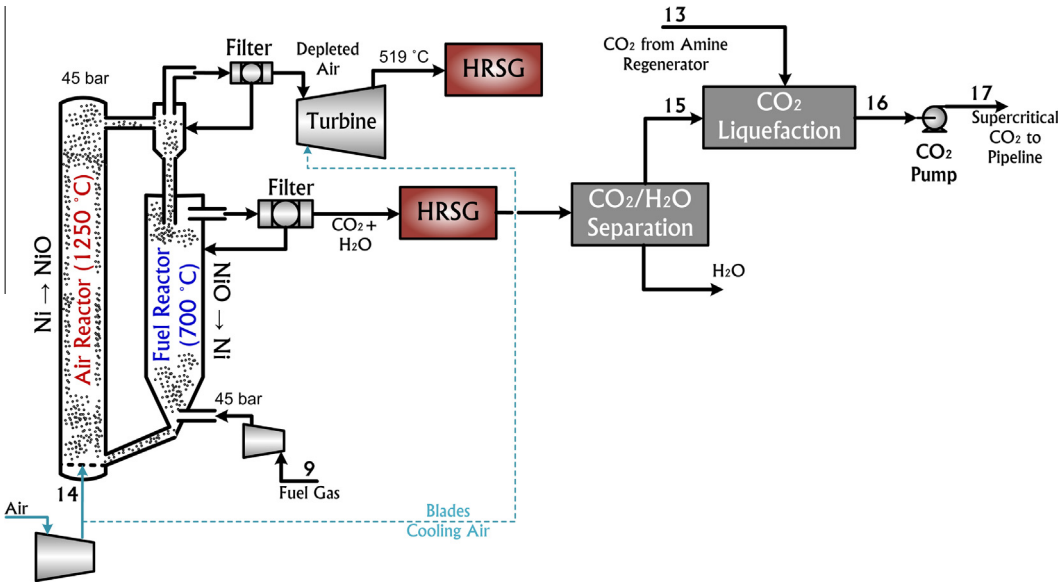

Fig. 4. Chemical looping combustion process for power generation.

Table 5
Base-case market prices and economic assumptions.

Natural gas price ($/MMBtu)	3.72, [74]
Electricity ($/MW h)	79.46, [75]
Nickel-oxide (commercial grade, 76 wt.%) ($/kg)	20, [76]
Nickel-oxide disposal cost ($/kg)	5
Ethylene ($/tonne)	1384, [77]
CO_2 sale price ($/tonne)	10, [78]
Economic assumptions, [50,70]	
Operation time (h/year)	8760
Capacity factor	85%
Plant lifetime (year)	30 [45,73]
Loan lifetime (year)	30 [45,73]
Interest rate on loan	9.5%
Debt percentage	50%
Inflation	2.79%
Federal + state tax rate	40%
Equity return rate	20%
Chemical engineering plant cost index	582.2, [79]
Indirect cost	20% fixed capital cost
Working capital cost	15% total investment
Operating labor	10% total production cost
Direct supervisory and clerical labor	10% operating labor
Utilities	10% total product cost
Maintenance and repairs	5% fixed capital investment
Operating supplies	10% maintenance and repair
Laboratory charges	10% operating labor
Plant-overhead	50% of cost for operating labor, supervision, and maintenance
Administrative costs	15% of cost for operating labor, supervision, and maintenance
Distribution and selling costs	2% of total product cost
Research and development	2% of total product cost

shows that since 2009, there is a correlation between natural gas and ethane prices, where the ethane price was usually higher than natural gas by about 50%, except for some short periods. It should be noted that all scenarios used in this work were scaled to the same energy input of 1111.1 MW (LHV). A conservative value for the debt equity ratio is assumed, to incorporate the risk of investment in this novel non-proven technology, as recommended by the NETL for high risk projects [72]. The plant lifetime value is assumed to be 30 years based on recommended values reported by National Energy Technology Laboratory (NETL) for the cost estimation of industrial scale, coal and natural gas to electricity plants [45,73]. To be able to calculate the capital cost of heat exchangers, a preliminary sizing was performed for all exchangers in Aspen Icarus.

For the CLC cases, the capital cost of the inventory of nickel solid particles and the corresponding cost of particle replenishment because of reactivity loss are two important factors which are to be considered [80]. Based on the work of Kolbitsch et al. [81,82] and Wolf et al. [83], 300 s was assumed for the required residence time of solids in air and fuel reactors. This number was chosen because 170 s was the largest required residence time reported in those references, so 300 s was used as an over-design parameter in order to produce a conservative cost estimate. The estimated life span of NiO varies, with estimated life spans including 4500 h (Linderholm et al. [80], 160 h operation, 10 kW_{th}), 10,000 h (Adánez et al. [43], 100 h operation, 120 kW_{th}), 33,000 h (Linderholm et al. [84], 1000 h operation, 10 kW_{th}), and even 40,000 h [43]. In this work, 10,000 h was assumed for the lifetime of NiO for operating cost calculations.

In this analysis, both CO_2 taxes and revenue from the sale of CO_2 as a product are considered as appropriate. This is discussed in Section 4.5.

3.9. Optimization

Each process was subject to optimization considering two degrees of freedom: (i) the inlet molar ratio of methane to oxygen routed to the OCM reactor (CH_4/O_2 of stream 4 shown in Fig. 3 with feasibility bounds between 2 and 8 based on [35]) and (ii) the recycle ratio of unreacted gas to OCM reactor (with bounds between 0% and 100%) as identified in Fig. 1. Because there were only two decision variables, a "coarse grain exhaustive search" method was used in which 1440 simulations were performed in Aspen Plus using different, evenly spaced combinations of the decision variables. This was used to identify a small region of the decision variable space which contained the global optima, and it was visually evident that only one local optimum existed in every case studied (see Section 4.1, for example). Then, the particle swarm optimization (PSO) method was implemented in Matlab and linked to the simulation file via a Visual Basic interface to fine-tune the decision variables and locate the true global optima within small tolerances. This was necessary because the optimization tool

Table 6
PSO algorithm parameters.

Parameter	Value
Minimum number of function evaluation (NFE_{min})	70
Maximum number of function evaluation (NFE_{max})	100
Number of particles	5
a_1, a_2	2.05,[87]
φ	$a_1 + a_2$, [87]
w	$\frac{2}{\lvert 2-\varphi-\sqrt{\varphi^2-4\varphi}\rvert}$, [87]
$c1$; $c2$	$a_1 w$; $a_2 w$ [87]
$r1$; $r2$	*Rand* (0,1), [87]

provided within Aspen Plus had technical issues arising from the use of external Visual Basic models integrated into the Aspen Plus flowsheets.

It is worth noting that when using commonly used PSO heuristics [85] as shown in Table 6, the PSO method was very effective, and located a global optimum in only about 5% of the time as the exhaustive search, even when no information from the exhaustive search was provided. As such, PSO was used for all sensitivity analyses (Sections 4.2–4.5) without the exhaustive search component, to save time. Similarly, genetic algorithms [86] were tested for comparison, but they were unable to determine the global optimum as quickly as PSO. Although PSO cannot guarantee the global optimum of any problem, we can visually confirm from the coarse grain method that it is the true global optimum for the cases examined in this paper.

4. Results and discussion

4.1. Results for base-case market conditions

The optimization results for two different types of shale gases using the CLC option are depicted in Fig. 5 and shown in Table 7. Fayetteville shale gas is selected to be the representative methane-rich feedstock with no propane, and the New Albany shale gas is selected to represent a methane-lean feed with some propane. Both decision variables (the CH_4/O_2 molar ratio and the recycle ratio of the unreacted gases to the OCM reactor) are varied to illustrate the maximum NPV of each feed considering the base case prices (Table 5). In the figure, the input shale gas rate has been adjusted so that the energy input value is fixed at around 1111.1 MW (LHV) for each case. It can be seen that the optimum CH_4/O_2 ratio is between 3.6 and 4. Furthermore, the NPV drastically decreases by increasing the recycle ratio of unreacted gases to the OCM reactor. This means that power generation is a more profitable option than ethylene production for the base case market conditions, regardless of the composition of the shale gas. The optimization was repeated for the GCT power generation option, as shown in Table 7. The GCT scenario is significantly more profitable than the CLC option, but again, power generation is favored over olefin production. However, as will be shown in the sensitivity analysis, even small perturbations in the market prices of ethylene or electricity result in different product mixes containing a greater percentage of ethylene, and changes in carbon tax policy can result in the CLC option being the preferred choice.

In order to compare to existing naphtha cracking and ethane cracking strategies, the production cost of ethylene is computed. This is because the existing literature contains many examples of costs using this metric, but with insufficient information for computing NPV on a fair basis. Note that, for this scenario, the production cost of ethylene is between \$0.77–0.79/kg ethylene for the CLC cases and –\$0.35–0.39/kg ethylene for the GCT cases. This is computed by taking the total plant annualized cost, subtracting the revenues from ethane and power production, and dividing by the ethylene production rate. The negative value indicates that the power produced is significantly more than the amount of ethylene produced at the optimum condition, and so the metric for the production cost of ethylene is not particularly meaningful for comparison with traditional ethylene plants. This is a common problem associated with polygeneration plants with multiple products. Instead, a more useful metric is to compute the ethylene production cost without considering the credit from the other products. This is computed by taking the total annualized cost, dividing it by the ethylene production rate, and multiplying it by the fraction of energy leaving the process as ethylene. This fraction is computed by taking the higher heating value of the ethylene produced and dividing it by the sum of the higher heating value of the ethylene, the higher heating value of the ethane, and wattage of the net electric power produced. This allows us to allocate the costs of production to the ethylene on an energy basis. With this approach, the cost of ethylene is more reasonable at \$0.89–0.98/kg for the CLC cases and \$0.73–0.75/kg for the GCT cases.

In the second optimization scenario, the objective function was to maximize the rate of ethylene production while still achieving a worthwhile business investment—i.e., with an additional constraint that the NPV is zero or greater. This results in a significantly different plant design in which the recycle ratio is significantly higher (72–84%), such that most of the unreacted off-gases are recycled. Consequently, the rate of ethylene production is more than twice the previous case. For either case, the products are roughly 30% ethylene, 70% power on an energy basis. Both ethylene

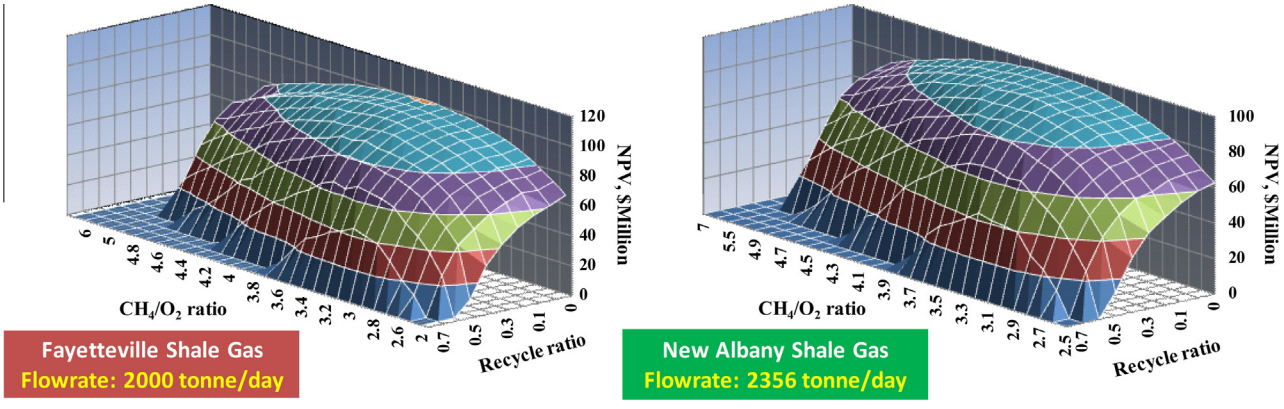

Fig. 5. The effect of varying input CH_4/O_2 molar ratio and the recycle ratio of the unreacted gases (see Fig. 2) on the NPV of the proposed process using the CLC option, note that negative NPV regions are hidden for clarity, and both processes have the same total energy input on an LHV basis.

Table 7
Cost and thermal analysis results of different scenarios (1111.1 MW inlet shale gas).

Shale gas type	Fayetteville (methane-rich feedstock)				New Albany (methane-lean feedstock)			
Optimization scenario	Maximum NPV		Maximum economic olefin production		Maximum NPV		Maximum economic olefin production	
Power generation option	CLC	GCT	CLC	GCT	CLC	GCT	CLC	GCT
NPV ($ million)	100.3	353.0	0	0	93.5	339.4	0	0
Tot. capital investment ($ million)	430.7	602.1	520.5	661.0	428.1	587.4	517.9	659.5
Tot. annual expenses ($million/yr)	216.4	219.3	220.2	223.7	216.1	218.2	220.3	223.6
Total revenue, $million/yr	293.7	377.9	287.8	309.4	291.5	371.7	287.7	309.2
Ethylene revenue ($million/yr)	77.7	77.7	173.7	208.3	73.2	73.2	160.1	195.1
Ethane revenue ($million/yr)	10.0	10.0	16.4	18.7	9.9	9.9	15.9	18.3
Propane revenue ($million/yr)	0.0	0.0	0.0	0.0	16.2	16.1	16.1	16.1
Electricity revenue ($million/yr)	192.3	290.2	86.9	82.5	178.1	272.4	84.0	79.7
CO_2 revenue ($ million/yr)	13.7	0.0	10.9	0.0	14.1	0.0	11.6	0.0
Ethylene production cost, with credit from other products ($/kg)	0.79	−0.35	1.27	1.26	0.78	−0.39	1.26	1.25
Ethylene production cost, without credit from other products ($/kg)	0.98	0.75	1.03	0.97	0.89	0.73	0.96	0.92
Gross power generation (MW)	386.5	548.4	298.5	344.3	367.7	522.1	286.8	332.2
ASU required power (MW)	−8.3	−8.3	−17.6	−21.0	−7.7	−7.7	−16.1	−19.4
OCM compression (MW)	−8.2	−8.2	−18.4	−24.9	−8.4	−8.5	−17.6	−23.8
Refrigeration power (MW)	−41.5	−41.5	−109.9	−159.0	−45.5	−45.4	−106.1	−154.3
CO_2 compression power (MW)	−3.6	0.0	−5.6	0.0	−5.1	0.0	−5.1	0.0
Net power generation (MW)	324.9	490.4	146.9	139.4	301.0	460.5	141.9	134.6
CO_2 emission (tonne/day)	0.0	3779.0	0.0	2711.8	0.0	3892.4	0.0	2888.7
Thermal efficiency (%HHV)	40.6	54.0	40.4	44.9	42.9	55.8	42.9	47.5
Decision variables								
CH_4/O_2 to the reactor	3.69	3.69	3.69	3.69	3.77	3.77	3.77	3.77
Recycle ratio to the OCM reactor	0.0	0.0	0.73	0.84	0.00	0.0	0.72	0.83
% Net power generation[a]	64.9%	73.6%	29.5%	25.2%	64.0%	73.1%	30.1%	25.5%

[a] % Net power generation = net power generation/(net power + ethylene + ethane) * 100.

cost metrics for either case are only slightly higher, at just over $1/kg.

In both cases, these production costs are quite comparable with existing cracking units. The production cost and CO_2 emissions of typical naphtha cracking units are 50–60 ¢/lb (1.1–1.32 $/kg) [88] and 0.85–1.35 tonne CO_2/tonne products [4] respectively. These values are 20–30 ¢/lb (0.44–0.66 $/kg) [88] and 0.75–1.1 tonne CO_2/tonne products [4] for ethane cracking. Note that, for the CLC cases, almost no CO_2 is emitted. This means that the proposed CLC is an economical way of co-producing power and olefins in about equal proportion without process CO_2 emissions. Similarly, the power required to capture and compress the CO_2 is very small due to the lack of N_2 present in the exhaust gas leaving the fuel reactor, the high pressure of that exhaust gas, and the efficient design of the CO_2 separation process.

It can also be seen that the power requirement of the refrigeration cycles is the most significant parasitic load, consisting of about 67–78% of plant total power requirement. This indicates that future improvements to the process might be best focused on reducing the costs of the demethanizer and C_2 splitter. The thermal efficiency for each case is also computed and shown in Table 7. Here, thermal efficiency is the sum of the net power produced and higher heating values of the produced ethylene, ethane and propane, divided by the higher heating value of the shale gas feed to the process. Note that no external energy inputs were required—the process is entirely self-sufficient. For polygeneration plants, it is not particularly meaningful to compare the thermal efficiencies of one process to another due to the different nature and proportion of the products. Nevertheless, it is useful to make general comparisons for processes with similar product portfolios. For the same product portfolio, the GCT-based processes are generally much more expensive to construct than CLC-based processes, but also more efficient by roughly 5–10 percentage points resulting in greater revenues and usually higher NPV. However, the downside is that the GCT-based process produces a considerable amount of CO_2 emissions, while the CLC-based process produces essentially none.

Instead of thermal efficiencies, computing exergy efficiencies is a more appropriate way of comparing processes with different product portfolios. Although this information is academically interesting, it is not particularly useful for this study because the economic analysis serves as a more grounded basis of comparison in terms of which processes would actually be constructed. Thus, the exergy analysis is left to future work.

The breakdown of capital cost investment for the maximum NPV and maximum economic olefin production scenarios of Table 7 is shown in Fig. 6. As can be seen around 36–73% of the capital investment results from the power generation section, specifically the gas and steam turbines. This is consistent because electricity accounts for 30–70% of the products produced (on an energy basis) depending on the optimization scenario and power generation approach. In addition, the investment portion of the ASU is also significant which indicates that finding ways of producing olefins without as much pure oxygen would improve the economics of the liquid production section. For example, alternative strategies using carbonless heating sources might reduce the O_2 requirement while still allowing for a CO_2 emissions-free process [89]. This is a subject for future work.

The influence of market price on the maximum achievable NPV and optimum plant design are described next. In Section 4.2, a sensitivity analysis of these parameters as a function of shale gas and ethylene prices was carried out for different shale gas prices. In Section 4.3, the sensitivity analysis was repeated for changes in electricity price. In Section 4.4, a sensitivity analysis was performed for changes in ethylene and electricity prices. Finally, in Section 4.5, the effect of CO_2 tax policies are examined.

4.2. Sensitivity analysis – effects of shale gas and ethylene price

The sensitivity analysis of the maximum NPV scenario for the CLC-based design as a function of ethylene and shale gas price

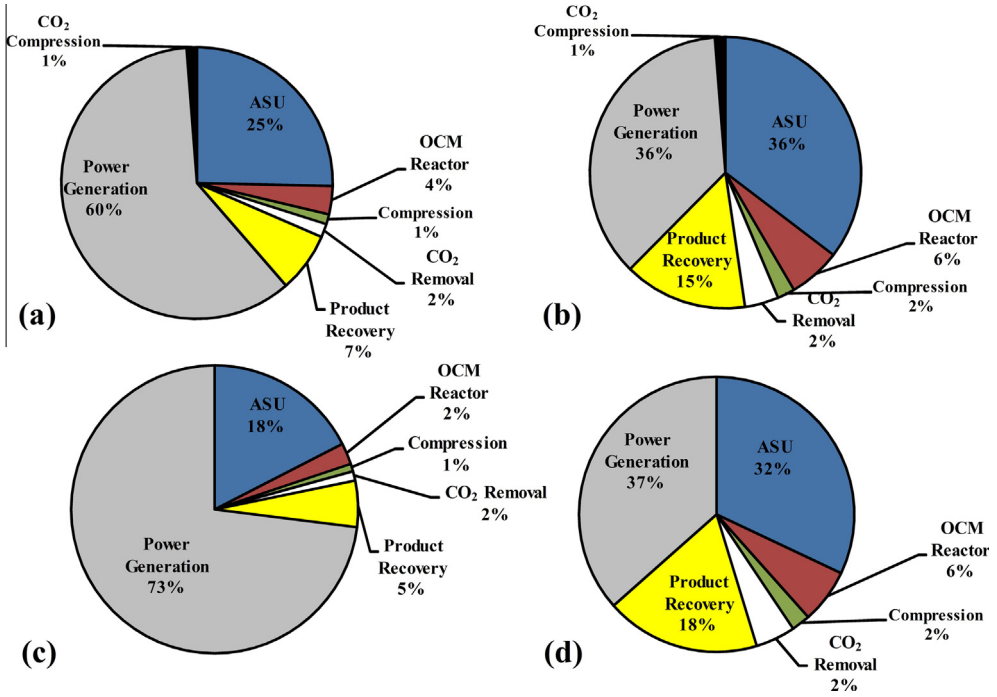

Fig. 6. Percentage of capital cost investment for each CLC and GCT scenario for Fayetteville shale gas: (a) maximum NPV-CLC; (b) maximum olefins production-CLC; (c) maximum NPV-GCT; (d) maximum olefins production-GCT.

(relative to their base case prices) is shown in Fig. 7 for both Fayetteville and New Albany shale gases. It can be seen that for the base case price of shale gas (SG/SGB = 1), the ethylene price can drop as low as $1200/tonne while still having positive NPV. On the other hand, the NPV is much more sensitive to the shale gas price. This is because for ethylene prices lower than $1300/tonne, the optimal design produces as much power as possible by not recycling waste gases, as shown in Fig. 7b and d. Once the ethylene price rises above $1300/tonne, the optimum design moves away from this bound, using more recycle and consequently increasingly more ethylene and less power as the product. Overall, both the NPV and the design itself is sensitive to the ethylene price, but only the NPV is sensitive to the shale gas price. This makes sense because the shale gas rate is fixed for all simulations considered.

4.3. Sensitivity analysis – effects of shale gas and electricity price

The impact of varying the electricity price on the optimum net power generation and maximum NPV for both methane-rich (Fayetteville) and methane-lean (New Albany) is depicted in Fig. 8. It

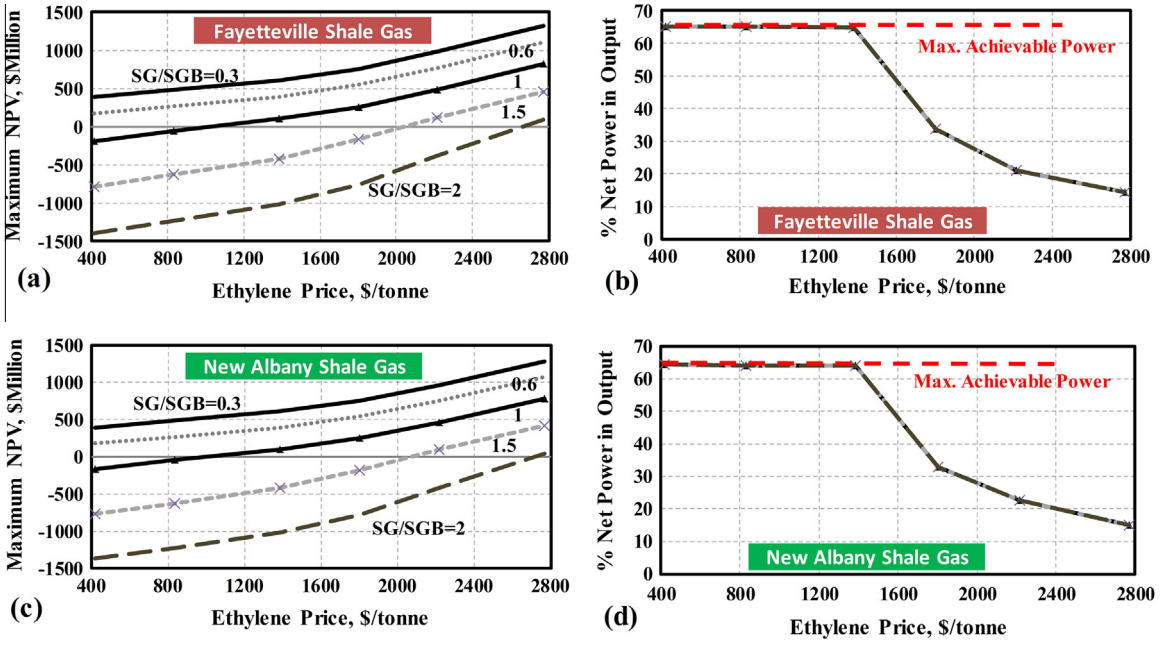

Fig. 7. Effect of ethylene and shale gas price on (a) and (c) the maximum NPV scenario and (b) and (d) optimum net power generation ratio [net power/(net power + ethylene + ethane)], for the CLC cases.

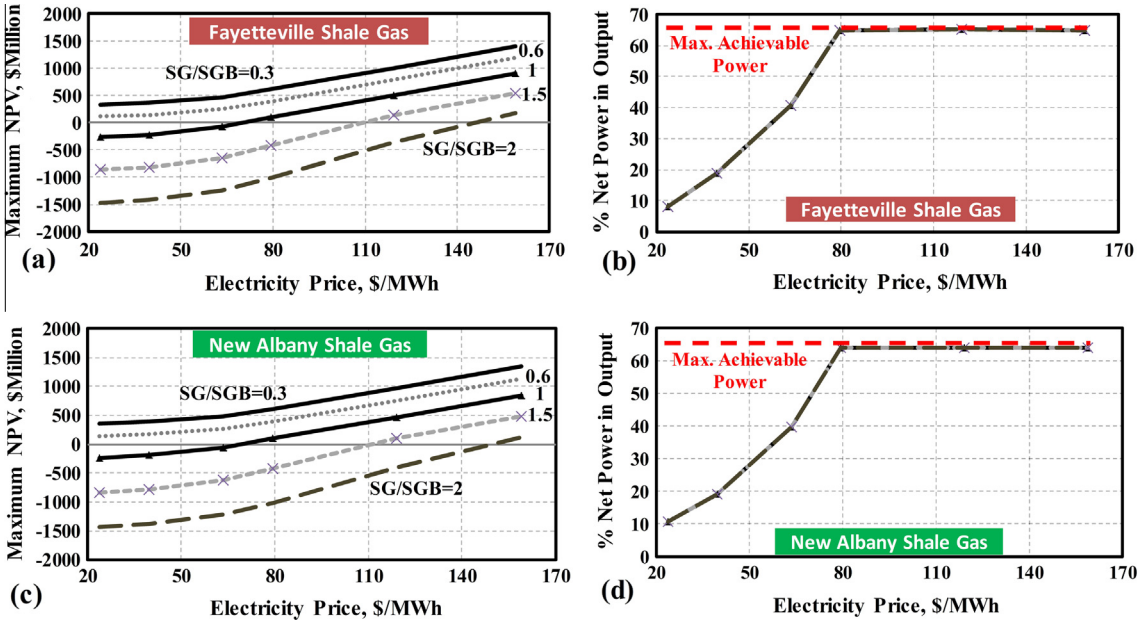

Fig. 8. Effect of ethylene price on (a) and (c) maximum NPV and (b) and (d) optimum net power generation ratio at different shale gas prices.

can be seen that for the base case (SG/SGB = 1), the NPV will be positive when the electricity price is more than $65/MW h (Fig. 8a and c). Overall, the NPV is roughly about as sensitive to the electricity price as it is to the shale gas price (roughly increasing the NPV by $800 million by doubling electricity price from the base case). The optimal designs also change with the electricity price, ranging from the maximum electricity production design at about 80% power for electricity prices above $80/MW h, to as low as about 10% electricity.

4.4. Sensitivity analysis – effects of ethylene and electricity price

The optimum net power generation ratios and maximum NPVs for different ethylene prices are depicted in Fig. 9 as a function of electricity price. When the ethylene price is 50% more than its base case price or higher and electricity wholesale price is around $50/MW h or less, the optimum conditions will be such that some part of the plant's electricity demand should be imported.

4.5. Carbon emission tax

A CO_2 emission tax is a potential regulatory device, which would encourage industries to reduce greenhouse gas emissions. In this analysis, three processes were considered. First, the CLC-based process for the maximum NPV scenario at the base case market conditions. Second, the same, but without CO_2 capture and compression such that the fuel reactor exhaust gas is vented to the atmosphere after heat recovery. Note that this process remains

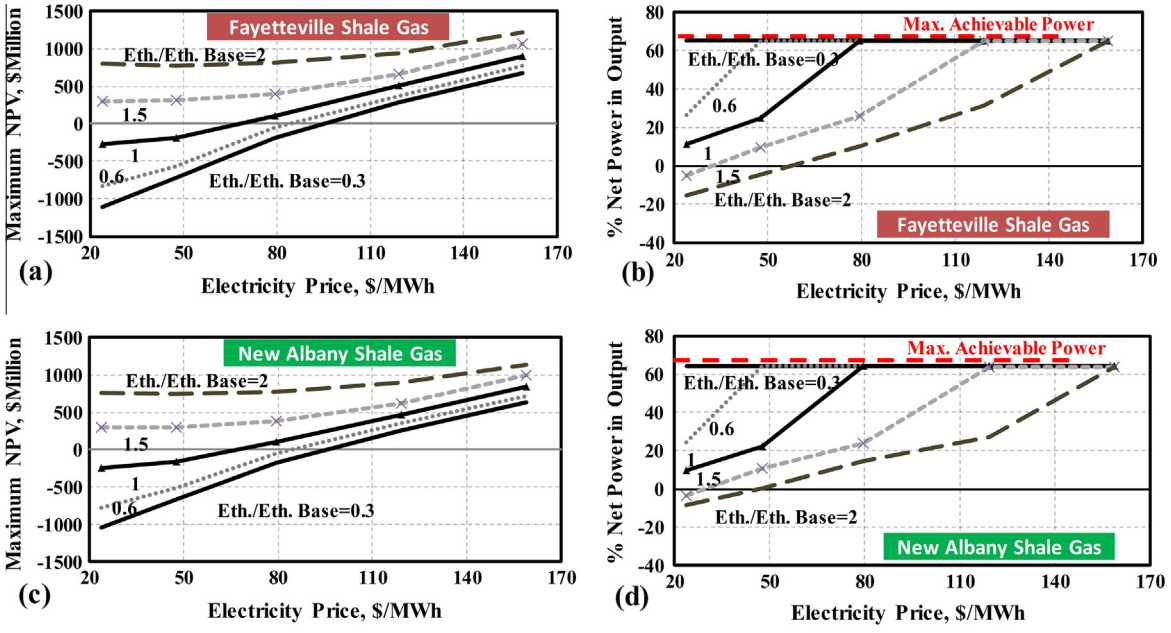

Fig. 9. Effect of ethylene and electricity price on (a) and (c) the maximum NPV scenario and (b) and (d) optimum net power generation ratio, for the CLC cases.

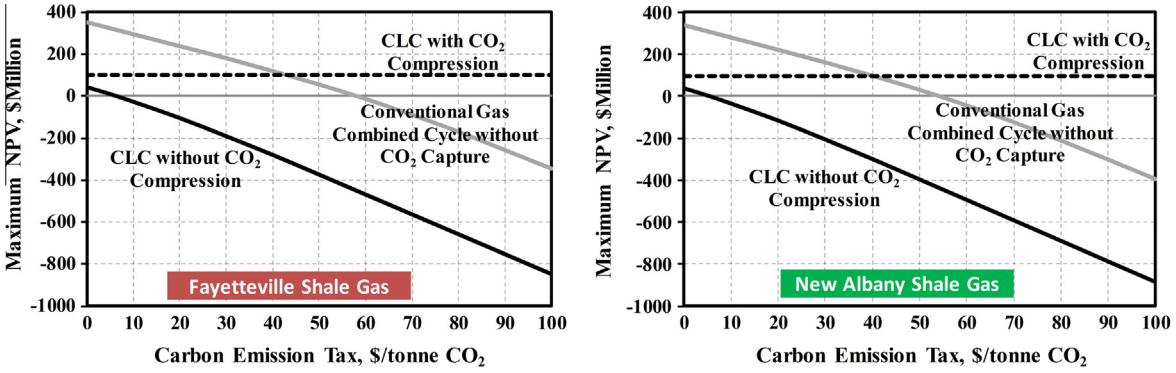

Fig. 10. Maximum achievable NPV of different CO_2 capture scenarios varying with carbon emission tax.

"CO_2-capture ready" since it is possible to retrofit the CO_2 capture section with minimal impact on the rest of the process. Third, the GCT-based process for the maximum NPV scenario at the base-case market conditions. In our analysis, the carbon tax is only applied to direct CO_2 emissions from the plant. Indirect emissions resulting from the use of any of the products downstream, or from the production and delivery of the feedstock (natural gas) or imported utilities (cooling water) upstream of our process are not considered subject to the tax.

As shown in Fig. 10, the GCT-based process is the most profitable design scenario when the carbon emission tax is below \$45/tonne CO_2 for the Fayetteville shale gas and \$40/tonne CO_2 for the New Albany shale gas. However, above those levels, the CLC-based process with CO_2 capture becomes the most economic. The economics of this process are essentially unaffected by the CO_2 tax since there are virtually no CO_2 emissions. Although the capital investment cost of the CLC-based process without CO_2 capture is less than the capital cost of the CLC-based process with CO_2 capture, it is virtually never the most economical choice. This is because the CLC process with CO_2 capture enjoys additional revenue from the sale of captured CO_2.

The CO_2 emission of traditional naphtha and ethane cracking processes are approximately 1.2 and 0.9 tonne CO_2/tonne olefins, respectively [4]. Using these numbers with a tax of \$45/tonne CO_2 and the base case market conditions, the production cost of the traditional approaches increased to 1.15–1.37 and 0.48–0.70 \$/kg olefin respectively. Thus, the production cost of the zero-emission CLC-based process even at maximum olefin production (\$0.96–1.03/kg as shown in Table 7) will be less than the naphtha cracking process in this scenario.

5. Conclusion

A novel ethylene production plant was proposed and simulated in this work, which to the best of our knowledge is the first polygeneration process that converts shale gas directly to ethylene, ethane, and electricity with zero carbon emissions using OCM. Furthermore, because the gas combustion turbine cooling system plays an important role on the efficiency of the power island, a detailed model was used to account for the nuances of the film-cooling strategy. In addition, a nickel-oxide CLC unit with corresponding CO_2 capture system is considered as an alternative power generation strategy which avoids any CO_2 emissions. A techno-economic analysis of the design and its variants was also presented in this paper. Under the base case market conditions, the highest NPV is achieved when the molar ratio of inlet shale gas to oxygen fed to the OCM reactor is between 3.69 and 3.77 (depending on the shale gas type) and essentially all of the unreacted gas is routed to the power generation section. In other words, this means that because of the poor selectivity and conversion of the OCM reactor it is not worth recycling the unreacted gas to the reactor or increasing the reactor conversion by lowering the gas to oxygen ratio under current market conditions. Sensitivity analyses results show that even relatively small perturbations in the ethylene and/or electricity prices from the base case can result in optimal designs containing a higher proportion of ethylene in the product portfolio. Similarly, a \$40–45/tonne CO_2 carbon emission tax is sufficient to incentivize using CLC with CO_2 capture instead of a conventional gas combustion turbine without carbon capture.

As mentioned in the introduction, the global production rate of ethylene in 2012 was about 155.9 million tonne per year and growing. Assuming that all of the existing olefin production units can be replaced with the proposed zero emission process, the worldwide carbon emission reduction would be about 117–210 million tonne per year, which is equivalent to the annual greenhouse gas emissions from 24 to 43 million passenger vehicles or carbon sequestered annually by 96–172 million acres of forests [6]. Consideration of other novel natural gas based olefin production routes like methanol-to-olefins is a subject of future work. In addition, it may be beneficial to use less expensive (but poorer performing) metal-oxides such as Fe_2O_3 as the oxygen carrier in the CLC section, which is also a subject of future work.

Appendix A

This section describes the model used for the gas combustion turbine, which includes film cooling as a key parameter that affects the turbine performance and overall system efficiency. The model was originally developed by Zhang et al. [49] and was implemented in this work with data for physical properties and other parameters taken from other sources, as described below.

A.1. Gas turbine work

The user must first specify the number of turbine stages, the desired final outlet pressure, and the polytropic efficiency, which are key design parameters. Then, the work produced in the gas turbine can be computed for each stage. The power generated in each stage of the gas turbine equals the enthalpy change at that stage:

$$W_{GT} = m_g \int_{T_{g,out}}^{T_{g,in}} c_{p,g}(T)dT \tag{A1}$$

where $T_{g,in}$ is the hot gas inlet temperature and $T_{g,out}$ is the outlet temperature of each stage before mixing with coolant and $c_{p,g}$ is the hot gas specific heat which is a function of temperature [62]. To incorporate this equation in the gas turbine model, the hot gas

outlet temperature of stage must be calculated. The temperature and pressure of each stage are related by [62]:

$$\frac{dT}{T} = \left[\frac{R\eta}{c_{p,g}}\right]\frac{dP}{P} \tag{A2}$$

where R is the gas constant and η is the polytropic efficiency of gas turbine. The pressure drop of each stage is defined by assuming a linear pressure drop in the turbine.

A.2. Coolant requirement

Various approaches to compute the cooling requirement are presented in several other works. For example, calculations based on a continuous expansion model have been proposed in some works such as Bolland and Stadaas [57], Najjar et al. [90] and Sanjay [61–63,91]. Other methods consider turbine layout (both stator and rotor in each stage) such as those proposed by Wilcock et al. [92], Young and Wilcock [93] and Horlock [94,95]. In the latter approach, which has been used in this paper, the effect of cooling on each blade rows is considered [94].

The calculation method is described by Wilcock et al. [92] and Young and Wilcock [93] in more detail. In summary, the internal cooling efficiency ($\eta_c = 0.7$ [92]) and film cooling effectiveness ($\varepsilon_f = 0.4$ [92]) are determined using temperature information at different locations of the turbine according to:

$$\eta_c = \frac{T_{c,out} - T_{c,in}}{T_{m,internal} - T_{c,in}} \tag{A3}$$

$$\varepsilon_f = \frac{T_{g,in} - T_{aw}}{T_{g,in} - T_{c,out}} \tag{A4}$$

where $T_{c,in}$ and $T_{c,out}$ are the coolant inlet and outlet temperatures, T_{aw} is the mean adiabatic wall temperature and $T_{m,internal}$ is the internal metal temperature. The blade cooling effectiveness ε_0 is:

$$\varepsilon_0 = \frac{T_{g,in} - T_{m,external}}{T_{g,in} - T_{c,in}} \tag{A5}$$

After determining ε_0, the dimensionless coolant requirement (m_{c+}) can be calculated with (see the appendix of Wilcock et al. [92] and Young and Wilcock [93] for more details):

$$(1 + Bi_{TBC})m_{c+} = \frac{\varepsilon_0}{\eta_{c,external}(1-\varepsilon_0)} - \varepsilon_f\left[\frac{1}{\eta_{c,external}(1-\varepsilon_0)} - 1\right] \tag{A6}$$

$$\eta_{c,external} = \frac{T_{c,out} - T_{c,in}}{T_{m,external} - T_{c,in}} = \frac{\eta_c}{1 + m_{c+}\eta_c Bi_m} \tag{A7}$$

Some empirical values are introduced for metal Biot number ($Bi_m = 0.15$ [92]) and thermal barrier coating (TBC) Biot number ($Bi_{TBC} = 0.3$ [92]) according to:

$$Bi_m = \frac{T_{m,external} - T_{m,internal}}{T_{aw} - T_w} \tag{A8}$$

$$Bi_{TBC} = \frac{T_w - T_{m,external}}{T_{aw} - T_w} \tag{A9}$$

Using m_{c+}, the coolant requirement of each stage, m_c, is determined by [93]:

$$m_c = K_{cool} m_g m_{c+} \tag{A10}$$

where K_{cool} is the cooling flow factor (=0.045 [49]). Then, the coolant exit temperature, $T_{c,out}$, can be calculated by using Eq. (A7).

The algorithm used in this work is illustrated in Fig. A1. In this algorithm, after defining the fixed geometric variants like the number of gas turbine stages, gas turbine outlet pressure and polytropic efficiency, the outlet pressure of each stage is calculated assuming a fixed inlet/outlet pressure ratio for each stage. Then, for each stage, the gas outlet temperature and power generated are expressed as shown in Eqs. (A1) and (A2). The required coolant rate is related to the hot gas temperature, pressure and flowrate and can be defined using Eqs. A6–10. The effect of mixing in each stage of the gas turbine (Siemens V94.3A) is calculated based on the work of Zhang et al. [49] which determines the efficiency loss because of hot gas mixing with exit coolant. The actual polytropic efficiency of each stage is given as a function of the theoretical polytropic efficiency (η_{pt}), inlet and outlet pressures (P_{in}, P_{out}), stage inlet pressure ($P_{in,s}$) and turbine inlet temperature using the following experimental equation based on published data for Siemens V94.3A [49]:

$$\eta = \eta_{pt} - \ln\left(\frac{P_{in}}{P_{out}}\right)\cdot\frac{P_{in,s}}{P_{in} - P_{out}}\cdot\frac{m_c}{m_g}\cdot(-0.000425T_{g,in} + 0.695) \tag{A11}$$

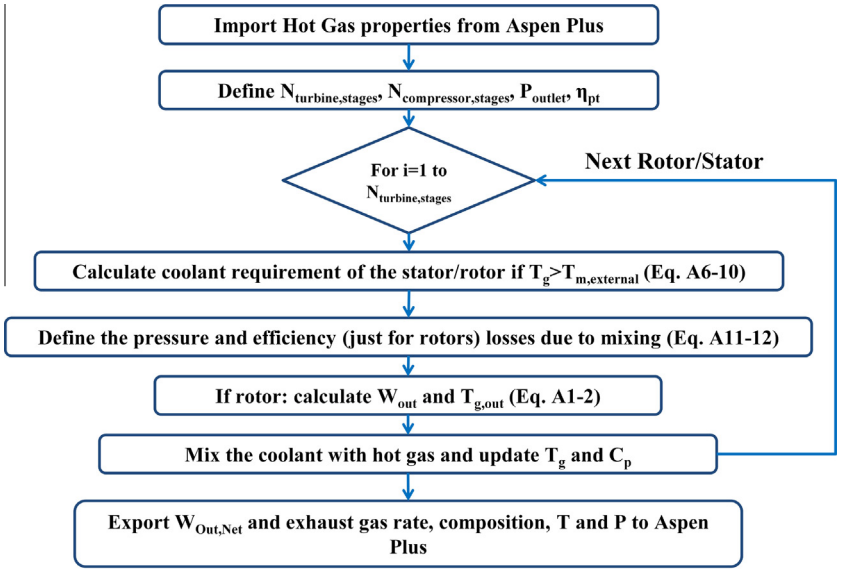

Fig. A1. Algorithm of coolant requirement calculation.

The pressure loss because of mixing is shown by Bolland and Stadaas [57]:

$$\frac{dP_{loss}}{P_{in}} = \frac{m_c}{m_g}.\gamma.M^2.Y \quad (A12)$$

where Y is cooling air mixing loss factor (=0.3 [57]), γ is the heat capacity ratio and M is Mach number (=0.85 [57]). Therefore, after calculation of coolant requirement, the effect of mixing is determined to define the actual hot gas temperature, pressure (Eq. (A12)), flowrate (hot gas + coolant) and polytropic efficiency (Eq. (A11)). Using these values, the calculations of work outlet and coolant requirement will be repeated for the next stage of the gas turbine. Finally, the resulting net power generated of the gas turbine and the exhaust gas conditions are sent to the Aspen Plus model.

Appendix B. Supplementary material

Supplementary data associated with this article can be found, in the online version, at http://dx.doi.org/10.1016/j.enconman.2014.12.081.

References

[1] Seifzadeh Haghighi S, Rahimpour MR, Raeissi S, Dehghani O. Investigation of ethylene production in naphtha thermal cracking plant in presence of steam and carbon dioxide. Chem Eng J 2013;228:1158–67.
[2] True WR. Global ethylene capacity poised for major expansion. Oil Gas J 2013.
[3] Carr C. IHS: global ethylene outlook: one product. Many Strategies 2013.
[4] Ren T, Patel MK, Blok K. Steam cracking and methane to olefins: energy use, CO_2 emissions and production costs. Energy 2008;33:817–33.
[5] Xiang D, Yang S, Li X, Qian Y. Life cycle assessment of energy consumption and GHG emissions of olefins production from alternative resources in China. Energy Convers Manage 2015;90:12–20.
[6] United States Environmental Protection Agency. Greenhouse gas equivalencies calculator, <http://www.epa.gov/cleanenergy/energy-resources/calculator.html>.
[7] Asche F, Oglend A, Osmundsen P. Gas versus oil prices the impact of shale gas. Energy Policy 2012;47:117–24.
[8] Yang C-J, Jackson RB. China's growing methanol economy and its implications for energy and the environment. Energy Policy 2012;41:878–84.
[9] Adams II TA. Challenges and opportunities in the design of new energy conversion systems. In: Mario JDS, Eden R, Gavin PT, editors. Computer aided chemical engineering. Elsevier; 2014. p. 5–14.
[10] Bell DA, Towler BF, Fan M. Coal gasification and its applications. Elsevier Inc.; 2011.
[11] Chen JQ, Bozzano A, Glover B, Fuglerud T, Kvisle S. Recent advancements in ethylene and propylene production using the UOP/hydro MTO process. Catal Today 2005;106:103–7.
[12] Keil FJ. Methanol-to-hydrocarbons: process technology. Microporous Mesoporous Mater 1999;29:49–66.
[13] Xiang D, Yang S, Liu X, Mai Z, Qian Y. Techno-economic performance of the coal-to-olefins process with CCS. Chem Eng J 2014;240:45–54.
[14] Holmgren KM, Berntsson T, Andersson E, Rydberg T. System aspects of biomass gasification with methanol synthesis – process concepts and energy analysis. Energy 2012;45:817–28.
[15] Wang W, Jiang Y, Hunger M. Mechanistic investigations of the methanol-to-olefin (MTO) process on acidic zeolite catalysts by in situ solid-state NMR spectroscopy. Catal Today 2006;113:102–14.
[16] Wilson S, Barger P. The characteristics of SAPO-34 which influence the conversion of methanol to light olefins. Microporous Mesoporous Mater 1999;29:117–26.
[17] Wu X, Abraha MG, Anthony RG. Methanol conversion on SAPO-34: reaction condition for fixed-bed reactor. Appl Catal A: Gen 2004;260:63–9.
[18] Taheri Najafabadi A, Fatemi S, Sohrabi M, Salmasi M. Kinetic modeling and optimization of the operating condition of MTO process on SAPO-34 catalyst. J Ind Eng Chem 2012;18:29–37.
[19] Bos ANR, Tromp PJJ, Akse HN. Conversion of methanol to lower olefins. Kinetic modeling, reactor simulation, and selection. Ind Eng Chem Res 1995;34:3808–16.
[20] Sedighi M, Keyvanloo K. Kinetic study of the methanol to olefin process on a SAPO-34 catalyst. Front Chem Sci Eng 2014;8:306–11.
[21] Branco JB, Ferreira AC, do Rego AMB, Ferraria AM, Lopes G, Gasche TA. Oxidative coupling of methane over KCl–$LnCl_3$ eutectic molten salt catalysts. J Mol Liq 2014;191:100–6.
[22] Kaarsholm M, Joensen F, Nerlov J, Cenni R, Chaouki J, Patience GS. Phosphorous modified ZSM-5: deactivation and product distribution for MTO. Chem Eng Sci 2007;62:5527–32.
[23] Wu W, Guo W, Xiao W, Luo M. Methanol conversion to olefins (MTO) over H-ZSM-5: evidence of product distribution governed by methanol conversion. Fuel Process Technol 2013;108:19–24.
[24] Keller GE, Bhasin MM. Synthesis of ethylene via oxidative coupling of methane: I. determination of active catalysts. J Catal 1982;73:9–19.
[25] Mimoun H, Robine A, Bonnaudet S, Cameron CJ. Oxypyrolysis of natural gas. Appl Catal 1990;58:269–80.
[26] Brophy JH, Manning RP. Conversion process. United States Patent, 4 1988; p. 726–913.
[27] Sinev MY, Fattakhova ZT, Lomonosov VI, Gordienko YA. Kinetics of oxidative coupling of methane: bridging the gap between comprehension and description. J Nat Gas Chem 2009;18:273–87.
[28] Mleczko L, Baerns M. Catalytic oxidative coupling of methane—reaction engineering aspects and process schemes. Fuel Process Technol 1995;42:217–48.
[29] Zaman J. Oxidative processes in natural gas conversion. Fuel Process Technol 1999;58:61–81.
[30] Huff GA, Vasalos IA. Oxidative pyrolysis of natural gas in a spouted-bed reactor: reaction stoichiometry and experimental reactor design. Catal Today 1998;46:223–31.
[31] Becker S, Baerns M. Oxidative coupling of methane over La_2O_3–CaO catalysts effect of bulk and surface properties on catalytic performance. J Catal 1991;128:512–9.
[32] Stansch Z, Mleczko L, Baerns M. Comprehensive kinetics of oxidative coupling of methane over the La_2O_3/CaO catalyst. Ind Eng Chem Res 1997;36:2568–79.
[33] Cordi EM, Pak S, Rosynek MP, Lunsford JH. Steady-state production of olefins in high yields during the oxidative coupling of methane: utilization of a membrane contactor. Appl Catal A: Gen 1997;155:L1–7.
[34] Holst N, Jašo S, Godini HR, Glöser S, Arellano-Garcia H, Wozny G, et al. Two-dimensional model for oxidative coupling of methane in a packed-bed membrane reactor. Chem Eng Technol 2012;35:294–301.
[35] Godini HR, Xiao S, Jašo S, Stünkel S, Salerno D, Son NX, et al. Techno-economic analysis of integrating the methane oxidative coupling and methane reforming processes. Fuel Process Technol 2012;106:684–94.
[36] Edwards JH, Do KT, Tyler RJ. The OXCO process. A new concept for the production of olefins from natural gas. Fuel 1992;71:325–34.
[37] Xu L, Xie S, Liu S, Lin L, Tian Z, Zhu A. Combination of CH_4 oxidative coupling reaction with C_2H_6 oxidative dehydrogenation by CO_2 to C_2H_4. Fuel 2002;81:1593–7.
[38] David J. Economic evaluation of leading technology options for sequestration of carbon dioxide. Master of Science Thesis, 2000.
[39] Adams II TA, Barton PI. High-efficiency power production from coal with carbon capture. AIChE J 2010;56:3120–36.
[40] Hong J, Chaudhry G, Brisson JG, Field R, Gazzino M, Ghoniem AF. Analysis of oxy-fuel combustion power cycle utilizing a pressurized coal combustor. Energy 2009;34:1332–40.
[41] Adams TA, Nease J, Tucker D, Barton PI. Energy conversion with solid oxide fuel cell systems: a review of concepts and outlooks for the short- and long-term. Ind Eng Chem Res 2012;52:3089–111.
[42] Fan LS. Chemical looping systems for fossil energy conversions. John Wiley & Sons, Inc.; 2010.
[43] Adanez J, Abad A, Garcia-Labiano F, Gayan P, de Diego LF. Progress in chemical-looping combustion and reforming technologies. Prog Energy Combust Sci 2012;38:215–82.
[44] Bullin K, Krouskop P. Composition variety complicates processing plans for US shale gas. Bryan Research and Engineering Inc report, 2009.
[45] Haslbeck JL, Kuehn NJ, Lewis EG, Pinkerton LL, Simpson J, Turner MJ, et al. Cost and performance baseline for fossil energy plants volume 1: bituminous coal and natural gas to electricity. DOE, National Energy Technology Laboratory (NETL); 2010.
[46] C.F. Inc., Liquid methane fuel characterization and safety assessment report. Report No CFI-1600, 1991.
[47] Chen CC, Mathias PM. Applied thermodynamics for process modeling. AIChE J 2002;48:194–200.
[48] GPSA. Engineering data book. Gas Processors Suppliers Association; 1998.
[49] Zhang J, Ma L, Li Z, Ni W. Modeling an air-cooled gas turbine of the integrated gasification combined cycle in aspen plus. In: International conference on future electrical power and energy systems (ICFEPES), Elsevier Ltd., Sanya, China, 2012.
[50] Adams II TA, Barton PI. Combining coal gasification and natural gas reforming for efficient polygeneration. Fuel Process Technol 2011;92:639–55.
[51] Nghiem XS. Ethylene production by oxidative coupling of methane: new process flow diagram based on adsorptive separation. PhD thesis, Technische Universität Berlin, 2014.
[52] Mafi M, Amidpour M, Naeynian SMM. Development in mixed refrigerant cycles used in olefin plants. In: Proceedings of the 1st annual gas processing symposium, Elsevier, Amsterdam, 2009. p. 154–61.
[53] Kohl AL, Nielsen RB. Gas purification. Houston: Gulf Professional Publishing; 1997.
[54] Seagraves J, Weiland RH. Treating high CO_2 gases with MDEA. Gas 2009:103–8.
[55] Weiland R, Sivasubramanian M, Dingman J. Effective amine technology: controlling selectivity, increasing slip, and reducing sulfur. In: Proceedings of the Laurance reid gas conditioning conference, 2003. p. 79–98.
[56] Tusiani MD, Shearer G. LNG: a nontechnical guide. PennWell Books; 2007.

[57] Bolland O, Stadaas JF. Comparative evaluation of combined cycles and gas turbine systems with water injection, steam injection, and recuperation. ASME J Eng Gas Turb Power 1995;117:138–45.
[58] Canière H, Willockx A, Dick E, De Paepe M. Raising cycle efficiency by intercooling in air-cooled gas turbines. Appl Therm Eng 2006;26:1780–7.
[59] Cerri G, Giovannelli A, Battisti L, Fedrizzi R. Advances in effusive cooling techniques of gas turbines. Appl Therm Eng 2007;27:692–8.
[60] Chiesa P, Macchi E. A thermodynamic analysis of different options to break 60% electric efficiency in combined cycle power plants. J Eng Gas Turb Power 2004;126:770–85.
[61] Sanjay OS, Prasad BN. Influence of different means of turbine blade cooling on the thermodynamic performance of combined cycle. Appl Therm Eng 2008;28:2315–26.
[62] Sanjay OS, Prasad BN. Comparative performance analysis of cogeneration gas turbine cycle for different blade cooling means. Int J Therm Sci 2009;48:1432–40.
[63] Sanjay, Singh O. Thermodynamic evaluation of different gas turbine blade cooling techniques. Thermal Issues in Emerging Technologies, Cairo, Egypt, 2008. p. 237–44.
[64] Dyson TE, Bogard DG, Piggush JD, Kohli A. Overall effectiveness for a film cooled turbine blade leading edge with varying hole pitch. J Turbomach 2013;135:1–8.
[65] Garg VK. Heat transfer research on gas turbine airfoils at NASA GRC. Int J Heat Fluid Flow 2002;23:109–36.
[66] Linderholm C, Jerndal E, Mattisson T, Lyngfelt A. Investigation of NiO-based mixed oxides in a 300-W chemical-looping combustor. Chem Eng Res Des 2010;88:661–72.
[67] Hossain MM, de Lasa HI. Chemical-looping combustion (CLC) for inherent separations—a review. Chem Eng Sci 2008;63:4433–51.
[68] Chiu P-C, Ku Y. Chemical looping process – a novel technology for inherent CO_2 capture. Aerosol Air Qual Res 2012;12:1421–32.
[69] Lyngfelt A. Oxygen carriers for chemical looping combustion – 4000 h of operational experience. Oil Gas Sci Technol – Rev IFP Energies Nouvelles 2011;66:161–72.
[70] Peters MS, Timmerhaus KD. Plant design and economics for chemical engineers. 4th ed. 1991.
[71] Ethane prices trail other natural gas liquids. Energy Information Administration (eia), <http://www.eia.gov/todayinenergy/detail.cfm?id=1170>; 2011.
[72] Worhach P, Haslbeck J. Recommended project finance structures for the economic analysis of fossil-based energy projects. DOE/NETL-401/090808, 2008.
[73] Bibber LV, Shuster E, Haslbeck J, Rutkowski M, Olson S, Kramer S. Baseline technical and economic assessment of a commercial scale fischer-tropsch liquids facility. DOE/NETL-2007/1260, 2007.
[74] US Energy Information Administration. Natural gas weekly update, Henry Hub spot price, <http://www.eia.gov/naturalgas/weekly/>; (26.06.13).
[75] EIA. U.S. wholesale electricity price, Mass Hub, New England, <http://www.eia.gov/electricity/wholesale/>; (24.06.13).
[76] Nickel Monoxide. CAS No.: 1313-99-1, <http://www.alibaba.com/product-gs/1036820506/The_good_and_guanranteed_nickel_oxide.html>.
[77] DEWITT & COMPANY Incorporated. Petrochemical portal, ethylene annual price, <http://www.dewittworld.com/portal/Default.aspx?ProductID=101>; (January 2013).
[78] Luckow P, Stanton EA, Biewald B, Fisher J, Ackerman F, Hausman E. 2013 Carbon dioxide price forecast. Synapse Energy Economics, Inc.; 2013.
[79] Chemical Engineering Plant Cost Index. Chemical Engineering 2012; 119: p. 64.
[80] Linderholm C, Abad A, Mattisson T, Lyngfelt A. 160 h of chemical-looping combustion in a 10 kW reactor system with a NiO-based oxygen carrier. Int J Greenhouse Gas Control 2008;2:520–30.
[81] Kolbitsch P, Bolhàr-Nordenkampf J, Pröll T, Hofbauer H. Operating experience with chemical looping combustion in a 120 kW dual circulating fluidized bed (DCFB) unit. Int J Greenhouse Gas Control 2010;4:180–5.
[82] Kolbitsch P, Pröll T, Bolhar-Nordenkampf J, Hofbauer H. Design of a chemical looping combustor using a dual circulating fluidized bed (DCFB) reactor system. Chem Eng Technol 2009;32:398–403.
[83] Wolf J, Anheden M, Yan J. Comparison of nickel- and iron-based oxygen carriers in chemical looping combustion for CO_2 capture in power generation. Fuel 2005;84:993–1006.
[84] Linderholm C, Mattisson T, Lyngfelt A. Long-term integrity testing of spray-dried particles in a 10-kW chemical-looping combustor using natural gas as fuel. Fuel 2009;88:2083–96.
[85] Wetter M, Wright J. A comparison of deterministic and probabilistic optimization algorithms for nonsmooth simulation-based optimization. Build Environ 2004;39:989–99.
[86] Goldberg DE. Genetic algorithms in search, optimization, and machine learning. Addison-Wesley; 1989.
[87] Parsopoulos KE, Vrahatis MN. Particle swarm optimization and intelligence: advances and applications. IGI Global 2010.
[88] Roberts T. Ethylene – good today, better tomorrow – a year later. Goldman Sachs Chemical Intensity Day, 2012.
[89] Khojasteh Salkuyeh Y, Adams II TA. Combining coal, natural gas, and nuclear heat for liquid fuels production with reduced CO_2 emissions. In: Ian David Lockhart B, Michael F, editors. Computer aided chemical engineering. Elsevier; 2012. p. 247–51.
[90] Najjar YSH, Alghamdi AS, Al-Beirutty MH. Comparative performance of combined gas turbine systems under three different blade cooling schemes. Appl Therm Eng 2004;24:1919–34.
[91] Kumar S, Singh O. Thermodynamic performance evaluation of gas turbine cycle with transpiration cooling of blades using air vis-à-vis steam. Proc Inst Mech Eng, Part A: J Power Energy 2010;224:1039–47.
[92] Wilcock RC, Young JB, Horlock JH. The effect of turbine blade cooling on the cycle efficiency of gas turbine power cycles. J Eng Gas Turb Power 2005;127:109–20.
[93] Young JB, Wilcock RC. Modeling the air-cooled gas turbine: Part 2—coolant flows and losses. J Turbomach 2002;124:214–21.
[94] Horlock JH, Watson DT, Jones TV. Limitations on gas turbine performance imposed by large turbine cooling flows. J Eng Gas Turb Power 2001;123:487–94.
[95] Horlock JH. Advanced gas turbine cycles. Elsevier Science Ltd.; 2003.

Chapter 4- Supplementary Material 1

P-xy Ethane & Ethylene Mixture

Experimental	Temperature		-17.77 C	
VLE 013	Liquid Mol	Temperatu	Vapor Mol	Total pressure(bar)
1	0	255.38	0	26.648
2	0.0315	255.38	0.023	26.269
3	0.111	255.38	0.083	25.407
4	0.351	255.38	0.271	22.753
5	0.364	255.38	0.291	22.546
6	0.573	255.38	0.475	20.167
7	0.662	255.38	0.564	19.236
8	0.829	255.38	0.757	17.168
9	0.907	255.38	0.859	16.203
10	0.9665	255.38	0.95	15.548
11	1	255.38	1	15.134

Experimental	Temperature		-111.75 C	
VLE 038	Liquid Mol	Temperatu	Vapor Mol	Total pressure(bar)
1	0	161.4	0	0.6168
2	0.2056	161.4	0.1071	0.5544
3	0.3022	161.4	0.1597	0.5242
4	0.446	161.4	0.246	0.4768
5	0.4673	161.4	0.26	0.4695
6	0.4888	161.4	0.2745	0.4622
7	0.6021	161.4	0.3597	0.4212
8	0.7145	161.4	0.465	0.3769
9	0.7745	161.4	0.5333	0.3522
10	1	161.4	1	0.2367

Reference:
Hanson, G. H.; Hogan, R. J.; Ruehlen, F. N.; Cines, M. R. Chem. Eng. Prog. Symp. Ser., 1953, 49(6), 37 Ethane - ethylene system vapor-liquid equilibria at 0!31, -40!31, and -100! 31f

Reference:
Calado, J. C. G.; Gomes de Azevedo, E. J. S.; Clancy, P.; Gubbins, K. E. J. Chem. Soc., Faraday Trans. 1, 1983, 79, 2657-67 Thermodynamic study of liquid mixtures of ethane and ethene

PR-BM (Aspen Plus)			
	TOTAL PRES	VAPOR MOLEFRAC C2H6	LIQUID MOLEFRAC C2H6
	bar		
	26.88689	0	0
	25.94155	0.052	0.071429
	25.02256	0.105577	0.142857
	24.12742	0.161022	0.214286
	23.24277	0.218599	0.285714
	22.37522	0.278633	0.357143
	21.52347	0.341462	0.428571
	20.68638	0.407454	0.5
	19.86296	0.477017	0.571429
	19.05232	0.550611	0.642857
	18.25369	0.62875	0.714286
	17.46638	0.712025	0.785714
	16.68977	0.801113	0.857143
	15.9233	0.896799	0.928571
	15.16601	1	1

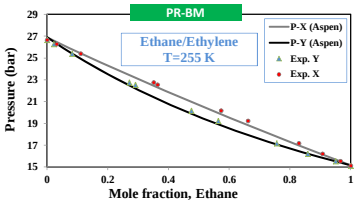

PR-BM (Aspen Plus)			
	TOTAL PRES	VAPOR MOLEFRAC C2H6	LIQUID MOLEFRAC C2H6
	bar		
	0.632386	0	0
	0.60419	0.029134	0.071429
	0.576091	0.061006	0.142857
	0.548041	0.096032	0.214286
	0.520034	0.13472	0.285714
	0.492069	0.177692	0.357143
	0.464142	0.225717	0.428571
	0.436251	0.279758	0.5
	0.408392	0.341043	0.571429
	0.380565	0.411153	0.642857
	0.352765	0.492165	0.714286
	0.324993	0.586864	0.785714
	0.297245	0.69907	0.857143
	0.269521	0.834168	0.928571
	0.241812	1	1

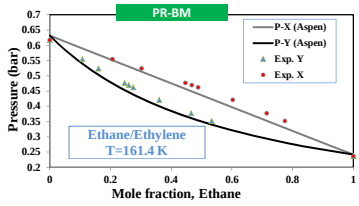

Ethylene Package (Aspen Plus)			
	TOTAL PRES	VAPOR MOLEFRAC C2H6	LIQUID MOLEFRAC C2H6
	bar		
	26.92745	0	0
	25.99319	0.05202	0.071429
	25.08359	0.105625	0.142857
	24.19662	0.161102	0.214286
	23.32	0.218714	0.285714
	22.45963	0.278785	0.357143
	21.61429	0.341649	0.428571
	20.78288	0.407671	0.5
	19.96446	0.477259	0.571429
	19.15819	0.550865	0.642857
	18.36332	0.629004	0.714286
	17.5792	0.71226	0.785714
	16.80524	0.801304	0.857143
	16.04091	0.896915	0.928571
	15.2853	1	1

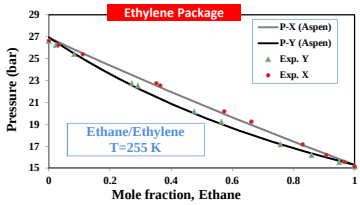

Ethylene Package (Aspen Plus)			
	TOTAL PRES	VAPOR MOLEFRAC C2H6	LIQUID MOLEFRAC C2H6
	bar		
	0.61915	0	0
	0.590814	0.027922	0.071429
	0.562582	0.058537	0.142857
	0.534396	0.092271	0.214286
	0.506254	0.129642	0.285714
	0.478151	0.171292	0.357143
	0.450083	0.218018	0.428571
	0.422047	0.27083	0.5
	0.394039	0.331025	0.571429
	0.366057	0.400291	0.642857
	0.338097	0.480875	0.714286
	0.310157	0.575832	0.785714
	0.282235	0.689419	0.857143
	0.254329	0.827763	0.928571
	0.22643	1	1

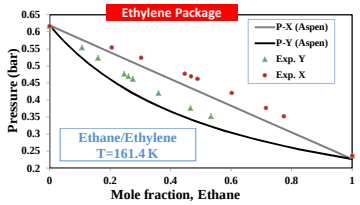

P-xy Methane & Ethane Mixture

Experimental		Temperature		-101.14 C
VLE 013	Liquid Mol	Temperatu	Vapor Mol	Total pressure(bar)
1	0	172.01	0	0.48946
2	0.0685	172.01	0.7681	2.1236
3	0.07	172.01	0.7768	2.2063
4	0.1087	172.01	0.8469	3.1371
5	0.205	172.01	0.9161	5.5847
6	0.2626	172.01	0.9322	6.8948
7	0.3164	172.01	0.9434	8.2737
8	0.5042	172.01	0.9656	12.411
9	0.5708	172.01	0.9704	13.79
10	0.7082	172.01	0.9788	17.065
11	0.8609	172.01	0.9878	20.615
12	0.8673	172.01	0.9887	20.684
13	0.9175	172.01	0.99209	22.339
14	0.9513	172.01	0.99531	23.408
15	1	172.01	1	24.925

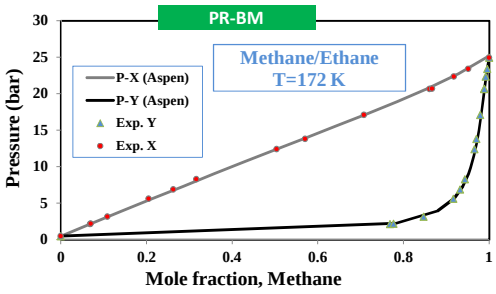

Reference:

Wichterle, I.; Kobayashi, R. Low Temperature VLE ..., 1970,, Monograph, Rice University, Houston,

PR-BM (Aspen Plus)		
TOTAL PRES	VAPOR MOLEFRAC CH4	LIQUID MOLEFRAC CH4
bar		
0.492539	0	0
2.223878	0.781693	0.071429
3.944536	0.87931	0.142857
5.652316	0.917714	0.214286
7.345433	0.9384	0.285714
9.022702	0.951464	0.357143
10.6827	0.960595	0.428571
12.32888	0.967447	0.5
13.96482	0.972909	0.571429
15.59946	0.977503	0.642857
17.25069	0.981583	0.714286
18.94327	0.985445	0.785714
20.73613	0.989388	0.857143
22.74272	0.993875	0.928571
25.22086	1	1

Ethylene Package (Aspen Plus)		
TOTAL PRES	VAPOR MOLEFRAC CH4	LIQUID MOLEFRAC CH4
bar		
0.469944	0	0
2.271505	0.795874	0.071429
4.052332	0.88769	0.142857
5.809877	0.923389	0.214286
7.542099	0.942524	0.285714
9.246507	0.954589	0.357143
10.92457	0.962999	0.428571
12.57749	0.969315	0.5
14.21019	0.974356	0.571429
15.83245	0.978608	0.642857
17.46212	0.982402	0.714286
19.13255	0.98601	0.785714
20.89543	0.989736	0.857143
22.87361	0.994031	0.928571
25.3312	1	1

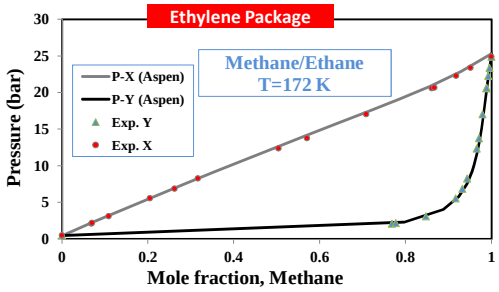

P-xy Methane & Ethylene Mixture

Experimental		Temperature		-123.14 C
VLE 007	Liquid Mol	Temperatu	Vapor Mol	Total pressure(bar)
1	0	150.01	0	0.276
2	0.0848	150.01	0.8338	1.547
3	0.1273	150.01	0.8783	2.039
4	0.209	150.01	0.9244	3.035
5	0.2896	150.01	0.9455	3.95
6	0.4043	150.01	0.9627	5.022
7	0.5118	150.01	0.972	5.991
8	0.6327	150.01	0.979	7.02
9	0.758	150.01	0.9859	8.03
10	0.8724	150.01	0.9927	9.03

Experimental		Temperature		-103.14 C
VLE 038	Liquid Mol	Temperatu	Vapor Mol	Total pressure(N/sqm)
1	0	170.01	0	1.057
2	0.0328	170.01	0.4815	2.028
3	0.1105	170.01	0.7463	4.038
4	0.1951	170.01	0.8372	6.034
5	0.2811	170.01	0.8842	8
6	0.3778	170.01	0.9128	10.01
7	0.4872	170.01	0.9339	12.17
8	0.5859	170.01	0.9489	14.07
9	0.6897	170.01	0.9612	16.01
10	0.7891	170.01	0.9728	18
11	0.7908	170.01	0.974	18.03
12	0.8797	170.01	0.984	19.96

Reference:

Miller, R. C.; Kidnay, A. J.; Hiza, M. J. J. Chem. Thermodyn., 1977, 9, 167-78 Liquid + Vapor equilibria in methane + ethene and in methane + ethane from 150.00 to 190.00 K

Reference:

Miller, R. C.; Kidnay, A. J.; Hiza, M. J. J. Chem. Thermodyn., 1977, 9, 167-78 Liquid + Vapor equilibria in methane + ethene and in methane + ethane from 150.00 to 190.00 K

PR-BM (Aspen Plus)

TOTAL PRES	VAPOR MOLEFRAC CH4	LIQUID MOLEFRAC CH4
bar		
0.285617	0	0
1.06432	0.742902	0.071429
1.826403	0.857222	0.142857
2.57209	0.903854	0.214286
3.301854	0.929387	0.285714
4.016629	0.94566	0.357143
4.717918	0.957075	0.428571
5.40797	0.96565	0.5
6.090024	0.972448	0.571429
6.76866	0.97809	0.642857
7.450329	0.982974	0.714286
8.14418	0.987384	0.785714
8.863434	0.991544	0.857143
9.629478	0.995666	0.928571
10.47284	1	1

PR-BM

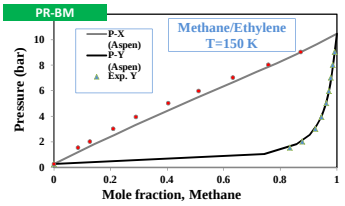

Ethylene Package (Aspen Plus)

TOTAL PRES	VAPOR MOLEFRAC CH4	LIQUID MOLEFRAC CH4
bar		
0.274953	0	0
1.071242	0.754095	0.071429
1.847278	0.864067	0.142857
2.603348	0.908506	0.214286
3.340128	0.932743	0.285714
4.05877	0.948162	0.357143
4.761045	0.958971	0.428571
5.449514	0.967093	0.5
6.126987	0.973544	0.571429
6.799911	0.978904	0.642857
7.474686	0.983559	0.714286
8.161859	0.987777	0.785714
8.8737	0.991779	0.857143
9.631827	0.995771	0.928571
10.46752	1	1

Ethylene Package

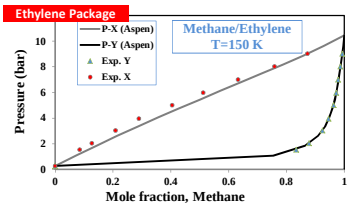

PR-BM (Aspen Plus)

TOTAL PRES	VAPOR MOLEFRAC CH4	LIQUID MOLEFRAC CH4
bar		
1.067969	0	0
2.611995	0.601842	0.071429
4.143485	0.756871	0.142857
5.66236	0.828427	0.214286
7.169322	0.869973	0.285714
8.665884	0.897405	0.357143
10.15475	0.917132	0.428571
11.6403	0.932249	0.5
13.12933	0.944455	0.571429
14.63215	0.954781	0.642857
16.16798	0.963918	0.714286
17.7589	0.972415	0.785714
19.44725	0.980776	0.857143
21.30952	0.989615	0.928571
23.48316	1	1

PR-BM

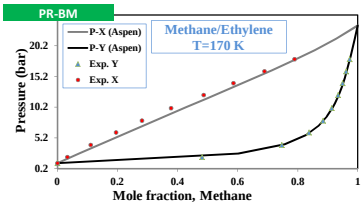

Ethylene Package (Aspen Plus)

TOTAL PRES	VAPOR MOLEFRAC CH4	LIQUID MOLEFRAC CH4
bar		
1.054761	0	0
2.645694	0.611658	0.071429
4.216889	0.763933	0.142857
5.768353	0.833528	0.214286
7.300898	0.873752	0.285714
8.816244	0.900248	0.357143
10.3174	0.919281	0.428571
11.80919	0.933867	0.5
13.29893	0.945654	0.571429
14.79764	0.955645	0.642857
16.32387	0.964513	0.714286
17.90331	0.972791	0.785714
19.57839	0.980977	0.857143
21.42652	0.989688	0.928571
23.58691	1	1

Ethylene Package

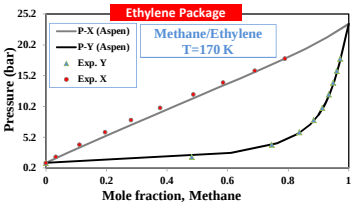

P-xy Hydrogen & Ethane Mixture

Experimental	Temperature		-83.59 C	
VLE 013	Liquid Mol	Temperatu	Vapor Mol	Total pressure(bar)
1	0.6205	189.56	0.0612	903.7
2	0.6666	189.56	0.0525	774.6
3	0.7046	189.56	0.0466	665.1
4	0.7136	189.56	0.045	639.1
5	0.716	189.56	0.045	636
6	0.7468	189.56	0.0405	559.1
7	0.7528	189.56	0.0389	537
8	0.7677	189.56	0.0398	501.6
9	0.7947	189.56	0.036	433.2
10	0.816	189.56	0.0318	379.4
11	0.8298	189.56	0.0303	349.1
	0.8469	189.56	0.0294	313.8
	0.8647	189.56	0.0282	278.5
	0.8838	189.56	0.0264	227.1
	0.9211	189.56	0.026	152
	0.932	189.56	0.0251	127.6
	0.9474	189.56	0.0298	98.6
	0.9675	189.56	0.0395	57.5

Reference:

Heintz, A.; Streett, W. B. J. Chem. Eng. Data, 1982, 27,
465-469 Phase equilibria in the H2/C2Hsystem at temperatures from 92.5 to 280.1 k and pressures to 560 mpa

PR-BM (Aspen Plus)		
TOTAL PRES	VAPOR MOLEFRAC C2H6	LIQUID MOLEFRAC C2H6
bar		
920.0797	0.075053	0.6
830.129	0.069337	0.625
746.6416	0.06408	0.65
668.221	0.059103	0.675
594.9998	0.054477	0.7
526.5382	0.050186	0.725
462.4555	0.046225	0.75
402.4607	0.042615	0.775
346.0843	0.039338	0.8
293.171	0.036461	0.825
243.4597	0.034058	0.85
196.7365	0.032273	0.875
152.7658	0.03137	0.9
111.4047	0.032013	0.925
72.47281	0.036094	0.95
35.82607	0.052861	0.975

Ethylene Package (Aspen Plus)		
TOTAL PRES	VAPOR MOLEFRAC C2H6	LIQUID MOLEFRAC C2H6
bar		
1305.99	0.034527	0.714286
727.2337	0.028475	0.785714
388.1943	0.023675	0.857143
163.0056	0.022741	0.928571
1.289736	1	1

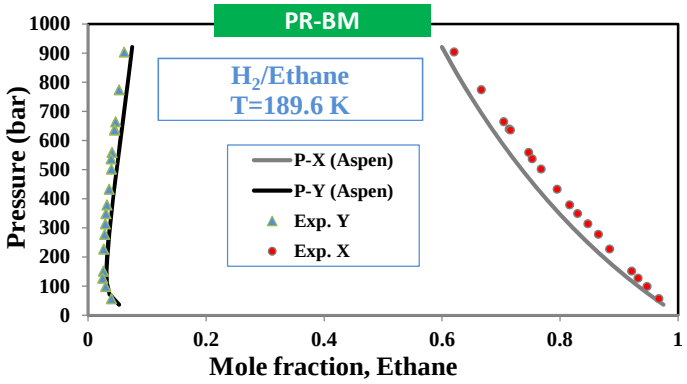

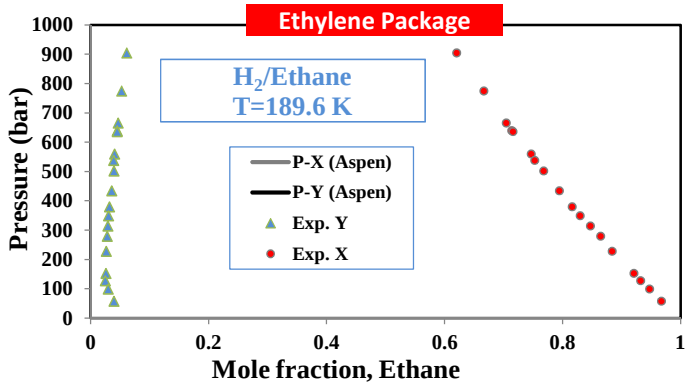

P-xy H_2 & Ethylene Mixture

Experimental		Temperature		-73.3 C
VLE 013	Liquid Mol	Temperatu	Vapor Mol	Total pressure(bar)
1	0.6922	199.85	0.1023	551.58
2	0.6922	199.85	0.1022	551.58
3	0.8378	199.85	0.0754	275.79
4	0.8385	199.85	0.0737	275.79
5	0.8387	199.85	0.074	275.79
6	0.841	199.85	0.0729	275.79
7	0.915	199.85	0.0859	137.9
8	0.9153	199.85	0.0824	137.9
9	0.9154	199.85	0.0852	137.9
10	0.9579	199.85	0.1144	68.948
11	0.958	199.85	0.117	68.948
12	0.9587	199.85	0.1158	68.948
13	0.959	199.85	0.1155	68.948
14	0.9799	199.85	0.1862	34.474
15	0.9802	199.85	0.1846	34.474
16	0.9804	199.85	0.186	34.474
17	0.9806	199.85	0.1849	34.474
18	0.9915	199.85	0.3182	17.237
19	0.9919	199.85	0.3186	17.237
20	0.9921	199.85	0.3174	17.237
21	0.9926	199.85	0.317	17.237

Reference:

Williams, R. B.; Katz, D. L. Ind. Eng. Chem., 1954, 46, 2512 Hydrogen with ethylene, ethane, propylene, and propane

PR-BM (Aspen Plus)			
	TOTAL PRES	VAPOR MOLEFRAC C2H4	LIQUID MOLEFRAC C2H4
	bar		
	547.375	0.142602	0.6
	506.2113	0.133913	0.625
	466.6818	0.12652	0.65
	427.6305	0.11954	0.675
	389.384	0.113235	0.7
	351.9916	0.107549	0.725
	315.5148	0.102498	0.75
	279.9977	0.09814	0.775
	245.4685	0.094586	0.8
	211.9368	0.092009	0.825
	179.4138	0.090737	0.85
	147.8819	0.091306	0.875
	117.3306	0.094818	0.9
	87.7418	0.103757	0.925
	59.09467	0.125167	0.95
	31.36529	0.189891	0.975
	4.531944	1	1

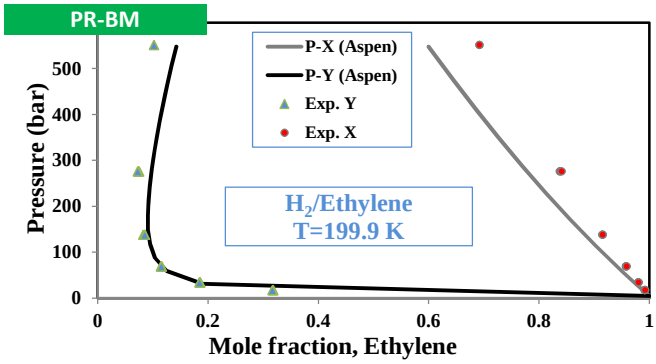

Ethylene Package (Aspen Plus)			
	TOTAL PRES	VAPOR MOLEFRAC C2H4	LIQUID MOLEFRAC C2H4
	bar		
	771.7381	0.097617	0.642857
	549.2022	0.084321	0.714286
	372.1033	0.074881	0.785714
	227.5096	0.071256	0.857143
	107.0068	0.084605	0.928571
	4.538519	1	1

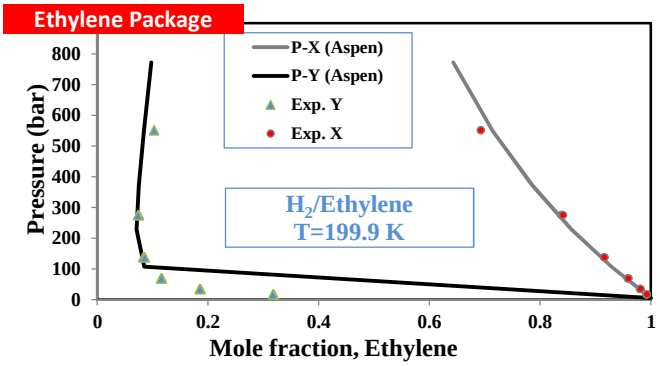

P-xy CO & Ethane Mixture

Experimental		Temperature		-99.99 C
VLE 001	Liquid Mol	Temperatu	Vapor Mole fra	Total pressure(bar)
1	0.172	173.16	0.117	93.079
2	0.431	173.16	0.0543	82.737
3	0.572	173.16	0.0273	68.948
4	0.814	173.16	0.0216	34.474
5	0.9304	173.16	0.0341	13.79

Reference:

Trust, D. B.; Kurata, F. AIChE J., 1971, 17, 415-9
Vapor-liquid and liquid-liquid vapor phase behavior of the carbon monoxide - propane and the carbon monoxide - ethane systems

PR-BM (Aspen Plus)

TOTAL PRES	VAPOR MOLEFRAC C2H6	LIQUID MOLEFRAC C2H6
bar		
86.94718	0.070135	0.475
83.05856	0.062888	0.5
79.08912	0.056701	0.525
75.04758	0.051477	0.55
70.95518	0.047073	0.575
66.8264	0.043396	0.6
62.67215	0.040359	0.625
58.50085	0.037888	0.65
54.31855	0.035928	0.675
50.1305	0.034429	0.7
45.94418	0.033383	0.725
41.75879	0.032776	0.75
37.57882	0.032636	0.775
33.40679	0.033025	0.8
29.24487	0.034062	0.825
25.09495	0.035967	0.85
20.95868	0.039151	0.875
16.83757	0.044442	0.9
12.73261	0.053745	0.925
8.645844	0.072597	0.95
4.577575	0.126068	0.975
0.528975	1	1

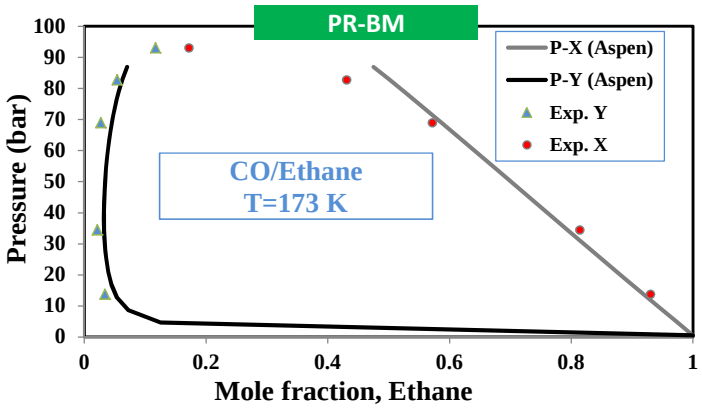

Ethylene Package (Aspen Plus)

TOTAL PRES	VAPOR MOLEFRAC C2H6	LIQUID MOLEFRAC C2H6
bar		
92.47156	0.072271	0.5
79.87242	0.051972	0.5714286
66.83472	0.039708	0.6428571
53.61343	0.033024	0.7142857
40.32309	0.030577	0.7857143
27.01501	0.032981	0.8571429
13.73288	0.048392	0.9285714
0.505608	1	1

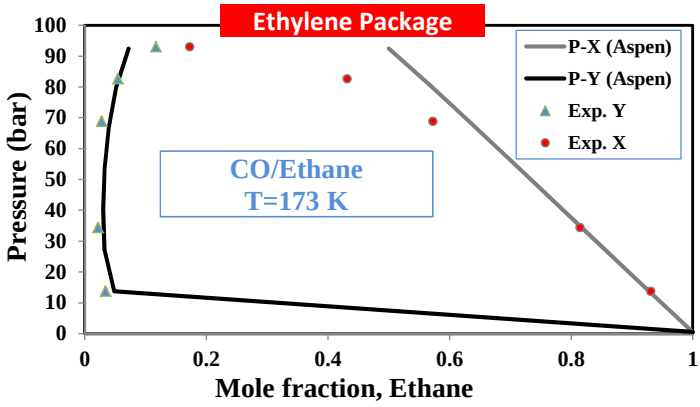

P-xy Ethane & Water Mixture

Experimental		Temperature		200.053 C
VLE 001	Liquid mole	Temperatu	Vapor mole	Total pressure(bar)
1	0.00095	473.203	0.55	29.42
2	0.0015	473.203	0.65	39.23
3	0.0021	473.203	0.72	49.03
4	0.00265	473.203	0.76	58.83
5	0.0037	473.203	0.81	78.45
6	0.00475	473.203	0.85	98.07
7	0.00575	473.203	0.87	117.68
	0.00655	473.203	0.88	137.29
	0.00732	473.203	0.99	156.91

Reference:

Tsiklis, D. S.; Kulikova, A. I.; Shenderei, L. I. Khim. Prom-st. (Moscow), 1960, , 401-6
Phase equilibria in the system ethanol + ethylene + water at high pressures and temperatures

PR-BM (Aspen Plus)		
TOTAL PRES	VAPOR MOLEFRAC C2H4	LIQUID MOLEFRAC C2H4
bar		
15.6068	0	0
20.07492	0.204288	0.000256
24.62567	0.336249	0.000513
29.26712	0.428371	0.000769
34.00247	0.496224	0.001026
38.83651	0.548192	0.001282
43.77436	0.589187	0.001538
48.8215	0.622281	0.001795
53.98379	0.649492	0.002051
59.26752	0.6722	0.002308
64.67941	0.69138	0.002564
70.2267	0.70774	0.002821
75.93333	0.721762	0.003077
81.7802	0.733929	0.003333
87.78862	0.744509	0.00359
93.96837	0.753746	0.003846
100.33	0.761832	0.004103
106.8848	0.768919	0.004359
113.6448	0.775135	0.004615
120.6232	0.780582	0.004872
127.8339	0.785344	0.005128
135.2918	0.789495	0.005385
143.013	0.793094	0.005641
151.0145	0.796193	0.005897
159.3147	0.798838	0.006154
167.933	0.801068	0.00641
176.8901	0.802918	0.006667
186.2079	0.80442	0.006923
195.9098	0.805603	0.007179
206.0202	0.806496	0.007436
216.5653	0.807123	0.007692
227.5725	0.80751	0.007949
239.1243	0.807617	0.008205
251.1575	0.80758	0.008462
263.7481	0.807369	0.008718
276.9315	0.807004	0.008974
290.745	0.806505	0.009231
305.2288	0.805893	0.009487
320.426	0.805184	0.009744
336.3827	0.804396	0.01

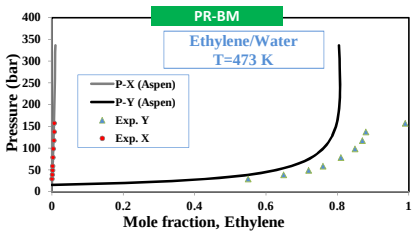

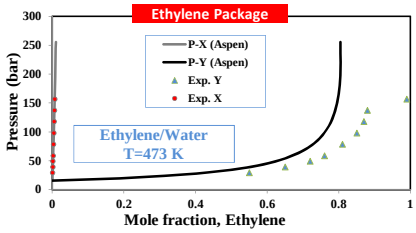

Ethylene Package (Aspen Plus)		
TOTAL PRES	VAPOR MOLEFRAC C2H4	LIQUID MOLEFRAC C2H4
bar		
15.60513	0	0
19.60831	0.187767	0.000256
23.66875	0.313275	0.000513
27.78935	0.402979	0.000769
31.97241	0.470203	0.001026
36.22057	0.522382	0.001282
40.5366	0.563997	0.001538
44.92348	0.597903	0.001795
49.38431	0.626011	0.002051
53.92241	0.649643	0.002308
58.54128	0.669747	0.002564
63.24463	0.687016	0.002821
68.0364	0.701972	0.003077
72.93429	0.714974	0.003333
77.91902	0.726403	0.00359
83.00611	0.736471	0.003846
88.20064	0.745371	0.004103
93.50803	0.753263	0.004359
98.93403	0.760273	0.004615
104.4847	0.766509	0.004872
110.1666	0.772058	0.005128
115.9866	0.776994	0.005385
121.952	0.781378	0.005641
128.0706	0.785264	0.005897
134.3506	0.788697	0.006154
140.8007	0.791716	0.00641
147.4303	0.794355	0.006667
154.2492	0.796642	0.006923
161.2676	0.798605	0.007179
168.4966	0.800267	0.007436
175.9476	0.801648	0.007692
183.6329	0.802769	0.007949
191.5652	0.803647	0.008205
199.758	0.8043	0.008462
208.2254	0.804742	0.008718
216.9822	0.804989	0.008974
226.0439	0.805056	0.009231
235.477	0.804895	0.009487
245.2074	0.804634	0.009744
255.2957	0.804233	0.01

P-xy Ethylene & CO Mixture

Experimental		Temperature		-39.42 C
VLE 001	Liquid mole	Temperatu	Vapor mole fra	Total pressure(bar)
1	0.582	233.73	0.4833	90.283
2	0.592	233.73	0.4749	90.132
3	0.613	233.73	0.464	89.424
4	0.6333	233.73	0.446	87.608
5	0.651	233.73	0.4318	85.775
6	0.666	233.73	0.425	83.726
7	0.689	233.73	0.414	80.469
8	0.698	233.73	0.4074	78.872
9	0.732	233.73	0.401	73.746
10	0.764	233.73	0.4005	68.651
11	0.8045	233.73	0.406	62.731
12	0.8065	233.73	0.4095	62.375
13	0.8524	233.73	0.433	52.417
14	0.896	233.73	0.463	42.278
15	0.9288	233.73	0.524	34.055
16	0.9589	233.73	0.6362	26.144
17	0.9764	233.73	0.7423	21.414
18	0.9862	233.73	0.8248	18.598
19	0.9864	233.73	0.828	18.649
20	0.9912	233.73	0.8804	17.291
21	0.9955	233.73	0.9336	16.159
22	0.999	233.73	0.9827	15.106
23	1	233.73	1	14.76

Reference:

Ahmar, E. E.; Valtz, A.; Ferrando, N.; Coquelet, C.; Mougin, P. J. Chem. Eng. Data, 2012, 57, 2744-2749 System Vapor-Liquid Equilibrium (PTxy) Measurements and Modeling for the CO-C2H4 Binary

PR-BM (Aspen Plus)		
TOTAL PRES	VAPOR MOLEFRAC C2H4	LIQUID MOLEFRAC C2H4
bar		
84.8003	0.408452	0.688
83.45136	0.407021	0.696
82.0364	0.405551	0.704
80.59077	0.404361	0.712
79.11381	0.40344	0.72
77.60684	0.402795	0.728
76.07102	0.402434	0.736
74.5075	0.402368	0.744
72.91737	0.402608	0.752
71.30167	0.403168	0.76
69.66142	0.404064	0.768
67.99758	0.405315	0.776
66.31108	0.40694	0.784
64.60281	0.408964	0.792
62.87361	0.411412	0.8
61.12431	0.414316	0.808
59.3557	0.417709	0.816
57.56852	0.421632	0.824
55.76351	0.426131	0.832
53.94836	0.431339	0.84
52.10856	0.43714	0.848
50.25308	0.443702	0.856
48.38252	0.451107	0.864
46.4975	0.459451	0.872
44.5986	0.46885	0.88
42.68639	0.479437	0.888
40.76143	0.491377	0.896
38.82424	0.504864	0.904
36.87534	0.520137	0.912
34.91524	0.537489	0.92
32.9444	0.557283	0.928
30.96332	0.579977	0.936
28.97242	0.606153	0.944
26.97217	0.636563	0.952
24.96299	0.672202	0.96
22.94528	0.714402	0.968
20.91946	0.765002	0.976
18.88345	0.82659	0.984
16.84505	0.903	0.992
14.79704	1	1

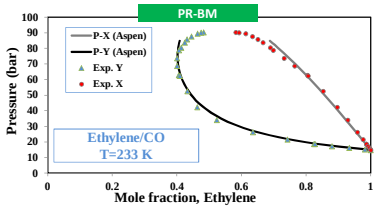

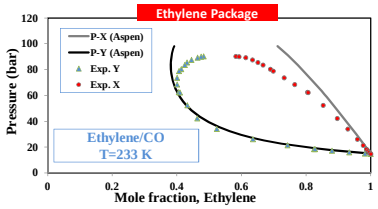

Ethylene Package (Aspen Plus)		
TOTAL PRES	VAPOR MOLEFRAC C2H4	LIQUID MOLEFRAC C2H4
bar		
98.15655	0.391315	0.712
96.40733	0.389225	0.72
94.62532	0.387251	0.728
92.79915	0.385545	0.736
90.93143	0.384122	0.744
89.02322	0.382992	0.752
87.07564	0.382166	0.76
85.08981	0.381657	0.768
83.06678	0.381484	0.776
81.00762	0.381664	0.784
78.91333	0.382221	0.792
76.78493	0.38318	0.8
74.62335	0.38457	0.808
72.42955	0.386425	0.816
70.20441	0.388784	0.824
67.94881	0.391691	0.832
65.6636	0.3952	0.84
63.34959	0.399371	0.848
61.00759	0.404274	0.856
58.6441	0.410067	0.864
56.24698	0.41669	0.872
53.82423	0.424352	0.88
51.37653	0.433195	0.888
48.90457	0.443396	0.896
46.40901	0.455168	0.904
43.89049	0.468777	0.912
41.34965	0.484557	0.92
38.78709	0.502932	0.928
36.20341	0.52445	0.936
33.5992	0.549829	0.944
30.975	0.580033	0.952
28.33138	0.61638	0.96
25.66888	0.660729	0.968
22.98802	0.715779	0.976
20.28931	0.785615	0.984
17.57327	0.876712	0.992
14.84012	1	1

CO_2 Absorbtion Reactions

Reaction (1): $2H_2O + DGACOO^- \leftrightarrow DGA + HCO3^-$

Reaction (2): $H_2O + DGA^+ \leftrightarrow DGA + H_3O^+$

Reaction (3): $H_2O + HCO3^- \leftrightarrow CO3^{--} + H_3O^+$

Reaction (4): $2H_2O + CO_2 \leftrightarrow HCO3^- + H_3O^+$

Reaction (5): $2H_2O \leftrightarrow OH^- + H_3O^+$

Ref. 1

M. Al-Juaied, G.T. Rochelle. Journal of Chemical & Engineering Data. 51 (2006) 708-17.

Thermodynamics and Equilibrium Solubility of Carbon Dioxide in Diglycolamine/Morpholine/Water.

Temperature Dependence of Equilibrium Constants (K_i)

$\ln(K_i)=A+B/T+C\ln(T)+DT$

	Reaction (1)		**Reaction (2)**		**Reaction (3)**		**Reaction (4)**		**Reaction (5)**	
	Aspen Plus	Ref. 1	Aspen Plus	Ref. 1	Aspen Plus	Ref. 1	Aspen Plus	Ref. 1	Aspen Plus	Ref. 1
A	3.6611	-	-13.3373	1.7	216.05	216	231.465	231.4	132.899	132.9
B	-3696.17	-	-4218.71	-8432	-12431.7	-12432	-12092.1	-12092	-13445.9	-13446
C	0	-	0	0	-35.4819	-35.48	-36.7816	-36.78	-22.4773	-22.48
D	0	-	0	-0.00504	0	0	0	0	0	0
Sample Temperature (K)	-	-	313	313	313	313	313	313	313	313
Value at 313 K	-	-	**2.3E-12**	**2.3E-12**	**1.1E-12**	**1.0E-12**	**9.0E-09**	**8.5E-09**	**9.3E-18**	**9.1E-18**

CO_2 Henry Constant (H_{CO2})

$\ln(H_{CO2})=A+B/T+C\ln(T)+DT$

	Aspen Plus	Ref. 1
A	170.71	170.7
B	-8477.71	-8477
C	-21.96	-22
D	0.00578	0.003383
Sample Temperature (K)	313	313
Value at 313 K	**2.3E+08**	**8.5E+07**

Chapter 4- Supplementary Material 2

OCM Reactor Model Results

Experimental (H.R. Godini, S. Xiao, S. Jašo, S. Stünkel, D. Salerno, N.X. Son, et al. Techno-e

CH4/O2	X(CH4)	X(O2)	S(C2+)	S(CO2)	CO2+C2+	S(CO)	Ethylene/Ethane
2	39	97	38	51	89	11	4
2.5	33	98	47	46	93	7	3.5
3.3	28	97	55	35	90	10	3.2
5	25	96	57	22	79	21	2.8
6	23	92	56	20	76	24	2.4
8	18	90	65	19	84	16	1

Reactor Model (Table 3 & 4)

CH4/O2	X(CH4)	X(O2)	S(C2+)	S(CO2)	CO2+C2+	S(CO)	Ethylene/Ethane
2	39.004	97.15902	37.9928	51.2524	89.2452	10.7548	3.9982
2.5	32.98406	97.61882	47.02534	45.38669	92.41203	7.587969	3.495359
3.3	28.01125	97.26904	54.98942	35.52856	90.51798	9.48202	3.184116
5	24.9925	95.97774	57.0455	21.7045	78.75	21.25	2.692
6	23.0032	91.97473	56.0616	20.1852	76.2468	23.7532	2.1446
8	17.9956	90.01905	65.1992	19.0828	84.282	15.718	0.9898

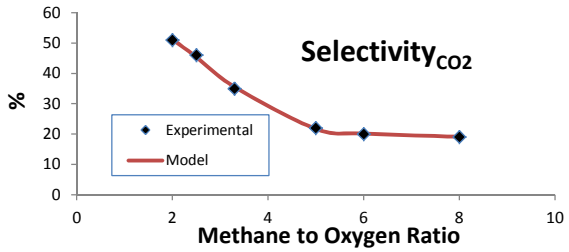

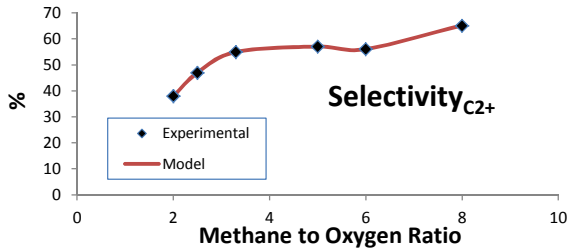

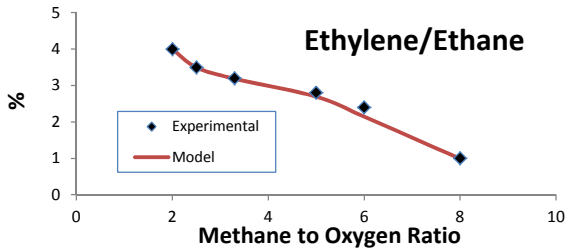

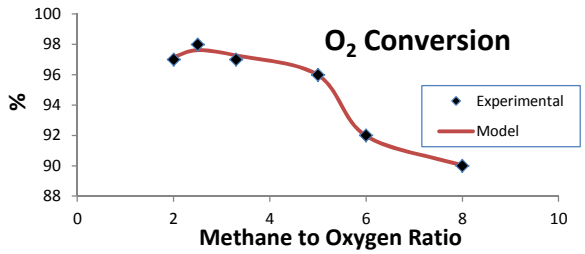

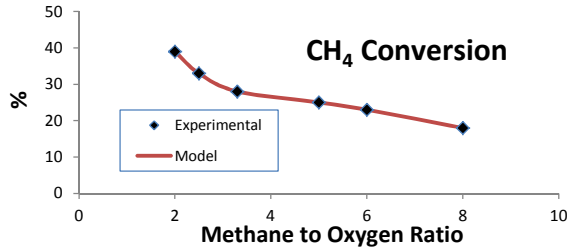

Chapter 4- Supplementary Material 2

Shale Gas Type: Fayetteville

Design Basis: Maximum NPV

Power Generation Option: CLC

Stream No.	**1**	**2**	**3**	**4**	**5**	**6**	**7**	**8**	**9**	**10**	**11**	**12**	**13**	**14**	**15**	**16**	**17**
Temperature (°C)	30.0		15.0	27.3	40.0	30.0	-80.0	-120.0	16.2	-18.0	-38.9	-13.7	40.0	30.0	30.0	30.0	44.0
Pressure (bar)	30.0		6.0	6.0	26.2	25.3	24.3	20.0	19.0	22.0	15.0	17.0	1.5	45.0	44.1	80.0	153.0
Mass Vapor Fraction	1.0		1.0	1.0	1.0	1.0	1.0	1.0	1.0	0.0	0.0	0.0	1.0	1.0	1.0	0.0	0.0
Total Flow (kmole/hr)	5000		1323	6323	4891	4396	4394	3963	3963	431	269	162	482	34803	3724	4206	4206
Total Flow (kg/hr)	83363		42345	125708	97364	75962	75893	63471	63471	12422	7543	4880	21194	1004073	163639	184833	184833
Mole Percent																	
O_2	0.00%		99.36%	20.79%	0.71%	0.79%	0.79%	0.87%	0.87%	0.00%	0.00%	0.00%	0.00%	21.00%	0.00%	0.00%	0.00%
CH_4	97.00%		0.00%	76.71%	72.50%	80.66%	80.70%	89.48%	89.48%	0.00%	0.00%	0.00%	0.05%	0.00%	0.00%	0.01%	0.01%
CO	0.00%		0.00%	0.00%	3.22%	3.57%	3.58%	3.96%	3.96%	0.00%	0.00%	0.00%	0.04%	0.00%	0.00%	0.00%	0.00%
CO_2	1.50%		0.00%	1.19%	9.84%	0.00%	0.00%	0.00%	0.00%	0.03%	0.04%	0.00%	99.73%	0.00%	99.61%	99.62%	99.62%
C_2H_4	0.00%		0.00%	0.00%	5.71%	6.36%	6.36%	0.30%	0.30%	62.07%	99.54%	0.03%	0.02%	0.00%	0.00%	0.00%	0.00%
C_2H_6	1.50%		0.00%	1.19%	3.37%	3.75%	3.75%	0.04%	0.04%	37.89%	0.42%	99.94%	0.01%	0.00%	0.00%	0.00%	0.00%
H_2O	0.00%		0.00%	0.00%	0.32%	0.05%	0.00%	0.00%	0.00%	0.01%	0.00%	0.03%	0.15%	0.00%	0.17%	0.16%	0.16%
H_2	0.00%		0.00%	0.00%	4.16%	4.62%	4.63%	5.13%	5.13%	0.00%	0.00%	0.00%	0.00%	0.00%	0.00%	0.00%	0.00%
DGA	0.00%		0.00%	0.00%	0.00%	0.01%	0.00%	0.00%	0.00%	0.00%	0.00%	0.00%	0.00%	0.00%	0.00%	0.00%	0.00%
N_2	0.00%		0.32%	0.07%	0.09%	0.10%	0.10%	0.11%	0.11%	0.00%	0.00%	0.00%	0.00%	79.00%	0.11%	0.10%	0.10%
Argon	0.00%		0.32%	0.07%	0.09%	0.10%	0.10%	0.11%	0.11%	0.00%	0.00%	0.00%	0.00%	0.00%	0.11%	0.10%	0.10%
Total	**100.00%**	**0.00%**	**100.00%**	**100.00%**	**100.00%**	**100.00%**	**100.00%**	**100.00%**	**100.00%**	**100.00%**	**100.00%**	**100.00%**	**100.00%**	**100.00%**	**100.00%**	**100.00%**	**100.00%**

OCM Reactor	
Conversion	
CH_4	26.86%
O_2	97.37%
Selectivity	
C2+	56.73%
CO_2	31.19%
CO	12.07%
Ethylene/Ethane	3.1052

Decision variables	
CH_4/O_2 to the reactor	**3.69**
Recycle ratio to the OCM reactor	**0**

Chapter 4- Supplementary Material 2

Shale Gas Type: New Albany

Design Basis: Maximum NPV

Power Generation Option: CLC

Stream No.	1	2	3	4	5	6	7	8	9	10	11	12	13	14	15	16	17
Temperature (°C)	30	59.06478	15	-17.59	40	30	-80	-120	40	-17.8083	-38.9352	-13.6994	40.0	30.0	30.0	30.0	44.0
Pressure (bar)	30	20.95	6	6	26.2	25.25	24.25	20	19	21.95	15	16.95	1.5	45.0	44.1	80.0	153.0
Mass Vapor Fraction	1	0	1	1	1	1	1	1	1	0	0	0	1.0	1.0	1.0	0.0	0.0
Total Flow (kmole/hr)	5183.0761	93.29537	1230.05516	6319.836	5000.274	4208.518	4206.048	3791.253	3791.253	414.795	253.0084	161.7866	779	33200	3553	4332	4332
Total Flow (kg/hr)	98165.1808	4111.416	39375.8257	133429.6	107103	72671.02	72582.42	60614.52	60614.52	11967.9	7101.303	4866.594	34239	957834	156141	190381	190381
Mole Percent																	
O_2	0.00%	0.00%	99.36%	19.34%	0.64%	0.76%	0.76%	0.84%	0.84%	0.00%	0.00%	0.00%	0.00%	21.00%	0.00%	0.00%	0.00%
CH_4	88.90%	0.00%	0.00%	72.91%	67.54%	80.24%	80.29%	89.08%	89.08%	0.00%	0.00%	0.00%	0.03%	0.00%	0.00%	0.01%	0.01%
CO	0.00%	0.00%	0.00%	0.00%	3.12%	3.70%	3.70%	4.10%	4.10%	0.00%	0.00%	0.00%	0.03%	0.00%	0.00%	0.00%	0.00%
CO_2	7.80%	0.01%	0.00%	6.40%	15.55%	0.00%	0.00%	0.00%	0.00%	0.05%	0.07%	0.01%	99.78%	0.00%	99.61%	99.64%	99.64%
C_2H_4	0.00%	0.00%	0.00%	0.00%	5.29%	6.28%	6.29%	0.30%	0.30%	61.00%	99.79%	0.34%	0.01%	0.00%	0.00%	0.00%	0.00%
C_2H_6	1.50%	0.20%	0.00%	1.23%	3.26%	3.88%	3.88%	0.05%	0.05%	38.90%	0.15%	99.51%	0.01%	0.00%	0.00%	0.00%	0.00%
H_2O	0.00%	0.00%	0.00%	0.00%	0.32%	0.05%	0.00%	0.00%	0.00%	0.01%	0.00%	0.01%	0.15%	0.00%	0.17%	0.16%	0.16%
H_2	0.00%	0.00%	0.00%	0.00%	4.11%	4.88%	4.89%	5.42%	5.42%	0.00%	0.00%	0.00%	0.00%	0.00%	0.00%	0.00%	0.00%
DGA	0.00%	0.00%	0.00%	0.00%	0.00%	0.01%	0.00%	0.00%	0.00%	0.00%	0.00%	0.00%	0.00%	0.00%	0.00%	0.00%	0.00%
N_2	0.00%	0.00%	0.32%	0.06%	0.08%	0.09%	0.09%	0.10%	0.10%	0.00%	0.00%	0.00%	0.00%	79.00%	0.11%	0.09%	0.09%
Argon	0.00%	0.00%	0.32%	0.06%	0.08%	0.09%	0.09%	0.10%	0.10%	0.00%	0.00%	0.00%	0.00%	0.00%	0.11%	0.09%	0.09%
C_3H_8	1.80%	99.79%	0.00%	0.00%	0.00%	0.00%	0.00%	0.00%	0.00%	0.05%	0.00%	0.12%	0.00%	0.00%	0.00%	0.00%	0.00%
Total	**100.00%**	**100.00%**	**100.00%**	**100.00%**	**100.00%**	**100.00%**	**100.00%**	**100.00%**	**100.00%**	**100.00%**	**100.00%**	**100.00%**	**100.00%**	**100.00%**	**100.00%**	**100.00%**	**100.00%**

OCM Reactor	
Conversion	
CH_4	26.69%
O_2	97.38%
Selectivity	
C2+	56.96%
CO_2	30.38%
CO	12.67%
Ethylene/Ethane	3.08906

Decision variables	
CH_4/O_2 to the reactor	**3.77**
Recycle ratio to the OCM reactor	**0**

Chapter 4- Supplementary Material 2
Shale Gas Type: Fayetteville
Design Basis: Maximum NPV
Power Generation Option: CLC

Decision variables	
CH_4/O_2 to the reactor	3.69
Recycle ratio to the OC	0

Cost Index (2007)	525.4
Cost Index, Jul 2012	582.2
Operation Time (hr/yr)	8760
Capacity Factor	85.0%
Plant Lifetime (Years)	30
Loan Lifetime (Years)	30
Interest Rate on Loan	9.5%
Debt Percentage	50%
Inflation	2.79%
Federal + State Tax Rt	40%
Equity Return Rate	20%

Total Capital Investment, USD	***430,121,950***
Direct Cost, USD	292,482,926
Indirect Cost, USD (20% of Fixed)	73,120,732
Fixed Capital Investment, USD	365,603,658
Working Capital Investment, USD	64,518,293

Feed and Product Prices	
Natural Gas Price, $/MMBtu	3.72
Ethylene Price, $/tonne	1384.72
Ethane Price, $/kg	0.27
Propane, $/m3	224.28
Electricity, cents/kwh	7.95
NiO Solid, $/kg	32.89
CO2, $/tonne	10.00

Total Annual Expense, $/yr	***216,330,786***
Natural Gas & Solid, $/yr	110,848,146
Operating Labor, $/yr	22,169,629
Direct supervisory, $/yr	2,216,963
Utilities, $/yr	22,169,629
Maintenance and repairs, $/yr	18,280,183
Operating supplies, $/yr	1,828,018
Laboratory charges, $/yr	2,216,963
Plant-overhead costs, $/yr	21,333,387
Administrative costs, $/yr	6,400,016
Distribution and selling costs, $/yr	4,433,926
Research and development costs	4,433,926

Total Revenue, $/yr	***293,624,570***
Ethylene Sale, $/yr	77,768,797
Ethane Sale, $/yr	9,957,375
Power, $/yr	192,167,307
CO2, $/yr	13,731,092
Propane, $/yr	

Gross Earning, $/yr	77,293,784
Debt Taken, $	215,060,975
Equity Expended, $	215,060,975
Annual Payment on Loan, $	21,867,526

Direct Capital Cost Estimate Breakdown	
OCM Reactor	$9,813,189
Compression	$3,499,310
CO_2 Removal	$4,324,866
Cold Box	$1,090,577
De-Methanizer (Including Refrigeration Cycle)	$9,748,507
C_2 Splitter (Including Refrigeration Cycle)	$10,324,537
HRSG	$3,979,266
Steam Turbines	$47,097,921
Air & Fuel Compression	$28,015,450
Gas Turbine	$59,473,424
Solid Reactors	$31,837,961
Solid Cost	$7,948,056
CO_2/H_2O Separation	$225,498
CO_2 Compression	$3,578,180
ASU	$71,526,183
Total	**292,482,926**

MACRS CASH FLOW - Depreciation	
2013	36,560,366
2014	65,808,658
2015	52,646,927
2016	42,117,541
2017	33,708,657
2018	26,944,990
2019	23,947,040
2020	23,947,040
2021	23,983,600
2022	23,947,040
2023	11,991,800

Loan Principal Balance at start of	
2013	215,060,975
2014	213,624,242
2015	212,051,020
2016	210,328,341
2017	208,442,007
2018	206,376,472
2019	204,114,712
2020	201,638,084
2021	198,926,176
2022	195,956,637
2023	192,704,992
2024	189,144,441
2025	185,245,637
2026	180,976,447
2027	176,301,683
2028	171,182,818
2029	165,577,660
2030	159,440,012
2031	152,719,287
2032	145,360,094
2033	137,301,777
2034	128,477,920
2035	118,815,797
2036	108,235,772
2037	96,650,645
2038	83,964,930
2039	70,074,073
2040	54,863,584
2041	38,208,099
2042	19,970,343

Interest Payed	
2013	20,430,793
2014	20,294,303
2015	20,144,847
2016	19,981,192
2017	19,801,991
2018	19,605,765
2019	19,390,898
2020	19,155,618
2021	18,897,987
2022	18,615,881
2023	18,306,974
2024	17,968,722
2025	17,598,335
2026	17,192,762
2027	16,748,660
2028	16,262,368
2029	15,729,878
2030	15,146,801
2031	14,508,332
2032	13,809,209
2033	13,043,669
2034	12,205,402
2035	11,287,501
2036	10,282,398
2037	9,181,811
2038	7,976,668
2039	6,657,037
2040	5,212,041
2041	3,629,769
2042	1,897,183

CASH FLOW - Taxable Earnings	
2013	20,302,625
2014	-6,655,787
2015	8,868,785
2016	21,836,874
2017	32,763,391
2018	42,126,863
2019	47,810,223
2020	50,584,874
2021	53,416,063
2022	56,417,565
2023	71,439,290
2024	86,603,746
2025	89,887,503
2026	93,287,612
2027	96,809,678
2028	100,459,685
2029	104,244,031
2030	108,169,559
2031	112,243,600
2032	116,474,009
2033	120,869,217
2034	125,438,272
2035	130,190,902
2036	135,137,567
2037	140,289,529
2038	145,658,917
2039	151,258,808
2040	157,103,312
2041	163,207,659
2042	169,588,307

CASH FLOW - Net Earnings	
2013	-204,316,133
2014	-8,229,009
2015	3,598,592
2016	11,215,791
2017	17,592,499
2018	23,014,357
2019	26,209,506
2020	27,639,017
2021	29,080,099
2022	30,598,894
2023	39,303,022
2024	48,063,444
2025	49,663,312
2026	51,297,804
2027	52,966,941
2028	54,670,653
2029	56,408,771
2030	58,181,011
2031	59,986,967
2032	61,826,089
2033	63,697,673
2034	65,600,840
2035	67,534,516
2036	69,497,413
2037	71,488,003
2038	73,504,493
2039	75,544,796
2040	77,606,502
2041	79,686,839
2042	81,782,641

CASH FLOW - Discounted Cash Flow	
2013	-167,755,767
2014	57,579,649
2015	56,245,519
2016	53,333,332
2017	51,301,157
2018	49,959,347
2019	50,156,545
2020	51,586,056
2021	53,063,699
2022	54,545,933
2023	51,294,822
2024	48,063,444
2025	49,663,312
2026	51,297,804
2027	52,966,941
2028	54,670,653
2029	56,408,771
2030	58,181,011
2031	59,986,967
2032	61,826,089
2033	63,697,673
2034	65,600,840
2035	67,534,516
2036	69,497,413
2037	71,488,003
2038	73,504,493
2039	75,544,796
2040	77,606,502
2041	79,686,839
2042	81,782,641

CASH FLOW - Cumulative Cash Flow (PV,	
2013	-167,755,767
2014	-119,772,726
2015	-80,713,338
2016	-49,849,141
2017	-25,109,000
2018	-5,031,459
2019	11,765,867
2020	26,162,588
2021	38,503,509
2022	49,074,876
2023	57,359,276
2024	63,828,038
2025	69,398,109
2026	74,192,601
2027	78,318,014
2028	81,866,439
2029	84,917,470
2030	87,539,877
2031	89,793,050
2032	91,728,260
2033	93,389,753
2034	94,815,700
2035	96,039,015
2036	97,088,074
2037	97,987,330
2038	98,757,848
2039	99,417,769
2040	99,982,712
2041	100,466,118
2042	100,879,550

NPV, $ Million	**101**

Chapter 4- Supplementary Material 2
Shale Gas Type: New Albany
Design Basis: Maximum NPV
Power Generation Option: CLC

Decision variables	
CH_4/O_2 to the reactor	3.77
Recycle ratio to the OC	0

Cost Index (2007)	525.4
Cost Index, Jul 2012	582.2
Operation Time (hr/yr)	8760
Capacity Factor	85.0%
Plant Lifetime (Years)	30
Loan Lifetime (Years)	30
Interest Rate on Loan	9.5%
Debt Percentage	50%
Inflation	2.79%
Federal + State Tax Rt	40%
Equity Return Rate	20%

Total Capital Investment, USD	***428,147,645***
Direct Cost, USD	291,140,399
Indirect Cost, USD (20% of Fixed)	72,785,100
Fixed Capital Investment, USD	363,925,498
Working Capital Investment, USD	64,222,147

Feed and Product Prices	
Natural Gas Price, $/MMBtu	3.72
Ethylene Price, $/tonne	1384.72
Ethane Price, $/kg	0.27
Propane, $/m3	224.28
Electricity, cents/kwh	7.95
NiO Solid, $/kg	32.89
CO2, $/tonne	10.00

Total Annual Expense, $/yr	***216,146,462***
Natural Gas & Solid, $/yr	110,825,605
Operating Labor, $/yr	22,165,121
Direct supervisory, $/yr	2,216,512
Utilities, $/yr	22,165,121
Maintenance and repairs, $/yr	18,196,275
Operating supplies, $/yr	1,819,627
Laboratory charges, $/yr	2,216,512
Plant-overhead costs, $/yr	21,288,954
Administrative costs, $/yr	6,386,686
Distribution and selling costs, $/yr	4,433,024
Research and development costs	4,433,024

Total Revenue, $/yr	***291,546,579***
Ethylene Sale, $/yr	73,219,060
Ethane Sale, $/yr	9,930,771
Power, $/yr	178,097,318
CO2, $/yr	14,145,496
Propane, $/yr	16,153,933

Gross Earning, $/yr	75,400,117
Debt Taken, $	214,073,823
Equity Expended, $	214,073,823
Annual Payment on Loan, $	21,767,151

Direct Capital Cost Estimate Breakdown	
OCM Reactor	8,423,718
Compression	3,551,330
CO_2 Removal	4,247,808
Cold Box	953,312
De-Methanizer (Including Refrigeration Cycle)	9,886,721
C_2 Splitter (Including Refrigeration Cycle)	8,613,107
De-Propanizer	12,354,256
HRSG	3,810,484
Steam Turbines	44,875,687
Air & Fuel Compression	27,031,483
Gas Turbine	56,938,720
Solid Reactors	30,431,496
Solid Cost	7,914,084
CO2/H2O Separation	221,134
CO2 Compression	4,155,744
ASU	67,731,317
Total	**291,140,399**

MACRS CASH FLOW - Depreciation	
2013	36,392,550
2014	65,506,590
2015	52,405,272
2016	41,924,217
2017	33,553,931
2018	26,821,309
2019	23,837,120
2020	23,837,120
2021	23,873,513
2022	23,837,120
2023	11,936,756

Loan Principal Balance at start of	
2013	214,073,823
2014	212,643,684
2015	211,077,683
2016	209,362,911
2017	207,485,237
2018	205,429,183
2019	203,177,804
2020	200,712,544
2021	198,013,084
2022	195,057,175
2023	191,820,456
2024	188,276,248
2025	184,395,340
2026	180,145,746
2027	175,492,440
2028	170,397,070
2029	164,817,641
2030	158,708,165
2031	152,018,289
2032	144,692,876
2033	136,671,547
2034	127,888,193
2035	118,270,420
2036	107,738,958
2037	96,207,008
2038	83,579,522
2039	69,752,426
2040	54,611,755
2041	38,032,720
2042	19,878,677

Interest Payed	
2013	20,337,013
2014	20,201,150
2015	20,052,380
2016	19,889,477
2017	19,711,097
2018	19,515,772
2019	19,301,891
2020	19,067,692
2021	18,811,243
2022	18,530,432
2023	18,222,943
2024	17,886,244
2025	17,517,557
2026	17,113,846
2027	16,671,782
2028	16,187,722
2029	15,657,676
2030	15,077,276
2031	14,441,737
2032	13,745,823
2033	12,983,797
2034	12,149,378
2035	11,235,690
2036	10,235,201
2037	9,139,666
2038	7,940,055
2039	6,626,480
2040	5,188,117
2041	3,613,108
2042	1,888,474

CASH FLOW - Taxable Earnings	
2013	18,670,554
2014	-8,206,989
2015	7,202,257
2016	20,065,525
2017	30,895,331
2018	40,167,970
2019	45,776,056
2020	48,487,413
2021	51,253,641
2022	54,187,951
2023	69,085,823
2024	84,124,241
2025	87,334,921
2026	90,659,804
2027	94,104,423
2028	97,674,688
2029	101,376,921
2030	105,217,884
2031	109,204,824
2032	113,345,509
2033	117,648,277
2034	122,122,082
2035	126,776,549
2036	131,622,034
2037	136,669,687
2038	141,931,521
2039	147,420,490
2040	153,150,575
2041	159,136,871
2042	165,395,690

CASH FLOW - Net Earnings	
2013	-204,301,628
2014	-9,772,990
2015	2,606,582
2016	10,161,640
2017	16,481,145
2018	21,849,403
2019	25,000,373
2020	26,392,988
2021	27,796,276
2022	29,276,051
2023	37,907,286
2024	46,593,637
2025	48,151,359
2026	49,742,577
2027	51,367,284
2028	53,025,383
2029	54,716,677
2030	56,440,855
2031	58,197,480
2032	59,985,977
2033	61,805,612
2034	63,655,476
2035	65,534,468
2036	67,441,270
2037	69,374,327
2038	71,331,816
2039	73,311,623
2040	75,311,310
2041	77,328,080
2042	79,358,737

CASH FLOW - Discounted Cash Flow	
2013	-167,909,078
2014	55,733,600
2015	55,011,854
2016	52,085,858
2017	50,035,076
2018	48,670,712
2019	48,837,494
2020	50,230,108
2021	51,669,789
2022	53,113,171
2023	49,844,042
2024	46,593,637
2025	48,151,359
2026	49,742,577
2027	51,367,284
2028	53,025,383
2029	54,716,677
2030	56,440,855
2031	58,197,480
2032	59,985,977
2033	61,805,612
2034	63,655,476
2035	65,534,468
2036	67,441,270
2037	69,374,327
2038	71,331,816
2039	73,311,623
2040	75,311,310
2041	77,328,080
2042	79,358,737

CASH FLOW - Cumulative Cash Flow (PV)	
2013	-167,909,078
2014	-121,464,412
2015	-83,261,735
2016	-53,119,457
2017	-28,989,887
2018	-9,430,219
2019	6,925,359
2020	20,943,660
2021	32,960,401
2022	43,254,090
2023	51,304,181
2024	57,575,125
2025	62,975,620
2026	67,624,754
2027	71,625,575
2028	75,067,213
2029	78,026,723
2030	80,570,695
2031	82,756,653
2032	84,634,266
2033	86,246,407
2034	87,630,067
2035	88,817,154
2036	89,835,176
2037	90,707,843
2038	91,455,586
2039	92,095,999
2040	92,644,234
2041	93,113,331
2042	93,514,510
NPV, $ Million	**94**

Chapter 5

Co-Production of Olefins, Fuels, and Electricity from Conventional Pipeline Gas and Shale Gas with Near-Zero CO_2 Emissions

The text and materials provided in this chapter are submitted to the *Energies* journal for peer review.

Co-Production of Olefins, Fuels, and Electricity from Conventional Pipeline Gas and Shale Gas with Near-Zero CO_2 Emissions

Yaser Khojasteh Salkuyeh [1], Thomas A. Adams II [1, *]

[1] Department of Chemical Engineering, McMaster University, 1280 Main St W, Hamilton, Ontario, L8S 4L7, Canada; E-Mail: khojasy@mcmaster.ca

***** Author to whom correspondence should be addressed; E-Mail: tadams@mcmaster.ca; Tel.: +1 (905) 525-9140 (ext. 24782).

External Editor:

Received: / Accepted: / Published:

Abstract: A novel polygeneration process is presented in this paper that co-produces olefins, methanol, dimethyl ether, and electricity from conventional pipeline natural gas and different kinds of shale gases. Techno-economic analyses of many variants of the process are performed, considering differences in power generation strategy and gas type. Derivative-free optimization algorithms were coupled with Aspen Plus simulation models to determine the optimum product portfolio as a function of a wide variety of market prices. The optimization results show that the proposed plant is capable of producing olefins with the same production costs as traditional petrochemical routes while having effectively zero process CO_2 emissions (including the utilities). This provides an economic and more sustainable alternative to traditional naphtha cracking.

Keywords: polygeneration; gas-to-olefins; gas-to-liquids, methanol-to-olefins, CO_2 capture

---

1. Introduction

In the chemical and petrochemical industries, high-value products such as ethylene and propylene are traditionally produced from crude oil. Although the industry is growing (around 4.5% per year [1]), it currently faces two significant challenges. First, the price of crude oil is now quite high—currently almost six times the price it was in early 1999 (adjusting for inflation). However, natural gas is comparatively much cheaper, being less than one third of the price of oil for the same energy content [2]. Second, the negative environmental impact of these processes is quite significant. The olefin industry is one of the largest consumers of primary energy, resulting in a total of 30% of direct CO_2 emitted from chemical plants [3]. The indirect CO_2 emissions attributed to electricity consumption by olefin production processes is roughly 12% of the total CO_2 emissions of chemical and petrochemical plants [4].

Polygeneration processes, which are systems that co-produce a variety of products such as fuels, chemicals, and electricity, are a promising new strategy of chemical processing. By design, polygeneration systems tightly integrate different production trains together in an attempt to exploit synergies between them to yield higher efficiencies and profits. This can take the form of the integration of waste heat, clever reuse of waste gases, or strategic blending of certain streams. Often, these tightly integrated processes are both more profitable and more environmentally friendly processes compared to their stand-alone counterparts [5-7]. For example, Adams and Barton performed a techno-economic analysis that produces transportation fuels, methanol and power from coal and natural gas in response to market price fluctuations, product portfolios and CO_2 emissions tax [8, 9]. Cormos provided a detailed techno-economic analysis of a hybrid system that co-produces hydrogen and power showing reduced cost and greenhouse gas emissions compared to standalone power generation system [10]. In another example, the implementation of a coal-oven gas-to-olefins polygeneration concept was studied by Man et al. aiming to reduce the CO_2 mitigation cost [11]. In their work, the H_2/CO ratio of syngas was adjusted to its optimum value (around 2) by using an integrated coal gasification-coke oven dry reforming system.

The main goal of the present work is to attack both environmental and economic issues by proposing novel polygeneration processes that co-produce methanol, liquid transportation fuel (dimethyl ether), and olefins from natural gas. In the work, four different advanced power generation options are examined in which electricity is produced from waste gases that enable 90-100% capture of all CO_2 produced inside the plant boundary. These are chemical looping combustion using nickel oxide, chemical looping combustion using iron oxide, oxyfuel combustion, and conventional combustion with a gas turbine, each with an integrated CO_2 capture process. There is more than sufficient energy from the waste gases to provide for all electricity, cooling, and heat needs in each process. All process heat, water and electricity integration has been explicitly accounted. Thus, no utility is imported across the plant boundary. Only natural gas, process water, and air are consumed, and only water vapor, spent air, liquefied CO_2, and products are output.

In addition to using conventional pipeline natural gas as the primary feedstock, four different qualities of shale gas are considered as the feedstock, due to its rapid growth in North America. The process steps for conventional pipeline natural gas and shale gas are similar, but their geographic location can be very different. All of the steps in the process using conventional gas are located at the same place, using a connection to a conventional natural gas pipeline as the feed. However, for the shale gas cases, gas is first converted not to conventional pipeline gas, but to methanol at a point near a collection of shale gas wellheads. The methanol is then transported to the main plant location where it is then converted to the various products. It is also possible that the main plant receives methanol from a variety of different methanol sources or shale gas sites over a wider area. This possibility was examined because it may be more economical to transport methanol as an intermediary rather than convert shale gas to pipeline quality natural gas and transport that, especially since methanol has to be created as an intermediate product anyway in the proposed process. In addition, because some CO_2 is captured at the smaller upstream processes closer to the shale gas source, there is the potential for even more synergistic benefits because the CO_2 can be used for enhanced gas recovery or enhanced oil recovery with minimum transportation penalty [12]. However, because this decision is highly dependent on each particular business supply chain circumstance, it is not the scope of this work to decide which is better. Rather, the objective is to propose and study several process options and

estimate their efficiency, optimal configuration, and profitability, each of which might be the best choice in some circumstances.

As shown in Figure 1A, in the process using conventional gas, the gas is reformed to synthesis gas first and then used for methanol production. Depending on the market prices, the methanol can either be sold as a product, or converted into dimethyl ether (DME), olefins and C_{3+} via the methanol-to-olefins (MTO) process. DME is a non-toxic fuel that can be used as a substitute for diesel [13-15]. The unreacted gases from methanol synthesis are either recycled to the methanol reactor or are mixed with an off-gas stream coming from the MTO unit and sent to the power generation unit. Four different advanced power generation systems with 90-100% CO_2 capture are considered in this study in order to determine the best CO_2 removal approach (section 2.4).

The steps in the processes which use shale gas directly, as shown in Figure 1B, are very similar to the conventional natural gas process. However, in the shale-gas processes, methanol and DME are co-produced near the shale gas source in the "upstream" section. Depending on the type of shale gas, the upstream section may also contain additional separation steps to remove higher hydrocarbons from the shale gas that are not as prevalent in conventional pipeline gas. The methanol is then transported to the "downstream" section in which methanol is converted to olefins in a central locality. The key difference from a process perspective is that the upstream and downstream sections each require their own power generation, heat recovery & steam generation (HRSG), and CO_2 capture and compression islands to handle waste gases and CO_2 capture, and their performances will be different because the off-gases from upstream and downstream processes will not be mixed and the quality of available heat sources and sinks is also different. However, in this work, the processes were designed to ensure that both the upstream and downstream sections each independently produce their own utilities on site and virtually no CO_2 is emitted from either one (in most cases).

In this work, chemical process simulations were performed to determine the mass and energy flows of each stream in each variants of the process. Optimization algorithms were used in an economic analysis to determine the design parameters which resulted in either the highest profitability for each design variant, or the highest production rate of olefins (both are considered as separate objective functions in separate optimization problems), considering a selected subset of the most important design parameters. Because market conditions are always subject to change, this was repeated for a wide variety of market conditions, ranging from low to high prices for the various products generated in each process. Finally, the most promising variants of the MTO concept were compared to naphtha cracking and ethane cracking processes for olefin production, the closest competing processes, showing promising results. The models used for each of the individual unit operations were either developed in the prior work of our group or other groups.

The present work focuses on the conversion of gas to more valuable products with minimum environmental effects. However, there are some other open research areas in the production of olefins and fuels from alternative resources such as biomass [16, 17] and plastic wastes [18], which are out of scope of this paper. The primary novelty of this work is the proposal of the first complete MTO process with low-to-zero CO_2 emissions (and all of its variants), as well as its techno-economic analysis, neither of which have been put forth in the open literature to the best of our knowledge. We also note that the upstream/downstream approach (Figure 1B) could also be applied to conventional natural gas as well. Although that case is not modelled separately in this work, the results would be

very similar to the case of Fayetteville shale gas reported herein since it has a similar makeup and heating value.

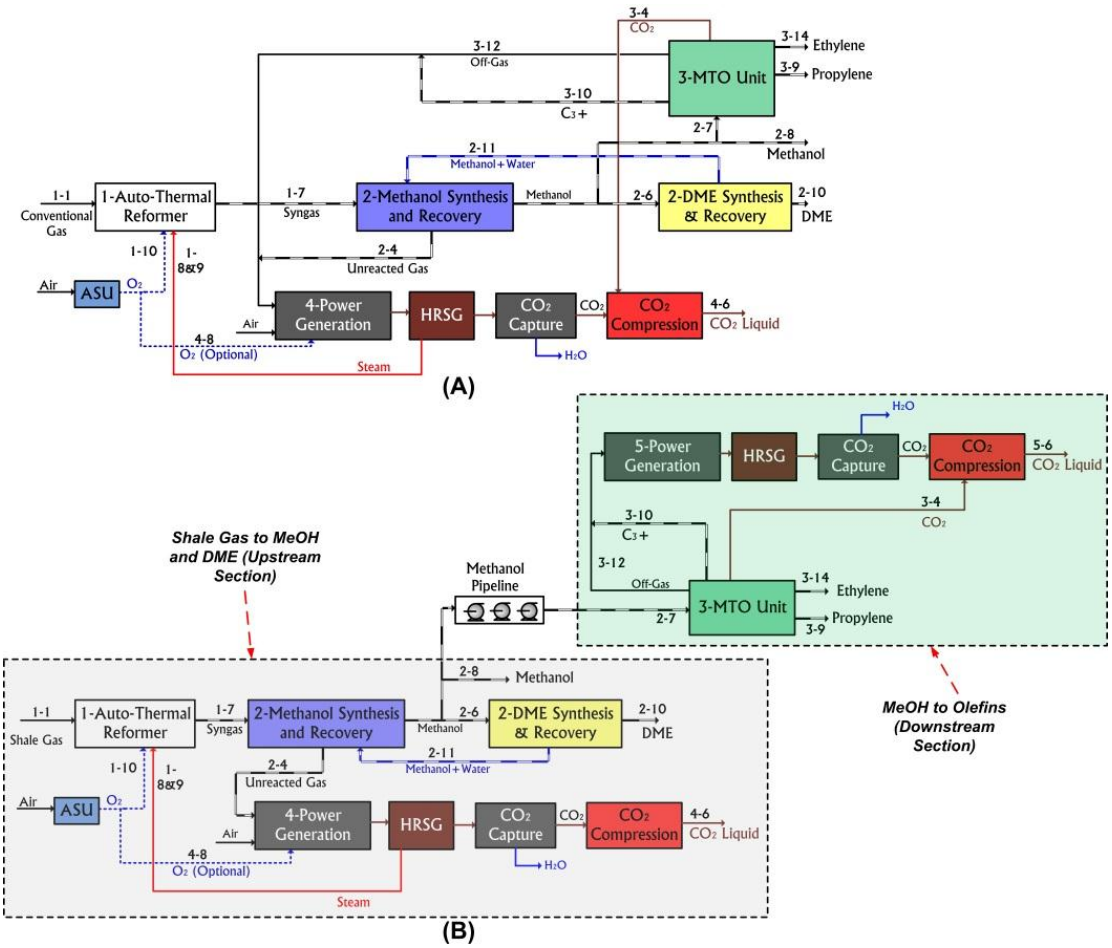

Figure 1. Scheme of the proposed polygeneration process.

2. Process Model and Simulations

Each process variant was simulated using standard chemical unit operation models contained in Aspen Plus 2006.5, except for the gas turbines which were simulated by using a custom model integrated into Aspen Plus via the Microsoft Excel interface (section 2.4). The feed rate for each case was fixed at 1111 MW (LHV), which is 1976-2356 tonne/day depending on the composition of the gas used (see Table 1). The PR-BM equation of state was used for all units except for water-only unit operations (especially in the HRSG section and steam turbines) and amine units that were simulated by using NBS/NRC and Elec-NRTL models as suggested by Chen and Mathias [19]. The PR-BM model was chosen because it was found to predict experimentally determined vapor-liquid equilibrium data quite well for many different chemical pairs encountered in the process, as shown in the supplementary material-section 1. Other physical property packages such as the Ethylene package, which might be appropriate for some of the units of the process, were found to predict the equilibrium properties less accurately than the chosen methods, as shown in the supplementary material-section 1. The thermal efficiency calculations of the plant consider all external utility requirements, such as electricity, process steam, and steam for reboiler heating.

Table 1. Gas feedstocks composition, (molar).

Gas type	CH_4	C_2H_6	C_3H_8	C_4H_{10}	CO_2	N_2	Flowrate (tonne/day)	Energy Content, MW (LHV)	HHV
Marcellus [20]	0.872	0.095	0.025	0.000	0.005	0.003	1976	1228 (1111)	
Fayetteville [20]	0.97	0.015	0.000	0.000	0.015	0.000	2000	1232 (1111)	
New Albany [20]	0.889	0.015	0.018	0.000	0.078	0.000	2356	1231 (1111)	
Haynesville [20]	0.948	0.001	0.000	0.000	0.05	0.001	2200	1233 (1111)	
Conventional Gas [21]	0.939	0.032	0.007	0.004	0.01	0.008	2007	1231 (1111)	

2.1. Natural gas reformer

The process of synthesis gas production from gas, called gas reforming, is an endothermic reaction that occurs at high temperature (700-1000°C). Depending on the reforming temperature and inlet steam-to-gas ratio, the gas conversion varies between 50 to 95% [8]. For this section, the models and optimum operating conditions developed and used in our prior work [8, 9, 22] were re-used in this simulation, and is briefly described next. As shown in Figure 2, the natural gas is sent to the pre-reformer after being heated by the reformer effluent. In the pre-reformer, ethane and heavier hydrocarbons are converted to syngas. The output stream is sent then to the reformer, where methane is converted to H_2, CO and CO_2 based on the following equilibrium reactions [22]:

$$CH_4 + H_2O \leftrightarrow CO + 3H_2 \quad (1)$$

$$CO + H_2O \leftrightarrow CO_2 + H_2 \quad (2)$$

$$CH_4 + CO_2 \leftrightarrow 2CO + 2H_2 \quad (3)$$

In addition, a portion of the methane is simultaneously oxidized with high purity (99.5%) O_2 inside the reactor in order to provide the heat requirements of the reforming reactions (the air separation unit (ASU) is not modeled in detail but all costs, parasitic loads, and other relevant mass and energy balances are included in the analysis). After cooling the hot syngas stream, it is dehydrated, compressed, and then sent to the methanol synthesis unit (Stream 1-7). The REquil model was used for the simulation of both reactors.

2.2. Methanol & DME production unit

In this unit, the synthesis gas produced in the reforming unit (Stream 1-7) is first mixed with a recycle stream containing unreacted gases and sent to the methanol reactor (Figure 3). The main reactions that occur in the MeOH reactor are [23]:

$$CO_2 + 3H_2 \rightleftharpoons CH_3OH + H_2O \quad \Delta H_{25}\text{=-49.51 kJ/mol} \quad (M1)$$

$$CO_2 + H_2 \rightleftharpoons CO + H_2O \quad \Delta H_{25}\text{=41 kJ/mol} \quad (M2)$$

with corresponding reaction rate laws:

$$r_{M1} = \frac{k_{M1} p_{CO_2} p_{H_2} [1 - (1/K_{eq,M1})(p_{H_2O} p_{CH_3OH} / p_{H_2}^3 p_{CO_2})]}{(1 + K_1(p_{H_2O}/p_{H_2}) + K_2\sqrt{p_{H_2}} + K_3 p_{H_2O})^3}, \frac{kmol}{kg_{cat}.sec}$$

$$r_{M2} = \frac{k_{M2} p_{CO_2} [1 - (1/K_{eq,M2})(p_{H_2O} p_{CO} / p_{CO_2} p_{H_2})]}{(1 + K_1(p_{H_2O}/p_{H_2}) + K_2\sqrt{p_{H_2}} + K_3 p_{H_2O})}, \frac{kmol}{kg_{cat}.sec}$$

where r_{M1} and r_{M2} are the reaction rates, p_i is the partial pressure of species *i*, and the *k* and *K* terms are constants shown in Table 3 as suggested by Vanden bussche et al., as well as the operating

conditions for the reactor (shown in Table 2) [23]. The reactor dimensions were adjusted to achieve 40% CO conversion.

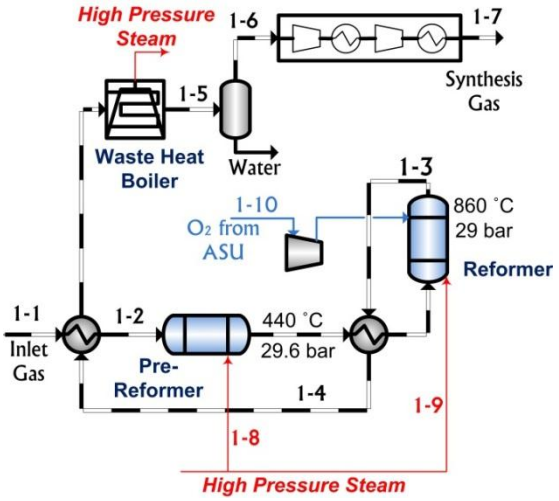

Figure 2. Section 1: Auto-thermal gas reforming.

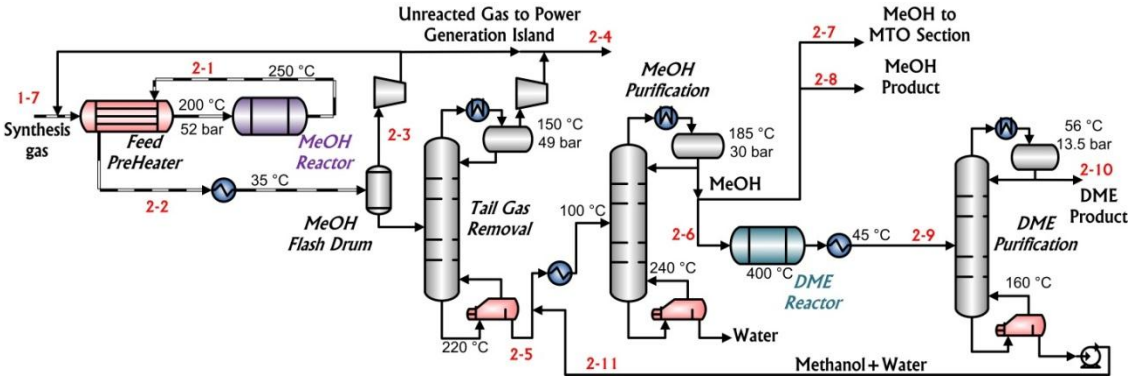

Figure 3. Section 2: Methanol and DME synthesis.

Table 2. Main design parameters of the Methanol/DME synthesis section.

MeOH reactor	Temperature: 250°C, Pressure: 51 bar RPlug reactor model
MeOH flash drum	35°C, 50.5 bar
DME reactor	Temperature: 400°C, Pressure: 15 bar RPlug reactor model
Tail gas removal	25 stages, 49 bar MeOH mass recovery: 98%
MeOH purification	30 stages, 30 bar, RadFrac model MeOH mass recovery: 99.5%, MeOH mole purity (industrial grade): 99.5% [24]
DME purification	30 stages, 13.5 bar, RadFrac model DME mass recovery: 99.5%, DME mole purity (fuel grade): 99.9% [25]

Table 3. Kinetic values of the MeOH/DME synthesis reactions [23, 26].

Parameter ($k_i = Aexp(\frac{B}{RT})$)	A	B (kJ/kmol)
K_1	3453.38	0
K_2 (1/bar$^{0.5}$)	0.499	17197
K_3 (1/bar)	6.62×10^{-11}	124119
K_4 (m^3/kmol)	5.39×10^{-4}	70560.92
K_5 (m^3/kmol)	8.47×10^{-2}	42151.98
k_{M1} (kmol/kg$_{cat}$.bar^2.sec)	1.07×10^{-3}	36696
k_{M2} (kmol/kg$_{cat}$.bar.sec)	1.22×10^{7}	-94765
k_{D1} (kmol/kg$_{cat}$.sec)	1.49×10^{10}	-143666
$K_{eq,M1}$(1/bar^2)	2.56×10^{-11}	58694.56
$K_{eq,M2}$	87.57	-36581.6

Unreacted gases and water are removed from the MeOH product by first cooling the reactor effluent at 35°C and collecting the liquid in a flash drum. A portion of the vapour product (stream 2-3, mostly unreacted syngas) from the flash drum is recycled to the reactor, and the rest is sent for power generation. The percentage that is recycled is subject to optimization, discussed later. Additional gasses still present in the liquid product are removed in a tail gas removal column, leaving primarily MeOH and water in the bottoms product. The bottom is sent to a MeOH purification column in which water is recovered in the bottoms and MeOH is recovered in the distillate. Key design parameters for these columns are shown in Table 2, based on our previous work [27]. The MeOH product is then split into three streams: Stream 2-6 which is the feedstock for the DME synthesis reactor (described next); Stream 2-7 which is the feedstock of the MTO unit (see section 2.3); and Stream 2-8 which is sent to the storage tanks for sale of MeOH as a final product. The split ratio between these streams is subject to optimization and discussed later.

The DME synthesis reaction and corresponding rate law is as follows:

$$2CH_3OH \rightleftharpoons CH_3OCH_3 + H_2O \quad \Delta H_{25}\text{=-24 kJ/mol} \qquad \text{(D1)}$$

$$r_{D1} = \frac{k_{D1}K_4^2[C_{CH_3OH}^2 - (1/K_{eq,D1})C_{H_2O}C_{CH_3OCH_3}]}{(1 + 2\sqrt{K_4C_{CH_3OH}} + K_5C_{H_2O})^4}, \frac{kmol}{kg_{cat}.sec}$$

$$ln\,(K_{eq,D1}) = \frac{2835.2}{T} + 1.675ln(T) - 2.39\times10^{-4}T - 0.21\times10^{-6}T^2 - 13.36$$

where r_{D1} is the reaction rate, C_i is the concentration of species *i*, and the *k* and *K* terms are constants shown in Table 3 as suggested by Bercic and Levec [26]. Further details of design parameters are summarized in Table 2, based on our previous work [27].

The DME reactor effluent is then sent to the DME purification column to get DME product with 99.9% molar purity (fuel grade), with key design parameters also shown in Table 2, chosen for recovering 99.5% of DME.

2.3. Methanol to Olefins (MTO)

The MTO technology is based on the dehydration of MeOH to light olefins in a catalytic reactor. The main reaction products are [28]:

$$MeOH \leftrightarrow \begin{cases} C_2H_4/C_2H_6 \\ C_3H_6/C_3H_8 \\ C_4H_8/C_5H_{10} \\ CO_2/H_2O \\ CH_4 \end{cases}$$

The SAPO-34 catalyst, which was developed by Union Carbide, is known to have one of the highest selectivity and conversion rates of MeOH-to-olefins and thus is utilized by UOP in its licensed UOP/Hydro MTO process [29, 30], shown in more detail Figure 4. In this work, the MTO reactor was modelled based on the experimentally determined selectivities for this catalyst described in detail by Wilson et al. [31]. As such, the model used for the MTO reactor fixes the temperature, pressure, feed conditions and selectivity to those results, as shown in Table 4.

Next, the reactor effluent is cooled to 40°C and flashed in order to recover unreacted water and MeOH as a liquid, which is the recycled to the MTO reactor. The vapour product from the flash drum is then sent to the CO_2 removal section, which uses a classic absorption / regenerator loop using 70 wt% diglycolamine (DGA) / 30 wt% water mixture as the solvent. Note that other solvents are possible, such as MDEA, but for this particular application it was found to outperform MDEA (MDEA model not shown for brevity). The absorber / regenerator cycle was modeled using RadFrac in Aspen Plus and designed to achieve 99.9% CO_2 removal. Design parameters are shown in Table 4.

The remaining gases are compressed to 35 bar and cooled to remove the remaining water (some water escapes from the solvent mixture). Then, the dehydrated gas is fed to the De-Ethanizer column to remove ethylene, ethane and other light gases such as CO_2 (Stream 3-7) from the propylene and heavier components (Stream 3-8). The De-Propanizer column splits propylene from the heavier hydrocarbons (C_{3+}) which can be sold as unstabilized naphtha or used as fuel for power generation. The light gases are fed to the De-Methanizer column to split the methane and light gases (Stream 3-12) from ethylene and ethane (Stream 3-13). The light gases are sent to the power generation island while the ethylene and ethane are sent to the C_2-Splitter. The C_2-Splitter is then used to recover ethylene from ethane, noting that in this design, some ethylene remains in the ethylene stream. Ethylene and ethane have close boiling points and a large number of stages and high boilup rates are required to achieve greater yields. This is subject to optimization but is outside of the scope of this work. The design parameters for all of these columns can be found in Table 4.

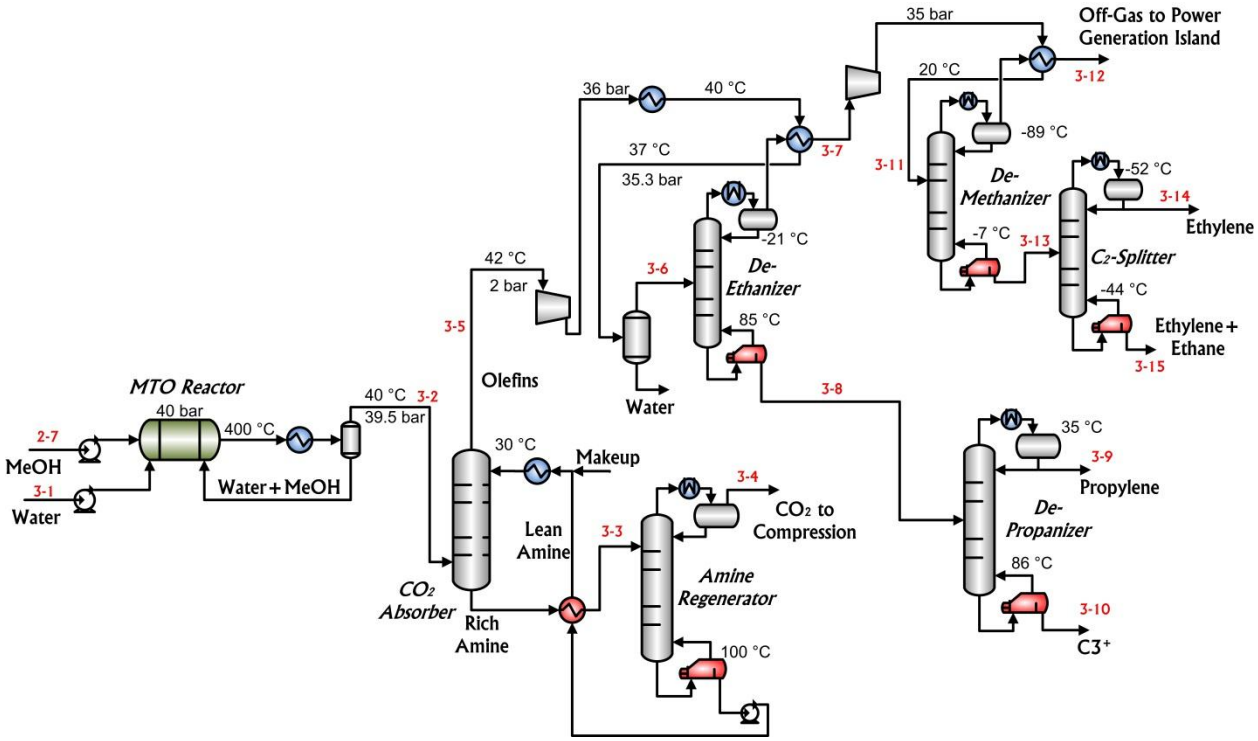

Figure 4. Section 3: Methanol-to-olefins process (MTO) based on UOP/Hydro technology [32, 33].

It should be noted that two refrigeration cycles are required to provide low temperature for the condensers. A three-stage propane refrigeration cycle was used to provide low temperatures for the condenser of De-Ethanizer columns [34]. The De-Methanizer and C_2 Splitter columns utilize a two-stage ethylene refrigeration cycle, which is integrated with the propane refrigeration cycle [35]. Please note that these cycles were not individually modeled and have not been shown in Figure 4 for brevity, but their capital costs, operating costs, and parasite power consumption have been considered in thermal and cost analysis, using Aspen Icarus 2006.5 and Gas Processors Suppliers Association (GPSA) [36].

Table 4. Main design parameters of the MTO section.

Olefins production method	*UOP/Hydro* MTO process [32]
MTO reactor	RYield reactor model; Temperature: 400 °C, Pressure: 40 bar
MTO reactor catalyst	*SAPO-34* [31]
Reactor selectivity	Experimental results by Wilson et al. [31]
	Molar Selectivity: CH_4: 0.013; C_2H_4: 0.43; C_2H_6: 0.008; C_3H_6: 0.418; C_3H_8: 0.005; C_4H_8: 0.108; C_5H_{10}: 0.017
CO_2 removal	Amine type: DGA; Elec-NRTL model [19]
CO_2 absorber	20 stages, 2 bar
Amine regenerator	20 stages, 1.5 bar
%CO_2 removal	99.9
Olefin products recovery	
De-Ethanizer	32 stages, 35 bar
	Reflux ratio: 2.6; Boilup ratio: 4
	%Ethane recovery: 99.8

	Power consumption of refrigeration cycle: 0.35 MW/MW [36]
De-Methanizer	35 stages, 34 bar
	Reflux ratio: 3.85; Boilup ratio: 1.03
	%Methane removal: 99.99
	Power consumption of refrigeration cycle: 1.21 MW/MW [36]
C_2 Splitter	30 stages, 10 bar
	Reflux ratio: 1.7; Boilup ratio: 29.8
	%Ethylene recovery: 95; Ethylene mole purity (polymer grade): 99.9% [37]
	Power consumption of refrigeration cycle: 0.64 MW/MW [36]
De-Propanizer	30 stages, 25 bar
	Reflux ratio: 6.0; Boilup ratio: 25.6
	%Propylene recovery: 98; Propylene mole purity (polymer grade): 99.2% [38]

2.4. Power Island

In this work, four different power generation systems with CO_2 capture were investigated for use in the power island, using unreacted syngas (Stream 2-4), off-gas (Stream 3-12) and C_{3+} (Stream 3-10) as the fuel gas. In conventional pipeline gas cases, streams 2-4,3-10 and 3-12 are mixed, and in the shale gas cases, a separate power generation island is used for 2-4 (at the upstream location) and 3-10 and 3-12 (at the downstream location). First, a traditional gas combustion turbine system with post-combustion capture was considered with a solvent-based system to recover CO_2 from the combustion exhaust. This is a commercially available technology [39]. Second, oxy-fuel combustion was considered, in which the fuel gas is combusted with an oxygen-rich stream instead of air. Since only limited N_2 mixes with the fuel CO_2 capture is achieved by simply condensing water from the combustion exhaust, leaving a high purity CO_2 stream behind. Then, chemical looping combustion with two different metal oxides was considered, which achieves indirect combustion of fuel gas by using a metal oxygen carrier such as iron-oxide (Fe_2O_3) in option three or nickel-oxide (NiO) in option four [40]. In either process, the combustion reaction takes place in the Fuel reactor with the oxygen provided by metal oxide while N_2 is absent. Then the reduced metal is regenerated in Air reactor, and the depleted air sent to the turbine. Both oxy-fuel combustion and chemical looping combustion technologies are in active development, and have been demonstrated at pilot scales [41-43]. The main process design assumptions and specifications of each approach are listed in Table 5, and are described in detail in the following subsections.

2.4.1. Option 1: Gas Combustion Turbines with Post-Combustion Capture

In this classic process, shown in Figure 5, the waste gases are combusted with air at high pressure and then expanded through a gas combustion turbine, generating electricity. Additional power is produced in a combined cycle by using the waste heat from the combustion exhaust to generate steam for steam turbines. As shown in Figure 5, Condensing steam turbine is used for the last stage and the vacuum pressure is provided by condensing steam in the condenser. It should be noted that the additional cost of this type of turbine has been considered in the economic analysis of process. In Aspen Plus, standard models for the compressors, turbines, heat exchangers, and pump were used with design assumptions shown in Table 5. As illustrated in Figure 5, a simple train was used for the steam

turbines. However, reheating the steam is an alternative that can improve the performance of the power island. The optimal design pressures and temperatures of the steam cycle were chosen using the built-in optimization algorithm in Aspen Plus, considering typical turbine efficiencies [27]. The built-in Aspen Plus model for a gas turbine was not used, but rather used a more accurate, empirical model based on the Siemens V94.3A turbine developed by Wilcock et al. [44-46]. This model is more rigorous because it considers the detailed effects of the coolant when predicting the system efficiencies, which in this case is air used with a film-cooling mechanism. This model was implemented inside Microsoft Excel and used within Aspen Plus through the user model interface.

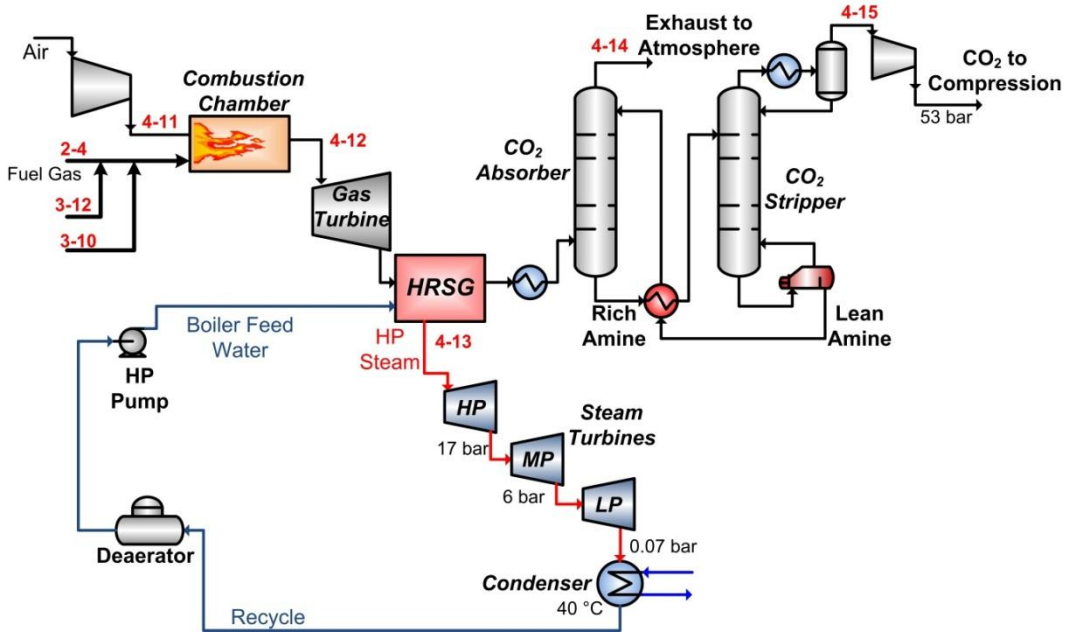

Figure 5. Section 4 Option 1: Power generation with post-combustion capture

Next, CO_2 is removed from the exhaust gas of the gas turbine using an amine-based absorption process. Although not commonly used at very high capture rates in current power plants, it is a well-known carbon capture technique. Moreover, the CO_2 capture section can be readily retrofitted to a gas turbine power plant after construction [39, 47]. This means it is possible to neglect the CO_2 capture step and vent the cooled combustion exhaust to the atmosphere instead (noting some small cleanup steps may be needed first), and retrofit the CO_2 capture section onto the end of the proposed polygeneration process at some later date only when politically or economically necessary. However, this is outside the scope of this work, and only processes with CO_2 capture enabled are considered.

Table 5. Process design specifications of the power island.

Gas turbines (options 1, 3, and 4)	Model: Siemens V94.3A [46]
	Outlet pressure: 1.1 bar
	Polytropic efficiency: 0.92, mechanical efficiency: 0.983
	Number of turbine stages: 4
	Maximum metal surface temperature ($T_{m,external}$): 850°C
	Gas turbine model based upon algorithm presented by Wilcock [44] and Young [45]

Steam turbines (all four options)	High pressure steam: 470 °C, 40.75 bar
	Turbines outlet pressure (HP/IP/LP): 17/5.8/0.07 bar
	Turbines outlet temperature (HP/IP/LP): 351/230/42 °C
	Isentropic efficiency: 0.875, Mechanical efficiency: 0.983
Post combustion capture (option 1)	Amine type: DGA; Elec-NRTL model [19]
	%CO_2 capture: 90
	CO_2 absorber: 30 actual stages, 1.8 bar, CO_2 Murphree efficiency: 0.33 [48]
	CO_2 stripper: 30 actual stages, 1.3 bar, CO_2 Murphree efficiency: 0.5 [48]
Oxy-fuel combustion (option 2)	RGibbs reactor model.
Excess O_2	3% (mole) [49]
O_2/recycle CO_2 ratio	27% (mole) [49]
Air Separation Unit	Oxygen purity (molar): 0.995 [50]
Chemical looping combustion (options 3 and 4)	RGibbs model for both Air and Fuel reactors. See [51] for more details on Aspen model setup.
Residence time of Air & Fuel reactors	300 seconds [52-54]
Iron oxide (option 3)	Air reactor temperature: 960°C
	Air/Solid rate: 1.312 (mole)
	Fuel reactor temperature: 710°C
	Fe_2O_3 in/Fuel gas: 1.81 (mole)
Nickel oxide (option 4)	Air reactor temperature: 1250°C
	Air/Ni rate: 2.39 (mole)
	Fuel reactor temperature: 700°C
	NiO in/Fuel gas: 1.57 (mole)
CO_2 compression (all four options)	Compressor outlet pressure: 80 bar
	Delivery condition: Temperature: 44 °C, Pressure: 153 bar

For the post-combustion CO_2 capture step used in this work, an amine is used to absorb the CO_2 component based on a set of electrolyte reactions [55, 56]. As shown in Figure 5, the exhaust gas from the gas turbine is cooled first and then contacted with lean amine in the absorption column. The exhaust gas leaving from the absorber is lean in CO_2 and can be vented to atmosphere. The CO_2-Rich amine stream is pumped into the stripper column, where a reboiler supplies the required heat to break the CO_2-amine chemical bound and separate the CO_2. Even though there are different kinds of amines that can be applied to this process, primary amines like monoethanolamine (MEA) and diglycolamine (DGA) are more suitable for low-pressure gas streams [57, 58]. DGA was chosen for this work since it can be used at higher concentration (50-70 wt% [58]), its circulation rate is less than MEA, which affects the size and energy requirement of the plant. This was verified through simulation of both solvents, although MEA results are not reported here for brevity. An exhaustive comparison of solvent selection is outside the scope of this work. The system is designed to achieve 90% capture with the captured CO_2 at 96% purity. The CO_2 product stream is then sent to the compression train, where the remaining water impurity is removed and liquid CO_2 with high purity (≥98%) is produced.

2.4.2. Option 2: Oxy-Fuel Combustion

The primary downside to using the solvent-based post-combustion capture approach is that it has a very high parasitic load, which contributes to significant efficiency loss. One proposed alternative is the oxy-fuel combustion process, in which the fuel is combusted in high-purity oxygen instead of air. An air separation unit is used to remove nitrogen and other impurities from the air and produce the oxygen. Thus, the exhaust gas produced from oxy-combustion consists of mainly CO_2 and steam that can be separated in a solvent-free process (by condensing out the water) [59]. Although the ASU is energy intensive, the CO_2 capture step requires little energy, and the process as a whole should have a higher efficiency than traditional post-combustion carbon capture.

The oxy-fuel process used in this work (shown in Figure 6 with details in Table 5) is based on the process of Tan et al. [41], who developed a 0.3 MWh_{th} pilot plant constructed in the CANMET energy center. In this process, the oxy-combustion is performed in a boiler where the heat is used to make steam for the steam cycle, the only source of power generation in this scenario. The oxy-combustion is performed at high pressure and is not expanded, such that the CO2 is captured at high pressure, which greatly reduces compression costs. Note that some of the captured CO_2 is recycled and used as a diluent, such that the feed oxygen composition and combustion mechanism are similar to traditional air combustion [41, 60, 61]. In this work, all unit operations are modeled using standard models for the pump, turbines, heat exchangers, and flash drum, and the RGibbs model was used for the combustor (this model assumes chemical equilibrium).

2.4.3. Options 3 and 4: Chemical Looping Combustion

Chemical looping combustion is another power generation alternative that is also designed to avoid the large parasitic energy loads of solvent-based CO_2 capture by keeping nitrogen separate from the fuel. However, in this process, oxygen is introduced to the fuel using a solid oxide as an oxygen carrier. The process works as shown in Figure 7 by taking solid metal particles and reacting with air to produce the metal oxide, which is easily separated from the remaining air. The metal oxides are then reacted with the fuel gas in a second reactor, producing heat, the exhaust gas (CO_2 and steam), and more solid metals for reuse. The hot, depleted air is expanded in a turbine for power production, and additional waste heat from the hot air and the hot combustion exhaust is used to produce steam in a steam cycle for additional power. Like oxy-fuel combustion, the chemical looping combustion reactors operate at high pressure such that CO_2 can also be captured via water condensation in a similar manner, reducing downstream compression costs considerably.

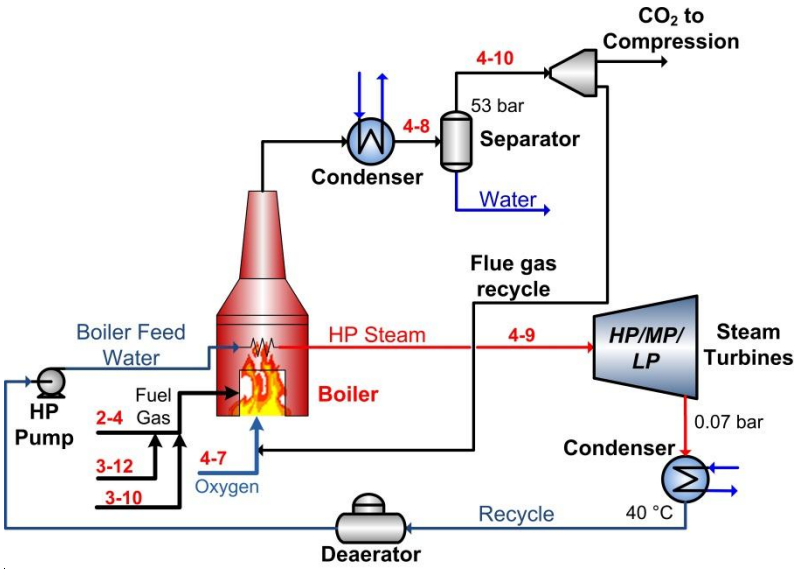

Figure 6. Section 4 Option 2: Power generation with Oxy-fuel combustion

Nickel-oxide and iron-oxide were investigated as two possible oxygen carriers, since it is not immediately obvious which would be better. Prior experimental test results by Cho et al. [62] and Adanez et al. [63] have shown that NiO has one of the highest reaction rates with a relatively high lifespan and low circulation rate. On the other hand, iron-oxide is less expensive than most other metals while having relatively high activity [64]. Lyngfelt tested both Fe and Ni loops successfully for 4000 hours of continuous operation with almost 100% CO_2 capture [65]. Linderholm et al. [66] and Kolbitsch et al. [52, 53] have also analyzed the operability of 10-kW and 120-kW Ni-based demonstration plants respectively and achieved promising results.

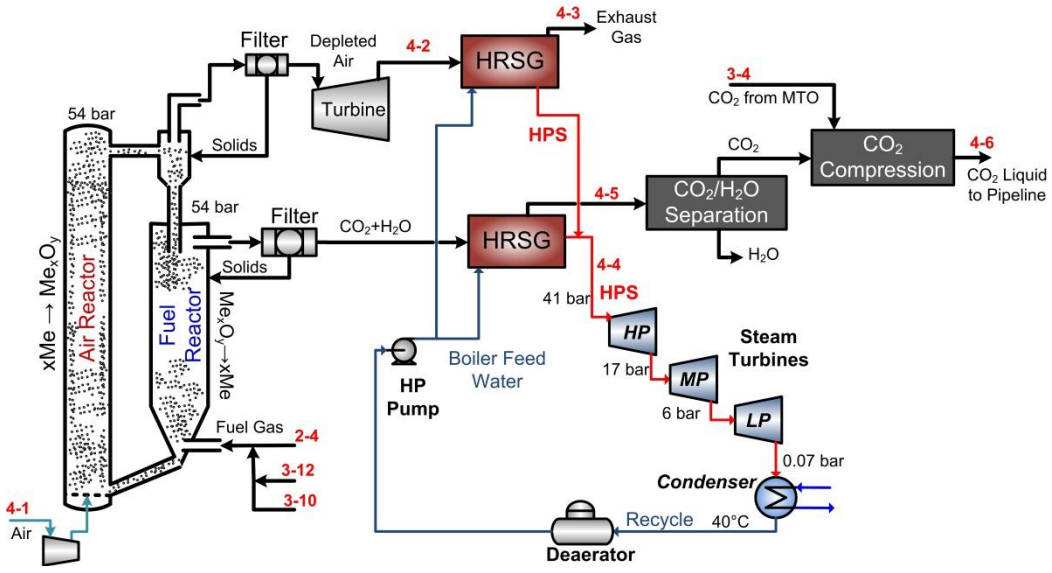

Figure 7. Section 4 Options 3 and 4: Power generation with Chemical looping combustion based on sub-pilot plant constructed by Ishida et al. [42, 43].

The main reactions of the fuel reactor and air reactor for each metal are listed as follows:

Nickel oxide [51]:

Fuel reactor: $C_xH_y + [(4x + y)/2]NiO \rightarrow xCO_2 + y/2H_2O + [(4x + y)/2]Ni$ (4)

$$CO + NiO \rightarrow CO_2 + Ni \quad (5)$$

$$H_2 + NiO \rightarrow H_2O + Ni \quad (6)$$

Air reactor:

$$2Ni + O_2 \rightarrow 2NiO \quad (7)$$

Iron Oxide [67]:

Fuel reactor: $C_xH_y + \left[(6x + \frac{3}{2}y)/3\right] Fe_2O_3 \rightarrow xCO_2 + y/2H_2O + [(12x + 3y)/3]FeO$ (8)

$$CO + Fe_2O_3 \rightarrow CO_2 + 2FeO \quad (9)$$

$$H_2 + Fe_2O_3 \rightarrow H_2O + 2FeO \quad (10)$$

Air reactor:

$$4FeO + O_2 \rightarrow 2Fe_2O_3 \quad (11)$$

In this work, Aspen Plus was used to simulate the different unit operations for both metal oxide options. Standard Aspen Plus models for all of the unit operations were used with design conditions shown in Table 5. The two chemical looping reactors were modeled assuming chemical equilibrium (RGibbs). Note that due to a lack of available data and the complexity of the system, the model did not consider leakage of solids or gases from the system or the effects of carrying spent solid particles (unusable) along with the useable ones. However, the different degradation rates and associated replacements costs were reflected in the economic analysis since the rate of catalyst replacement and costs were significantly different for the two oxides considered. If the effects of leakage or inert particles on the mass or energy balances were considered, one would expect the system performance to be slightly lower than the results reported, but should not deviate too significantly such that we can still make useful comparisons with Options 1 and 2 in this study.

2.5. Economic Analysis

The profitability of each process was determined by computing the net present value (NPV) as the primary economic indicator. Capital costs were determined from published sources wherever possible, such as for the reformer section, MeOH synthesis section, power generation section and carbon sequestration units [8, 21]. The capital costs of other units which did not have available cost data were estimated using the Aspen Icarus software package. This tool is commonly used to predict the capital cost of common chemical engineering unit operations and is updated regularly. In this work, it was used to predict the capital costs of individual unit operations such as pumps, compressors, and distillation columns which were not included in the sections listed previously. Table 6 lists all economic analysis parameters, market prices and assumptions for calculating the net present value (NPV) of all design cases, with citations to justify each parameter included in that table. Note that the utility and market prices shown are those used only for “base-case” calculations. Since prices vary from place to place and change somewhat unpredictably in the future, a sensitivity analysis which includes the effects of changes in price is discussed in section 4. All financial parameters, such as interest rates, are chosen based on recommendations of prior work. Other business related expenses such as labor, overhead, laboratory operations, and maintenance are included using estimate formulas common to most analyses of this type. A detailed listing of the costs of each line item for each specific design option can be found in the supplementary material-section 2. Although all of these parameters can change from case to case, an extensive sensitivity analysis of all parameters considered is outside

the scope of this work. However, even though there is uncertainty in the exact values of the NPV, the parameters are applied equally to all process variants and so meaningful conclusions can be made about the relative comparison of one process option to another.

Table 6. Base-case market prices and economic assumptions.

Feeds and products prices	
Natural gas & Ethane prices, $/MMBtu	3.88, [68]
NiO (commercial grade, 76% wt.), $/kg	20, [69]
NiO Disposal Cost, $/kg	5 (1)
NiO life span, hours	10000, [63]
Fe_2O_3 (commercial grade, 96% wt.), $/kg	1.44, [70]
Fe_2O_3 Disposal Cost, $/kg	0.36 (1)
Fe_2O_3 life span, hours	3000, [51] (page 203)
Electricity, ¢/kWh	5.67, [71]
MeOH price, $/tonne	482, [72]
DME, $/tonne	962, [25]
Propylene, $/tonne	1340, [73]
Ethylene, $/tonne	1424, [74]
Economic assumptions, [8, 75]	
Plant capacity (shale gas inlet rate)	1111 MW, LHV
Operation time (hr/year)	8760
Capacity factor	85%
Chemical engineering plant cost index	574.3 [76]
Plant lifetime (year)	30
Loan lifetime (year)	30
Interest rate on loan	9.5%
Debt percentage	50%
Inflation	2.79%
Federal + state tax rate	40%
Equity return rate	20%
NPV calculation elements, [75]	
Indirect cost	20% Fixed capital cost
Working capital cost	15% Total investment
Operating labor	10% Total production cost
Direct supervisory and clerical labor	10% Operating labour
Utilities	10% Total product cost
Maintenance and repairs	5% Fixed capital investment
Operating supplies	10% Maintenance and repair
Laboratory charges	10% Operating labour
Plant-overhead	50% of cost for operating labour, supervision, and maintenance
Administrative costs	15% of cost for operating labor, supervision, and maintenance
R&D, distribution and selling costs	4% of total product cost

(1) Due to lack of published data, assumed to be 25% of the metal-oxide price.

2.6. Process Optimization

For each process variant, three design variables were subject to optimization, as noted in Figure 3: the recycle ratio of unreacted gas sent to the MeOH reactor, the split ratio of MeOH which is sent to the MTO section (stream 2-7), and the split ratio of the MeOH stored as the final product (stream 2-8). Other process variables are adjusted to either meet the process constraints and product specifications (which are listed in Tables 2-5), or selected based on suggested values in literatures. The feasibility range of all decision variables is fixed between 1% and 99%. Bounds of 0% and 100% were not used in order to avoid simulation problems in the software associated with zero flows. Instead, if the lower bound of 1% on a variable was reached, the simulation was reconstructed manually using 0% and adjusting the others proportionally (where in some cases the corresponding process section was eliminated), and if it improved the objective function, it was taken as the final result for that instance. A similar technique was used for 99%, which was reconstructed manually using 100%.

Because there were only three decision variables, a coarse-grain method (an exhaustive search over a grid) was used to sample the decision space in three dimensions for each design variant. For example, the effect of the recycle ratio and the ratio of MeOH to the MTO section are shown in Figure 8 for two different MeOH to MTO ratios. It can be seen that unlike the low olefin production ratio (Figure 8a), the optimum MeOH to DME ratio is between 20-40% in the high olefin production scenario (Figure 8b). In addition, the influence of electricity, MeOH, DME and olefin market price fluctuations as a function of different process variables are depicted in Figure 9.

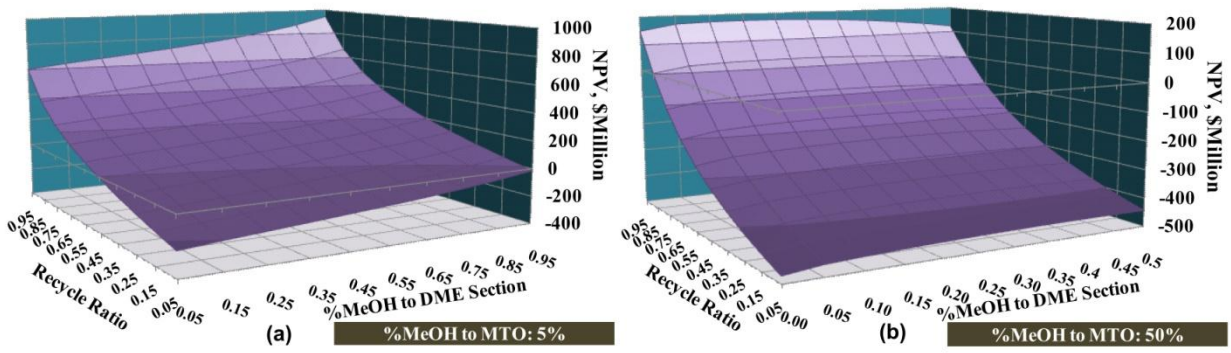

Figure 8. Effect of recycle ratio of unreacted gases to the methanol synthesis reactor and %MeOH to DME section on the NPV of plant at (a) low olefin (5%); (b) high olefin (50%) production ratios.

The sensitivity analysis shown in Figures 8 and 9 illustrate the impact of the main three decision variables on the NPV of plant at different market prices. Due to the relative long run time required per simulation (approximately one minute), the spacing between sample points was too large to sufficiently locate an optimum in a reasonable amount of time. The built-in Aspen Plus optimization tool was also found to be insufficient and improved the results only trivially compared to the coarse-grain method, even when starting from a variety of different initial conditions.

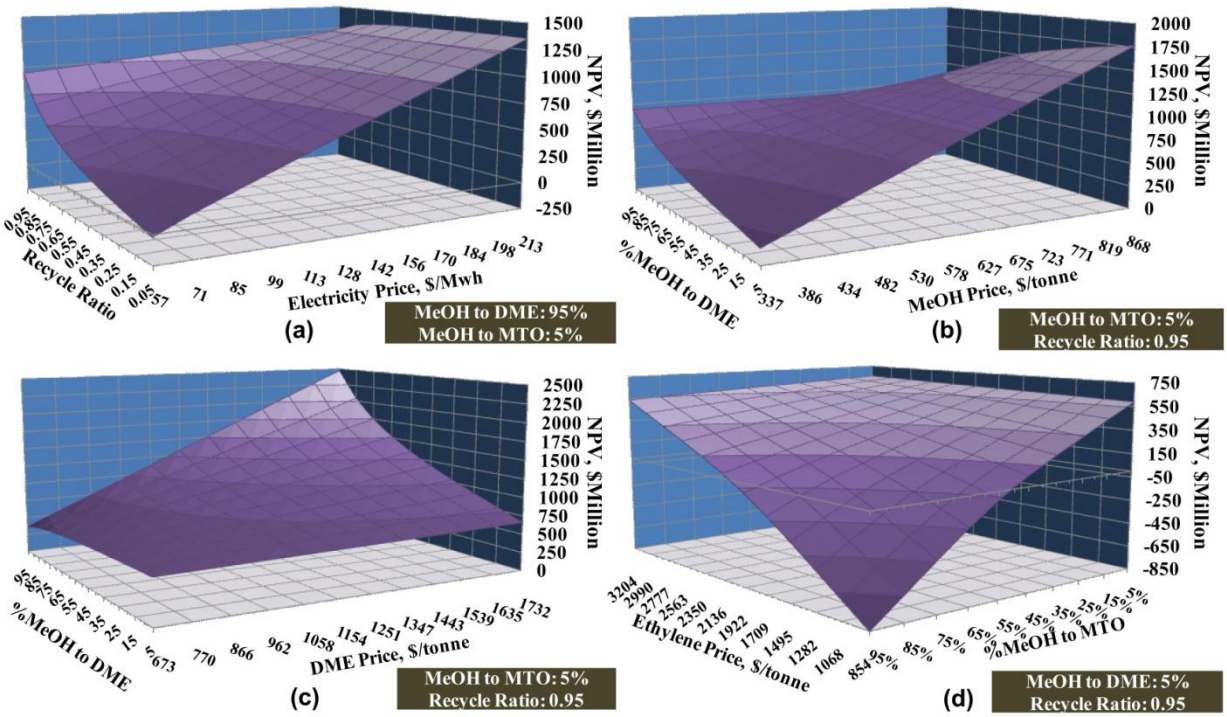

Figure 9. The NPV of plant at different market prices and selected decision variables changes.

Instead, three heuristic-based, derivative-free black box optimization algorithms were considered, namely particle swarm optimization, genetic algorithms, and simulated annealing. These are stochastic methods which use different strategies of exploring the decision variable space broadly at first and then later exploring promising subspaces in more and more depth. Eventually, the algorithms terminate once no more improvements can be found, and the best known point is usually locally optimal within tolerances, with a good chance that it is also the global optimal if the problem is not too "bumpy" and the heuristics were chosen correctly. Fortunately, finding the true optimum point is not critical to this work, and since the coarse-grain method samples points across the entire range of the state space, suboptimum results are expected to deviate from the true global optimum by only small amounts. These algorithms were implemented in Matlab and were coupled with the Aspen Plus simulations through the Excel interface. The three algorithms were used on a subset of cases to determine which derivative-free algorithm was the most promising. Standard algorithms have been used for each optimization technique and have not been detailed here for brevity. However, the heuristic parameters chosen for each algorithm are listed and referenced in the supplementary material-section 2. Particle swarm optimization was found to give the best results in all test cases, and so this algorithm was chosen for all remaining cases used in this study.

Several objective functions were used: maximizing the NPV, maximizing the power production, maximizing the olefin production, and maximizing the olefin production with the added constraint that the NPV must be non-negative (the constraint was implemented by adding a huge penalty to the objective function when violated). These four objective functions were run for each of the three process variants for each of the four shale gas types, and for each of these the particle swarm optimization was rerun a total of 10 times using different initial guesses, to ensure that the exploration was sufficiently broad. Thus a total of 160 optimization runs were performed, requiring about 15 minutes each for a total of about 40 hours of computer processing time on a modern desktop PC.

3. Economic Results

Selected stream and energy conditions of each process section for each optimization scenario for the Fayetteville shale gas case, are shown in Table 7. Stream tables for the "Maximum olefin with non-negative NPV constraint" optimization scenario are shown in supplementary material-section 3. Furthermore, the NPV maximization results of the chemical looping combustion (both NiO and Fe_2O_3 oxygen carriers), oxy-fuel combustion and post-combustion technologies for Fayetteville shale gas are shown in Table 9. Looking at the results, the highest NPV is obtained at the base case prices (Table 6) when the split ratios and unreacted gas recycle ratio are such that DME production is maximized in the chemical looping and oxyfuel cases. It can also be seen that the NiO-CLC system achieved the highest NPV compared to other options. Although the efficiency of the post-combustion system is relatively high, its NPV is less than other systems due to its higher capital cost. This is mostly because this option requires an amine unit to absorb CO_2 from the exhaust gas at atmospheric pressure, which requires a high recirculation rate of the amine and subsequently large size of the CO_2 removal unit. It also needs a separate compressor to send the captured CO_2 to the CO_2 compression unit. As shown in Table 8, the optimal MeOH split ratio to the DME section is 70% in the post-combustion approach, which is lower than other configurations. This is due to the high energy demand of the reboiler of the CO_2 stripper column (Figure 5) which consumes most of the stream generated in the HRSG unit. Therefore, there is not sufficient steam generation to supply the energy demand of the DME purification column (Figure 3) when the MeOH-to-DME ratio is more than 70% without the import of utilities from external sources.

Table 7. Selected results of four different optimization scenarios (Fayetteville shale gas). The energy output is defined as the electricity produced plus the higher heating values of methanol, DME and olefins produced.

Optimization Scenario	***Maximum NPV***						***Maximum olefin***						
Stream No.	**1-1**	**2-8**	**2-10**	**3-9**	**3-14**	**4-6**	**Stream No.**	**1-1**	**2-8**	**2-10**	**3-9**	**3-14**	**4-6**
Description	**Shale Gas**	**MeOH**	**DME**	**Propylene**	**Ethylene**	**CO_2 Liquid**	**Description**	**Shale Gas**	**MeOH**	**DME**	**Propylene**	**Ethylene**	**CO_2 Liquid**
Temperature (°C)	30.0	-	56.0	-	-	30.0	Temperature (°C)	30.0	-	-	35.7	-51.8	30.0
Pressure (bar)	30.0	-	13.5	-	-	153.0	Pressure (bar)	30.0	-	-	15.0	10.0	153.0
Total Flow (kg/hr)	83363	-	76862	-	-	72830	Total Flow (kg/hr)	83363	-	-	8274	9474	72285
Energy Input, HHV	1232 MW		Energy Output, HHV		641.77 MW		Energy Input, HHV	1232 MW		Energy Output, HHV		268.10 MW	
Net Power Generation (Upstream of Pipeline)	27.0 MW		Net Power Generation (Downstream of Pipeline)		0 MW		Net Power Generation (Upstream of Pipeline)	11.2 MW		Net Power Generation (Downstream of Pipeline)		22.3 MW	
Power Consumption (MW)							*Power Consumption (MW)*						
Reformer	10.3		MeOH & DME Synthesis		2.4		Reformer	10.3		MeOH & DME Synthesis		4.3	
MTO process	0.0		Refrigeration		0.0		MTO process	4.5		Refrigeration		4.8	
Optimization Scenario	***Maximum Power***						***Maximum olefin with non-negative NPV constraint***						
Stream No.	**1-1**	**2-8**	**2-10**	**3-9**	**3-14**	**4-6**	**Stream No.**	**1-1**	**2-8**	**2-10**	**3-9**	**3-14**	**4-6**
Description	**Shale Gas**	**MeOH**	**DME**	**Propylene**	**Ethylene**	**CO_2 Liquid**	**Description**	**Shale Gas**	**MeOH**	**DME**	**Propylene**	**Ethylene**	**CO_2 Liquid**
Temperature (°C)	30.0	-	56.0	-	-	30.0	Temperature (°C)	30.0	-	56.0	35.7	-51.8	30.0
Pressure (bar)	30.0	-	13.5	-	-	153.0	Pressure (bar)	30.0	-	13.5	15.0	10.0	153.0
Total Flow (kg/hr)	83363	-	25483	-	-	172386	Total Flow (kg/hr)	83363	-	21038	6260	7168	67998
Energy Input, HHV	1232 MW		Energy Output, HHV		476.28 MW		Energy Input, HHV	1232 MW		Energy Output, HHV		409.21 MW	
Net Power Generation (Upstream of Pipeline)	274.3 MW		Net Power Generation (2nd)		0 MW		Net Power Generation (Downstream of Pipeline)	45.3 MW		Net Power Generation (2nd)		16.9 MW	
Power Consumption (MW)							*Power Consumption (MW)*						
Reformer	10.3		MeOH & DME Synthesis		1.2		Reformer	10.3		MeOH & DME Synthesis		4.4	
MTO process	0.0		Refrigeration		0.0		MTO process	3.4		Refrigeration		3.6	

Table 8. Comparison of the power generation options using Fayetteville shale gas.

Power Generation Option	Chemical Looping		Oxy-fuel Combustion	Post Combustion
	Iron-Oxide	Nickel-Oxide		
NPV, $Million	1138	1165	1026	709
Efficiency, %HHV	52.5	52.1	48.2	54.5
%CO_2 capture	100	100	100	90
Decision Variables				
Recycle ratio of unreacted gases	0.956	0.956	0.950	0.950
MeOH ratio to the MTO section	0.000	0.000	0.000	0.000
MeOH ratio to the DME section	1.000	1.000	1.000	0.700
Product Portfolio (%)				
Net electricity	5.0	4.2	1.0	11.1
MeOH	0.0	0.0	0.0	47.2
DME	95.0	95.8	99.0	41.7
Olefins	0.0	0.0	0.0	0.0
Capital investment, $Million	565	509	535	714

3.1. Different Feed Compositions

The thermal efficiency and NPV results of various scenarios are shown in Table 9 for each type of shale gas and conventional pipeline gas using NiO-CLC as the power generation configuration since it had the highest NPV. In addition, the breakdowns of products are shown in this table based on their energy content. In the first scenario, the objective function was to maximize the NPV of the process. It can be seen from the optimization results that most of the output must be DME for all types of shale gases. In the second and fourth scenarios, the objective function was to maximize the olefins production rate. Their difference is that there is an NPV constraint in the fourth scenario, which must always be non-negative. Therefore, this scenario shows that the maximum possible olefins production while still having a profitable plant is between 45-54%, depending on the gas type. In the third scenario, the objective function was to maximize the power output of our proposed polygeneration plant. The maximum power generation is around 60% of the output in this scenario.

Table 9. Comparison of optimization results different shale gases at the same energy input (1111 MW) and with NiO-CLC as the selected power generation approach.

Optimization Scenario	**Maximum NPV**					**Maximum olefin**				
Gas Type	Marcellus	Fayetteville	New Albany	Haynesville	Conventional Gas	Marcellus	Fayetteville	New Albany	Haynesville	Conventional Gas
NPV, $Million	1139	1165	1158	1177	1143	-813	-769	-746	-728	-803
%HHV	51.9	52.1	51.8	52.1	52.5	21.9	22.0	22.5	22.7	22.8
Product portfolio										
%Power	4.5	4.2	4.3	4.2	4.3	14.3	11.7	12.5	12.9	18.5
%MeOH	0.0	0.0	0.0	0.0	0.0	0.0	0.0	0.0	0.0	0.0
%DME	95.5	95.8	95.7	95.8	95.7	0.0	0.0	0.0	0.0	0.0
%Olefins	0.0	0.0	0.0	0.0	0.0	85.7	88.3	87.5	87.1	81.5
Capital, $Million	519	509	503	501	558	694	678	684	676	705
Optimization Scenario	**Maximum power**					**Maximum olefin with non-negative NPV constraint**				
Gas Type	Marcellus	Fayetteville	New Albany	Haynesville	Conventional Gas	Marcellus	Fayetteville	New Albany	Haynesville	Conventional Gas
NPV, $Million	28	30	38	35	39	0	0	0	0	0
%HHV	38.8	38.8	38.7	38.7	40.3	33.7	33.3	33.1	32.9	34.8
Product portfolio										
%Power	57.9	57.4	56.1	56.6	57.5	15.8	14.8	13.4	13.2	20.1
%MeOH	0.0	0.0	0.0	0.0	0.0	0.0	0.0	0.0	0.0	0.0
%DME	42.1	42.6	43.9	43.4	42.5	43.5	41.1	41.4	40.8	40.7
%Olefins	0.0	0.0	0.0	0.0	0.0	40.7	44.1	45.3	45.9	39.2
Capital, $Million	530	536	539	538	584	681	666	670	661	698

3.2. Olefins Production Cost

The effect of changing the olefin production ratio on its production cost is shown in Figure 10. The olefin production of traditional cracking processes varied between 0.44-1.3 $/kg in 2012, depending on feedstock type and price [77]. It can be seen that the production cost of the proposed novel system is lower than the average production cost of commercial naphtha cracking and ethane cracking plants when the olefin production ratio is around 44% and 33% of output respectively. The calculated production cost of olefins is the total plant annualized cost subtracted by the revenue from other products. Therefore, its value can be negative when the credit from other products is more than the total cost of plant.

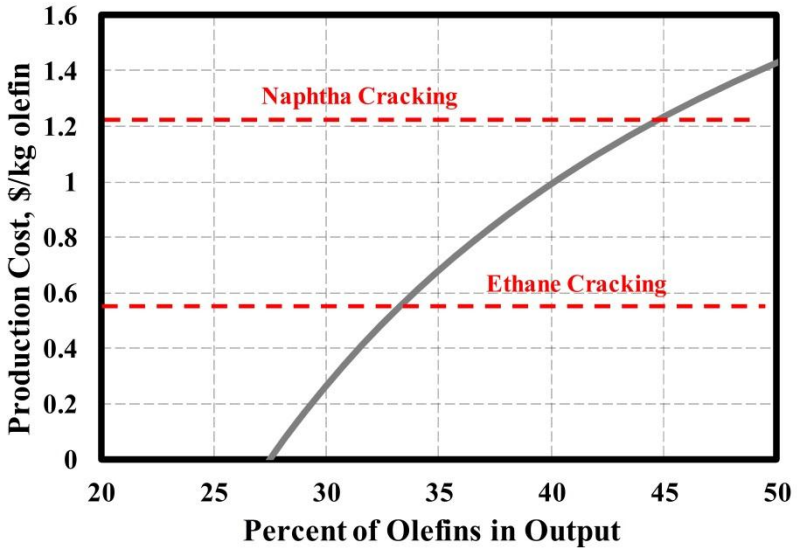

Figure 10. Sensitivity analysis of olefin production cost as a function of olefin production ratio (Fayetteville shale gas).

3.3. Sensitivity Analysis- Effect of MeOH and DME Prices

A sensitivity analysis was performed to determine how changes in the MeOH and DME prices affect the optimization results. For each set of MeOH and DME prices, the optimization was repeated using the maximum NPV objective function, resulting in a potentially different optimal configuration of recycle and product ratios. As shown in Figure 11a, the design with the maximum NPV is always positive when the MeOH price is $300/tonne (60% of its base case value) or more. Furthermore, the maximum NPV is always positive when the DME price is $577/tonne (60% of its base case price) or more. Figure 11b depicts a "price map" of the optimal product portfolios depending on the market prices. For example, maximizing the amount of olefins produced is the most profitable choice when MeOH prices are below about $150/tonne and DME prices are below about $300/tonne (the lower-left corner of Figure 11b). Above those prices, either maximum DME production or maximum MeOH production is the most profitable choice depending on the prices, corresponding to the upper left and lower right regions of the diagram, respectively.

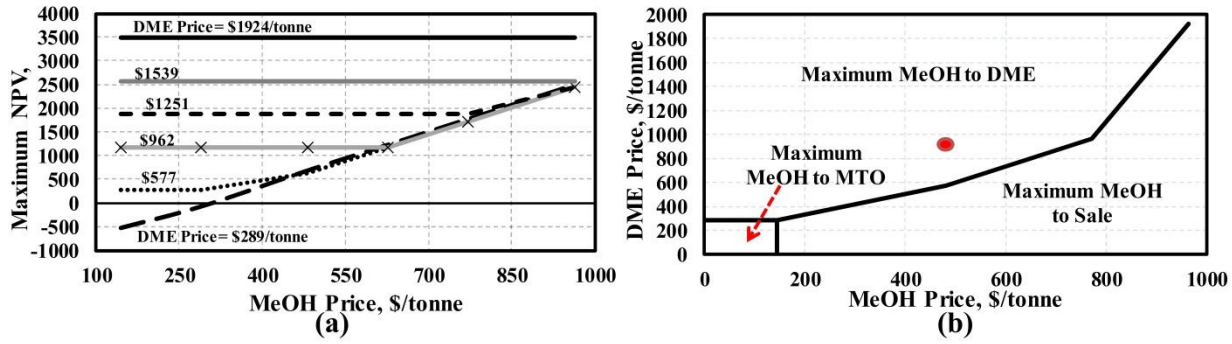

Figure 11. Effect of MeOH and DME price on the maximum NPV of process (Fayetteville shale gas). The location of the chosen base case market conditions is indicated as a red circle.

3.4. Sensitivity Analysis- Effect of Olefins Prices

Similarly, the effect of varying the price of olefins (ethylene and propylene) on the maximum NPV is shown in Figure 12. It is assumed that the propylene price changes at the same ratio as the ethylene price varies compared to their base case prices (Table 6). It can be seen that the NPV of the process is always positive regardless the price of olefins and DME products when methanol and electricity prices are at their base case market conditions. The reason is that at low olefins and DME prices, the maximum methanol production option is favoured over the others as shown in Figure 12b. Similarly, maximum DME or maximum olefin production is favoured for relatively high DME or olefin prices (the upper left and lower right regions of Figure 12b). However, when both DME and olefin prices are high, a mixture of DME and olefin products is actually more profitable than maximizing just one.

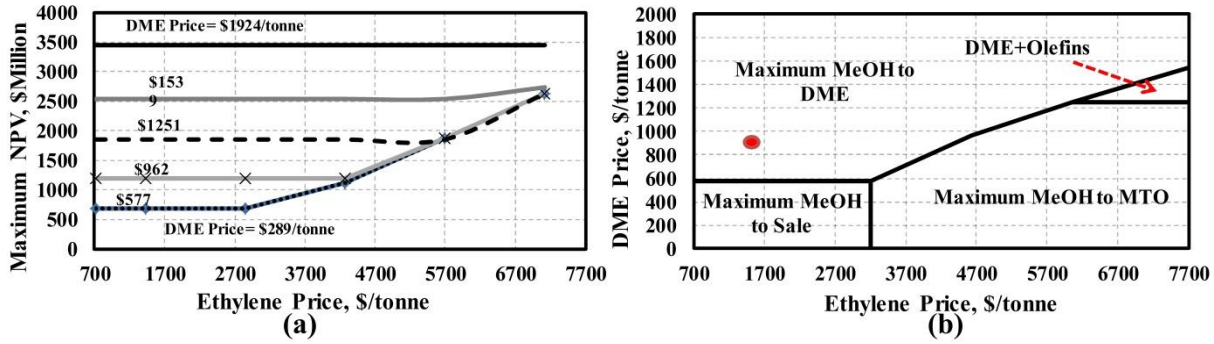

Figure 12. Effect of olefins and DME prices on the maximum NPV of process (Fayetteville shale gas). The base case prices are marked with a red circle.

4. Conclusion

In this work, a process (with many variants) to co-produce some combination of olefins, electricity, DME, and methanol using conventional natural gas or shale gas as the feedstock with little-to-zero direct CO_2 emissions was presented. Five different gas compositions, four different power generation options, and a variety of product portfolios were considered. Each process (including upstream and downstream sections for the shale gas cases) is self-sufficient, needing no external import of energy or utilities except for the primary feedstock, air, and water. In addition, 90-100% of the CO_2 produced can be captured from both sections of each process (where applicable) using different techniques depending on the advanced power generation technique. Because no utilities are imported, the direct and indirect emissions associated with each process are very small, except for the recovery and transport of the natural gas itself.

The simulation and techno-economic analysis results showed that the CLC technology with nickel oxide was not only the most profitable choice compared to the other power generation options, but it had essentially zero CO_2 emissions as well. The results also showed that the composition of the feed gas had small but measurable effects on the product portfolio and economics, meaning that some types of gas might be more profitable to use than others, but all of those considered were still suitable. The results of the sensitivity analysis showed that it in most market conditions, it was usually optimal for only one of methanol, DME, or olefins to be co-generated along with electricity. However, the co-production of DME and olefins was optimal for some cases with very high product prices. At current (base case) market conditions, olefin production was not favored. However, using the polygeneration

concept, it is possible to produce a mixture of olefins and electricity with 100% CO_2 capture in current market conditions at costs similar to naphtha or ethane cracking without any CO_2 capture. Thus, the proposed process may be a promising way of displacing traditional olefin production using abundant natural gas sources at similar costs but with significantly reduced environmental impact.

Nomenclature

Abbreviations

ASU	Air separation unit
CLC	Chemical looping combustion
DGA	Diglycolamine
DME	Dimethyl ether
HHV	Higher heating value
HRSG	Heat recovery steam generator
LHV	Lower heating value
MDEA	Methyl diethanolamine
NPV	Net present value
PSO	Particle swarm optimization

Notations

C_i	Concentration of component *i*, kmol/m^3
$K_{eq,i}$	Equilibrium constant of reaction *i*
k_i	Rate constant of reaction *i*
K_i	Adsoption constant *i*
p_i	Partial pressure of component *i*, bar
r_i	Rate of reaction *i*, kmol/kg$_{cat}$.sec
R	Gas constant, 8.314 kj/kmol.K
T	Temperature, K

References

[1] J.-K. Bok, H. Lee, S. Park. Robust investment model for long-range capacity expansion of chemical processing networks under uncertain demand forecast scenarios. Computers & Chemical Engineering. 22 (1998) 1037-49.
[2] T.A. Adams II. Challenges and Opportunities in the Design of New Energy Conversion Systems. in: J.D.S. Mario R. Eden, P.T. Gavin, (Eds.), Computer Aided Chemical Engineering. Elsevier2014. pp. 5-14.
[3] T. Ren, M.K. Patel, K. Blok. Steam cracking and methane to olefins: Energy use, CO_2 emissions and production costs. Energy. 33 (2008) 817-33.
[4] T. Benchaita. Greenhouse Gas Emissions from New Petrochemical Plants. TECHNICAL NOTE, No IDB - TN - 562. (2013).
[5] L. Gao, H. Li, B. Chen, H. Jin, R. Lin, H. Hong. Proposal of a natural gas-based polygeneration system for power and methanol production. Energy. 33 (2008) 206-12.
[6] X. Zhang, T. Gundersen, S. Roussanaly, A.L. Brunsvold, S. Zhang. Carbon chain analysis on a coal IGCC — CCS system with flexible multi-products. Fuel Processing Technology. 108 (2012) 146-53.
[7] C.A. Floudas, J.A. Elia, R.C. Baliban. Hybrid and single feedstock energy processes for liquid transportation fuels: A critical review. Computers and Chemical Engineering. 41 (2012) 24–51.
[8] T.A. Adams II, P.I. Barton. Combining coal gasification and natural gas reforming for efficient polygeneration. Fuel Processing Technology. 92 (2011) 639-55.
[9] T.A. Adams II, P.I. Barton. Combining coal gasification, natural gas reforming, and solid oxide fuel cells for efficient polygeneration with CO_2 capture and sequestration. Fuel Processing Technology. 92 (2011) 2105-15.
[10] C.-C. Cormos. Assessment of flexible energy vectors poly-generation based on coal and biomass/solid wastes co-gasification with carbon capture. International Journal of Hydrogen Energy. 38 (2013) 7855-66.

[11] Y. Man, S. Yang, J. Zhang, Y. Qian. Conceptual design of coke-oven gas assisted coal to olefins process for high energy efficiency and low CO_2 emission. Applied Energy. 133 (2014) 197-205.
[12] D. Hussain, D.A. Dzombak, P. Jaramillo, G.V. Lowry. Comparative lifecycle inventory (LCI) of greenhouse gas (GHG) emissions of enhanced oil recovery (EOR) methods using different CO_2 sources. International Journal of Greenhouse Gas Control. 16 (2013) 129-44.
[13] H.C. F. Ju, X. Ding, H. Yang, X. Wang, S. Zhang, Z. Dai. Process simulation of single-step dimethyl ether production via biomass gasification. Biotechnology Advances. 27 (2009) 599-605.
[14] T.A. Semelsberger, R.L. Borup. Thermodynamic equilibrium calculations of hydrogen production from the combined processes of dimethyl ether steam reforming and partial oxidation. Journal of Power Sources. 155 (2006) 340-52.
[15] T.A. Semelsberger, R.L. Borup, H.L. Greene. Dimethyl ether (DME) as an alternative fuel. Journal of Power Sources. 156 (2006) 497–511.
[16] S.P. Pyl, C.M. Schietekat, M.-F. Reyniers, R. Abhari, G.B. Marin, K.M. Van Geem. Biomass to olefins: Cracking of renewable naphtha. Chemical Engineering Journal. 176–177 (2011) 178-87.
[17] P.S. Rezaei, H. Shafaghat, W.M.A.W. Daud. Production of green aromatics and olefins by catalytic cracking of oxygenate compounds derived from biomass pyrolysis: A review. Applied Catalysis A: General. 469 (2014) 490-511.
[18] W. Kaminsky, B. Schlesselmann, C. Simon. Olefins from polyolefins and mixed plastics by pyrolysis. Journal of Analytical and Applied Pyrolysis. 32 (1995) 19-27.
[19] C.C. Chen, P.M. Mathias. Applied thermodynamics for process modeling. AIChE Journal. 48 (2002) 194-200.
[20] K. Bullin, P. Krouskop. Composition Variety Complicates Processing Plans for US Shale Gas. Bryan Research and Engineering Inc report. (2009).
[21] J.L. Haslbeck, N.J. Kuehn, E.G. Lewis, L.L. Pinkerton, J. Simpson, M.J. Turner, et al. Cost and Performance Baseline for Fossil Energy Plants Volume 1: Bituminous Coal and Natural Gas to Electricity, DOE. National Energy Technology Laboratory (NETL). (2010).
[22] T.A. Adams II, P.I. Barton. High-efficiency power production from natural gas with carbon capture. Journal of Power Sources. 195 (2010) 1971-83.
[23] K.M. Vanden bussche, G.F. Froment. A steady-state kinetic model for methanol synthesis and the water gas shift reaction on a commercial $Cu/ZnO/Al_2O_3$ catalyst. Journal of Catalysis. 161 (1996) 1-10.
[24] Methanol Industrial Grade, http://www.alibaba.com/product-detail/2012-Methanol-99-5-_551002733.html.
[25] DiMethyl Ether, http://www.alibaba.com/product-detail/DiMethyl-Ether_1659793013.html.
[26] G. Bercic, J. Levec. Catalytic dehydration of methanol to dimethyl ether. Kinetic investigation and reactor simulation. Industrial & Engineering Chemistry Research. 32 (1993) 2478-84.
[27] Y. Khojasteh Salkuyeh, T.A. Adams II. A new power, methanol, and DME polygeneration process using integrated chemical looping systems. Energy Conversion and Management. 88 (2014) 411-25.
[28] A. Taheri Najafabadi, S. Fatemi, M. Sohrabi, M. Salmasi. Kinetic modeling and optimization of the operating condition of MTO process on SAPO-34 catalyst. Journal of Industrial and Engineering Chemistry. 18 (2012) 29-37.
[29] Y.-J. Lee, S.-C. Baek, K.-W. Jun. Methanol conversion on SAPO-34 catalysts prepared by mixed template method. Applied Catalysis A: General. 329 (2007) 130-6.
[30] J.Q. Chen, A. Bozzano, B. Glover, T. Fuglerud, S. Kvisle. Recent advancements in ethylene and propylene production using the UOP/Hydro MTO process. Catalysis Today. 106 (2005) 103-7.
[31] S. Wilson, P. Barger. The characteristics of SAPO-34 which influence the conversion of methanol to light olefins. Microporous and Mesoporous Materials. 29 (1999) 117-26.
[32] D.A. Bell, B.F. Towler, M. Fan. Coal Gasification and its Applications. William Andrew Publishing, Boston, United States, 2011.
[33] F.J. Keil. Methanol-to-hydrocarbons: process technology. Microporous and Mesoporous Materials. 29 (1999) 49-66.
[34] Bahadori A., M. S. Estimating Design Parameters in Propane Refrigerant Systems. Pumps & Systems. (2007) 68-71.
[35] M. Mafi, M. Amidpour, S.M.M. Naeynian. Development in Mixed Refrigerant Cycles Used in Olefin Plants. Proceedings of the 1st Annual Gas Processing Symposium. Elsevier, Amsterdam, Netherland, 2009. pp. 154-61.
[36] GPSA. Engineering Data Book, 11th edition Gas Processors Suppliers Association, Oklahoma, United States, 1998.
[37] Ethylene, Polymer Purity, https://www.mathesongas.com/pdfs/products/Ethylene-Pure-Gas.pdf.
[38] Propylene, Polymer Grade, http://www.dow.com/productsafety/finder/pro.htm.
[39] M.R.M. Abu-Zahra, J.P.M. Niederer, P.H.M. Feron, G.F. Versteeg. CO_2 capture from power plants: Part II. A parametric study of the economical performance based on mono-ethanolamine. International Journal of Greenhouse Gas Control. 1 (2007) 135-42.
[40] B. Moghtaderi. Review of the Recent Chemical Looping Process Developments for Novel Energy and Fuel Applications. Energy & Fuels. 26 (2011) 15-40.
[41] Y. Tan, M.A. Douglas, K.V. Thambimuthu. CO_2 capture using oxygen enhanced combustion strategies for natural gas power plants. Fuel. 81 (2002) 1007-16.
[42] H. Jin, M. Ishida. A novel gas turbine cycle with hydrogen-fueled chemical-looping combustion. International Journal of Hydrogen Energy. 25 (2000) 1209-15.
[43] M. Ishida, M. Yamamoto, T. Ohba. Experimental results of chemical-looping combustion with $NiO/NiAl_2O_4$ particle circulation at 1200 °C. Energy Conversion and Management. 43 (2002) 1469-78.

[44] R.C. Wilcock, J.B. Young, J.H. Horlock. The Effect of Turbine Blade Cooling on the Cycle Efficiency of Gas Turbine Power Cycles. Journal of Engineering for Gas Turbines and Power. 127 (2005) 109-20.
[45] J.B. Young, R.C. Wilcock. Modeling the Air-Cooled Gas Turbine: Part 2—Coolant Flows and Losses. Journal of Turbomachinery. 124 (2002) 214-21.
[46] J. Zhang, L. Ma, Z. Li, W. Ni. Modeling an Air-Cooled Gas Turbine of the Integrated Gasification Combined Cycle in Aspen plus. International Conference on Future Electrical Power and Energy Systems (ICFEPES). Elsevier Ltd., Sanya, China, 2012.
[47] M.R.M. Abu-Zahra, L.H.J. Schneiders, J.P.M. Niederer, P.H.M. Feron, G.F. Versteeg. CO_2 capture from power plants: Part I. A parametric study of the technical performance based on monoethanolamine. International Journal of Greenhouse Gas Control. 1 (2007) 37-46.
[48] D.H. Mackenzie, F.C. Prambil, C.A. Daniels, J.A. Bullin. Design & operation of a selective sweetening plant using MDEA. Energy Progress. 7 (1987).
[49] Y. Hu. CO_2 capture from oxy-fuel combustion power plants. Department of Chemical Engineering and Technology. KTH Royal Institute of Technology, Stockholm, Sweden, 2011.
[50] A.R. Smith, J. Klosek. A review of air separation technologies and their integration with energy conversion processes. Fuel Processing Technology. 70 (2001) 115-34.
[51] L.S. Fan. Chemical Looping Systems For Fossil Energy Conversions. John Wiley & Sons, Inc., , New Jersey, United States, 2010.
[52] P. Kolbitsch, J. Bolhàr-Nordenkampf, T. Pröll, H. Hofbauer. Operating experience with chemical looping combustion in a 120 kW dual circulating fluidized bed (DCFB) unit. International Journal of Greenhouse Gas Control. 4 (2010) 180-5.
[53] P. Kolbitsch, T. Pröll, J. Bolhar-Nordenkampf, H. Hofbauer. Design of a Chemical Looping Combustor using a Dual Circulating Fluidized Bed (DCFB) Reactor System. Chemical Engineering & Technology. 32 (2009) 398-403.
[54] J. Wolf, M. Anheden, J. Yan. Comparison of nickel- and iron-based oxygen carriers in chemical looping combustion for CO_2 capture in power generation. Fuel. 84 (2005) 993-1006.
[55] S. Naskar, K. Jana, S. De. Comparative performance study of CO_2 capture with Monoethyl and Diethyl Amines using Aspen Plus. International Journal of Emerging Technology and Advanced Engineering. 3 (2013) 490-7.
[56] G. Pellegrini, R. Strube, G. Manfrida. Comparative study of chemical absorbents in postcombustion CO_2 capture. Energy. 35 (2010) 851-7.
[57] J. Polasek, J. Bullin. Selecting amines for sweetening units. ENERGY PROGRESS. 4 (1984) 146-9.
[58] F.S. Manning, R.E. Thompson. Oilfield Processing of Petroleum Volume 1: Natural Gas. Pennwell Books, Oklahoma, United States, 1991.
[59] M.B. Toftegaard, J. Brix, P.A. Jensen, P. Glarborg, A.D. Jensen. Oxy-fuel combustion of solid fuels. Progress in Energy and Combustion Science. 36 (2010) 581-625.
[60] K. Tigges, F. Klauke, C. Bergins, K. Busekrus, J. Niesbach, M. Ehmann, et al. Oxyfuel combustion retrofits for existing power stations. The 33rd international technical conference on coal utilization & fuel systems Clearwater, Florida, USA2008.
[61] J. Hong, G. Chaudhry, J.G. Brisson, R. Field, M. Gazzino, A.F. Ghoniem. Analysis of oxy-fuel combustion power cycle utilizing a pressurized coal combustor. Energy. 34 (2009) 1332-40.
[62] P. Cho, T. Mattisson, A. Lyngfelt. Comparison of iron-, nickel-, copper- and manganese-based oxygen carriers for chemical-looping combustion. Fuel. 83 (2004) 1215-25.
[63] J. Adanez, A. Abad, F. Garcia-Labiano, P. Gayan, L.F. de Diego. Progress in Chemical-Looping Combustion and Reforming technologies. Progress in Energy and Combustion Science. 38 (2012) 215-82.
[64] B.M. Corbella, J.M. Palacios. Titania-supported iron oxide as oxygen carrier for chemical-looping combustion of methane. Fuel. 86 (2007) 113-22.
[65] A. Lyngfelt. Oxygen Carriers for Chemical Looping Combustion - 4000 h of Operational Experience. Oil Gas Sci Technol – Rev IFP Energies nouvelles. 66 (2011) 161-72.
[66] C. Linderholm, A. Abad, T. Mattisson, A. Lyngfelt. 160 h of chemical-looping combustion in a 10 kW reactor system with a NiO-based oxygen carrier. International Journal of Greenhouse Gas Control. 2 (2008) 520-30.
[67] P. Gayán, M.A. Pans, M. Ortiz, A. Abad, L.F. de Diego, F. García-Labiano, et al. Testing of a highly reactive impregnated Fe_2O_3/Al_2O_3 oxygen carrier for a SR–CLC system in a continuous CLC unit. Fuel Processing Technology. 96 (2012) 37-47.
[68] Henry hub spot, average wholesale price; Aug 2014. http://www.eia.gov/electricity/wholesale/.
[69] Nickel Monoxide, CAS No.: 1313-99-1, http://www.alibaba.com/product-gs/747545915/Factory_direct_sales_with_reasonable_price.html.
[70] Factory price of Iron Oxide (Fe_2O_3), CAS No.: 1309-37-1. http://wwwalibabacom/product-detail/factory-price-of-iron-oxide-fe2o3-_814503142html?s=p.
[71] Electricity wholesale price, Average 2014. http://www.eia.gov/electricity/wholesale/.
[72] Methanol Price, North America, October 2014, https://www.methanex.com/our-business/pricing.
[73] Platts Global Propylene Price Index, August 2014, http://www.platts.com/news-feature/2014/petrochemicals/pgpi/propylene.

[74] Platts Global Ethylene Price Index, August 2014, http://www.platts.com/news-feature/2014/petrochemicals/pgpi/ethylene.
[75] M. S. Peters, K.D. Timmerhaus. Plant Design and Economics for Chemical Engineers. 4th ed. McGraw-Hill, New York, United States, 1991.
[76] CEPCI. Chemical Engineering Plant Cost Index. Chemical Engineering. 121 (May 2014) 80.
[77] T. Roberts. Ethylene – Good Today, Better Tomorrow – A Year Later. Goldman Sachs Chemical Intensity Day. (2012).

Chapter 5, Supplementary 1

P-xy MeOH & DME Mixture

VLE 002

Experimental	Temperature		79.97906 C
No.	Liquid molt	Temperatu	Vapor mole fr	Total pressure (bar)
1	0	353.1291	0	22.43
2	0.083	353.1291	0.037	20.41
3	0.14	353.1291	0.055	19.44
4	0.251	353.1291	0.076	18
5	0.35	353.1291	0.098	16.55
6	0.443	353.1291	0.112	15.17
7	0.546	353.1291	0.131	13.44
8	0.637	353.1291	0.161	11.72
9	0.706	353.1291	0.182	10.27
10	0.73	353.1291	0.192	9.72
11	0.771	353.1291	0.216	8.76
12	0.833	353.1291	0.274	7.17
13	0.842	353.1291	0.287	6.89
14	0.867	353.1291	0.31	6.21
15	0.877	353.1291	0.329	5.65
16	0.919	353.1291	0.406	4.34
17	0.947	353.1291	0.502	3.52
18	0.979	353.1291	0.742	2.69
19	0.986	353.1291	0.786	2.21
20	1	353.1291	1	1.82

Reference:

Chang, E.; Calado, J. C. G.; Streett, W. B. J. Chem. Eng. Data, 1982, 27, 293
Vapor-liquid equilibrium in the system dimethyl ether + methanol from 0 to 180 c and at pressures to 6.7 mpa.

VLE 004

Experimental	Temperature		99.97437
No.	Liquid molt	Temperatu	Vapor mole fract	Total pressure (bar)
1	0	373.1244	0	32.56
2	0.073	373.1244	0.036	30.47
3	0.094	373.1244	0.047	29.79
4	0.18	373.1244	0.081	27.58
5	0.238	373.1244	0.1	26.2
6	0.314	373.1244	0.115	24.82
7	0.368	373.1244	0.13	23.51
8	0.429	373.1244	0.148	22.06
9	0.494	373.1244	0.165	20.75
10	0.56	373.1244	0.177	19.24
11	0.598	373.1244	0.188	18.2
12	0.648	373.1244	0.206	16.69
13	0.739	373.1244	0.26	13.93
14	0.784	373.1244	0.303	12.41
15	0.823	373.1244	0.336	11.17
16	0.838	373.1244	0.348	10.48
17	0.881	373.1244	0.424	8.69
18	0.922	373.1244	0.502	7.17
19	0.948	373.1244	0.609	5.79
20	0.967	373.1244	0.7	5.17
21	0.978	373.1244	0.772	4.62
22	1	373.1244	1	3.53

PR-BM (Aspen Plus)

TOTAL PRES	VAPOR MOLEFRAC Methanol	LIQUID MOLEFRAC Methanol
bar		
22.60526	0	0
21.02205	0.016871	0.0666666
19.61489	0.031868	0.1333333
18.33925	0.045609	0.2
17.16085	0.058567	0.2666667
16.05137	0.071162	0.3333333
14.98424	0.08382	0.4
13.93382	0.097041	0.4666667
12.87308	0.111483	0.5333333
11.7721	0.128115	0.6
10.59644	0.148516	0.6666667
9.305347	0.175546	0.7333333
7.849655	0.215121	0.8
6.169541	0.281965	0.8666667
4.191957	0.426146	0.9333333
1.82791	1	1

PR-BM

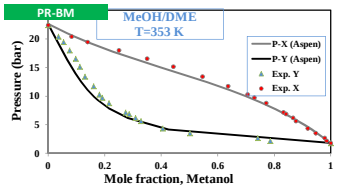

Ethylene Package (Aspen Plus)

TOTAL PRES	VAPOR MOLEFRAC METHANO	LIQUID MOLEFRAC METHANOL
bar		
22.52383	0	0
21.919	0.006594	0.025
21.34068	0.012853	0.05
20.78711	0.01882	0.075
20.25677	0.024535	0.1
19.75122	0.030032	0.125
19.25906	0.035336	0.15
18.78395	0.040475	0.175
18.32431	0.04548	0.2
17.87494	0.050361	0.225
17.44412	0.055152	0.25
17.02084	0.059871	0.275
16.60674	0.06454	0.3
16.20045	0.069179	0.325
15.80402	0.07382	0.35
15.40948	0.078471	0.375
15.0186	0.083163	0.4
14.62999	0.087925	0.425
14.24226	0.092787	0.45
13.85395	0.097783	0.475
13.46358	0.102951	0.5
13.06955	0.108336	0.525
12.67023	0.113992	0.55
12.26386	0.11998	0.575
11.8486	0.126377	0.6
11.42247	0.133276	0.625
10.98336	0.140791	0.65
10.529	0.149067	0.675
10.05698	0.158293	0.7
9.563079	0.168697	0.725
9.047912	0.180636	0.75
8.506564	0.194544	0.775
7.93573	0.211051	0.8
7.331839	0.231078	0.825
6.691031	0.256023	0.85
6.009133	0.288117	0.875
5.28164	0.331151	0.9
4.503685	0.392142	0.925
3.670023	0.485681	0.95
2.775003	0.647942	0.975
1.81255	1	1

Ethylene Package

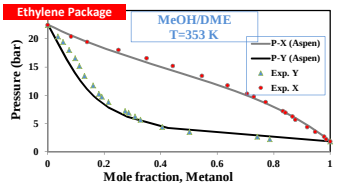

PR-BM (Aspen Plus)

TOTAL PRES	VAPOR MOLEFRAC Methanol	LIQUID MOLEFRAC Methanol
bar		
33.46041	0	0
31.01175	0.024391	0.0666666
28.86802	0.045426	0.1333333
26.93839	0.064444	0.2
25.16022	0.082302	0.2666667
23.48667	0.099666	0.3333333
21.87949	0.117164	0.4
20.30157	0.13548	0.4666667
18.71748	0.155487	0.5333333
17.08969	0.178428	0.6
15.37702	0.206273	0.6666667
13.53281	0.242462	0.7333333
11.50307	0.293776	0.8
9.224662	0.375873	0.8666667
6.623239	0.535263	0.9333333
3.611284	1	1

PR-BM

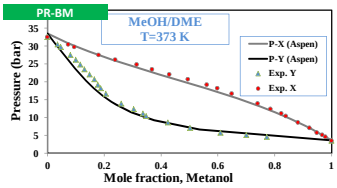

Ethylene Package (Aspen Plus)

TOTAL PRES	VAPOR MOLEFRAC METHANO	LIQUID MOLEFRAC METHANOL
bar		
33.39457	0	0
32.45087	0.009593	0.025
31.55387	0.018535	0.05
30.70468	0.026944	0.075
29.90152	0.034916	0.1
29.12541	0.042516	0.125
28.38023	0.049809	0.15
27.66232	0.056845	0.175
26.96845	0.063669	0.2
26.29574	0.070321	0.225
25.64596	0.076844	0.25
25.00564	0.083255	0.275
24.37944	0.089596	0.3
23.76541	0.095899	0.325
23.16148	0.102196	0.35
22.56563	0.108521	0.375
21.98082	0.114919	0.4
21.39591	0.121407	0.425
20.813	0.128033	0.45
20.23017	0.134843	0.475
19.64543	0.141887	0.5
19.05675	0.149222	0.525
18.46203	0.156916	0.55
17.85911	0.165047	0.575
17.24569	0.173709	0.6
16.61939	0.183018	0.625
15.9777	0.193113	0.65
15.31796	0.20417	0.675
14.63736	0.216409	0.7
13.93292	0.230118	0.725
13.20145	0.245671	0.75
12.43958	0.263572	0.775
11.64171	0.284497	0.8
10.80845	0.309466	0.825
9.933205	0.3399	0.85
9.011576	0.377996	0.875
8.038885	0.427293	0.9
7.010142	0.493868	0.925
5.920036	0.589118	0.95
4.762838	0.737224	0.975
3.532725	1	1

Ethylene Package

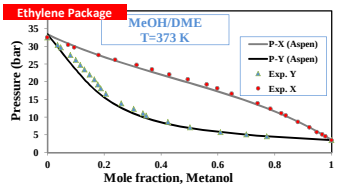

Chapter 5, Supplementary 1

P-xy MeOH & EtOH Mixture

Experimental		Temperature		24.99437 C
No.	Liquid mol	Temperatu	Vapor mole frac	Total pressure (bar)
1	0	298.1444	0	0.16916
2	0.0344	298.1444	0.0164	0.16604
3	0.1697	298.1444	0.0869	0.15365
4	0.2704	298.1444	0.1472	0.14442
5	0.3563	298.1444	0.2051	0.13657
6	0.3794	298.1444	0.2218	0.13451
7	0.4346	298.1444	0.264	0.12937
8	0.4437	298.1444	0.2712	0.12861
9	0.5157	298.1444	0.3322	0.12204
10	0.5865	298.1444	0.3989	0.11557
11	0.6121	298.1444	0.4248	0.11316
12	0.689	298.1444	0.5097	0.10628
13	0.7436	298.1444	0.577	0.10131
14	0.8871	298.1444	0.7888	0.08842
15	0.9569	298.1444	0.914	0.0823
16	1	298.1444	1	0.07859

Reference:

Kooner, Z. S.; Fenby, D. V. Aust. J. Chem., 1980, 33, 1943-6
Vapor pressure study of the deuterium exchange reaction in methanol + ethanol systems. equilibrium constant determination

PR-BM (Aspen Plus)		
TOTAL PRES	VAPOR MOLEFRAC EtOH	LIQUID MOLEFRAC EtOH
bar		
0.080836	1	1
0.086581	0.871828	0.9333333
0.092194	0.761085	0.8666667
0.097677	0.66425	0.8
0.103033	0.578663	0.7333333
0.108264	0.502271	0.6666667
0.113375	0.433463	0.6
0.118371	0.370948	0.5333333
0.123256	0.313678	0.4666667
0.128037	0.260781	0.4
0.132721	0.211525	0.3333333
0.137316	0.165278	0.2666667
0.14183	0.121486	0.2
0.146274	0.079649	0.1333333
0.150659	0.039301	0.0666666
0.154997	0	0

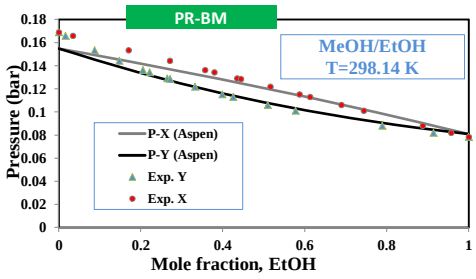

Ethylene Package (Aspen Plus)		
TOTAL PRES	VAPOR MOLEFRAC ETHANOL	LIQUID MOLEFRAC ETHANOL
bar		
0.168389	0	0
0.166721	0.015041	0.025
0.165033	0.029843	0.05
0.163327	0.04447	0.075
0.161601	0.058979	0.1
0.159855	0.073424	0.125
0.158087	0.08786	0.15
0.156297	0.102334	0.175
0.154483	0.116896	0.2
0.152644	0.131591	0.225
0.150779	0.146468	0.25
0.148886	0.16157	0.275
0.146965	0.176945	0.3
0.145013	0.192639	0.325
0.143031	0.208698	0.35
0.141017	0.225172	0.375
0.138969	0.24211	0.4
0.136889	0.259564	0.425
0.134773	0.277588	0.45
0.132623	0.296239	0.475
0.130438	0.315577	0.5
0.128217	0.335667	0.525
0.125959	0.356576	0.55
0.123665	0.378378	0.575
0.121336	0.401151	0.6
0.11897	0.424979	0.625
0.116568	0.449955	0.65
0.114131	0.476179	0.675
0.111658	0.503759	0.7
0.109152	0.532815	0.725
0.106611	0.563479	0.75
0.104038	0.595894	0.775
0.101433	0.63022	0.8
0.098797	0.666635	0.825
0.096131	0.705336	0.85
0.093438	0.746543	0.875
0.090717	0.790503	0.9
0.087971	0.837493	0.925
0.085201	0.887827	0.95
0.08241	0.941861	0.975
0.079598	1	1

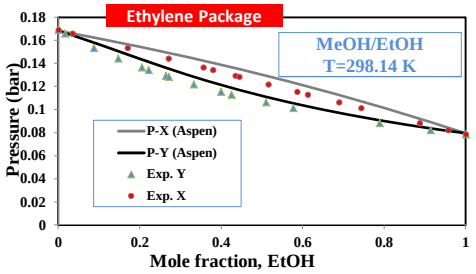

Chapter 5, Supplementary 1

P-xy DME & EtOH Mixture

Experimental		Temperature		80.1 C
No.	Liquid mol	Temperatu	Vapor mole fra	Total pressure (bar)
1	0.3641	353.25	0.0573	14.46
2	0.4088	353.25	0.0622	13.61
3	0.4258	353.25	0.0647	13.3
4	0.5151	353.25	0.0762	11.55
5	0.5506	353.25	0.0816	10.84
6	0.6003	353.25	0.0898	9.81
7	0.6824	353.25	0.1126	8.09

Reference:

Elbaccouch, M. M.; Elliott, J. R. J. Chem. Eng. Data, 2000, 45, 1080-1087
High-Pressure Vapor-Liquid Equilibrium for Dimethyl Ether + Ethanol and Dimethyl Ether + Ethanol + Wate

PR-BM (Aspen Plus)		
TOTAL PRES	VAPOR MOLEFRAC EtOH	LIQUID MOLEFRAC EtOH
bar		
22.66176	0	0
20.86951	0.009962	0.0666666
19.30428	0.018684	0.1333333
17.88247	0.026814	0.2
16.5505	0.034798	0.2666667
15.27166	0.04301	0.3333333
14.01731	0.051833	0.4
12.76562	0.061723	0.4666667
11.49848	0.073308	0.5333333
10.20059	0.087531	0.6
8.858718	0.105962	0.6666667
7.461189	0.131489	0.7333333
5.997615	0.17014	0.8
4.458663	0.23709	0.8666667
2.835924	0.384768	0.9333333
1.121812	1	1

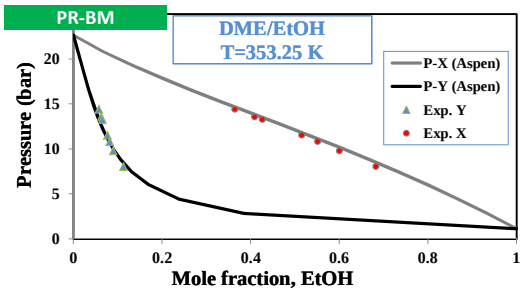

Ethylene Package (Aspen Plus)		
TOTAL PRES	VAPOR MOLEFRAC ETHANOL	LIQUID MOLEFRAC ETHANOL
bar		
22.58028	0	0
21.88775	0.003896	0.025
21.23432	0.007534	0.05
20.61492	0.010967	0.075
20.02491	0.014239	0.1
19.4597	0.017386	0.125
18.91767	0.02044	0.15
18.39002	0.023421	0.175
17.87745	0.026355	0.2
17.37603	0.029265	0.225
16.888	0.032165	0.25
16.407	0.03508	0.275
15.9327	0.038027	0.3
15.46353	0.041024	0.325
14.99806	0.044092	0.35
14.53494	0.047251	0.375
14.07296	0.050523	0.4
13.61097	0.053935	0.425
13.14791	0.057513	0.45
12.68278	0.061289	0.475
12.21464	0.0653	0.5
11.74261	0.069589	0.525
11.26583	0.074206	0.55
10.7835	0.079211	0.575
10.29485	0.08468	0.6
9.799152	0.090702	0.625
9.295696	0.097392	0.65
8.783804	0.104893	0.675
8.262823	0.113392	0.7
7.732124	0.123134	0.725
7.1911	0.134447	0.75
6.639164	0.147785	0.775
6.07575	0.163788	0.8
5.50031	0.183396	0.825
4.912314	0.208045	0.85
4.311248	0.24004	0.875
3.696617	0.283342	0.9
3.06794	0.345372	0.925
2.424754	0.441841	0.95
1.766608	0.612834	0.975
1.093072	1	1

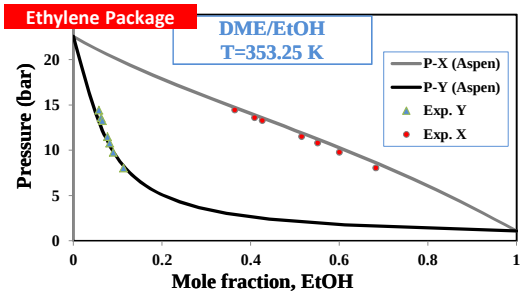

Chapter 5, Supplementary 1

P-xy Ethane & Propylene Mixture

Experimental		Temperature		-71.3892 C
		Temperat		
No.	Liquid mole	**ure (K)**	Vapor mole fra	Total pressure bar
1	0	201.7608	0	0.29864
2	0.024	201.7608	0.154	0.3733
3	0.145	201.7608	0.541	0.60795
4	0.21	201.7608	0.662	0.77594
5	0.292	201.7608	0.74	0.93459
6	0.364	201.7608	0.788	1.08791
7	0.421	201.7608	0.834	1.18124
8	0.525	201.7608	0.888	1.41455
9	0.676	201.7608	0.934	1.69986
10	0.783	201.7608	0.962	1.92384
11	0.915	201.7608	0.986	2.18382
12	1	201.7608	1	2.36114

Reference:

Hirata, M.; Suda, S.; Hakuta, T.; Nagahama, K. Mem. Fac. Technol., Tokyo Metrop. Univ., 1969, 19, 103-122 Light hydrocarbon vapor-liquid equilibria

PR-BM (Aspen Plus)		
TOTAL PRES	VAPOR MOLEFRAC Ethane	LIQUID MOLEFRAC Ethane
bar		
0.313963	0	0
0.462513	0.362072	0.0666666
0.607815	0.545806	0.1333333
0.750105	0.657363	0.2
0.889645	0.732628	0.2666667
1.026724	0.787106	0.3333333
1.161663	0.828598	0.4
1.294818	0.861456	0.4666667
1.426583	0.888305	0.5333333
1.557394	0.910826	0.6
1.687738	0.930144	0.6666667
1.818153	0.947047	0.7333333
1.949242	0.962106	0.8
2.081676	0.975744	0.8666667
2.216209	0.988289	0.9333333
2.353685	1	1

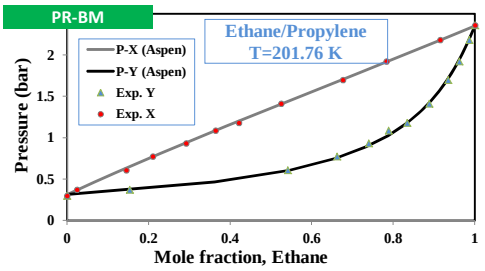

Ethylene Package (Aspen Plus)		
TOTAL PRES	VAPOR MOLEFRAC ETHAN-01	LIQUID MOLEFRAC ETHAN-01
bar		
2.32298	1	1
2.270386	0.996217	0.975
2.218255	0.992289	0.95
2.166057	0.988209	0.925
2.114067	0.983962	0.9
2.06227	0.979536	0.875
2.010652	0.974916	0.85
1.959202	0.970087	0.825
1.907905	0.965031	0.8
1.856752	0.95973	0.775
1.805732	0.954161	0.75
1.754834	0.948301	0.725
1.704051	0.942124	0.7
1.653372	0.9356	0.675
1.602792	0.928695	0.65
1.552301	0.921374	0.625
1.501894	0.913593	0.6
1.451564	0.905304	0.575
1.401304	0.896452	0.55
1.35111	0.886975	0.525
1.300976	0.8768	0.5
1.250897	0.865843	0.475
1.200869	0.854007	0.45
1.150888	0.841176	0.425
1.10095	0.827215	0.4
1.051051	0.811964	0.375
1.001188	0.79523	0.35
0.951357	0.77678	0.325
0.901556	0.75633	0.3
0.851783	0.733529	0.275
0.802034	0.707941	0.25
0.752307	0.679013	0.225
0.702601	0.646038	0.2
0.652913	0.608092	0.175
0.603242	0.563948	0.15
0.553585	0.511941	0.125
0.503942	0.449749	0.1
0.454311	0.374038	0.075
0.404691	0.27984	0.05
0.35508	0.159415	0.025
0.305464	0	0

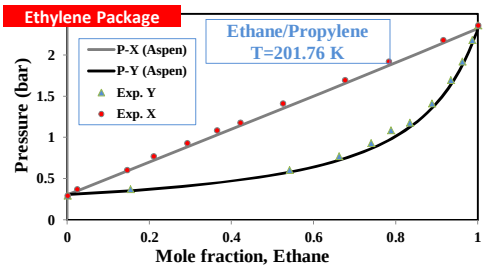

Chapter 5, Supplementary 1

P-xy H_2 & CO Mixture

Experimental	Temperature		-148.14 C
VLE 013	Liquid Mol	Temperatu	Vapor Mole	Total pressure(bar)
	0.9406	125.01	0.787	39.5
	0.9539	125.01	0.814	36.3
	0.967	125.01	0.8513	33
	0.9783	125.01	0.8935	29.8

Reference:

Tsang, C. Y.; Streett, W. B. Fluid Phase Equilib., 1981, 6, 261-273
Phase equilibria in the H(2) + CO system at temperatures from 70 to 125 k and pressures to 53 mpa.

PR-BM (Aspen Plus)		
	TOTAL PRES	VAPOR MOLEFRAC CO	LIQUID MOLEFRAC CO
	bar		
	40.34142	0.784837	0.9142857
	38.52117	0.797931	0.925
	36.63491	0.813707	0.9357143
	34.71097	0.832729	0.9464286
	32.7192	0.855331	0.9571429
	30.68127	0.882355	0.9678571
	28.58579	0.914593	0.9785714
	26.43305	0.953262	0.9892857
	24.23446	1	1

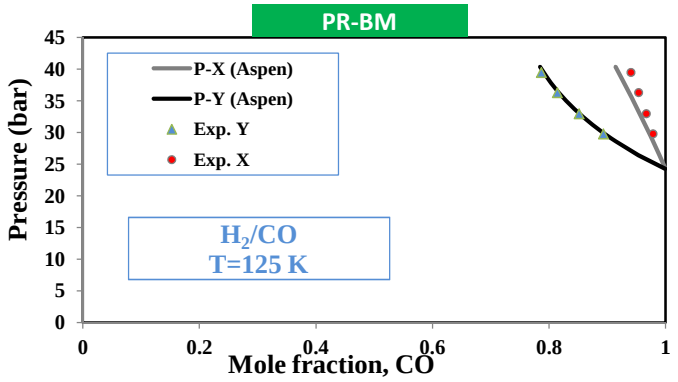

Ethylene Package (Aspen Plus)		
	TOTAL PRES	VAPOR MOLEFRAC CO	LIQUID MOLEFRAC CO
	bar		
	43.45492	0.75765	0.9175
	42.26928	0.765017	0.923
	41.09218	0.773357	0.9285
	39.89668	0.782529	0.934
	38.68281	0.792604	0.9395
	37.43508	0.803573	0.945
	36.1914	0.815757	0.9505
	34.92842	0.829124	0.956
	33.64215	0.843806	0.9615
	32.34807	0.859981	0.967
	31.03637	0.877792	0.9725
	29.70783	0.897445	0.978
	28.35506	0.919134	0.9835
	26.99372	0.943242	0.989
	25.61816	0.970063	0.9945
	24.22504	1	1

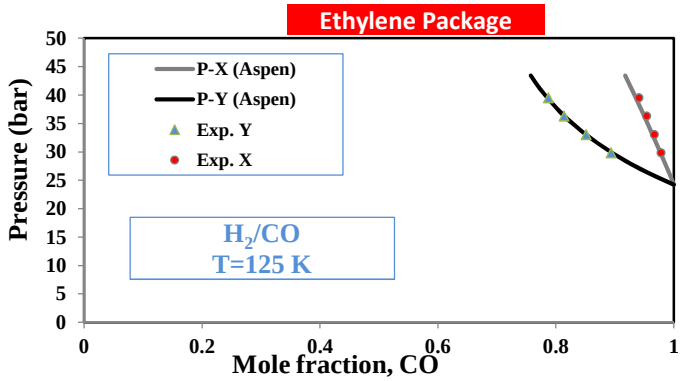

Chapter 5- Supplementary Material 2

Optimization Algorithms

Particle Swarm Optimization [1]	***Parameters***
Number of function evaluation (NFE)	200
Number of particles	5
a_1 , a_2	*2.05*
φ	$a_1 + a_2$
Inertia weight (w)	$\frac{2}{\lvert 2 - \varphi - \sqrt{\varphi^2 - 4\varphi} \rvert}$
Personal and global learning ratios *(c_1 ; c_2)*	$a_1 w$; $a_2 w$
Genetic Algorithm [2, 3]	***Parameters***
Number of function evaluation	200
Number of particles	10
Crossover ratio	0.9
Mutation ratio	0.6
Mutation rate	1 process variable
Simulate Annealing [4, 5]	***Parameters***
Number of function evaluation	200
Initial population	5
Number of particle moves in iteration *i*	3
Initial temperature (T_0)	10
Temperature decrement rate (α)	0.99

References

[1] K.E. Parsopoulos, M.N. Vrahatis, Particle Swarm Optimization and Intelligence: Advances and Applications, IGI Global,

[2] M. Gen, R. Cheng, Genetic algorithms and engineering optimization, John Wiley & Sons, 2000.

[3] D.E. Goldberg, Genetic Algorithms in Search, Optimization, and Machine Learning, Addison-Wesley, , 1989.

[4] U.M. Diwekar, Introduction to Applied Optimization, Springer, New York, 2008.

[5] D. Bertsimas, J. Tsitsiklis, Simulated annealing, Statistical science, 8 (1993) 10-15.

Chapter 5- Supplementary Material 2

Power Generation Option: Chemical Looping Combustion (NIO)
Optmization Scenario: Maximum Olefin with Non-negative NPV Constraint
Shale Gas Type: Fayetteville

Total Capital Investmen	665,718,099
Direct Cost, USD	452,688,307
Indirect Cost, USD (20% of Fixed)	113,172,077
Fixed Capital Investment, USD	565,860,384
Working Capital Investment, USD	99,857,715
Total Capital Investment, USD	665,718,099
Feed and Product Prices	
Natural Gas Price, $/MMBtu	3.88
Ethylene Price, $/tonne	1424.00
Ethane Price, $/kg	0.18
Electricity, cents/kwh	5.67
Methanol Price, $/tonne	482.00
DME Price, $/tonne	962.00
Propylene, $/tonne	1340.00
C4+, $/MJ	0.02
Solid, $/kg	32.89
CO2, $/tonne	10.00
Total Annual Expense, $	234,186,279
Natural Gas & Solid, $/yr	111,048,404
Operating Labor, $/yr	22,209,681
Direct supervisory, $/yr	2,220,968
Utilities, $/yr	22,209,681
Maintenance and repairs, $/yr	28,293,019
Operating supplies, $/yr	2,829,302
Laboratory charges, $/yr	2,220,968
Plant-overhead costs, $/yr	26,361,834
Administrative costs, $/yr	7,908,550
Distribution and selling costs, $/yr	4,441,936
Research and development costs	4,441,936
Total Revenue, $/yr	320,613,105
Ethylene Sale, $/yr	75,820,447
Ethane Sale, $/yr	631,071
Power, $/yr	24,896,390
Methanol Sale, $/yr	0
DME Sale, $/yr	151,893,560
Propylene, $/yr	62,309,738
C4+, $/yr	0
	5,061,899
Gross Earning, $/yr	86,426,826
Debt Taken, $	332,859,049
Equity Expended, $	332,859,049
Annual Payment on Loan, $	33,845,303
Carbon Taxes, $/yr	0

Installed Cost

	$	Percent
ASU	1.08E+08	23.94
Reformer	15388661	3.40
Methanol	2.01E+08	44.32
DME	2575951	0.57
MTO	31170164	6.88
Power Gener	90477137	19.98
CO_2 Compres	4123147	0.91
Total	4.53E+08	100

Shale Gas	kg/hr	83363.34	2000.72 tonne/day
HHV	MJ/kg	53.22	0.05 MMBtu/kg
LHV	MJ/kg	47.98	0.05 MMBtu/kg
HHV	MW	1232.37	4201.78 MMBtu/hr
LHV	MW	1111.07	3788.21 MMBtu/hr

Total Oxygen	kg/hr	75336.22
Power	MJ/kg	0.71
Power required	MW	16.09

Natural Gas Reformer		
Power Consumtion	MW	10.29

DME Unit		
Power Consumtion	MW	4.37
Methanol	kg/h	0.00
HHV	MJ/kg	19.92
LHV	MJ/kg	22.67
HHV	MW	0.00
LHV	MW	0.00
DME	kg/h	21205.15
HHV	MJ/kg	28.79
LHV	MJ/kg	31.65
HHV	MW	169.60
LHV	MW	186.45

MTO Unit		
Power Consumtion	MW	3.43
Ethylene	kg/h	7150.78
HHV	MJ/kg	47.16
LHV	MJ/kg	50.31
HHV	MW	93.68
LHV	MW	99.94
Propylene	kg/h	6244.94
HHV	MJ/kg	45.78
LHV	MJ/kg	48.92
HHV	MW	79.41
LHV	MW	84.87
C4+	kg/h	0.00
HHV	MJ/kg	45.11
LHV	MJ/kg	48.24
HHV	MW	0.00
LHV	MW	0.00
Ethane+Ethylene	kg/h	574.12
HHV	MJ/kg	47.00
LHV	MJ/kg	50.22
HHV	MW	7.50
LHV	MW	8.01
Naphtha HHV	MW	0.00
Naphtha LHV	MW	0.00
DeEthanizer Condenser	MW	-2.15
DeEthanizer Refrigenerat	MW/MW	0.35
DeEthanizer Refrigenerat	MW	0.75
DeMethanizer Condenser	MW	-1.26
Demethanizer Refrigener	MW/MW	1.21
DeMethanizer Refrigener	MW	1.53
C2-Splitter	MW	-2.12
C2-Splitter Refrigeratio	MW/MW	0.64
C2-Splitter Refrigeratio	MW	1.36
Total Power Consumptior	MW	7.07

Power Island		
	MW	96.82

Outputs			Percent	
Net Power Generation	MW	58.99	14.42	Power
Methanol, MW	HHV	0.00	0.00	Methanol
Methanol, MW	LHV	0.00		
DME, MW	HHV	169.60	41.45	DME
DME, MW	LHV	186.45		
Ethylene, MW	HHV	101.18	24.73	Ethylene
Ethylene, MW	LHV	107.94		
Propylene, MW	HHV	79.41	19.41	Propylene
Peopylene, MW	LHV	84.87		
Total, MW	HHV	409.18		

%Net Efficiency, LHV		39.44
%Net Efficiency, HHV		33.20
Liq/Liq+Power (%MW/MW)		85.58
		14.42

Solid inventory and makeup		
Residence Time	sec	300.00
Life-Time	hr	10000.00
Solid Rate	kg/hr	393230.79
Inventory	kg	65538.47
Refill	kg/yr	57411.70

NPV	0.04603
HHV	33.2027
%Power	14.4168
%Methanol	0
%DME+Naphtha	41.449
%Olefins	44.1342
Recycle Ratio	0.99
MeOH to DME	0.44
MeOH to MTO	0.56

MACRS CASH FLOW - Depreciation	
2014	56,586,038
2015	101,854,869
2016	81,483,895
2017	65,187,116
2018	52,172,327
2019	41,703,910
2020	37,063,855
2021	37,063,855
2022	37,120,441
2023	37,063,855
2024	18,560,221
Loan Principal Balance at start of	
2014	332,859,049
2015	330,635,356
2016	328,200,412
2017	325,534,149
2018	322,614,590
2019	319,417,674
2020	315,917,050
2021	312,083,867
2022	307,886,532
2023	303,290,450
2024	298,257,740
2025	292,746,923
2026	286,712,578
2027	280,104,970
2028	272,869,639
2029	264,946,952
2030	256,271,610
2031	246,772,110
2032	236,370,158
2033	224,980,021
2034	212,507,820
2035	198,850,760
2036	183,896,280
2037	167,521,124
2038	149,590,328
2039	129,956,106
2040	108,456,633
2041	84,914,711
2042	59,136,306
2043	30,908,952
Interest Payed	
2014	31,621,610
2015	31,410,359
2016	31,179,039
2017	30,925,744
2018	30,648,386
2019	30,344,679
2020	30,012,120
2021	29,647,967
2022	29,249,221
2023	28,812,593
2024	28,334,485
2025	27,810,958
2026	27,237,695
2027	26,609,972
2028	25,922,616
2029	25,169,960
2030	24,345,803
2031	23,443,350
2032	22,455,165
2033	21,373,102
2034	20,188,243
2035	18,890,822
2036	17,470,147
2037	15,914,507
2038	14,211,081
2039	12,345,830
2040	10,303,380
2041	8,066,898
2042	5,617,949
2043	2,936,350

CASH FLOW - Taxable Earnings	
2014	-1,780,822
2015	-44,430,566
2016	-21,353,354
2017	-2,259,412
2018	13,647,476
2019	27,107,186
2020	34,842,263
2021	38,045,839
2022	41,306,530
2023	44,799,583
2024	66,864,740
2025	89,117,806
2026	92,948,683
2027	96,924,777
2028	101,053,789
2029	105,343,984
2030	109,804,237
2031	114,444,086
2032	119,273,791
2033	124,304,397
2034	129,547,805
2035	135,016,845
2036	140,725,361
2037	146,688,300
2038	152,921,810
2039	159,443,354
2040	166,271,820
2041	173,427,656
2042	180,933,010
2043	188,811,885

CASH FLOW - Net Earnings	
2014	-336,863,564
2015	-46,865,509
2016	-24,019,618
2017	-5,178,970
2018	4,991,569
2019	12,763,688
2020	17,072,175
2021	18,630,168
2022	20,187,836
2023	21,847,040
2024	34,608,026
2025	47,436,338
2026	49,161,602
2027	50,919,535
2028	52,709,587
2029	54,531,048
2030	56,383,043
2031	58,264,499
2032	60,174,137
2033	62,110,437
2034	64,071,623
2035	66,055,627
2036	68,060,061
2037	70,082,184
2038	72,118,865
2039	74,166,540
2040	76,221,169
2041	78,278,188
2042	80,332,453
2043	82,378,179

CASH FLOW - Discounted Cash Flow	
2014	-280,277,525
2015	54,989,360
2016	57,464,278
2017	60,008,146
2018	57,163,896
2019	54,467,598
2020	54,136,030
2021	55,694,023
2022	57,308,277
2023	58,910,895
2024	53,168,247
2025	47,436,338
2026	49,161,602
2027	50,919,535
2028	52,709,587
2029	54,531,048
2030	56,383,043
2031	58,264,499
2032	60,174,137
2033	62,110,437
2034	64,071,623
2035	66,055,627
2036	68,060,061
2037	70,082,184
2038	72,118,865
2039	74,166,540
2040	76,221,169
2041	78,278,188
2042	80,332,453
2043	82,378,179

CASH FLOW - Cumulative Cash Flow (PV)	
2014	-280,277,525
2015	-234,453,059
2016	-194,547,311
2017	-159,820,374
2018	-132,252,909
2019	-110,363,603
2020	-92,233,556
2021	-76,690,376
2022	-63,362,302
2023	-51,944,976
2024	-43,358,007
2025	-36,973,646
2026	-31,459,845
2027	-26,700,708
2028	-22,595,339
2029	-19,055,976
2030	-16,006,336
2031	-13,380,166
2032	-11,119,963
2033	-9,175,853
2034	-7,504,605
2035	-6,068,773
2036	-4,835,938
2037	-3,778,052
2038	-2,870,860
2039	-2,093,402
2040	-1,427,573
2041	-857,740
2042	-370,418
2043	46,025
NPV, $ Million	0

Chapter 5- Supplementary Material 3
Shale Gas Type: Fayetteville
Optmization Scenario: Maximum Olefin with Non-negative NPV Constraint
Figure 2

Stream No.	**1-1**	**1-2**	**1-3**	**1-4**	**1-5**	**1-6**	**1-7**	**1-8**	**1-9**	**1-10**
Temperature (°C)	30.0	500.0	860.6	655.3	40.0	40.0	80.0	470.0	470.0	15.0
Pressure (bar)	30.0	30.0	28.9	28.9	28.4	28.4	52.0	40.8	40.8	12.9
Mass Vapor Fraction	1.00	1.00	1.00	1.00	0.65	1.00	1.00	1.00	1.00	1.00
Total Flow (kmole/hr)	5000	5000	23280	23280	23280	15209	15209	2625	7175	2140
Total Flow (kg/hr)	83363	83363	328435	328435	328435	182979	182979	47296	129260	68516
Mole Percent										
H_2O	0.0%	0.0%	34.8%	34.8%	34.8%	0.3%	0.3%	100.0%	100.0%	0.0%
N_2	0.0%	0.0%	0.0%	0.0%	0.0%	0.0%	0.0%	0.0%	0.0%	0.2%
O_2	0.0%	0.0%	0.0%	0.0%	0.0%	0.0%	0.0%	0.0%	0.0%	99.5%
AR	0.0%	0.0%	0.0%	0.0%	0.0%	0.0%	0.0%	0.0%	0.0%	0.3%
H_2	0.0%	0.0%	43.3%	43.3%	43.3%	66.3%	66.3%	0.0%	0.0%	0.0%
CO	0.0%	0.0%	10.8%	10.8%	10.8%	16.6%	16.6%	0.0%	0.0%	0.0%
CO_2	1.5%	1.5%	7.7%	7.7%	7.7%	11.8%	11.8%	0.0%	0.0%	0.0%
CH_4	97.0%	97.0%	3.3%	3.3%	3.3%	5.0%	5.0%	0.0%	0.0%	0.0%
C_2H_6	1.5%	1.5%	0.0%	0.0%	0.0%	0.0%	0.0%	0.0%	0.0%	0.0%
Total	100.0%	100.0%	100.0%	100.0%	100.0%	100.0%	100.0%	100.0%	100.0%	100.0%

Chapter 5- Supplementary Material 3
Shale Gas Type: Fayetteville
Optmization Scenario: Maximum Olefin with Non-negative NPV Constraint
Figure 3

Stream No.	1-7	2-1	2-2	2-3	2-4	2-5	2-6	2-7	2-8	2-9	2-10	2-11
Temperature (°C)	80.0	240.0	81.6	35.0	61.5	215.0	184.0	184.0		45.0	56.0	159.1
Pressure (bar)	52.0	51.0	51.0	50.5	55.0	50.0	30.0	30.0		28.5	13.5	33.0
Mass Vapor Fraction	1.00	1.00	1.00	1.00	1.00	0.00	0.00	0.00		0.00	0.00	0.00
Total Flow (kmole/hr)	15209	182506	182506	176888	2019	5368	2253	2867	0	2253	460	1793
Total Flow (kg/hr)	182979	2561344	2561344	2402440	32575	150353	72245	91948	0	72245	21205	51039
Mole Percent												
H_2O	0.3%	1.0%	1.0%	0.1%	0.4%	29.0%	0.2%	0.2%	0.0%	20.7%	0.0%	26.0%
N_2	0.0%	0.2%	0.2%	0.2%	0.2%	0.0%	0.0%	0.0%	0.0%	0.0%	0.0%	0.0%
AR	0.0%	0.4%	0.4%	0.4%	0.3%	0.0%	0.0%	0.0%	0.0%	0.0%	0.0%	0.0%
H_2	66.3%	40.8%	40.8%	42.1%	37.2%	0.0%	0.0%	0.0%	0.0%	0.0%	0.0%	0.0%
CO	16.6%	6.8%	6.8%	7.0%	6.2%	0.0%	0.0%	0.0%	0.0%	0.0%	0.0%	0.0%
CO_2	11.8%	8.3%	8.3%	8.5%	13.3%	0.0%	0.0%	0.0%	0.0%	0.0%	0.0%	0.0%
CH_4	5.0%	39.8%	39.8%	41.0%	37.9%	0.0%	0.0%	0.0%	0.0%	0.0%	0.0%	0.0%
MeOH	0.0%	2.8%	2.8%	0.7%	4.4%	70.8%	99.5%	99.5%	0.0%	58.5%	0.0%	73.5%
EtOH	0.0%	0.0%	0.0%	0.0%	0.0%	0.1%	0.2%	0.2%	0.0%	0.2%	0.0%	0.2%
Methanoate	0.0%	0.0%	0.0%	0.0%	0.0%	0.1%	0.1%	0.1%	0.0%	0.1%	0.1%	0.1%
DME	0.0%	0.0%	0.0%	0.0%	0.0%	0.0%	0.0%	0.0%	0.0%	20.5%	99.9%	0.1%
C_2H_6	0.0%	0.0%	0.0%	0.0%	0.0%	0.0%	0.0%	0.0%	0.0%	0.0%	0.0%	0.0%
Total	100.0%	100.0%	100.0%	100.0%	100.0%	100.0%	100.0%	100.0%	0.0%	100.0%	100.0%	100.0%

Chapter 5- Supplementary Material 3
Shale Gas Type: Fayetteville
Optmization Scenario: Maximum Olefin with Non-negative NPV Constraint
Figure 4

Stream No.	**3-1**	**3-2**	**3-3**	**3-4**	**3-5**	**3-6**	**3-7**	**3-8**	**3-9**	**3-10**	**3-11**	**3-12**	**3-13**	**3-14**	**3-15**
Temperature (°C)	45.0	40.0	91.0	55.2	42.2	37.0	22.7	85.0	35.7	86.9	20.0	28.6	-7.3	-51.8	-43.5
Pressure (bar)	2.0	39.5	2.5	1.5	2.0	35.3	34.5	35.3	15.0	15.5	34.5	33.5	34.2	10.0	10.5
Mass Vapor Fraction	0.00	1.00	0.33	1.00	1.00	1.00	1.00	0.00	0.00	0.00	1.00	1.00	0.00	0.00	0.00
Total Flow (kmole/hr)	2867	1176	301	81	1133	546	368	178	148	29	368	94	274	255	19
Total Flow (kg/hr)	51654	41554	14078	3663	38534	15938	8285	7654	6245	1409	8285	560	7725	7151	574
Mole Percent															
H_2O	100.0%	0.4%	48.5%	1.7%	3.7%	1.0%	0.0%	3.1%	0.0%	18.7%	0.0%	0.0%	0.0%	0.0%	0.0%
H_2	0.0%	6.8%	0.0%	0.0%	7.0%	13.6%	20.2%	0.0%	0.0%	0.0%	20.2%	79.3%	0.0%	0.0%	0.0%
CO_2	0.0%	3.0%	11.7%	43.3%	0.0%	0.0%	0.0%	0.0%	0.0%	0.0%	0.0%	0.0%	0.0%	0.0%	0.0%
CH_4	0.0%	1.2%	0.0%	0.1%	1.2%	2.0%	3.0%	0.0%	0.0%	0.0%	3.0%	11.8%	0.0%	0.0%	0.0%
MeOH	0.0%	0.0%	0.0%	0.0%	0.0%	0.0%	0.0%	0.0%	0.0%	0.0%	0.0%	0.0%	0.0%	0.0%	0.0%
C_2H_4	0.0%	38.7%	2.4%	9.0%	39.5%	50.6%	75.1%	0.0%	0.0%	0.0%	75.1%	8.9%	97.7%	99.9%	69.3%
C_2H_6	0.0%	0.7%	0.1%	0.2%	0.7%	0.8%	1.2%	0.0%	0.0%	0.0%	1.2%	0.0%	1.7%	0.1%	22.2%
C_3H_6	0.0%	37.6%	6.4%	23.3%	37.4%	27.8%	0.4%	84.5%	99.2%	10.2%	0.4%	0.0%	0.6%	0.0%	8.4%
C_3H_8	0.0%	0.4%	0.1%	0.3%	0.4%	0.3%	0.0%	0.9%	0.8%	1.5%	0.0%	0.0%	0.0%	0.0%	0.0%
C_4H_8	0.0%	9.7%	4.6%	16.5%	8.9%	3.5%	0.0%	10.8%	0.0%	65.6%	0.0%	0.0%	0.0%	0.0%	0.0%
C_5H_{10}	0.0%	1.5%	1.7%	5.6%	1.1%	0.2%	0.0%	0.7%	0.0%	4.0%	0.0%	0.0%	0.0%	0.0%	0.0%
DGA	0.0%	0.0%	24.4%	0.0%	0.0%	0.0%	0.0%	0.0%	0.0%	0.0%	0.0%	0.0%	0.0%	0.0%	0.0%
Total	100.0%	100.0%	100.0%	100.0%	100.0%	100.0%	100.0%	100.0%	100.0%	100.0%	100.0%	100.0%	100.0%	100.0%	100.0%

Chapter 5- Supplementary Material 3
Power Generation Option: Post-Combustion
Shale Gas Type: Fayetteville
Optmization Scenario: Maximum Olefin with Non-negative NPV Constraint
Power Plant: 4-Power Generation (Figure 1B); Power Generation for the Upstream Section
Figure 5

Stream No.	**4-11**	**4-12**	**4-13**	**4-14**	**4-15**
Temperature (°C)	544.3	1249.8	470.0	61.9	35.0
Pressure (bar)	54.0	53.8	40.8	2.0	1.4
Mass Vapor Fraction	1.00	1.00	1.00	1.00	1.00
Total Flow (kmole/hr)	32560	34187	15020	32890	1182
Total Flow (kg/hr)	939354	971929	270591	919249	50761
Mole Percent					
H_2O	0.0%	7.6%	100.0%	7.4%	3.5%
N_2	79.0%	74.6%	0.0%	77.5%	0.6%
O_2	21.0%	13.8%	0.0%	14.3%	0.3%
H_2	0.0%	0.0%	0.0%	0.0%	0.0%
CO	0.0%	0.0%	0.0%	0.0%	0.0%
CO_2	0.0%	3.7%	0.0%	0.4%	95.5%
CH_4	0.0%	0.0%	0.0%	0.0%	0.0%
AR	0.0%	0.3%	0.0%	0.4%	0.0%
Total	100.0%	100.0%	100.0%	100.0%	100.0%

Chapter 5- Supplementary Material 3
Power Generation Option: Post-Combustion
Shale Gas Type: Fayetteville
Optmization Scenario: Maximum Olefin with Non-negative NPV Constraint
Power Plant: 5-Power Generation (Figure 1B); Power Generation for the Downstream Section
Figure 5

Stream No.	**4-11**	**4-12**	**4-13**	**4-14**	**4-15**
Temperature (°C)	544.3	1249.8	470.0	61.9	35.0
Pressure (bar)	54.0	53.8	40.8	2.0	1.4
Mass Vapor Fraction	1.00	1.00	1.00	1.00	1.00
Total Flow (kmole/hr)	6994	7343	3226	7065	254
Total Flow (kg/hr)	201769	208766	58122	197451	10903
Mole Percent					
H_2O	0.0%	7.6%	100.0%	7.4%	3.5%
N_2	79.0%	74.6%	0.0%	77.5%	0.6%
O_2	21.0%	13.8%	0.0%	14.3%	0.3%
H_2	0.0%	0.0%	0.0%	0.0%	0.0%
CO	0.0%	0.0%	0.0%	0.0%	0.0%
CO_2	0.0%	3.7%	0.0%	0.4%	95.5%
CH_4	0.0%	0.0%	0.0%	0.0%	0.0%
AR	0.0%	0.3%	0.0%	0.4%	0.0%
Total	100.0%	100.0%	100.0%	100.0%	100.0%

Chapter 5- Supplementary Material 3
Power Generation Option: Oxy-Fuel Combustion
Shale Gas Type: Fayetteville
Optmization Scenario: Maximum Olefin with Non-negative NPV Constraint
Power Plant: 4-Power Generation (Figure 1B); Power Generation for the Upstream Section
Figure 6

Stream No.	**4-7**	**4-8**	**4-9**	**4-10**
Temperature (°C)	178.3	40.0	470.0	40.0
Pressure (bar)	54.0	53.0	40.8	53.0
Mass Vapor Fraction	1.00	0.34	1.00	1.00
Total Flow (kmole/hr)	2109	3740	32190	1274
Total Flow (kg/hr)	67518	100093	579914	55449
Mole Percent				
H_2O	0.0%	65.8%	100.0%	0.3%
N_2	0.2%	0.2%	0.0%	0.6%
O_2	99.5%	0.0%	0.0%	0.0%
H_2	0.0%	0.2%	0.0%	0.6%
CO	0.0%	0.0%	0.0%	0.1%
CO_2	0.0%	33.4%	0.0%	97.3%
CH_4	0.0%	0.0%	0.0%	0.0%
AR	0.3%	0.4%	0.0%	1.1%
Total	100.0%	100.0%	100.0%	100.0%

Chapter 5- Supplementary Material 3
Power Generation Option: Oxy-Fuel Combustion
Shale Gas Type: Fayetteville
Optmization Scenario: Maximum Olefin with Non-negative NPV Constraint
Power Plant: 5-Power Generation (Figure 1B); Power Generation for the Downstream Section
Figure 6

Stream No.	**4-7**	**4-8**	**4-9**	**4-10**
Temperature (°C)	178.3	40.0	470.0	40.0
Pressure (bar)	54.0	53.0	40.8	53.0
Mass Vapor Fraction	1.00	0.46	1.00	1.00
Total Flow (kmole/hr)	451	671	4846	307
Total Flow (kg/hr)	14424	20055	87304	13475
Mole Percent				
H_2O	0.0%	54.1%	100.0%	0.3%
N_2	0.2%	0.1%	0.0%	0.3%
O_2	99.5%	0.0%	0.0%	0.1%
H_2	0.0%	0.0%	0.0%	0.0%
CO	0.0%	0.0%	0.0%	0.0%
CO_2	0.0%	45.5%	0.0%	98.9%
CH_4	0.0%	0.0%	0.0%	0.0%
AR	0.3%	0.2%	0.0%	0.5%
Total	100.0%	100.0%	100.0%	100.0%

Chapter 5- Supplementary Material 3

Power Generation Option: Chemical Looping Combustion (NiO)

Shale Gas Type: Fayetteville

Optmization Scenario: Maximum Olefin with Non-negative NPV Constraint

Power Plant: 4-Power Generation (Figure 1B); Power Generation for the Upstream Section Figure 7

Stream No.	**4-1**	**4-2**	**4-3**	**4-4**	**4-5**	**4-6**
Temperature (°C)	30.0	254.2	170.0	470.0	40.0	30.0
Pressure (bar)	2.0	1.1	1.0	40.8	53.0	80.0
Mass Vapor Fraction	1.00	1.00	1.00	1.00	0.34	0.00
Total Flow (kmole/hr)	10486	9478	9478	20948	3730	1255
Total Flow (kg/hr)	302530	266827	266827	377381	99862	55063
Mole Percent						
H_2O	1.1%	1.2%	1.2%	100.0%	66.2%	0.3%
N_2	77.2%	94.5%	94.5%	0.0%	0.1%	0.3%
O_2	20.8%	3.3%	3.3%	0.0%	0.0%	0.0%
H_2	0.0%	0.0%	0.0%	0.0%	0.0%	0.0%
CO	0.0%	0.0%	0.0%	0.0%	0.0%	0.0%
CO_2	0.0%	0.0%	0.0%	0.0%	33.5%	98.9%
CH_4	0.0%	0.0%	0.0%	0.0%	0.0%	0.0%
AR	0.9%	1.0%	1.0%	0.0%	0.2%	0.5%
Total	100.0%	100.0%	100.0%	100.0%	100.0%	100.0%

Chapter 5- Supplementary Material 3
Power Generation Option: Chemical Looping Combustion (NiO)
Shale Gas Type: Fayetteville
Optmization Scenario: Maximum Olefin with Non-negative NPV Constraint
Power Plant: 5-Power Generation (Figure 1B); Power Generation for the Downstream Section
Figure 7

Stream No.	**4-1**	**4-2**	**4-3**	**4-4**	**4-5**	**4-6**
Temperature (°C)	30.0	254.2	170.0	351.4	40.0	30.0
Pressure (bar)	2.0	1.1	1.0	17.0	53.0	80.0
Mass Vapor Fraction	1.00	1.00	1.00	1.00	0.46	0.00
Total Flow (kmole/hr)	1209	1093	1093	4035	669	306
Total Flow (kg/hr)	34887	30770	30770	72696	19993	13420
Mole Percent						
H_2O	1.1%	1.2%	1.2%	100.0%	54.2%	0.3%
N_2	77.2%	94.5%	94.5%	0.0%	0.1%	0.1%
O_2	20.8%	3.3%	3.3%	0.0%	0.0%	0.0%
H_2	0.0%	0.0%	0.0%	0.0%	0.1%	0.1%
CO	0.0%	0.0%	0.0%	0.0%	0.0%	0.0%
CO_2	0.0%	0.0%	0.0%	0.0%	45.6%	99.2%
CH_4	0.0%	0.0%	0.0%	0.0%	0.0%	0.0%
AR	0.9%	1.0%	1.0%	0.0%	0.1%	0.2%
Total	100.0%	100.0%	100.0%	100.0%	100.0%	100.0%

Chapter 6

Integrated Petroleum Coke and Natural Gas Polygeneration Process with Zero Carbon Emissions

The text and materials provided in this chapter are submitted to the *Fuel Processing Technology* journal for peer review.

Integrated petroleum coke and natural gas polygeneration process with zero carbon emissions

Yaser Khojasteh Salkuyeh, Thomas A. Adams II[1]

Department of Chemical Engineering, McMaster University, 1280 Main St W, Hamilton, Ontario, L8S 4L7, Canada.

ABSTRACT

In the present work, a new polygeneration system is developed that uses petcoke and natural gas as feedstocks and coproduces different products such as chemicals, olefins, electricity and transportation fuels. Furthermore, by incorporation of chemical looping combustion and chemical looping gasification technologies, 100% of CO_2 emissions are captured effectively. The particle swarm optimization technique is implemented with Aspen Plus models to determine the optimum product portfolio at different market conditions. Techno-economic optimization results show that this plant can be profitable for a broad range of petcoke consumption (up to 74%) and various feeds and products price changes.

Keywords: Polygeneration, petcoke gasification, gas-to-liquids, methanol-to-olefins, CO_2 capture

1. Introduction

As the supply of light crude oils diminishes and the processing of heavier oil increases, crude oil refineries face growing challenges associated with this increased use of heavier crude. For instance, the API gravity of crude produced in the United States has been steadily decreasing [1]. One result of this change is an increasing rate in the production of extremely heavy residues called petroleum coke (or petcoke), even when upgrading units such as delayed coking and fluid coking are implemented [2, 3]. The global production of petcoke has been accelerated to about 4% per year [4] due to the invention of new technologies that can extract crude oil from shale oil and oil sand reservoirs.

[1]Corresponding author.1280 Main Street West, Hamilton, Ontario, Canada, L8S 4L7. Tel.: +1 (905) 525-9140 x24782; E-mail address: tadams@mcmaster.ca

Among the several emerging technologies available for the upgrading of petcoke, gasification has emerged as an effective approach that can convert petcoke to more valuable products with minimum environmental impacts compared to commercial combustion systems. In this approach, solid petcoke is converted to synthesis gas and, after purification, is used as a feedstock for other chemical units. Although different petcoke gasification mechanisms and technologies have been studied extensively [1, 5-7], little research has studied the techno-economic analysis on the polygeneration processes that use them. For example, a conceptual study of a large scale polygeneration plant that converts petcoke to power, chemicals such as ammonia and MeOH, hydrogen and transportation liquids was performed by Jacob Consultancy [8]. To the best of our knowledge, this report is the only techno-economic analysis of petroleum-based polygeneration systems. However, their preliminary results showed that the proposed system was not profitable in most cases with current technologies.

However, the incorporation of a natural gas reforming process which produces relatively inexpensive hydrogen rich synthesis gas can improve the performance of polygeneration plants significantly. Comprehensive studies which consider the coupling of pipeline natural gas reforming with commercial coal gasifiers [9, 10], as well as shale gas resources [11, 12] have shown promising results for a variety of different combinations of products and processing routes. Some of these proposed routes incorporate chemical looping gasification [13-15] and chemical looping combustion [16, 17], which can help facilitate low cost CO_2 capture.

Although these studies provide promising ways to produce energy products with low-to-zero process CO_2 emissions with coal and gas, petcoke has not yet been examined as a potential resource to use at the systems level. Even though petcoke and coal have some similarities, the results of the prior studies using coal cannot be readily extrapolated to petcoke. Fundamentally, coal is a valuable commodity, and petcoke is a low-quality waste product of limited use. As such, petcoke gasification and the resulting petcoke-derived syngas are different enough from the coal-based equivalent as to significantly affect the design and economics of the polygeneration plant at the systems level. Therefore, the purpose of this work is to determine how petcoke can best be used in combination with natural gas in a polygeneration system which produces different energy products while maintaining zero direct CO_2 emissions.

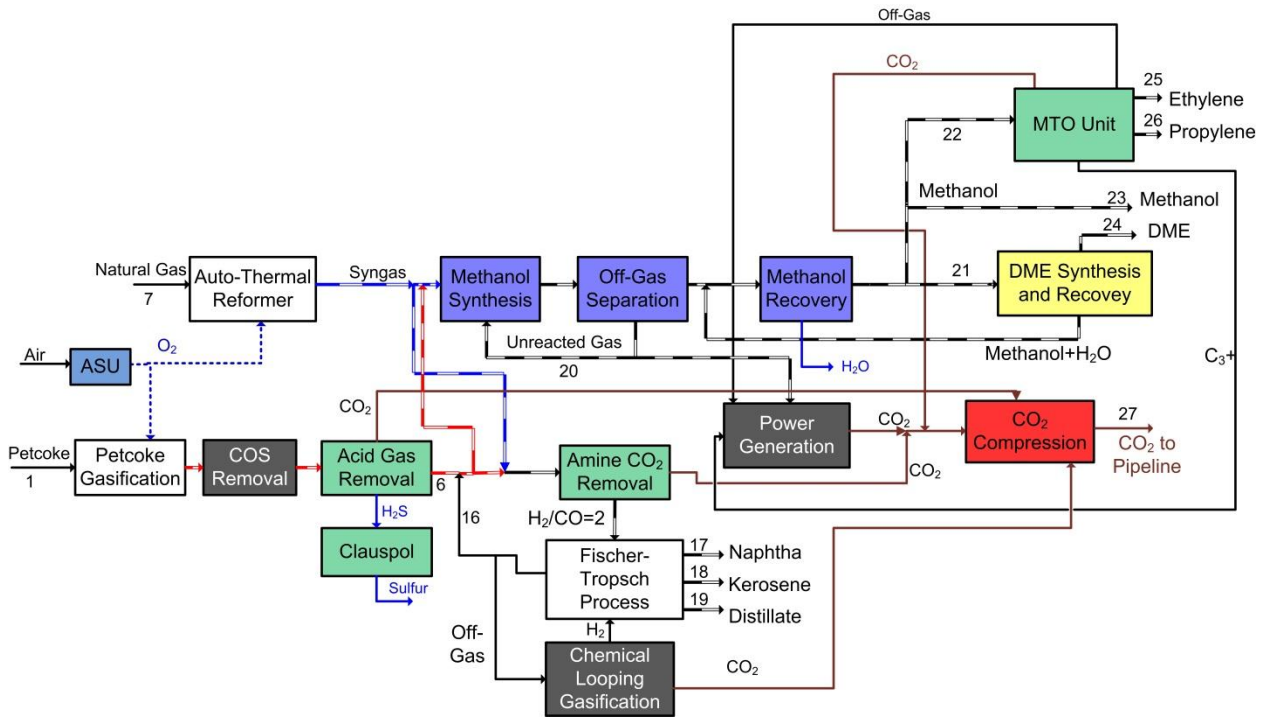

Figure 1. Scheme of the petcoke-natural gas superstructure.

In the present work, a novel polygeneration process is presented that consumes petcoke and natural gas as the main feedstock, utilizing novel technologies for power generation, hydrogen production and olefin production. Although many kinds of petcoke could be used, Syncrude coke was selected as the example for this work since it is produced and stockpiled in large amounts in Canada. In 2011, the total petcoke production rate in Canada was about 10 million tonnes per year [4], which is equivalent to 3500 MW electricity generated by typical IGCC plants [7]. Although conventional natural gas could be used, Haynesville shale gas was selected as the example gas feed in order to demonstrate that, if desired, it is possible to use desulfurized shale gas that has not been completely converted to conventional natural gas quality. Conventional pipeline natural gas or other shale gases could be used instead with minor operating changes to the reforming system [11, 12].

As illustrated in Figure 1, the syngas produced from petcoke gasification and shale gas reforming are routed into two parallel trains, the methanol (MeOH) and dimethyl ether (DME) synthesis unit, and the Fischer-Tropsch (FT) synthesis unit. In the MeOH/DME unit, syngas is converted to MeOH which can be stored or optionally routed to the DME reactor section to produce fuel-grade DME. In addition, the methanol-to-olefin (MTO) unit is coupled with the

MeOH/DME section to diversify the product portfolio by producing ethylene and propylene from MeOH. In the FT section, the syngas stream produced by the petcoke gasifier is sent to the FT reactor after being mixed with H_2-rich syngas to get the ratio $H_2/CO=2.1$ which is ideal for the FT chain reactions. It should be noted that prior to sending syngas to the FT reactor, it must be purified to remove CO_2. In our proposed system, a nickel-oxide (NiO) chemical looping combustion (CLC) system is used to supply the electricity demand of plant from purge gas streams. Furthermore, the heat, steam and hydrogen demands of the FT unit are provided by using an iron-oxide (Fe_2O_3) chemical looping gasification unit. One key advantage of the CLC system is that it facilitates 100% CO_2 capture from these purge gases. As a result, the proposed polygeneration process features essentially zero direct CO_2 emissions, and is profitable in a wide range of market prices and feedstock blends (different ratios of petcoke and natural gas can be used). In addition, the particle swarm optimization technique was employed to determine the optimum process conditions for a variety of objective functions, such as the maximization of profit or yield.

2. Process Simulation

Each polygeneration plant considered in this work was scaled to a combined 1111 MW (LHV) energy input of petcoke and shale gas, which is equivalent to around 2000 tonne per day of shale gas. The composition and other key properties of petcoke and shale gas are listed in Table 1. All process unit operation models were simulated in Aspen Plus 2006.5 simulation software, except for the gas turbines for which a custom model in Visual Basic for Applications (VBA) was linked into the Aspen simulation model instead. Details of this custom model were described in our previous work and not shown in this paper for brevity [12]. As in our prior works, the Peng Robinson with Boston-Matthias (PR-BM) equation of state was used for all equipment, except for amine units and the HRSG section (including steam turbines), in which Elec-NRTL and NBS/NRC models were used [18]. All utility requirements (electricity, process steam, reboiler steam and coolers) are considered in all thermal efficiency and profitability calculations for each plant. Since most of the units are already detailed in previous works [11, 12, 19, 20], only the new units are described in this paper. The main products specifications are also listed in Table 2. These values were used as the design specifications in the simulation of their corresponding production units.

Table 1. Properties of petcoke and shale gas feedstocks.

Petcoke [5]: Syncrude coke;					
Gross heating value: 13923 Btu/lb (HHV)					
Property proximate (wt. %)					
Moisture	0.25	*Ash*	4.83		
Volatiles	4.99	*Fixed carbon*	89.95		
Ultimate (wt. %)					
Carbon	83.74	*Chlorine*	0.25	*Nitrogen*	2.03
Hydrogen	1.77	*Sulfur*	6.52	*Oxygen*	0.88
Shale gas [21]: Haynesville					
Gas composition (% molar)					
Methane	0.948	CO_2	0.05		
Ethane	0.001	N_2	0.001		

Table 2. Main products properties and purity specifications.

MeOH	Mole purity (industrial grade): 99.5% [22]
DME	Mole purity (fuel grade): 99.9% [23]
Propylene	Mole purity (polymer grade): 99.2% [24]
Ethylene	Mole purity (polymer grade): 99.9% [25]
Naphtha	True boiling point temperature, 100% liquid: 150°C [26]
Kerosene	True boiling point temperature, 100% liquid: 260°C [26]
Diesel (Distillate)	True boiling point temperature, 100% liquid: 380°C [26]
CO_2 captured	Mole purity $\geq$ 0.966 [27]

2.1 Petcoke Gasification

Various types of petcoke gasification technologies have been developed in recent years. For example, Lee et al. [6] investigated the main characteristics of petcoke gasification by experimenting on a 1 tonne per day entrained flow gasifier pilot unit. A detailed study of different petcoke gasification mechanisms, provided by Murthy et al. [7], showed that entrained flow gasifiers are capable of offering higher efficiency and conversion compared to other kinds of gasifiers. In addition, our previous work [20] showed that coal-based polygeneration systems using slurry feed entrained gasifiers are generally more profitable than systems using dry gasifiers, and so it is likely to be a good choice for use in the petcoke-based polygeneration systems studied in this work. Thus, the slurry feed entrained gasifier was chosen as shown in

Figure 2. The typical operating range of this type of gasifier is 20-80 bar and 1200-1600°C [7]. Using a "full heat recovery" gasification system, described by Furimsky [1, 7], high pressure steam is generated in both radiant and convective coolers. The H_2/CO ratio of the produced syngas is around 0.39. This syngas stream is then sent to the purification unit to remove NH_3 and HCl. A COS conversion reactor is also required to hydrolysis the COS impurities to H_2S:

$$COS + H_2O \rightarrow CO_2 + H_2S$$

The reactor effluent must pass through an amine unit to remove H_2S and CO_2 from the syngas. Diglycolamine (DGA) solvent (70% wt. DGA/30% wt. H_2O) has been used as the scrubbing amine for the acid gas removal in this section and also for the CO_2 removal step of MTO (Figure 1) and FT units (Figures 1 and 4). MDEA was also investigated as a potential solvent, but our simulation results showed that at the same acid gas removal performance, the energy requirement and amine loss of DGA is lower than those of MDEA. The Elec-NRTL model was used for the simulation of the amine units, and the methodology for construction of the flowsheet and simulation is described in our prior work [28]. The clean syngas is then sent to the reforming section to be mixed with the H_2-rich syngas as described in the next section. The captured acid gases are sent to the Clauspol unit where H_2S is removed and converted to liquid sulphur. This unit is not modeled but its utility consumption and cost are considered in the techno-economic analysis of each plant [29]. The CO_2 recovered in the Clauspol process is sent to the CO_2 compression unit to be liquefied.

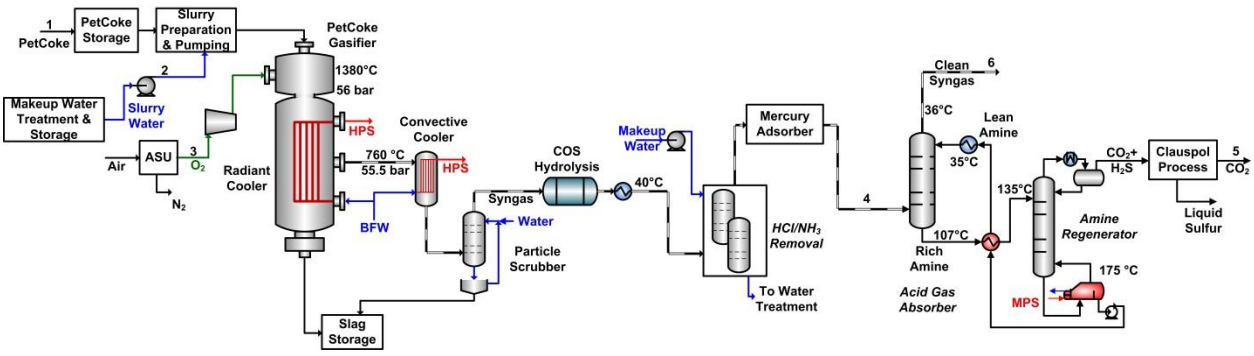

Figure 2. Petcoke gasification and purification unit [1].

2.1.1 Shale Gas Reforming

The synthesis gas produced by the petcoke gasifier is mixed with the unreacted gases from the FT unit (stream 16, Figures 3 and 4). This CO-rich syngas stream is mixed with the H_2-rich syngas provided by the shale gas reformer, and then divided into two streams and fed to FT (stream 12) and MeOH/DME (stream 13) units respectively. The ratio of blending is adjusted to create a ratio of H_2/CO around 2.1, which is required by FT unit. Conversion of shale gas to H_2-rich synthesis gas is performed in a low-temperature pre-reformer followed by a high-temperature reformer as shown in Figure 3. This system is applicable for different low N_2 content shale gases such as Marcellus, New Albany or Fayetteville [21]. Details of the operating conditions of the natural gas reforming section are described in [19, 20] and will not be described here for brevity.

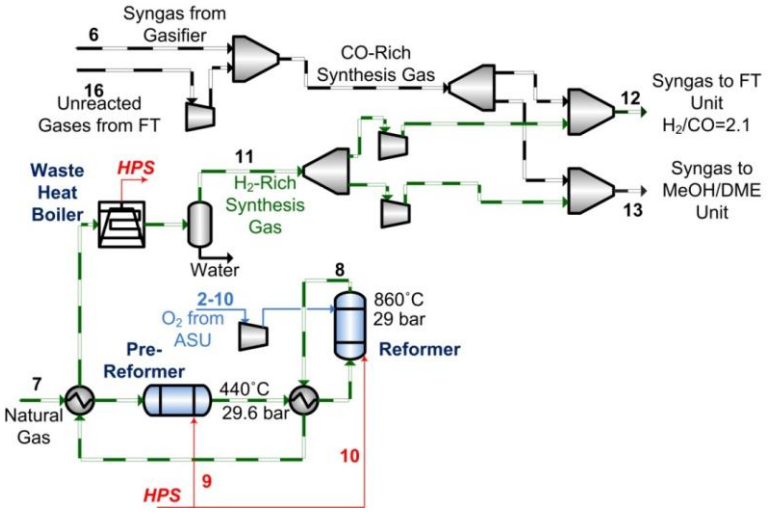

Figure 3. Shale gas reforming and syngas preparation.

2.2 Fischer-Tropsch Process

As shown in Figure 4, the syngas stream enters the second amine train to remove the CO_2 generated in the reforming section. An alternative configuration would be merging this amine unit with the first amine section (Figure 2) and recycling stream 16 and H_2-rich syngas to that. However, our results showed that the efficiency loss due to compression of the H_2-rich syngas and recycle streams and the additional energy consumption of the regeneration column are such that our chosen two-section system configuration outperforms this alternative single-section system. The clean gas stream is then fed to the FT reactor to convert CO and H_2 to a range of hydrocarbons from C_1 to C_{60} [19]:

$$n(2H_2 + CO) \rightarrow -C_nH_{2n}- + nH_2O$$

The reactor model, products distribution and recovery flowsheet are described in more detail by Adams and Barton [9]. The product stream is delivered to the first fractionation column to recover naphtha, kerosene and distillate products according to the specifications listed in Table 2. Further upgrading is performed by sending the heavy bottom residue to the hydrocracking catalytic reactor where heavy hydrocarbons are cracked at high temperature and in the presence of hydrogen. The product selectivity of the hydrocracker is adopted from the experimental data provided by Leckel et al. [30]. The reactor effluent is sent to the second fractionation column to recover the same products as the first column but with different rates. The naphtha is then sent to the naphtha stabilizer column to remove the light gases and recover the stabilized naphtha product. Furthermore, 70% of the unreacted off-gas stream is recycled to the reforming section (stream 16) and the rest must be sent to the chemical looping gasification (CLG) unit to produce hydrogen, process steam and excess heat required by heaters (upstream of the main fractionator column and cracking reactor). Thus, unlike typical FT processes [9], the hydrogen and heat requirement for FT processing is provided with essentially zero CO_2 emissions in this proposed system.

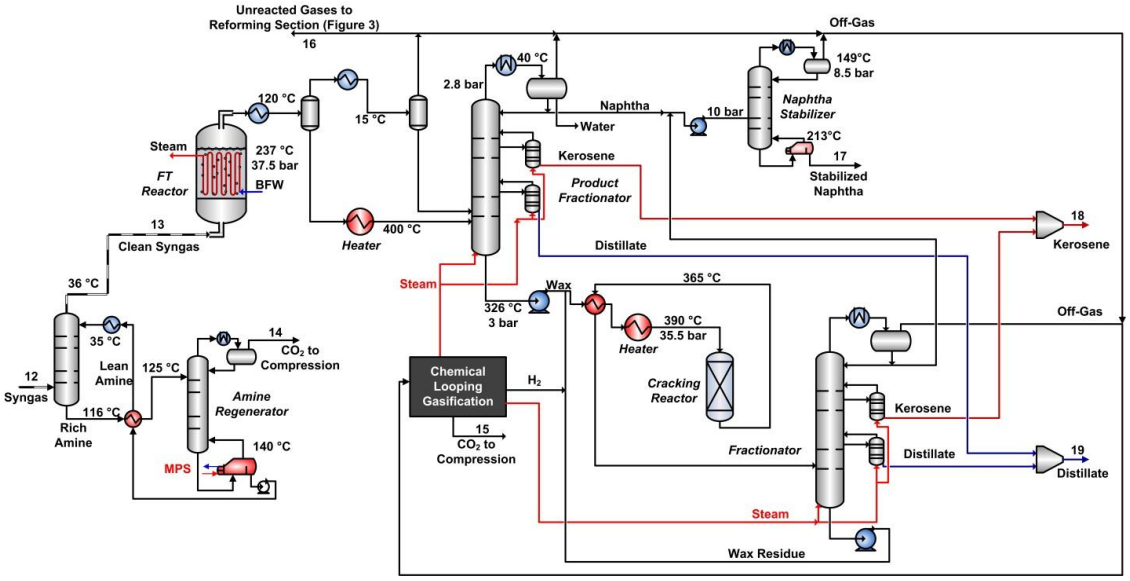

Figure 4. Fischer-Tropsch transportation liquid production process.

2.2.1 Chemical Looping Gasification

Instead of traditional commercial processes, H_2 can be produced via chemical looping gasification by using three tightly integrated reactors and an active oxygen carrier that circulates through the reactors [13-15]. This proposed system not only produces high purity hydrogen (>99.8% by mole) but also facilitates CO_2 capture by combusting the off-gas in absence of nitrogen (Figure 5). In this system, iron-oxide (Fe_2O_3) is used as the solid oxygen carrier with the following sub-reactions:

Reducer: $(0.5y+2x)\ Fe_2O_3 + C_xH_y \rightarrow (y+4x)\ FeO + (0.5y)\ H_2O + xCO_2$

$$Fe_2O_3 + CO \rightarrow 2FeO + CO_2$$

$$Fe_2O_3 + H_2 \rightarrow 2FeO + H_2O$$

Oxidizer: $3FeO + 4H_2O \rightarrow Fe_3O_4 + 4H_2$

Combustor: $4Fe_3O_4 + O_2 \rightarrow 6Fe_2O_3$

There are some other side-reactions that occur in the reducer and oxidizer and have been considered in the simulation but have not been shown here for brevity. Details of the operability and process description of this hydrogen production cycle is discussed in our previous work [20].

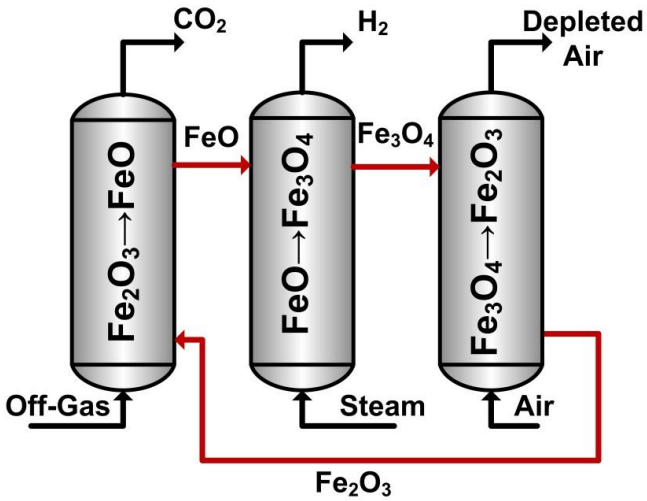

Figure 5. Simplified schematic of the chemical looping gasification system.

2.3 MeOH and DME production

The second syngas stream (stream 13 in Figure 3) is fed to the MeOH synthesis reactor (Figure 1) where syngas is converted to MeOH over $Cu/ZnO/Al_2O_3$ catalyst as follows [31]:

$$CO_2 + 3H_2 \leftrightarrow CH_3OH + H_2O$$

$$CO_2 + H_2 \leftrightarrow CO + H_2O$$

After removing the unreacted gases from the liquid product, MeOH is purified in the Methanol recovery column (see [20] for more details about kinetic reaction models and process description). Unreacted gases can be recycled to the reactor or optionally sent to the power generation island. The purified MeOH stream is split and routed to three different sections: 1) Stored as the final product. 2) Sent to the MTO unit for olefin production (described in the next section). 3) Sent to the DME unit to convert MeOH to dimethyl ether (CH_3OCH_3) fuel. In the third route, MeOH is delivered to the DME synthesis reactor where MeOH is dehydrated over γ-Al_2O_3 catalyst [32, 33]:

$$2CH_3OH \leftrightarrow CH_3OCH_3 + H_2O$$

The reactor effluent is then sent to the DME recovery column (Figure 1) to purify the DME product and recycle back MeOH+water to methanol recovery column.

2.4 MTO Unit

Catalytic conversion of methanol into light olefins such as ethylene and propylene is an alternative olefin production approach to commercial naphtha cracking processes. Several research groups and companies have been working on catalyst development and commercialization of this process [34, 35]. The experimental results of the SAPO-34 catalyst, developed by UOP/Hydro [36], are used in this work for the simulation of the MTO reactor. In addition to ethylene and propylene, C_3^+ is the by-product of this plant that can be sold as LPG product or sent to the power island as the alternative combustion fuel. The latter option was chosen in the present work. Details of the CO_2 removal and also product recovery train are described in our previous work [37].

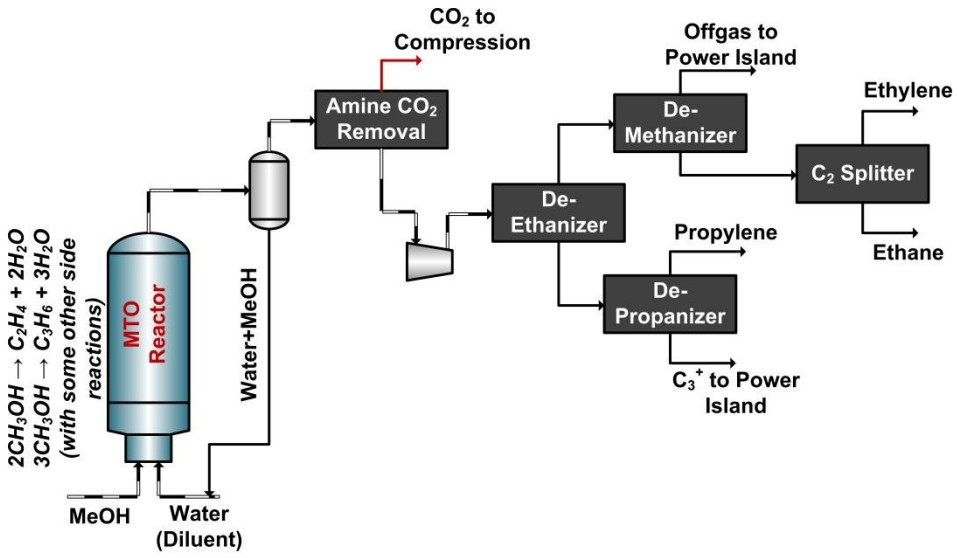

Figure 6. Simplified schematic of the MTO unit.

2.5 Power Generation and CO_2 Compression

In our prior work, the performances of three different power generation options were investigated [37]: amine-based post combustion [38], oxy-fuel combustion [39], and chemical looping combustion (CLC) [40]. Techno-economic optimization results showed that the CLC system achieves the highest thermal efficiency and net present value (NPV) compared to the other two technologies [37]. Thus, the CLC process with nickel-oxide as the oxygen carrier is chosen in the present work. As shown in Figure 7, it is very similar to the CLG concept (section 2.2.1), except that it employs only two reactors (instead of three) and air is used directly for metal regeneration (instead of steam):

Reducer: $(0.5y+2x)\ NiO + C_xH_y \rightarrow (0.5y+2x)\ Ni + (0.5y)\ H_2O + xCO_2$

$NiO + CO/H_2 \rightarrow Ni + CO_2/H_2O$

Oxidizer: $NiO + 0.5O_2 \rightarrow NiO$

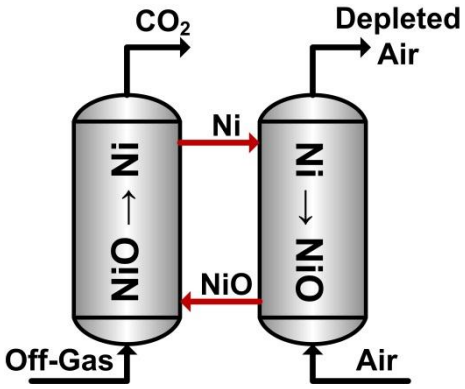

Figure 7. Chemical looping combustion for power generation purpose.

Finally, the captured CO_2 from all units are gathered and sent to the CO_2 compression section (Figure 1) where it is compressed to 80 bar and then condensed and pumped to 153 bar to obtain supercritical CO_2 [27]. The supercritical CO_2 can be then delivered via pipeline for different purposes, such as enhanced oil recovery (EOR), chemical uses, and so on.

2.6 Economic Analysis and Process Optimization

A summary of economic analysis parameters and market prices, used for the net present value analysis, are listed in Table 3. The details of the NPV calculation elements are described in [12, 20]. Capital cost estimates of the FT liquid production unit, shale gas reforming and gasification section, MeOH and DME synthesis section, heat recovery steam generation (HRSG) section, gas turbines, steam turbines and the air separation unit (ASU) are adopted from available published sources [9, 19, 20, 41]. Moreover, Aspen Capital Cost Estimator software was used for the capital cost estimation of units where economic data could not be found. It should be noted that due to a lack of reliable data for the price of petcoke, it is assumed that its price is the same as Illinois coal for the base case. However, the effect of variations in the petcoke price is investigated in detail in section 3.1 to determine the impact of this assumption on the profitability of our proposed system.

Table 3. Market prices and cost estimation parameters.

Feed and product prices	
Petcoke price, $/tonne	50.9 (assumed to be same price as Illinois coal) [42]
Shale gas & ethane prices, $/MMBtu	3.88 [43]
NiO (76% wt.), $/kg	20 [44]
NiO disposal cost, $/kg	5 (1)

NiO life span, hours	10000 [45]
Fe_2O_3 (96% wt.), $/kg	1.44 [46]
Fe_2O_3 disposal cost, $/kg	0.36 (1)
Fe_2O_3 life span, hours	3000 [47]
Electricity, ¢/kWh	5.67 [48]
MeOH, $/tonne	482 [49]
DME, $/tonne	962 [23]
Naphtha, $/liter	0.69 (assumed to be 90% of gasoline price) [50]
Kerosene, $/liter	0.68 (assumed to be 90% of jet-fuel price) [51]
Distillate, $/liter	0.91 (assumed to be 90% of diesel price) [52]
Propylene, $/tonne	1340 [53]
Ethylene, $/tonne	1424 [54]
Economic assumptions, [9, 55]	
Operation time (hr/year)	8760
Capacity factor	85%
Chemical Engineering Plant Cost Index	574.3 [56]
Plant and loan lifetimes (year)	30
Interest rate on loan	9.5%
Debt percentage	50%
Inflation	2.79%
Tax rate	40%
Equity return rate	20%

(1) Due to lack of published data, assumed to be 25% of the metal-oxide price.

2.6.1 Process Optimization

There are 5 main decision variables that affect the product portfolio of plant, its thermal efficiency, and its NPV:

1. Petcoke consumption (stream 1, Figure 1), which influences both product portfolio and subsequently the profitability of the plant. As mentioned earlier, when the petcoke rate is altered, the shale gas rate is automatically adjusted such that the total energy input remains the same. The petcoke rate is allowed to vary between 0 tonne/day and 3254 tonne/day (0-1111 MW (LHV), or 0%-100% of total input).
2. The split ratio of CO-rich syngas that is sent to FT section (Figure 3). By raising this ratio the FT liquid production increases, and thus, the MeOH, DME and olefin

production rates drop subsequently. The split ratio is allowed to vary between 0% and 100%.

3. The recycle ratio of unreacted gases that are sent back to the MeOH synthesis reactor (Steam 20, Figure 1). Raising this recycle ratio increases the MeOH production rate. On the other hand, the unreacted gases can be used for power generation to meet the plant's electricity demand or even be sold to the power grid. The recycle ratio is allowed to vary between 0% and 99%. Note that a 100% recycle ratio is not possible because a purge stream is required to allow impurities such as nitrogen to escape from the MeOH synthesis loop.
4. The percentage of the MeOH product that is fed to the DME synthesis reactor (Stream 21, Figure 1).
5. The percentage of the MeOH product that is fed to the MTO reactor (Stream 22, Figure 1). Both 4 and 5 impact the DME, olefins and stored MeOH rates relatively. The MeOH to DME and MTO ratios are allowed to vary between 5% and 95% and manually set to 0% when they reach the lower bound (5%).

Different scenarios are considered for the optimization of plant, as described in section 3, and for each scenario the objective function and constraints where changed respectively. Furthermore, the particle swarm optimization (PSO) technique was employed to obtain the optimum values of these five variables for each scenario. The PSO code was adopted from our previous work [12] in MATLAB and linked to the Aspen simulation file using VBA code. The only change is the maximum number of function evaluations (NFE) which has been increased to 150, since there were more decision variables to be considered and thus requiring more iterations. This optimization technique was much faster than other heuristic approaches such as genetic algorithm (GA) and simulated annealing (SA) and therefore is used for all sensitivity analyses to locate the optimum conditions at different market prices.

3. Results

The techno-economic results and breakdown of products and feedstocks are listed in Table 4 for different optimization scenarios: 1) Maximum NPV; 2) Maximum olefin production; 3) Maximum transportation fuel production; and 4) Maximum petcoke consumption. It can be seen that the maximum NPV (first scenario) is achieved when most of the output is DME. In the

second scenario, the objective function was to maximize the olefins production rate with an added constraint requiring non-negative NPV. This option shows that, at current market prices, the maximum olefin production ratio (ethylene + propylene) must be less than 35.8% to have a profitable plant. In the third scenario, the transportation fuel production is maximized with a non-negative NPV constraint. Based on the HHV energy content of outputs, around 59.2% of outputs are the produced transportation fuels (gasoline, kerosene and diesel). Furthermore, around 19.6% of feedstock is petcoke in this scenario. And finally the fourth scenario shows that the maximum petcoke consumption ratio while still having a profitable plant is around 74%. In addition, for each scenario, a summary of the most important economic parameters are listed in Table 5.

Table 4. Comparison of the results of different optimization scenarios. The thermal efficiency is defined as the total energy content in HHV of the chemicals plus the power produced, divided by the total HHV of the feed.

Optimization scenario	Maximum NPV	Maximum olefin production with non-negative NPV constraint	Maximum transportation fuel production with non-negative NPV constraint	Maximum petcoke consumption with non-negative NPV constraint
Thermal efficiency, %HHV	65.87	40.43	38.96	45.14
CO_2 Emissions, tonne/year	0.0	0.0	0.0	0.0
Product portfolio based on energy content (HHV basis where applicable)				
%*Methanol*	0.0	0.0	0.0	0.0
%*DME*	94.6	47.3	26.3	71.5
%*Ethylene*	0.0	18.9	0.0	0.0
%*Propylene*	0.0	16.9	0.0	0.0
%*Ethane*	0.0	1.6	0.0	0.0
%*Naphtha*	0.0	0.0	6.5	0.0
%*Kerosene*	0.0	0.0	12.0	0.0
%*Distillate*	0.0	0.0	40.7	0.0
%*Power*	5.4	15.3	14.5	28.5
Decision Variables (section 2.6.1)				
Petcoke rate, tonne/day	0	0	661	2434
CO-rich syngas to FT	0%	0%	100%	0%
Recycle ratio	99%	99%	99%	99%

MeOH to DME	100%	53%	100%	100%
MeOH to MTO	0%	47%	0%	0%
Feedstock ratio				
%Petcoke	0.0	0.0	19.6	74.0
%Shale gas	100.0	100.0	80.4	26.0
NPV, $million	$1,237	0	0	0
Capital cost, $million	$575	$595	$762	$937

Table 5. Economic summary of different optimization scenarios

	Maximum NPV	Maximum olefin production with non-negative NPV constraint	Maximum transportation fuel production with non-negative NPV constraint	Maximum petcoke consumption with non-negative NPV constraint
Direct capital cost breakdowns, $1000				
Petcoke handling and preparation	$0	$0	$36,035	$89,700
Petcoke gasification	$0	$0	$79,116	$196,937
Slag handling	$0	$0	$12,415	$30,903
Petcoke syngas cleaning	$0	$0	$39,076	$89,269
Shale gas reforming	$15,644	$15,644	$13,247	$6,923
MeOH synthesis and purification	$359,876	$357,221	$84,335	$198,496
DME synthesis and purification	$10,095	$2,662	$1,556	$4,403
MTO section	$5,199	$16,791	$5,199	$5,199
Power generation	$73,633	$90,993	$68,600	$148,515
Fischer-Tropsch, CO_2 removal unit	$0	$0	$95,036	$0
Fischer-Tropsch	$0	$0	$194,021	$0
Air separation unit (ASU)	$102,414	$102,414	$117,776	$140,104
CO_2 sequestration	$8,146	$9,399	$15,168	$26,784
Cost breakdowns at 85% of design capacity				
Total capital cost (direct+indirect+working), $1000	$845,658	$875,243	$1,119,972	$1,378,341
Feedstock cost, $1000/yr	$110,558	$110,621	$99,910	$69,990
Labour cost, $1000/yr	$22,112	$22,124	$19,982	$13,998
Other operating costs, $1000/yr	$114,084	$116,314	$129,556	$134,919
Sales				
Ethylene sale, $1000/yr	$0	$71,580	$0	$0
Ethane sale, $1000/yr	$0	$630	$0	$0
Power sale, $1000/yr	$18,396	$32,107	$29,093	$64,801
Methanol sale, $1000/yr	$0	$0	$0	$0
DME sale, $1000/yr	$625,907	$191,890	$101,842	$313,303
Propylene sale, $1000/yr	$0	$61,816	$0	$0

Gasoline sale, $1000/yr	$0	$0	$63,307	$0
Kerosene sale, $1000/yr	$0	$0	$32,995	$0
Distillate sale, $1000/yr	$0	$0	$157,424	$0
CO_2 sale, $1000/yr	$4,183	$4,480	$9,978	$20,403
Gross earning, $1000/yr	$401,731	$113,445	$145,190	$179,601
NPV, $million	$1,237	$0	$0	$0

3.1 Sensitivity analysis- effect of Petcoke consumption

Figure 8 shows the effect of the percentage of petcoke consumption on the maximum NPV at various petcoke prices. For example, when around 70% of the input is petcoke, the petcoke price must be less than $22/tonne to have a profitable plant. However, under base case market conditions, the most profitable strategy is to avoid the use of petcoke completely, regardless of the petcoke price. This is due to the extremely high capital investment cost imposed by the petcoke gasification and purification sections, which is much higher than the capital cost of the shale gas reforming unit, as can be seen in Table 5. Changing the petcoke input ratio can also have a significant influence on the thermal efficiency of the plant as shown in Figure 9.

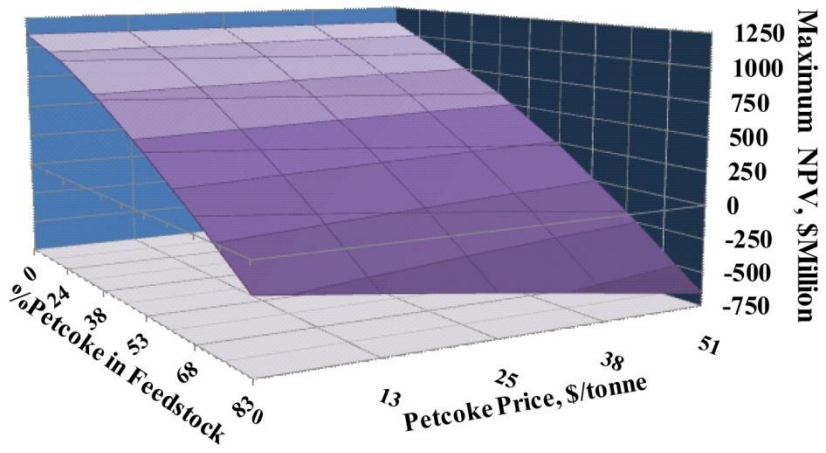

Figure 8. Effect of the petcoke inlet ratio and price on the maximum NPV of the plant.

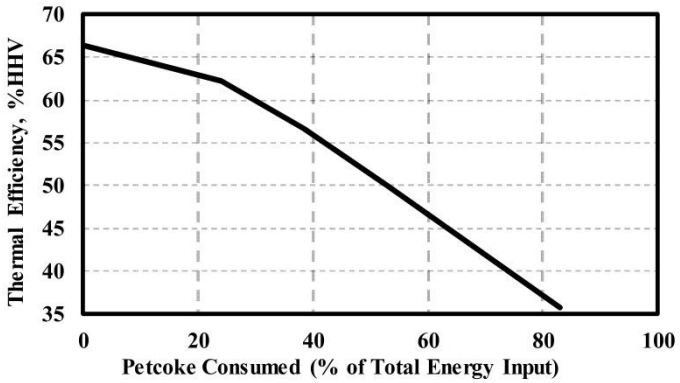

Figure 9. Thermal Efficiency of plant in %HHV as a function of petcoke consumption.

3.2 Sensitivity analysis- effect of DME and transportation fuels prices

To determine the impact of the market price changes on the optimum product portfolio, a sensitivity analysis was performed by rerunning the optimization at different gasoline and DME prices. It is assumed that the kerosene and diesel prices remain in the same proportion to gasoline as in the base case, such that if the gasoline price doubles, kerosene and diesel prices also double. The optimization results using the maximum NPV objective function is shown in Figure 10. It can be seen that when the DME price is $577 per tonne or less, the maximum NPV is only affected by the gasoline price since it is no longer optimal to produce DME at that low of a price. The optimum product portfolio and type of feedstock is shown in Figure 11. It can be seen that maximizing the production rate of MeOH is the most profitable choice only when the gasoline and DME prices are less than $0.697/liter and $577.2/tonne respectively. Furthermore, as can be seen in Figure 11b, in order for the use of petcoke gasification (which leads to the production of more transportation fuels) to be more profitable than a shale gas only system, the price of gasoline must be at some minimum price (starting at $0.69/L), which increases with increasing price of DME. In this case, the maximum petcoke consumption is 19.6% as shown in Table 4. It cannot go beyond this ratio because the blending H_2-rich syngas produced by the shale gas reformer would not be enough to make a syngas with $H_2/CO=2.1$, which is the constraint of the FT syngas stream (Figure 3).

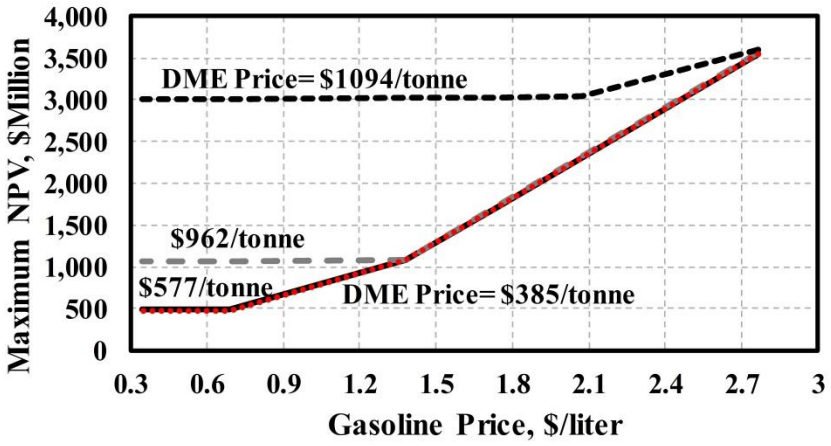

Figure 10. Effect of transportation fuels (gasoline, diesel and kerosene) and DME prices on the maximum NPV of plant.

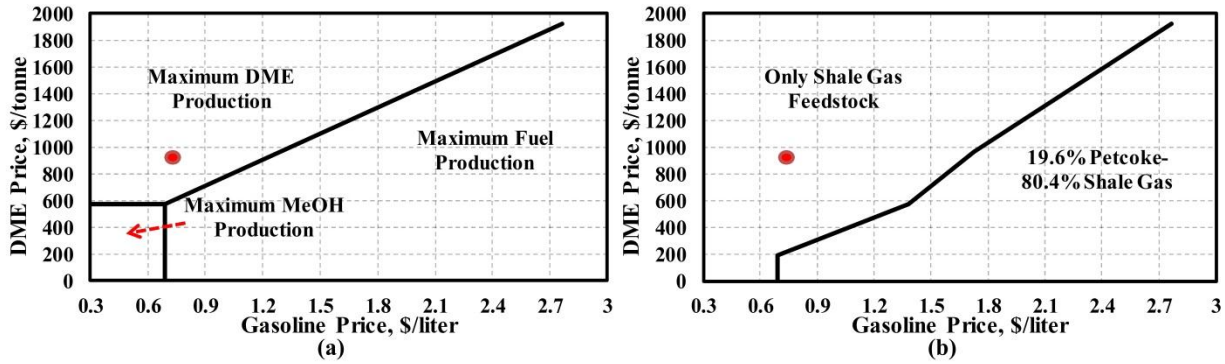

Figure 11. Effect of transportation fuels and DME prices on the optimum product portfolio and feedstock selection.

3.3 Sensitivity analysis- effect of MeOH and transportation fuels prices

A similar sensitivity analysis was performed to determine the effect of varying the prices of MeOH and gasoline on the maximum achievable NPV (Figure 12), optimum product portfolio (Figure 13a) and the optimum feedstock selection (Figure 13b). As depicted in Figure 12, the price of MeOH affects the maximum NPV only when the MeOH price is $482/tonne or more. Below this value, DME or transportation fuels are the major product of the plant, as shown in Figure 13a. Furthermore, as illustrated in Figure 13b, supplying syngas by using shale gas reforming-petcoke gasification trains is more profitable than using just the shale gas reforming system, only when the price of gasoline is more than $1.037/liter.

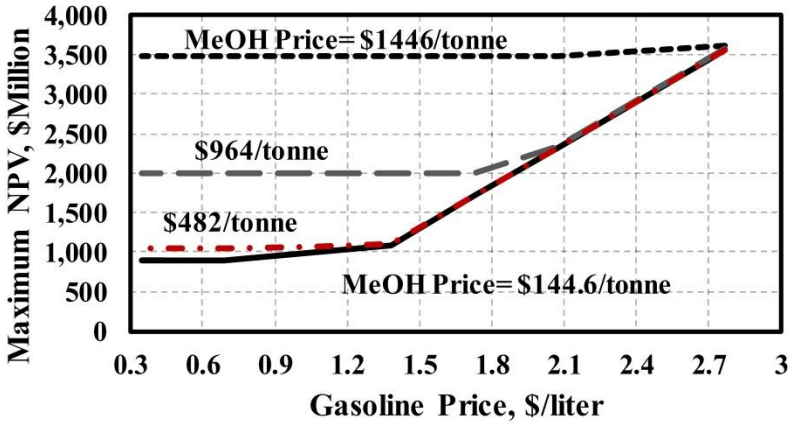

Figure 12. Effect of transportation fuels (gasoline, diesel and kerosene) and MeOH prices on the maximum NPV of plant.

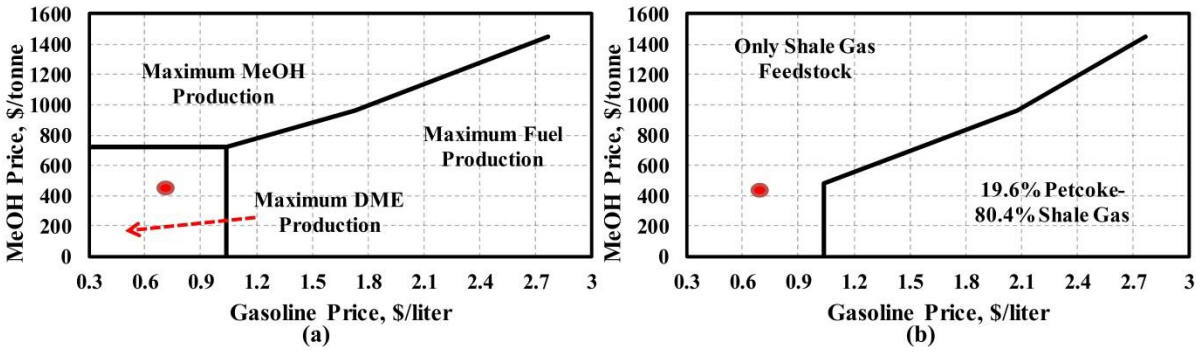

Figure 13. Effect of transportation fuels and MeOH prices on (a) optimum product portfolio, (b) feedstock selection.

3.4 Sensitivity analysis- effect of olefins and transportation fuels prices

Finally, the effect of varying the market prices of olefins and transportation fuels are analyzed in this section. Figure 14 depicts the maximum achievable NPV as a function of ethylene price for different gasoline prices. It is also assumed that the price of propylene always changes at the same ratio as the ethylene price varies (same for kerosene and diesel compared to gasoline price). As can be seen from Figure 14, the maximum NPV of the plant is never less than $1 billion,

regardless how inexpensive the price of olefins and transportation fuels is. The reason is illustrated in Figure 15a. Unless the gasoline price is more than $1.037/liter or ethylene price is more than $4272/tonne, maximizing the production of DME is the most profitable design scenario. In addition, it is more profitable to use the integrated petcoke gasification-shale gas reforming system only when the gasoline price is more than $1.037/liter, as shown in Figure 15b.

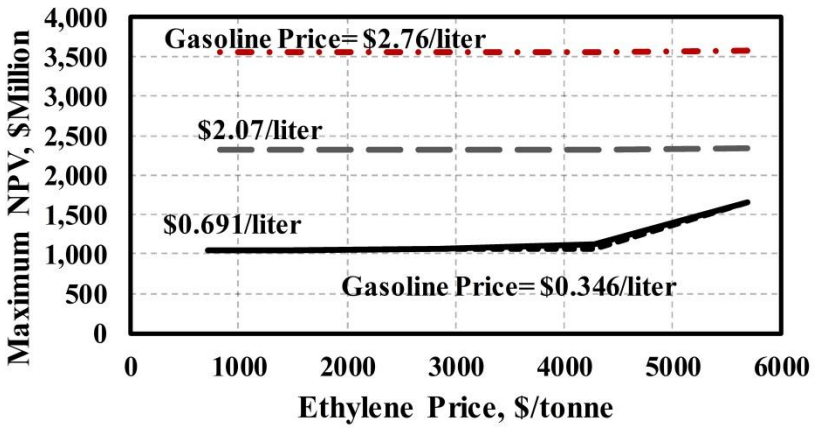

Figure 14. Effect of transportation fuels (gasoline, diesel and kerosene) and olefins (ethylene and propylene) prices on the maximum NPV of plant.

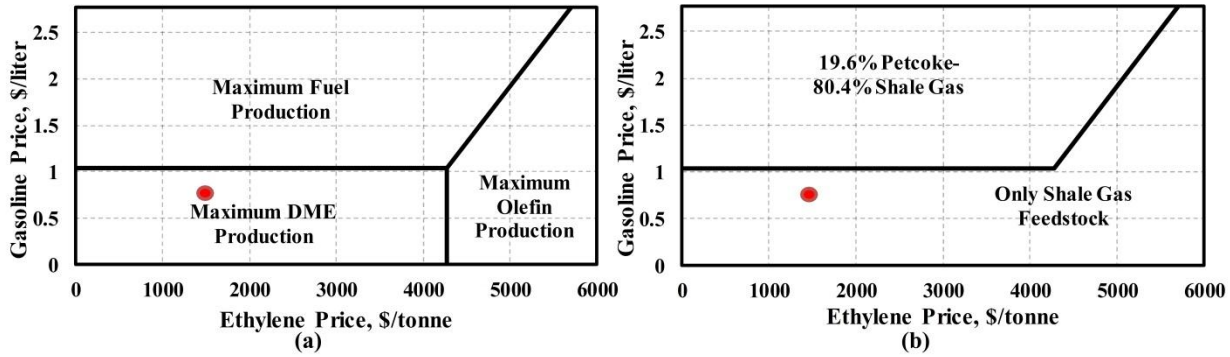

Figure 15. Effect of transportation fuels and MeOH prices on (a) optimum product portfolio, (b) feedstock selection.

4. Conclusion

In the present work, a novel polygeneration system was investigated that uses a combination of shale gas and petcoke feedstocks and co-produces methanol, DME, FT liquids, electricity and

olefins. Incorporation of petcoke gasification technology and coupling it with the shale gas reforming system is a great opportunity for petcoke producers such as oil sand upgrading plants and heavy oil refineries. This proposed process not only offers a zero carbon emissions model, but also can be an incentive for those producers to convert stockpiled petcoke to more valuable products, as an alternative to combusting petcoke or transporting it to regions or countries that do not control the environmental impacts of petcoke combustion.

Chemical looping combustion and chemical looping gasification alternatives were also considered for the power generation and FT units respectively, which both have beneficial effects on the performance of the plant. In addition, four optimization scenarios were investigated to determine the maximum achievable NPV, olefin production, FT liquid production and petcoke consumption. Optimization results showed that up to 74% of the feed can be petcoke while having a profitable plant. Moreover, a comprehensive sensitivity analysis was performed resulting that this integrated system can be profitable over a wide range of market conditions.

Nomenclature

Abbreviations

ASU	Air separation unit
CLC	Chemical looping combustion
CEPCI	Chemical engineering plant cost index
DGA	Diglycolamine
DME	Dimethyl ether

FT Fischer-Tropsch

HHV Higher heating value

HRSG Heat recovery steam generator

LHV Lower heating value

MDEA Methyl diethanolamine

NPV Net present value

PSO Particle swarm optimization

References

[1] E. Furimsky, Gasification in Petroleum Refinery of 21st Century, Oil & Gas Science and Technology - Rev. IFP, 54 (1999) 597-618.
[2] M. S. Rana, V. Sa´mano, J. Ancheyta, J.A.I. Diaz, A review of recent advances on process technologies for upgrading of heavy oils and residua, Fuel, 86 (2007) 1216-1231.
[3] D. Hammond, L. Lampert, C. Mart, S. Massenzio, G. Phillips, D. Sellards, A. Woerner, Review of fluid bed coking technologies, Petroleum technology quarterly, 8 (2003) 27-34.
[4] L. Stockman, Petroleum Coke: the coal hiding in the tar sands, Oil Chance International, Washington DC, USA, (2013).
[5] E. Furimsky, Gasification of oil sand coke: Review, Fuel Processing Technology, 56 (1998) 263-290.
[6] S.H. Lee, S.J. Yoon, H.W. Ra, Y.I. Son, J.C. Hong, J.G. Lee, Gasification characteristics of coke and mixture with coal in an entrained-flow gasifier, Energy, 35 (2010) 3239-3244.
[7] B.N. Murthy, A.N. Sawarkar, N.A. Deshmukh, T. Mathew, J.B. Joshi, Petroleum coke gasification: A review, The Canadian Journal of Chemical Engineering, 92 (2014) 441-468.
[8] JACOBS Consultancy, Executive Summary (Edited for RFP), .
[9] T.A. Adams II, P.I. Barton, Combining coal gasification and natural gas reforming for efficient polygeneration, Fuel Processing Technology, 92 (2011) 639-655.
[10] T.A. Adams II, P.I. Barton, Combining coal gasification, natural gas reforming, and solid oxide fuel cells for efficient polygeneration with CO_2 capture and sequestration, Fuel Processing Technology, 92 (2011) 2105-2115.
[11] Y. Khojasteh Salkuyeh, T. A. Adams II, Shale gas for the petrochemical industry: incorporation of novel technologies, in: Proceedings of the 8th International Conference on Foundations of Computer-Aided Process Design – FOCAPD, Washington, USA, 2014.
[12] Y. Khojasteh Salkuyeh, T.A. Adams II, A novel polygeneration process to co-produce ethylene and electricity from shale gas with zero CO_2 emissions via methane oxidative coupling, Energy Conversion and Management, 92 (2015) 406-420.
[13] L. Fan, F. Li, S. Ramkumar, Utilization of chemical looping strategy in coal gasification processes, Particuology, 6 (2008) 131-142.
[14] F. Li, H.R. Kim, D. Sridhar, F. Wang, L. Zeng, J. Chen, L. Fan, Syngas Chemical Looping Gasification Process: Oxygen Carrier Particle Selection and Performance, Energy & Fuels, 23 (2009) 4182–4189.
[15] L.G. Velazquez-Vargas, Development of chemical looping gasification processes for the production of hydrogen from coal, in, The Ohio State University, 2007.
[16] P. Kolbitsch, J. Bolhàr-Nordenkampf, T. Pröll, H. Hofbauer, Operating experience with chemical looping combustion in a 120 kW dual circulating fluidized bed (DCFB) unit, International Journal of Greenhouse Gas Control, 4 (2010) 180-185.
[17] P. Kolbitsch, T. Pröll, J. Bolhar-Nordenkampf, H. Hofbauer, Design of a Chemical Looping Combustor using a Dual Circulating Fluidized Bed (DCFB) Reactor System, Chemical Engineering & Technology, 32 (2009) 398-403.
[18] C.C. Chen, P.M. Mathias, Applied thermodynamics for process modeling, AIChE Journal, 48 (2002) 194-200.

[19] Y. Khojasteh Salkuyeh, T.A. Adams II, Combining coal gasification, natural gas reforming, and external carbonless heat for efficient production of gasoline and diesel with CO_2 capture and sequestration, Energy Conversion and Management, 74 (2013) 492-504.
[20] Y. Khojasteh Salkuyeh, T.A. Adams II, A new power, methanol, and DME polygeneration process using integrated chemical looping systems, Energy Conversion and Management, 88 (2014) 411-425.
[21] K. Bullin, P. Krouskop, Composition Variety Complicates Processing Plans for US Shale Gas, Bryan Research and Engineering Inc. report, (2009).
[22] Methanol Industrial Grade, http://www.alibaba.com/product-detail/2012-Methanol-99-5-_551002733.html.
[23] DiMethyl Ether, http://www.alibaba.com/product-detail/DiMethyl-Ether_1659793013.html.
[24] Propylene, Polymer Grade, http://www.dow.com/productsafety/finder/pro.htm.
[25] Ethylene, Polymer Purity, https://www.mathesongas.com/pdfs/products/Ethylene-Pure-Gas.pdf.
[26] J. Wauquier, Petroleum Refining, Vol. 1: Crude Oil, Petroleum Products, Process Flowsheets, in, Editions Technip, Paris, 1995.
[27] T.A. Adams II, P.I. Barton, High-Efficiency Power Production from Coal with Carbon Capture, AIChE Journal, 56 (2010) 3120-3136.
[28] T.A. Adams II, Y. Khojestah Salkuyeh, J. Nease, Chapter 6 - Processes and simulations for solvent-based CO_2 capture and syngas cleanup, in: F. Shi (Ed.) Reactor and Process Design in Sustainable Energy Technology, Elsevier, Amsterdam, 2014, pp. 163-231.
[29] C. Barrere-Tricca, D. Smith, J. Margotin, Thirty years of operating experience with the Clauspol process, Oil & Gas Science and Technology, 56 (2001) 199-206.
[30] D. Leckel, M. Liwanga-Ehumbu, Diesel-Selective Hydrocracking of an Iron-Based Fischer−Tropsch Wax Fraction (C_{15}−C_{45}) Using a MoO_3-Modified Noble Metal Catalyst, Energy & Fuels, 20 (2006) 2330-2336.
[31] K.M. Vanden bussche, G.F. Froment, A steady-state kinetic model for methanol synthesis and the water gas shift reaction on a commercial $Cu/ZnO/Al_2O_3$ catalyst, Journal of Catalysis, 161 (1996) 1-10.
[32] G. Bercic, J. Levec, Catalytic dehydration of methanol to dimethyl ether. Kinetic investigation and reactor simulation, Industrial & Engineering Chemistry Research, 32 (1993) 2478-2484.
[33] B.T. Diep, M.S. Wainwright, Thermodynamic equilibrium constants for the methanol-dimethyl ether-water system, Journal of Chemical & Engineering Data, 32 (1987) 330-333.
[34] T. Ren, M.K. Patel, K. Blok, Steam cracking and methane to olefins: Energy use, CO_2 emissions and production costs, Energy, 33 (2008) 817-833.
[35] J.Q. Chen, A. Bozzano, B. Glover, T. Fuglerud, S. Kvisle, Recent advancements in ethylene and propylene production using the UOP/Hydro MTO process, Catalysis Today, 106 (2005) 103-107.
[36] S. Wilson, P. Barger, The characteristics of SAPO-34 which influence the conversion of methanol to light olefins, Microporous and Mesoporous Materials, 29 (1999) 117-126.
[37] Y. Khojasteh Salkuyeh, T.A. Adams II, Co-Production of Olefins, Fuels, and Electricity from Conventional Pipeline Gas and Shale Gas with Near-Zero CO_2 Emissions, (Under Final Review), Energies, 18 (2015).
[38] M.R.M. Abu-Zahra, J.P.M. Niederer, P.H.M. Feron, G.F. Versteeg, CO_2 capture from power plants: Part II. A parametric study of the economical performance based on mono-ethanolamine, International Journal of Greenhouse Gas Control, 1 (2007) 135-142.
[39] Y. Tan, M.A. Douglas, K.V. Thambimuthu, CO_2 capture using oxygen enhanced combustion strategies for natural gas power plants, Fuel, 81 (2002) 1007-1016.
[40] B. Moghtaderi, Review of the Recent Chemical Looping Process Developments for Novel Energy and Fuel Applications, Energy & Fuels, 26 (2011) 15-40.
[41] J.L. Haslbeck, N.J. Kuehn, E.G. Lewis, L.L. Pinkerton, J. Simpson, M.J. Turner, E. Varghese, M.C. Woods, Cost and Performance Baseline for Fossil Energy Plants Volume 1: Bituminous Coal and Natural Gas to Electricity, DOE, National Energy Technology Laboratory (NETL), (2010).
[42] Illinois Basin coal, average wholesale price; Aug 2014. http://www.eia.gov/coal/news_markets/.
[43] Henry hub spot, average wholesale price; Aug 2014. http://www.eia.gov/electricity/wholesale/.
[44] Nickel Monoxide, CAS No.: 1313-99-1, http://www.alibaba.com/product-gs/747545915/Factory_direct_sales_with_reasonable_price.html.
[45] J. Adanez, A. Abad, F. Garcia-Labiano, P. Gayan, L.F. de Diego, Progress in Chemical-Looping Combustion and Reforming technologies, Progress in Energy and Combustion Science, 38 (2012) 215-282.
[46] Factory price of Iron Oxide (Fe_2O_3), CAS No.: 1309-37-1, http://www.alibaba.com/product-detail/factory-price-of-iron-oxide-fe2o3-_814503142.html?s=p.
[47] L.S. Fan, Chemical Looping Systems For Fossil Energy Conversions, John Wiley & Sons, Inc., , New Jersey, United States, 2010.
[48] Electricity wholesale price, Average 2014. http://www.eia.gov/electricity/wholesale/.
[49] Methanol Price, North America, October 2014, https://www.methanex.com/our-business/pricing.
[50] U.S. Regular Conventional Retail Gasoline Prices, 11/Nov/2014, http://www.eia.gov/petroleum/gasdiesel/.
[51] Kerosene-Type Jet Fuel, U.S. Gulf Coast, 08/Nov/2014, http://www.eia.gov/dnav/pet/pet_pri_spt_s1_d.htm.
[52] U.S. On-Highway Diesel Fuel Prices, 08/Nov/2014, http://www.eia.gov/petroleum/gasdiesel/.
[53] Platts Global Propylene Price Index, August 2014, http://www.platts.com/news-feature/2014/petrochemicals/pgpi/propylene.

[54] Platts Global Ethylene Price Index, August 2014, http://www.platts.com/news-feature/2014/petrochemicals/pgpi/ethylene.
[55] M. S. Peters, K.D. Timmerhaus, Plant Design and Economics for Chemical Engineers, 4th ed., McGraw-Hill, New York, United States, 1991.
[56] CEPCI, Chemical Engineering Plant Cost Index, Chemical Engineering, 121 (May 2014) 80.

Chapter 7 Conclusion

In this thesis, techno-economic analyses of different polygeneration systems were investigated to determine the optimum configurations with minimum environmental impacts. As the first step, a rigorous study was performed on different configurations of an integrated Fischer-Tropsch plant that uses coal, natural gas and nuclear energy as the principal feedstocks with and without CCS option (chapter 2). Incorporation of non-carbon energy into polygeneration process is a novel strategy that has been investigated in this work. The new integrated MHR-steam reformer system can improve the efficiency of plant by 4 percentage point compared to a coal-only system. Then, in order to facilitate the CO_2 removal and sequestration from the exhaust gases, chemical looping gasification and chemical looping combustion approaches were introduced to the plant (chapter 3).

In addition, the incorporation of two novel technologies that employ shale gas and petcoke for olefin production were studied in this thesis: 1) direct conversion of shale gas to ethylene based on the OCM reaction (chapter 4). 2) Indirect conversion of shale gas, and petcoke to ethylene and propylene based on the MTO process (chapters 5 and 6). Techno-economic analysis of a commercial scale OCM-based polygeneration process from shale gas had not been studied in any other research, to the best of our knowledge. However, our systematic comparison showed that the MTO-based polygeneration process is the superior route, due to its higher thermal efficiency and more valuable byproducts. Furthermore, using petcoke as a potential feedstock for polygeneration systems is studied in chapter 6.

After examining all of the various products, power generation options, feedstocks, and processing routes, some general conclusions can be made. First, significant improvements in efficiency, profitability, and environmental impact can be achieved by using chemical looping combustion instead of traditional combustion technology, especially when CCS is employed. For example, as described in chapter 5, the CLC system can raise the NPV of a polygeneration plant by up to 64%, compared to commercial combustion technology with post combustion CCS. In addition, the optimization results showed that at current market prices, DME is the most profitable product. However, the results also showed that the market conditions greatly affect

which product portfolios to choose. Accordingly, it is possible to have a profitable plant that uses petcoke as up to 74% of feedstock and with 100% carbon capture. Thus, instead of burning petcoke, the proposed system can be applied as a promising way of utilizing petcoke with less environmental impacts.

The cost effective polygeneration strategies, proposed in this work, can provide an incentive for energy sectors to even without financial encouragements or environmental regulations and leverages enforced by governments.

7.1 Future work

Despite promising results achieved by this work, the flexibility and dynamic behaviour of these tightly integrated systems has not been investigated and is subject of further research. It has been shown previously that flexible polygeneration systems can have massive improvements in NPV compared to inflexible ones. For example, one study showed that up to 62% increases in net present value were possible if the amount of methanol, synthetic fuels, or electricity produced by that particular process were allowed to change twice per day in response to changes in market prices with a 100% turndown ratio [1]. Other studies on polygeneration systems have shown that the optimal process design and corresponding product portfolio for inflexible polygeneration plants vary significantly with market prices [2]. These studies also showed that the historical variation in market prices experienced over a several year time period is sufficiently large enough such that flexible polygeneration may make economic sense. However, all of these studies assumed that transitions between operating steady states were feasible, instantaneous, and free. It is a significant future challenge to construct dynamic models of all of the relevant process units in sufficient detail such that the complex interaction between tightly integrated process sections can be understood well enough to know the information about the time required for transitions, feasible turndown ratios, off-spec products, and their associated costs. Some progress has been made in constructing dynamic models of certain individual process units specifically for the purposes of flexible polygeneration applications, such as for gasification [3], steam reforming [4], water gas shift [5], CO_2 capture [6], and solid oxide fuel cells [7]. However, combining these models into one system requires considerable effort and has not yet been

achieved.

Future work will also require a rigorous study on the market price prediction approaches to estimate the future prices before making any changes on desired feedstock portfolios and production strategies, during the operational stage. This feature is essential since market prices might vary significantly during the transition time between current steady conditions and the time that the new conditions, proposed by the optimizer, are reached. Artificial Neural Network (ANN) model can be considered as a useful approach to learn different market price relationships and establish a mathematical structure that is cable of predicting price trends with acceptable accuracy. For example, the preliminary results from an ANN model that predicts the weekly gasoline and diesel prices as a function of crude oil price are illustrated in Figure 1. A nonlinear feed forward time delay ANN model, composed of 5 hidden layers, was used to generate these trends. The Levenberg-Marquardt optimization approach was used as the training function. The number of time delays was 3 with a prediction horizon of 10 days. Thus, as an example, to predict the gasoline and diesel price on November 10, 2014, the ANN model has used the crude oil price data on October 10, 17, 24 and 31. The obtained results show that the ANN model can provide a perfect fit for the price of these two FT products compared to their actual prices. Similar approach can be applied to other products to estimate their short and long term market fluctuations. However, it should be noted that the number and type of parameters that dictate the price trend of each item might vary considerably. For instance, the olefin price might be affected by various items such as crude oil and natural gas prices, rate of annual growth in supply and demand, etc.

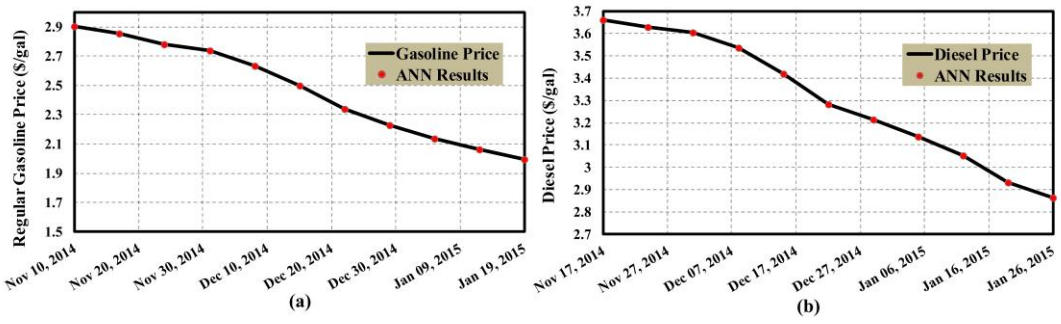

Figure 1. Obtained results from ANN model for (a) gasoline; (b) diesel price trends.

7.2 References

[1] Y. Chen, T.A. Adams II, P.I. Barton. Optimal Design and Operation of Flexible Energy Polygeneration Systems. Industrial & Engineering Chemistry Research. 50 (2011) 4553-66.

[2] T.A. Adams II, P.I. Barton. Combining coal gasification and natural gas reforming for efficient polygeneration. Fuel Processing Technology. 92 (2011) 639-55.

[3] J.S. Kasule, R. Turton, D. Bhattacharyya, S.E. Zitney. One-Dimensional Dynamic Modeling of a Single-Stage Downward-Firing Entrained-Flow Coal Gasifier. Energy & Fuels. 28 (2014) 4949-57.

[4] J.H. Ghouse, T.A. Adams II. A multi-scale dynamic two-dimensional heterogeneous model for catalytic steam methane reforming reactors. International Journal of Hydrogen Energy. 38 (2013) 9984-99.

[5] T.A. Adams II, P.I. Barton. A dynamic two-dimensional heterogeneous model for water gas shift reactors. International Journal of Hydrogen Energy. 34 (2009) 8877-91.

[6] N. Harun, T. Nittaya, P.L. Douglas, E. Croiset, L.A. Ricardez-Sandoval. Dynamic simulation of MEA absorption process for CO_2 capture from power plants. International Journal of Greenhouse Gas Control. 10 (2012) 295-309.

[7] N.F. Harun, D. Tucker, T.A. Adams II. Fuel Composition Transients in Fuel Cell Turbine Hybrid for Polygeneration Applications. Journal of Fuel Cell Science and Technology. 11 (2014) 061001 (1-8).

Appendix: modeling and optimization challenges

1) Process simulation: convergence issues

Aspen Plus simulation software provides reliable models for most of the chemical unit operations, which is very useful for the technical and economic evaluation of our proposed polygeneration systems and reduces the hand calculations and laboratory work significantly. However, it is not unusual to face convergence challenges caused by numerical problems or incorrect use of advanced model features. Unfortunately, finding the factors that cause the failure is usually a troublesome task.

A common problem is the convergence of the process flowsheet with multiple recycle streams. Manually setting the recycle as the tear stream can be a workaround to resolve this problem. Increasing the tolerance of the selected tear stream to a reasonable value is one option to troubleshoot the convergence issue. For example, the default tolerance for the convergence of temperature in a tear stream is 0.0001, and increasing this value to 0.0005 can help significantly. The additional error in temperature is still small and has little impact on the final results. For the distillation columns, it is much better to spread the design specs to the both top and bottom products instead of focusing on top or bottom of the column. For example, in a RadFrac block, it

is better to specify two design specs where one manipulates reflux ratio to achieve a certain distillate purity, and the other manipulates boilup ratio to achieve bottoms purity, as opposed to having two design specs which manipulate variables at the top, such as reflux ratio and condenser temperature. Furthermore, it is very helpful to use the Generate Estimates feature for each column after a successful convergence in order to make the convergence much faster for the next runs, since it uses these estimates as initial guesses in future runs. The position of the tear stream is an important factor that can reduce the computation time significantly, particularly when multiple tear streams are defined. Usually, it is better to place the tear stream upstream of separating unit operations (columns, separators, etc.). It is also better to place the tear on a stream that has less fluctuation. For example, downstream of mixers are usually more stable than other streams. Furthermore, changing the convergence solving method to Wegstein or Newton methods can increase the convergence rate in most cases.

2) Evaluation of the objective function

In this project, we decided to use an external spreadsheet for the calculation of objective function values, which can be the thermal efficiency, NPV or other cost or technical performance factors. Using a spreadsheet can also help us to monitor the impact of changes on other parameters more easily. For this purpose, the following steps can be performed to link the simulation variables and functions to the excel file by using an ActiveX Automation interface:

1. In the Excel file, go to Developer/View Code to go to VBA environment.

2. From Tools/References, select and add the Aspen Plus library.

3. Set the dimension of a new variable (for example "`getdata`") as an Aspen Plus variable by putting the following command in a VBA function or Subroutine:

```
Dim getdata As HappLS
```

Now the "`getdata`" has been introduced as an Aspen Plus function to VBA.

4. Introduce your simulation file to "`getdata`" by showing the place of your simulation file

as:

```
Set getdata = GetObject("C:\Research\...\Aspen.bkp")
```

Now the Aspen.bkp file has been introduced to "`getdata`".

5. Now the "`getdata`" and "Aspen.bkp" can communicate with each other. For instance, using "`getdata.run`" and "`getdata.save`", we can run and save the Aspen simulation file remotely from the VBA interface.

6. The place and name of the desired Aspen variables are also required to be defined. All input and output data can be viewed in the Aspen Plus file following a tree structure called "Variable Explorer". Depending on the version of Aspen Plus it can be viewed from the Tools or Customize tabs.

7. Each parameter can be called or adjusted from the VBA interface using the path obtained from the "Variable Explorer". As an example, the following line in VBA can be used to obtain the mass flowrate of stream 1 and put that into cell "A1" of "Sheet1":

```
Range("Sheet1!A1").Value=Getdata.Tree.FindNode("\Data\\Streams\
1\Output\MASSFLMX\MIXED").Value
```

3) Interaction between Optimization model (MATLAB code) and the Objective Function

Linking the objective function to the MATLAB optimization code can be done by using the following steps:

1. In the MATLAB main optimization code, write the following commands to link the excel sheet to the MATLAB code:

```
excelObject = actxserver('Excel.Application');

filename='C:\research\...\objectivefunction.xlsm';

Workbook=excelObject.Workbooks.Open(filename);
```

```
Activesheet=Workbook.Sheets.Item('Sheet1');
```

2. Now, "Sheet1" of the "objectivefunction.xlm" excel sheet has been introduced as the external objective function spreadsheet.

3. There are several ways to adjust the decision variables. For instance, another MATLAB function can be introduced to the main code using the following line:

```
ObjectiveFunction=@(Var)ObjectiveCost(Var,excelObject,filename,Workboo
k,Activesheet);
```

4. In the above command line, "Var" is the decision variable matrix, which can be set in the "ObjectiveCost" MATLAB function. During the optimization, the objective function can be called by using "ObjectiveFunction".

5. Another MATLAB function is required to call the objective function value and change the decision variables. This MATLAB function is called "ObjectiveCost" as mentioned above.

6. As an example, the following code in "ObjectiveCost" writes the values of "A1" and "A2" cells (as the decision variables) from MATLAB, runs the Aspen Plus file linked to the VBA code, and reads objective function value from the excel sheet (assuming the objective function value has been defined in "excelSheet2" cell "A3"):

```
Function
z=ObjectiveCost(var,excelObject,filename,Workbook,Activesheet)

ActivesheetRange = get(Activesheet, 'Range', 'A1');

set(ActivesheetRange, 'Value', var(1));

ActivesheetRange = get(Activesheet, 'Range', 'A2');

set(ActivesheetRange, 'Value', var(2));

k = Workbook.VBProject.Collection.get();
```

```
k =invoke(Workbook.Application,'run','Sheet1.RunSimulation_Click');

sheet = 2; xlRange = 'A3';

excelSheet2= Workbook.Sheets.Item('Sheet2');

ObjectiveFunction = excelSheet2.Range(xlRange);

z = ObjectiveFunction.Value;

end
```